DOCTOR OF PHILOSOPHY

Studies on micro algal fine-structure, taxonomy and systematics : cryptophyceae and bacillariophyceae.

Novarino, Gianfranco

Award date:
1990

Awarding institution:
Bangor University

Studies on microalgal fine-structure, taxonomy, and systematics: Cryptophyceae and Bacillariophyceae

In Two Volumes

Volume II (Plates)

by

Glanfranco Novarino, *Dottore In Scienze Biologiche (Rome)*

A Thesis submitted to the University of Wales in candidature for the degree of *Philosophiae Doctor*

University of Wales (Bangor)

School of Ocean Sciences

Marine Science Laboratories

Menai Bridge, Isle of Anglesey, United Kingdom

December 1990

Index

~~~~~~

Cryptomonads
~~~~~~

Diatoms

PLATE 1

Some cryptomonad cell features visible with the light microscope

Fig. 1. The freshwater '*Rhodomonas lacustris*' (Pascher & Ruttner) Javornicky, strain DK N750301, glutaraldehyde, phase-contrast. Fig. 2. *Proteomonas pseudobaltica* strain GN A, Lugol's iodine, bright-field. Figs 3, 4. *Rhinomonas reticulata* var. *elenlana* var. nov., strain IANL 97825/C, glutaraldehyde, phase-contrast. Fig. 3 is a lateral view, Fig. 4 a dorsal one. Fig. 5. *Pyrenomonas salina* var. *curvata* var. nov., glutaraldehyde, phase-contrast. CHLP = chloroplast, CV = contractile vacuole, F = flagella, PY = pyrenoid, T = posterior 'tail'. Scale bars = 5 µm.

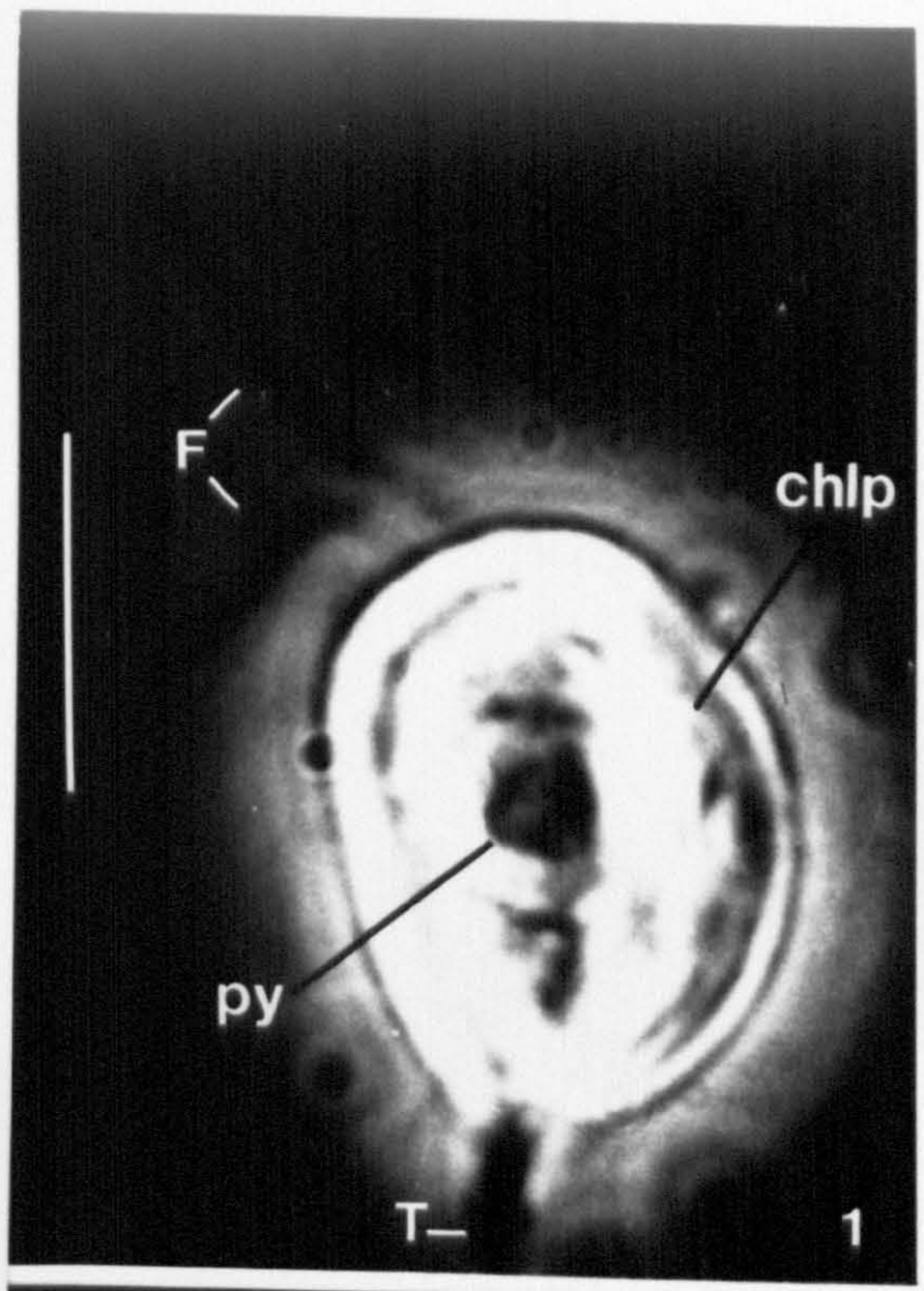

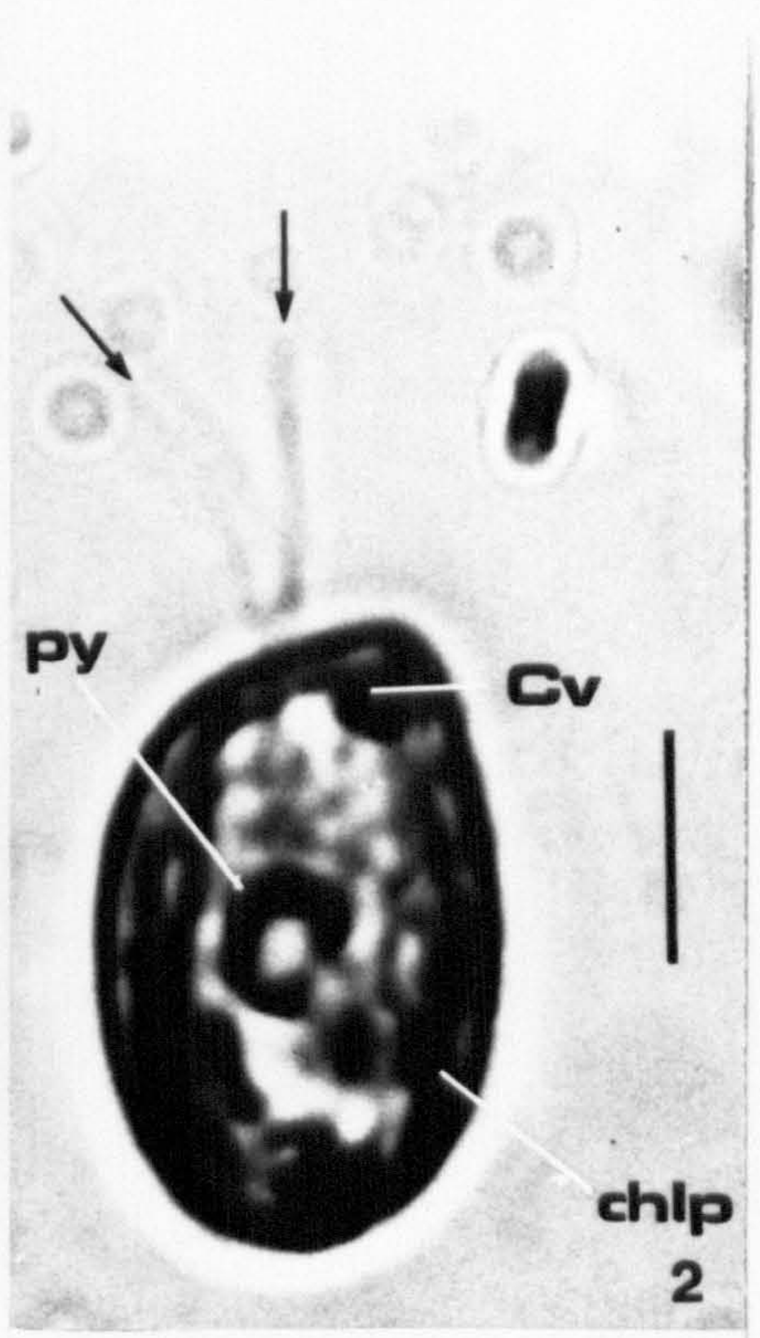

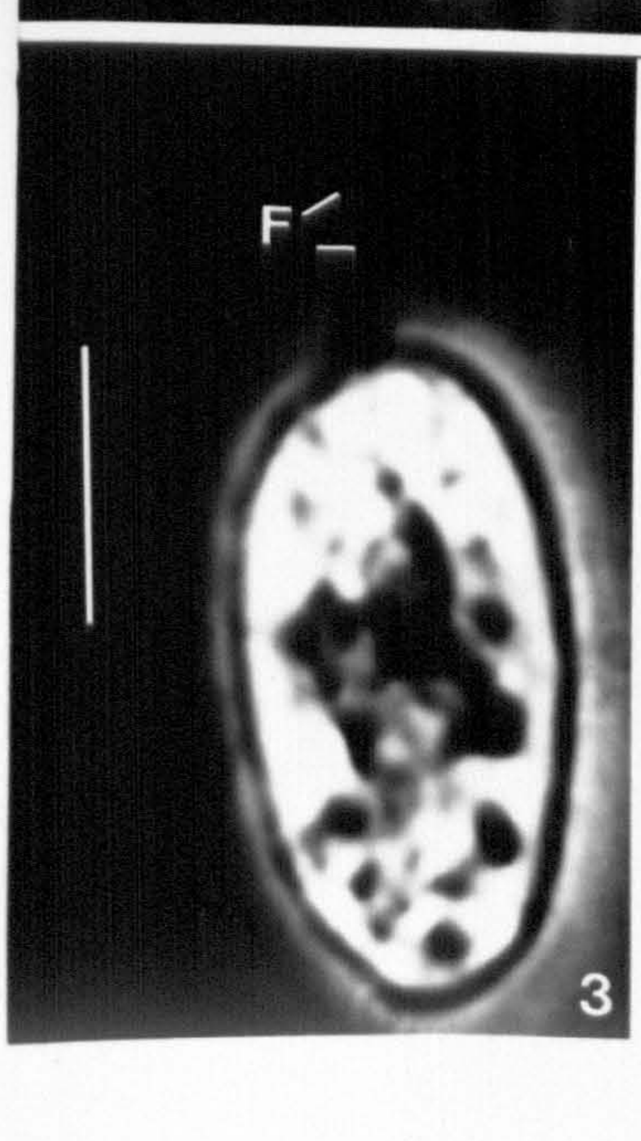

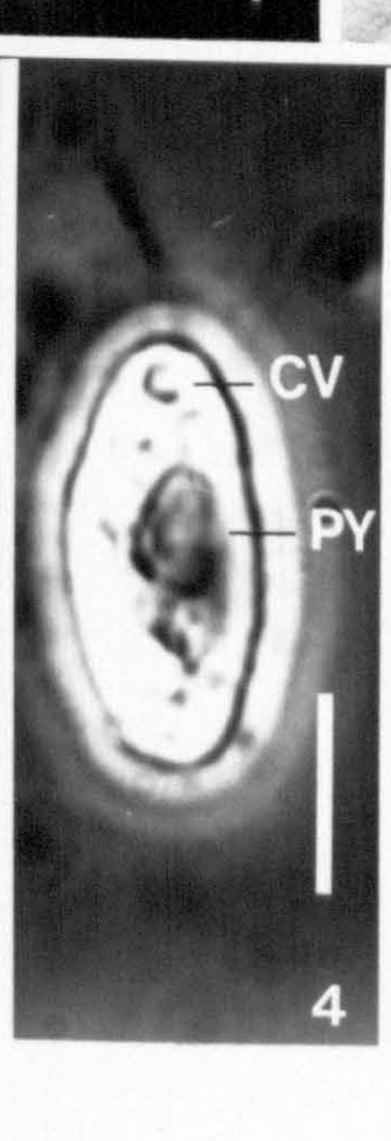

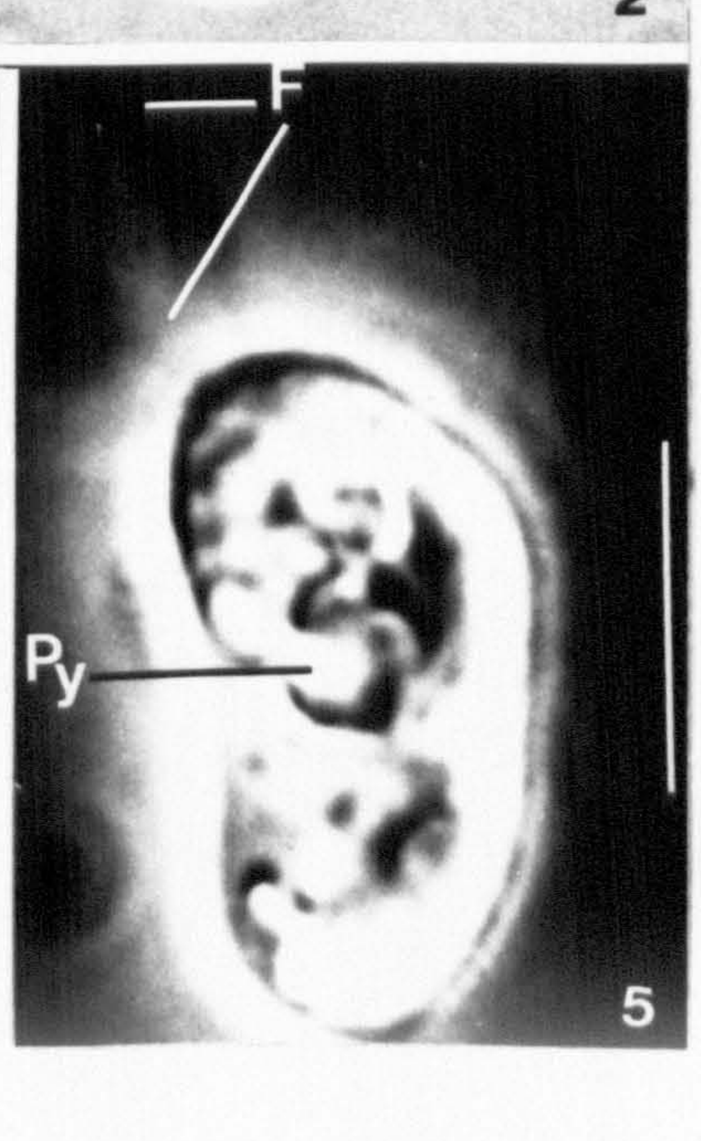

PLATE 1

PLATE 2

Hemiselmis rufescens strain PLY D, SEM, glutaraldehyde/osmium fixation.

Fig. 1. Cell with indistinct periplast. Fig. 2. Cell with circular, finely granular periplast areas, delineated by a lattice showing a repeated hexagonal pattern. Variations of the hexagonal pattern are sometimes visible; such is the case in the region of area 0, surrounded by a heptagonal lattice (arrows), each side of which separates area 0 from one of seven adjacent areas (1-7). Fig. 3. Cell with rectangular (1) or irregularly polygonal (2) periplast areas, showing a much coarser structure than that seen in Fig. 2. Periplasts with such an appearance may represent preparation artifacts. Note the similarity in size between the particles of the periplast areas and those of the delineating lattice (arrows). Scale bars = 1 μm.

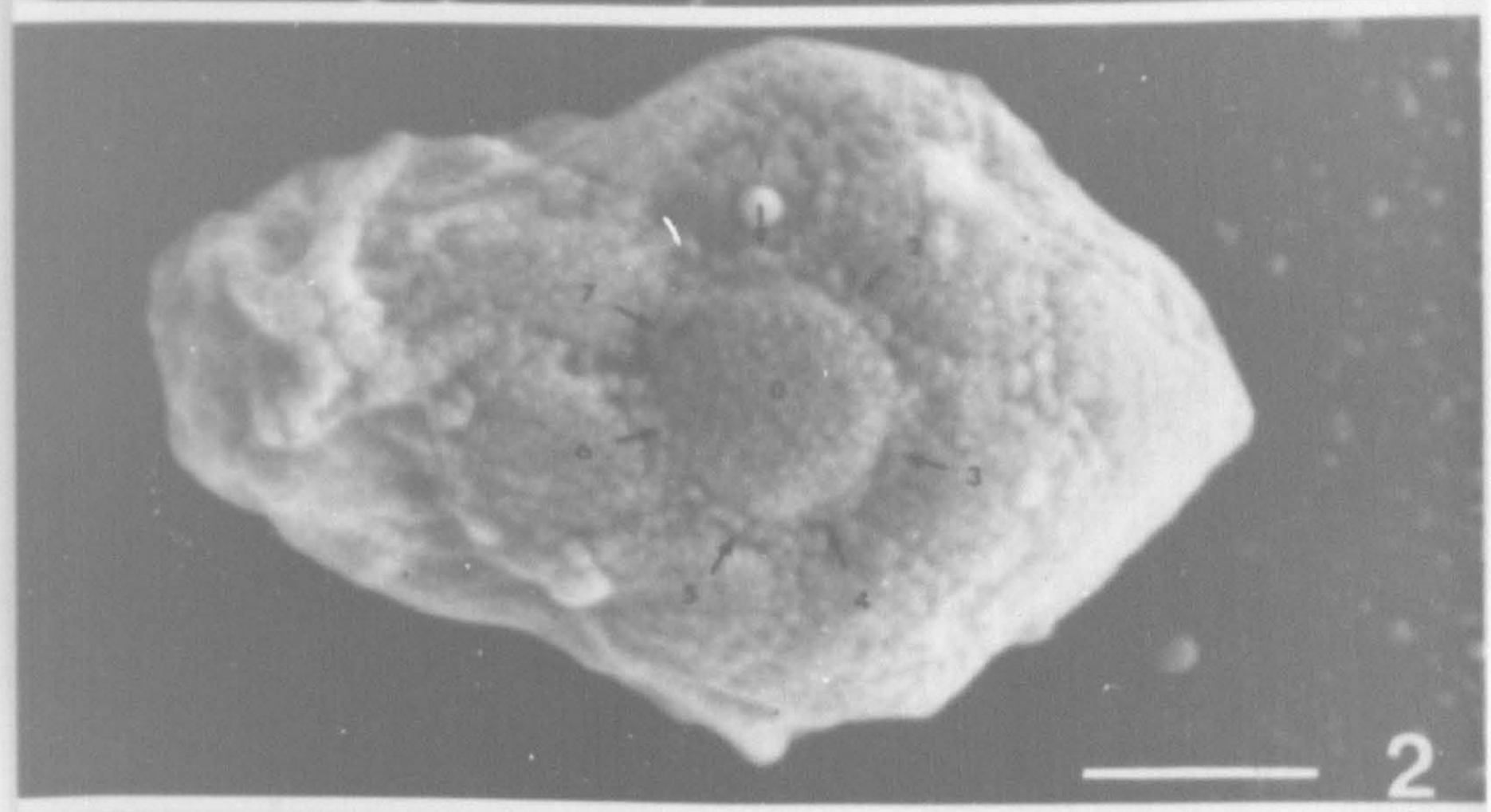

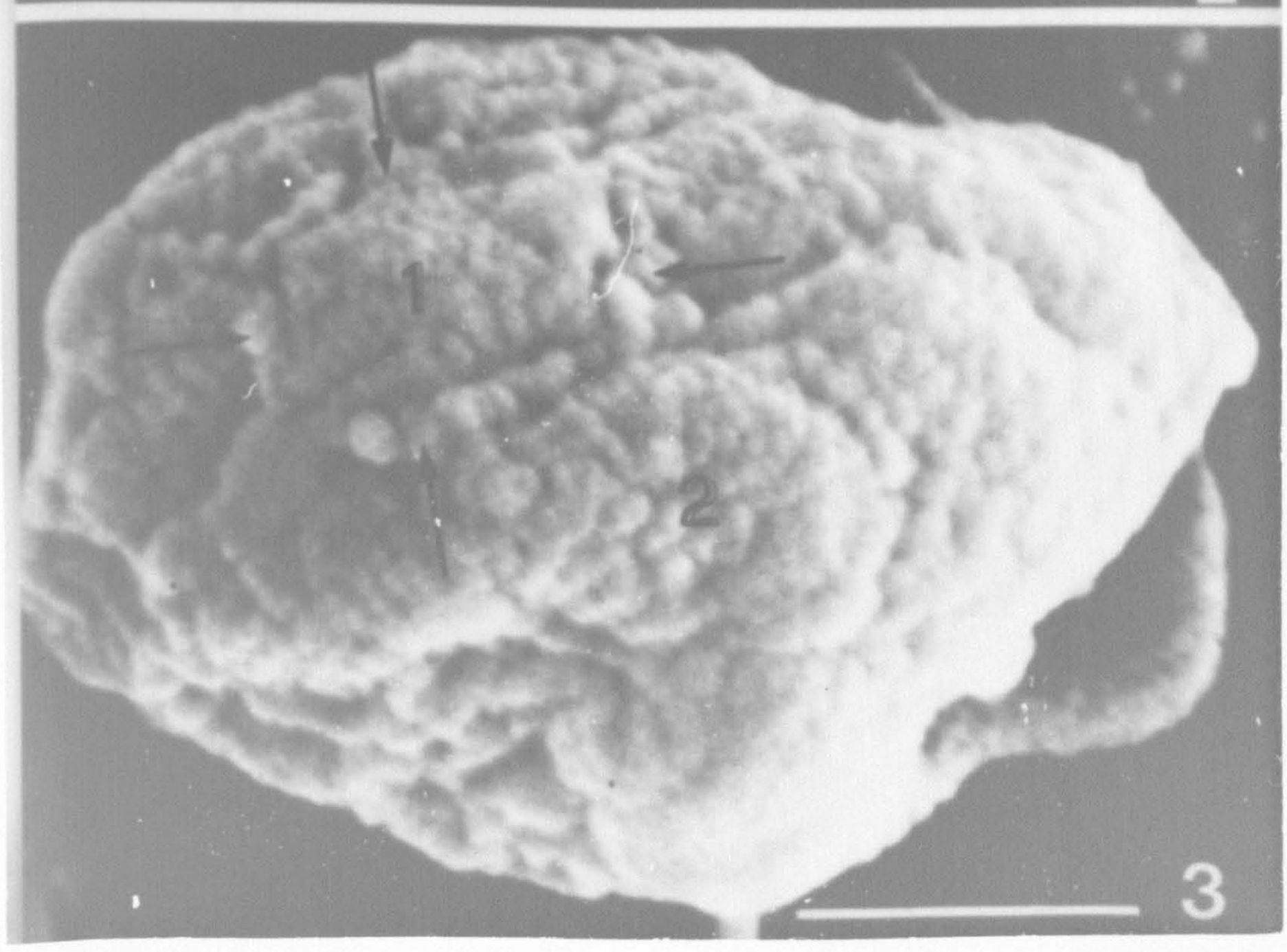

PLATE 2

PLATE 3

Hemiselmis virescens strain PLY 157, SEM, cold osmium fixation.

Fig. 1. A cell showing a periplast with distinct areas (nos 1-11), delineated by a hexagonal lattice having a granular appearance (arrows). Fig. 2. Cell with a relatively indistinct periplast. Fig. 3. Cell with a fissured hexagonal lattice (arrows). Scale bars = 2 µm.

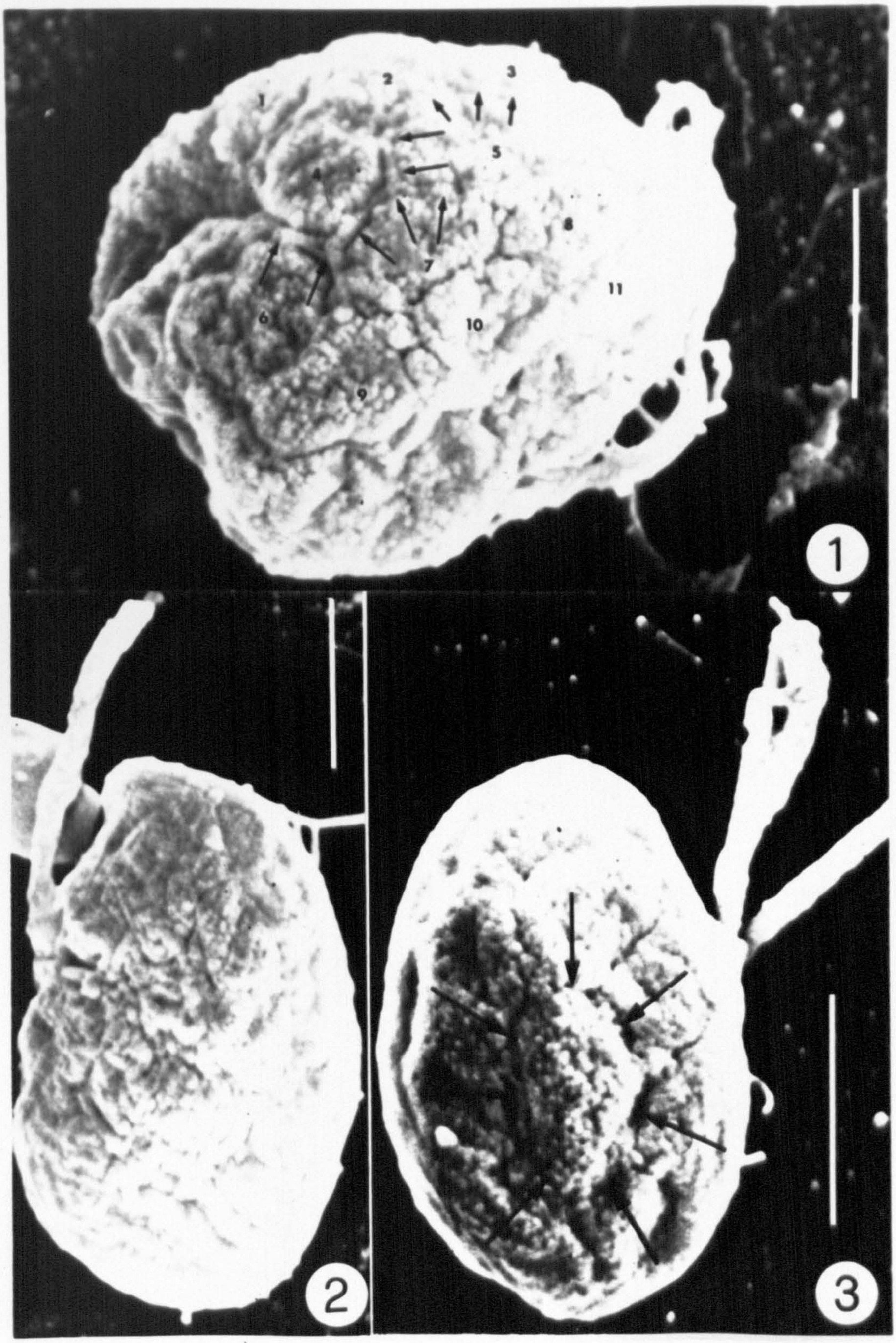

PLATE 3

PLATE 4

Hemiselmis virescens, origin unknown, TEM

Fig. 1. Longitudinal section; note the gullet, apparently divided in two branches (arrow and arrowhead), of which only the vertical one bears ejectosomes. Scale bar = 1 µm. Fig. 2. Grazing section, showing profiles of regularly arranged tubules of the endoplasmic reticulum (TER). Scale bar = 1 µm. Fig. 3. The cell surface; note the plasma membrane (arrows), and the overlying periplast layer (arrowheads). Scale bar = 0.1 µm. Fig. 4. Section similar to that in Fig. 3, but showing an interruption (I) of the periplast layer, in a position close to a peripheral ejectosome (E). Scale bar = 0.1 µm.

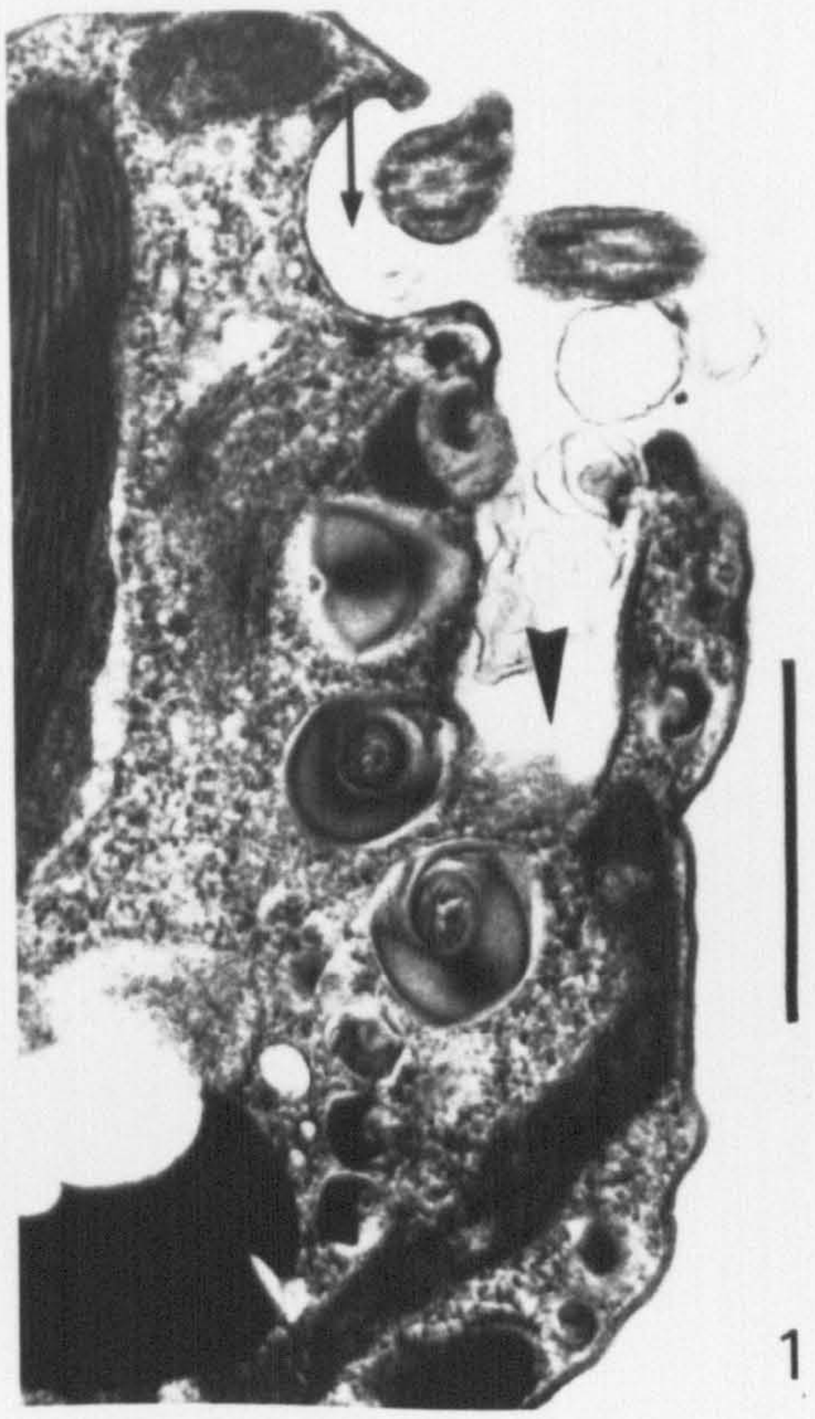

1

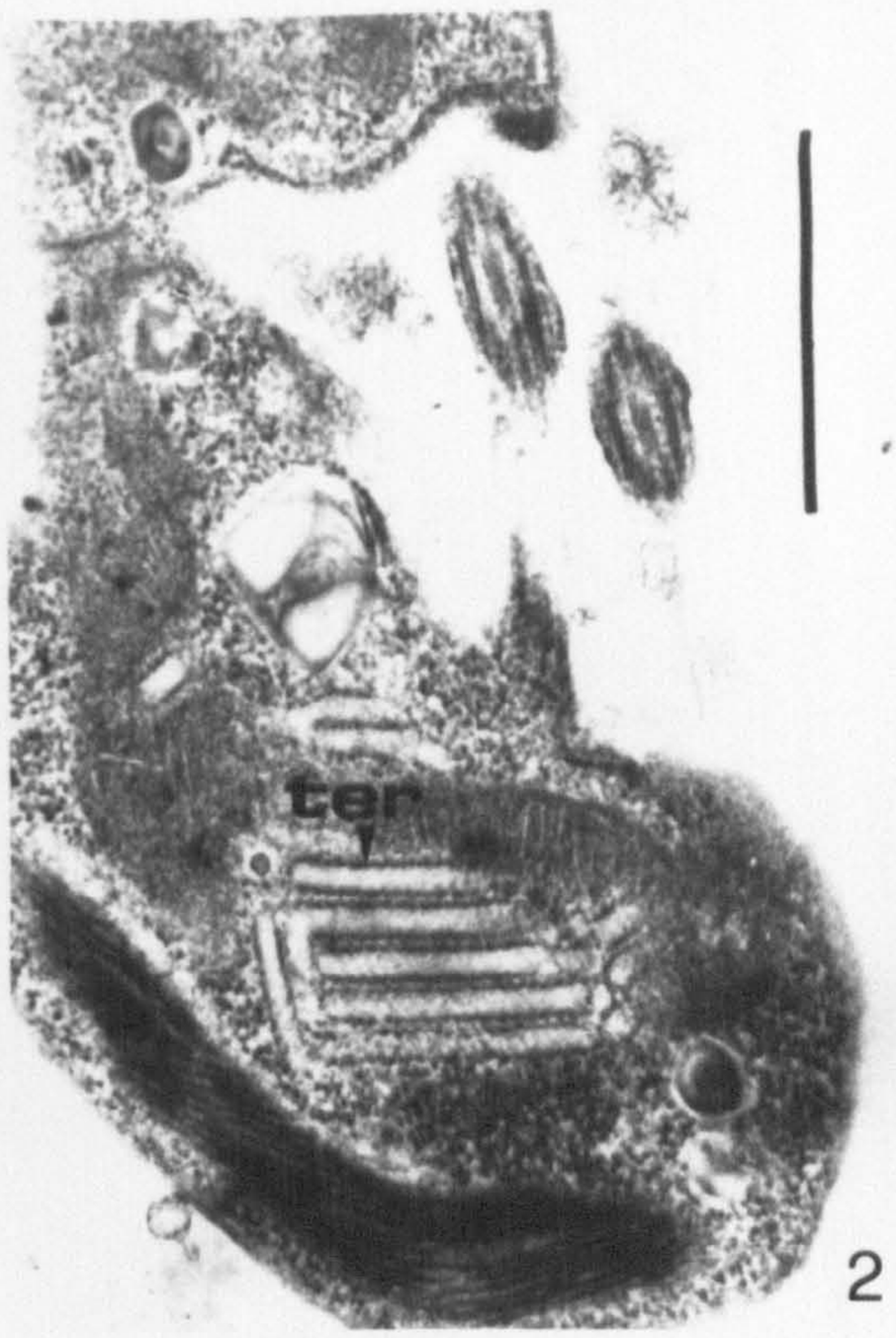

2

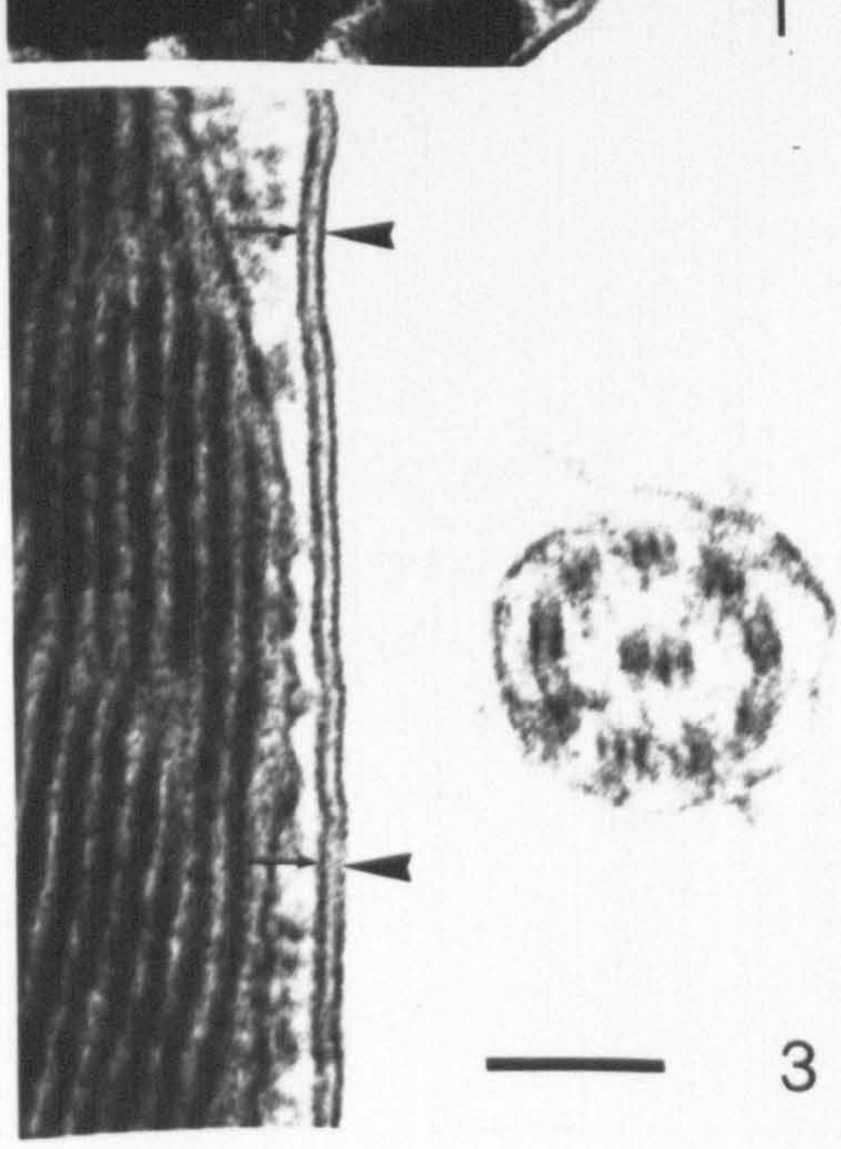

3

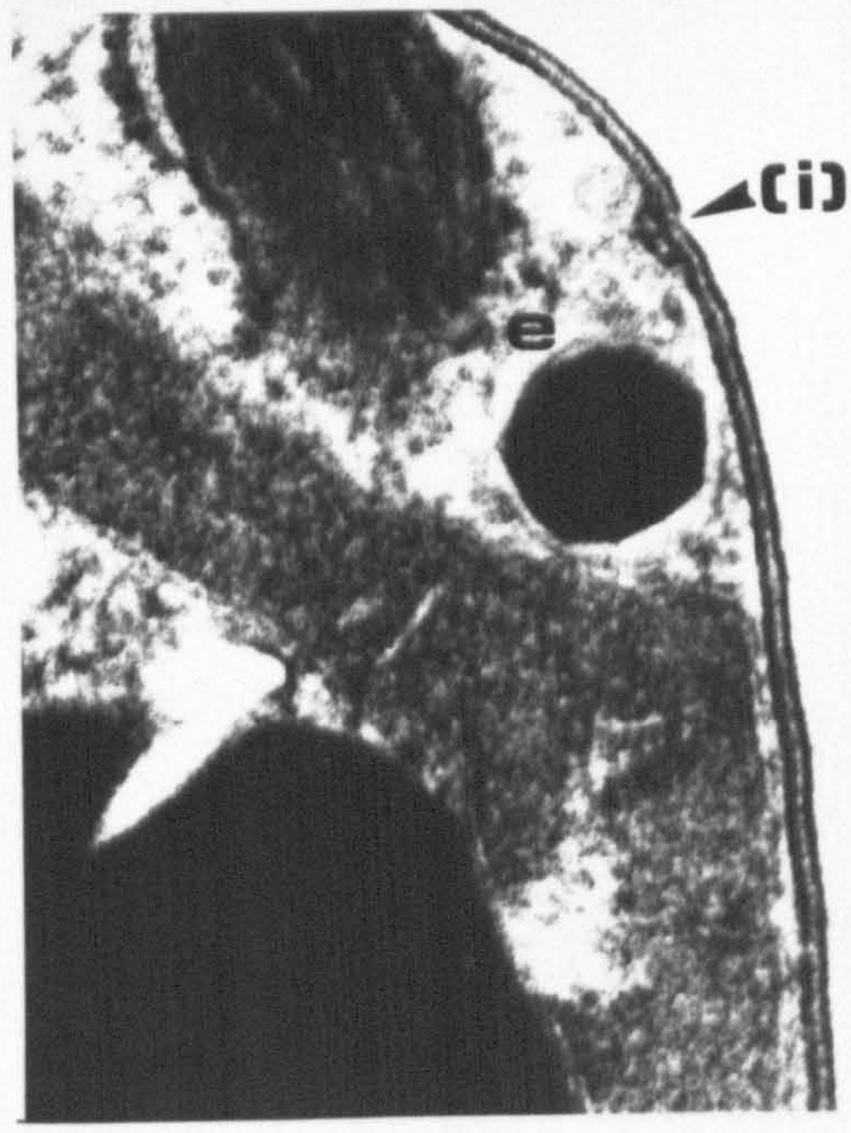

4

PLATE 4

PLATE 5A

Rhinomonas reticulata var. *reticulata* and var. *eleniana*, SEM, glutaraldehyde - osmium - critical point-drying.

Figs 1-4, 6: *Rhinomonas reticulata* var. *reticulata*. **Fig. 1.** Strain Theta/C. **Fig. 2.** Strain Rhodo. **Fig. 3.** Strain 3C. **Fig. 4.** Strain 995/2. **Fig. 5.** *Rhinomonas reticulata* var. *eleniana*, strain 97825/C. **Fig. 6.** Strain 358. Scale bars = 5 µm.

PLATE 5 A

PLATE 58

Further SEM views of *Rhinomonas reticulata* var. *reticulata*, strain CCAP 995/2, glutaraldehyde / osmium / critical point-drying.

Fig. 1. Ventral view. Fig. 2. Another ventral view, with an S-shaped fold running from the vestibular depression; this is interpreted as arising frtom cell shrinkage. Fig. 3. Dorsal view. Fig. 4. Periplast at higher magnification. Scale bars = 5 µm (Figs 1-3), or 1 µm (Fig. 4).

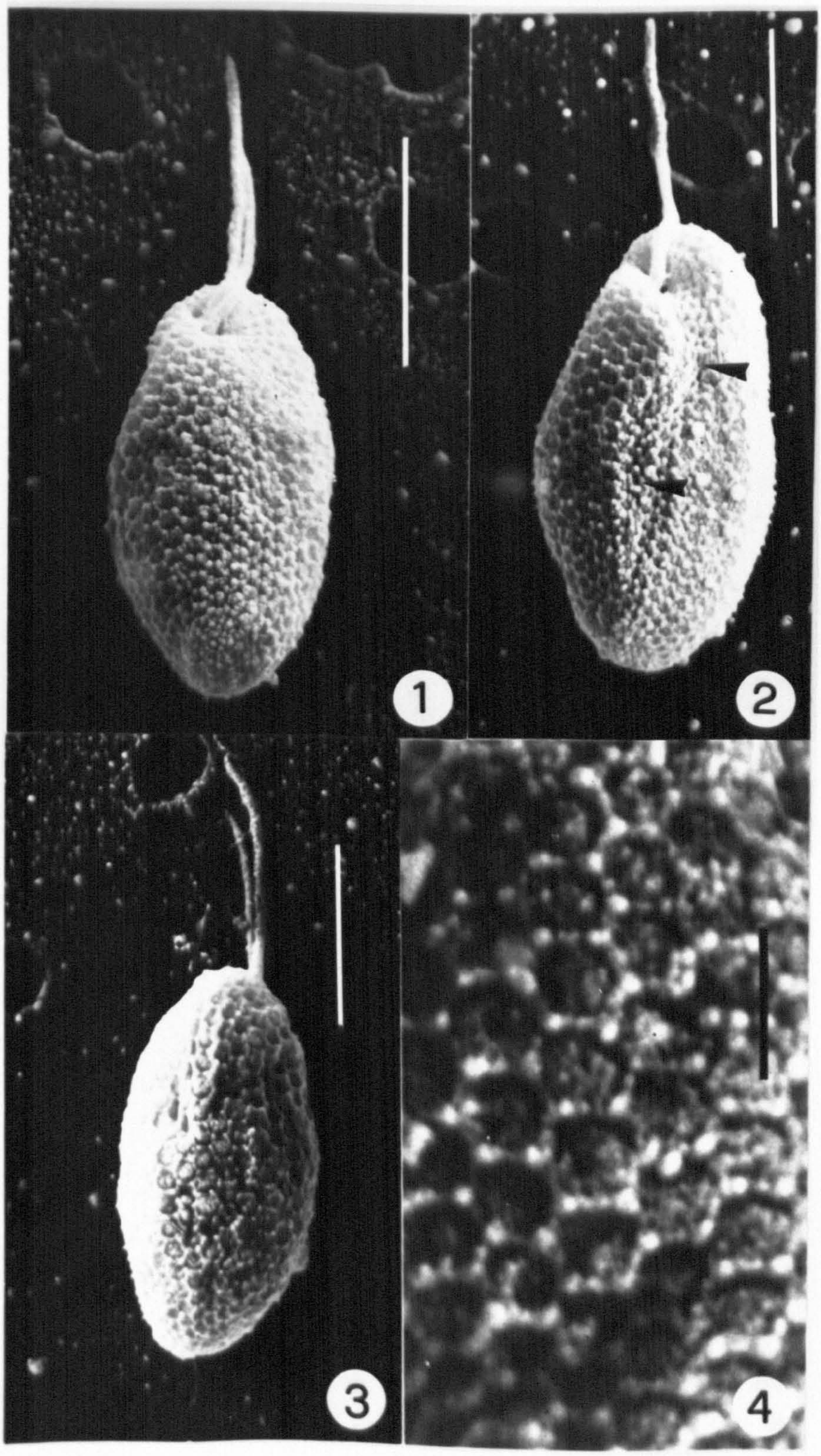

PLATE 5 B

PLATE 5C

Further SEM views of *Rhinomonas reticulata* var. *reticulata*, strain IANL Rhodo, glutaraldehyde / osmium / critical point-drying.

Fig. 1. Ventral view. Fig. 2. Ventro-lateral view of cell with spirochaete bacteria associated with the vestibular depression (arrowhead). Figs 3, 4. Views of the periplast towards the cell posterior, which give the impression that the periplast areas are imbricate; Fig. 3 is an inverted-polarity micrograph. Scale bars = 5 µm (Figs 1, 2) or 1 µm (Figs 3, 4).

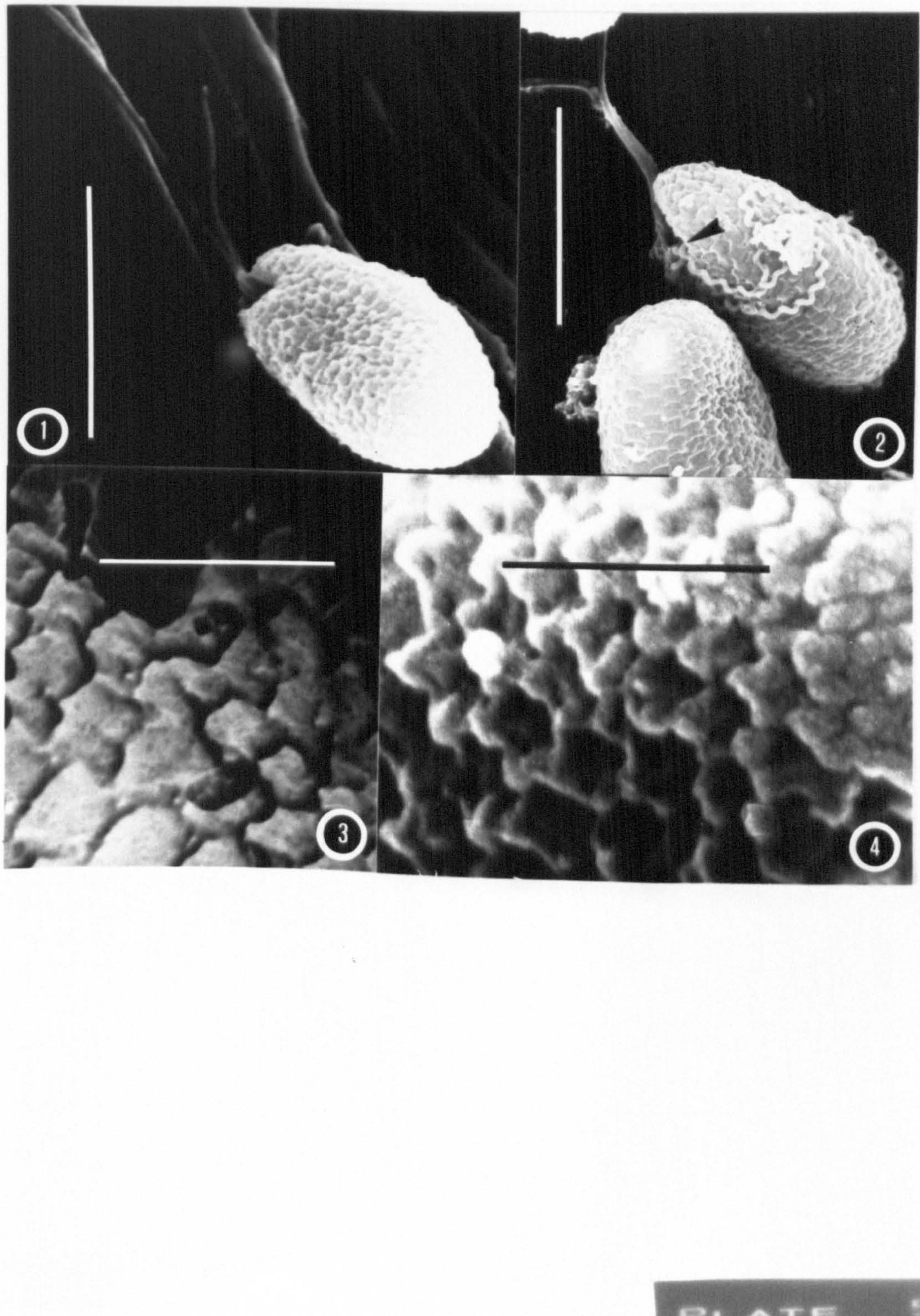

PLATE 5 C

PLATE 5D

Further SEM views of *Rhinomonas reticulata* var. *reticulata*, strain CCMP 3C, glutaraldehyde / osmium / critical point-drying.

Fig. 1. Ventral view; the furrow-like fold is interpreted as an artifact arising from cell shrinkage. **Fig. 2.** Ventro-lateral view; note that the furrow-like fold (arrows) is associated with signs of shrinkage in other regions of the cell (arrowheads). **Fig. 3, 4.** Details of the periplast, showing hexagonal periplast areas having a granular appearance, more pronounced in Fig. 3; the arrows point at pores arising from ejectosome discharge. Scale bars = 5 µm (Figs 1, 2), 1 µm (Fig. 3), or 0.5 µm (Fig. 4).

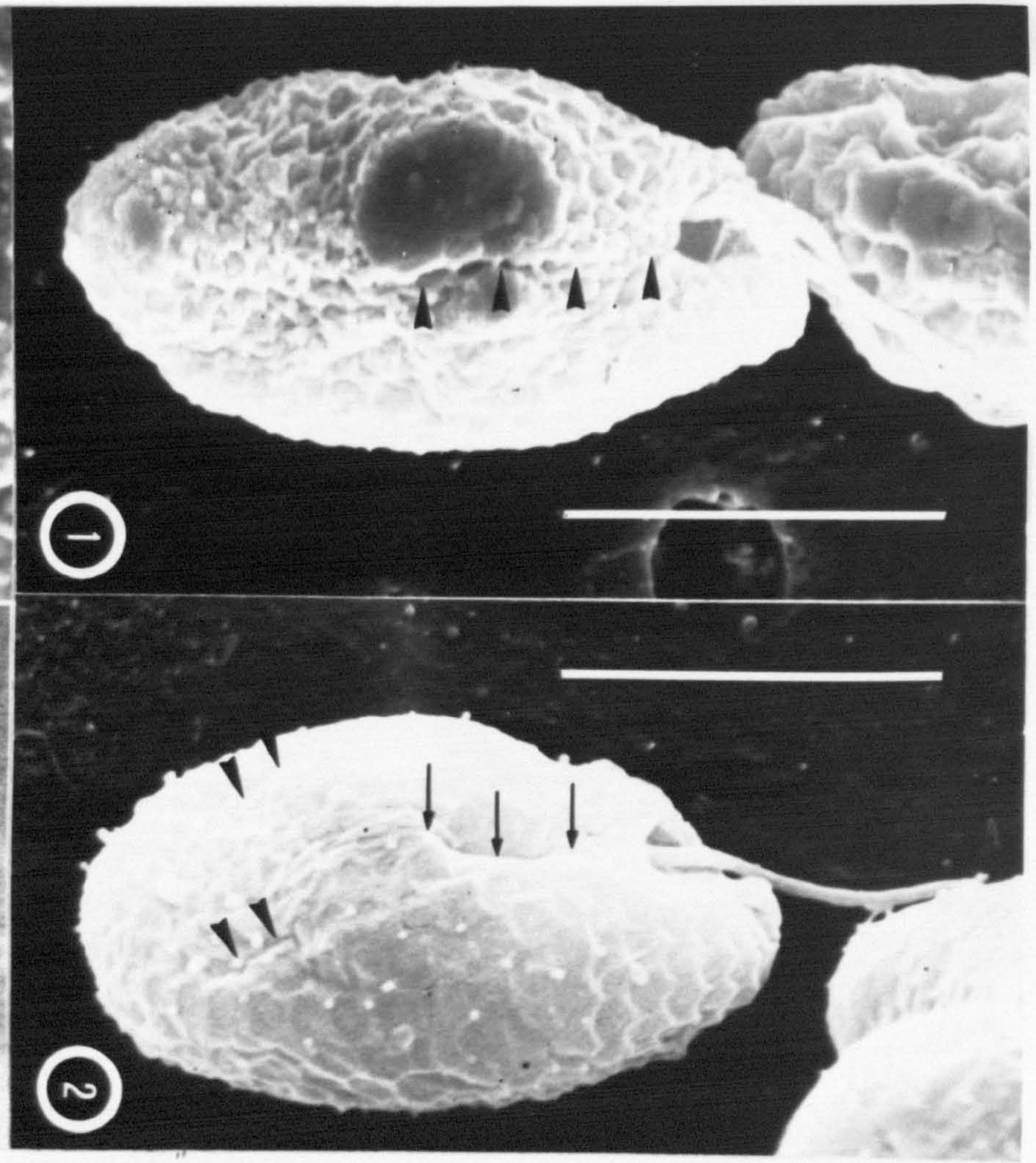
1

2

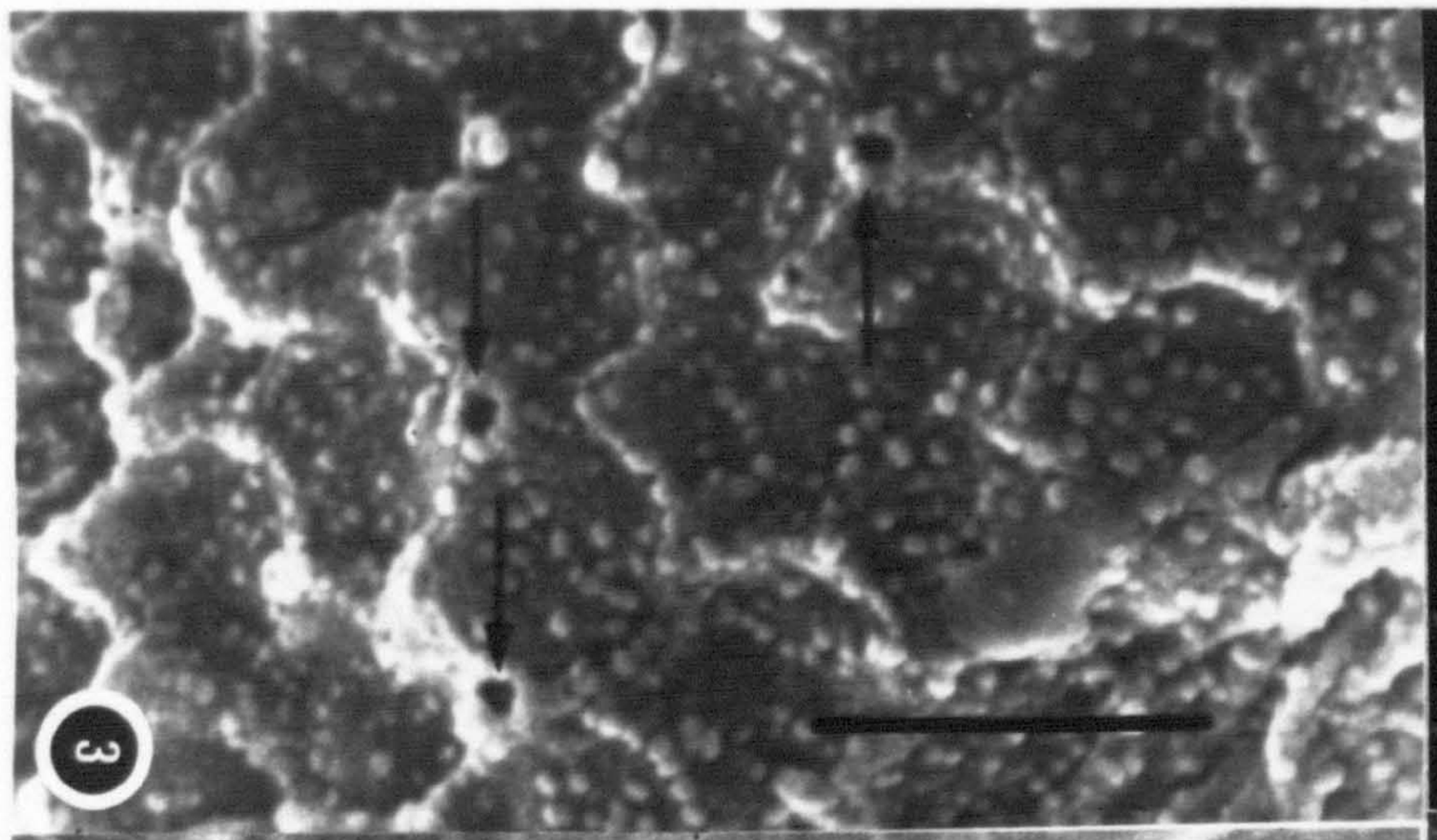
3

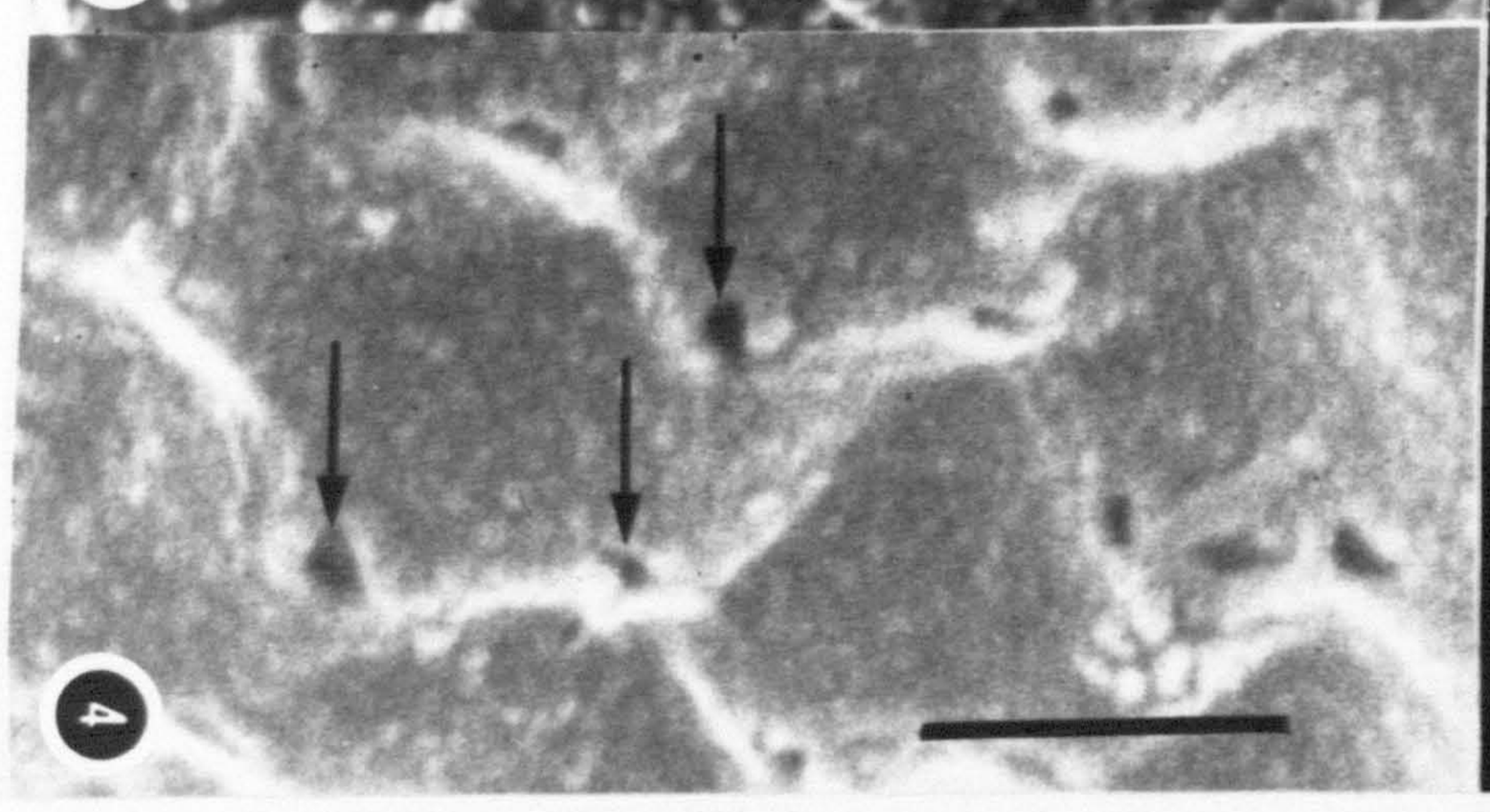
4

PLATE 5E

Further SEM views of *Rhinomonas reticulata* var. *eleniana*, strain IANL 97825/C, glutaraldehyde / osmium / critical point-drying unless otherwise stated.

Fig. 1. Ventral view. Figs 2, 3. Latero-ventral and ventral views; the short, notch-like 'furrows' (arrowheads), are interpreted as being due to cell shrinkage, also responsible for the folds in the lateral region (arrows); glutaraldehyde / CPD. Fig. 4. Detail of the periplast; the arrows point at pores caused by ejectosome discharge. Scale bars = 5 µm (Figs 1-3), or 1 µm (Fig. 4).

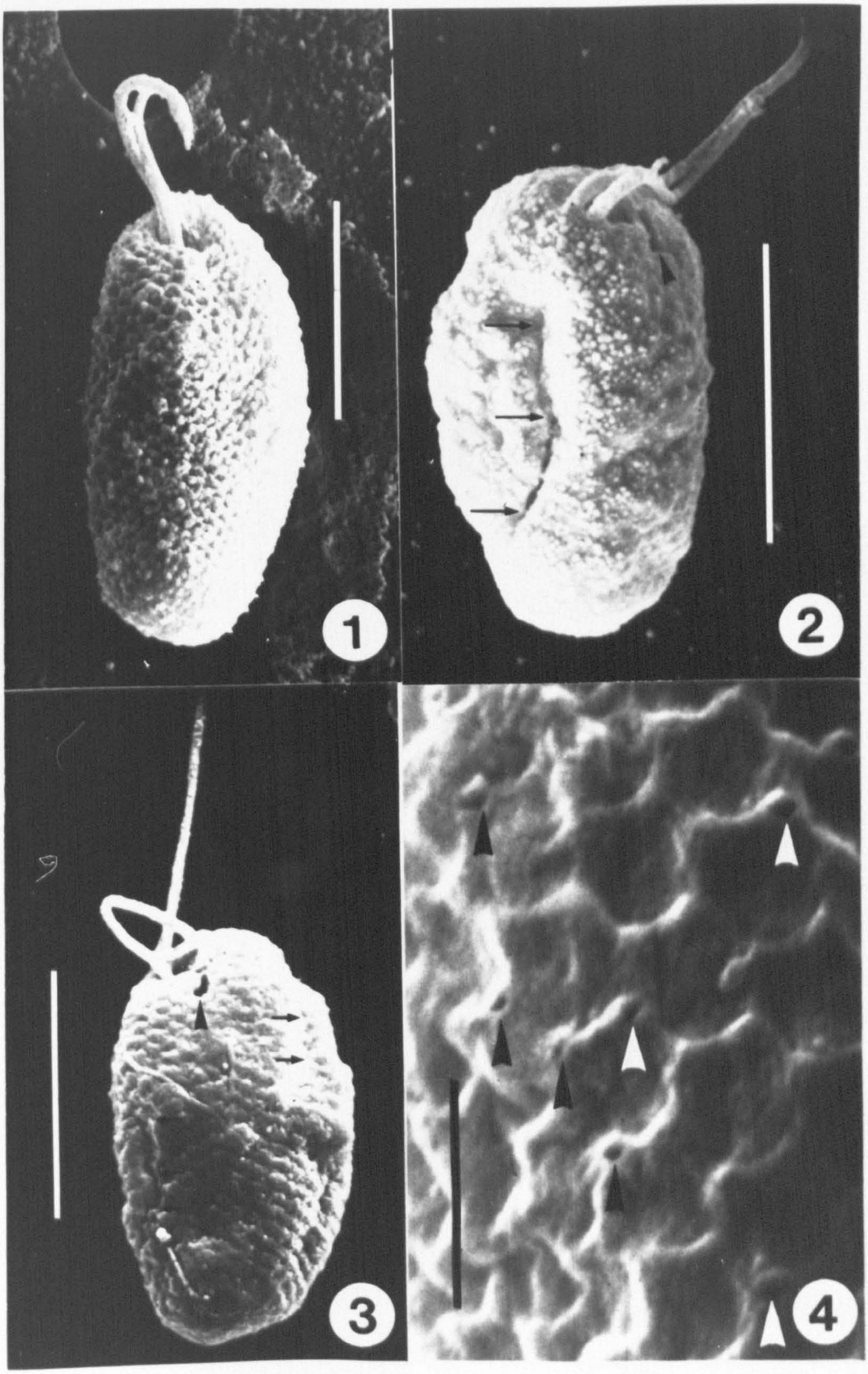

PLATE 5 E

PLATE 6

Rhinomonas reticulata var. atrorosea comb. et stat. nov., SEM, glutaraldehyde / osmium /critical point - drying, and LM (unfixed).

Fig. 1. Lateral view; scale bar = 5 µm. Fig. 2. Detail of the cell surface; scale bar = 1 µm. Fig. 3. Dorsal view; scale bar = 10 µm.

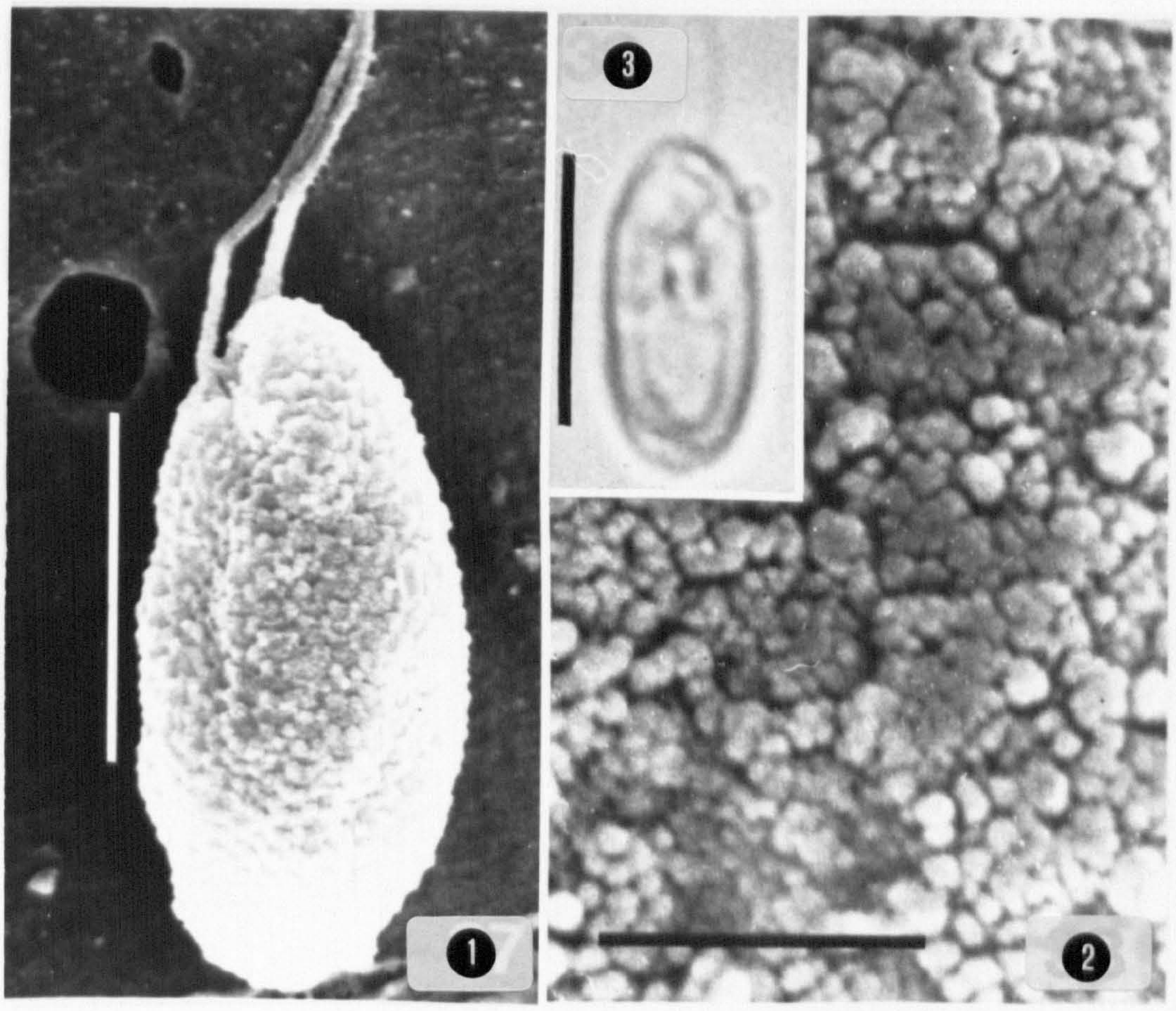

PLATE 6

PLATE 7

Rhinomonas reticulata var. *compressa* var. nov., SEM, glutaraldehyde / osmium /critical point-drying, and LM, unfixed.

Fig. 1. Lateral view; vestibular opening not visible. Scale bar = 5 µm. **Fig. 2.** Lateral view; vestibular opening visible. Scale bar = 5 µm. **Fig. 3.** Detail of the cell surface. Scale bar = 1 µm. **Fig. 4.** Lateral view; note prominent pyrenoid. Scale bar = 10 µm.

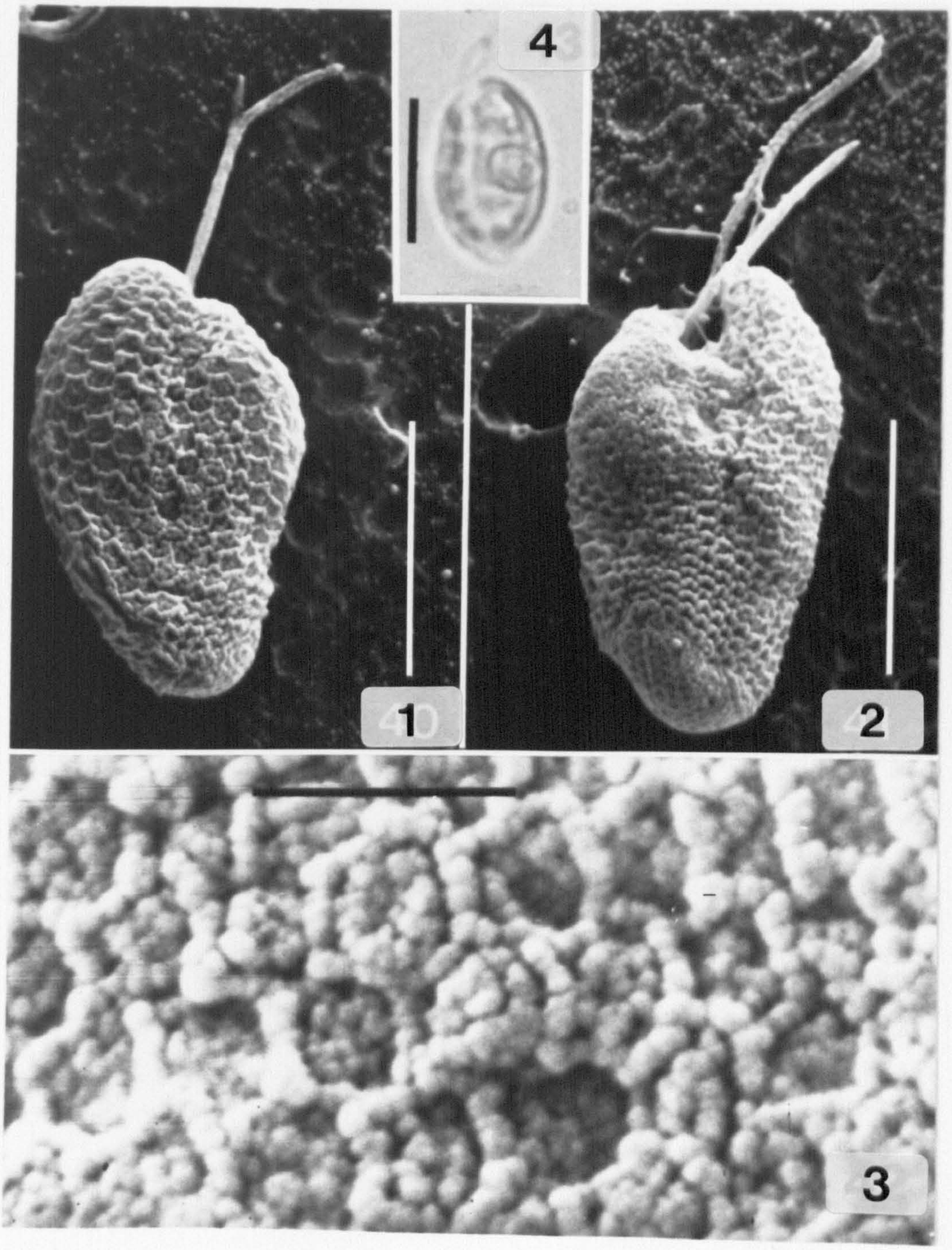

PLATE 7

PLATE 8

Details of the periplast features in *Rhinomonas reticulata* var. *reticulata* and *Pyrenomonas* sp. SEM, glutaraldehyde / osmium / critical point-drying, and TEM, glutaraldehyde / osmium .

Fig. 1. A cell of *R. reticulata* var. *reticulata* strain 358, showing two unornamented regions of the periplast, raised above the cell surface. Fig. 2. Periplast of strain 358 at higher magnification, showing hexagonal periplast areas delineated by a lattice which itself shows a hexagonal pattern. Fig. 3. Periplast of another cell of strain 358; one periplast area is roughly circular (asterisk), and the delineating lattice appears coarser than that in Fig. 2. Fig. 4. Longitudinal section of a cell of strain 3C; an accumulation of reserve material (arrow) bulges towards the cell surface on the ventral side of the cell, where unornamented regions of the periplast are visible with the SEM. Fig. 5. Detail at higher magnification of one unornamented region of the periplast. Fig. 6. A cell of *Pyrenomonas* sp., strain 11/8. Fig. 7. The periplast of *Pyrenomonas* sp. at higher magnification; note the periplast areas, rectangular or approximately so. Compare Figs 2, 3 (*Rhinomonas*). Scale bars = 5 µm (Figs 1, 6) or 1 µm (Figs 2-5 & 7).

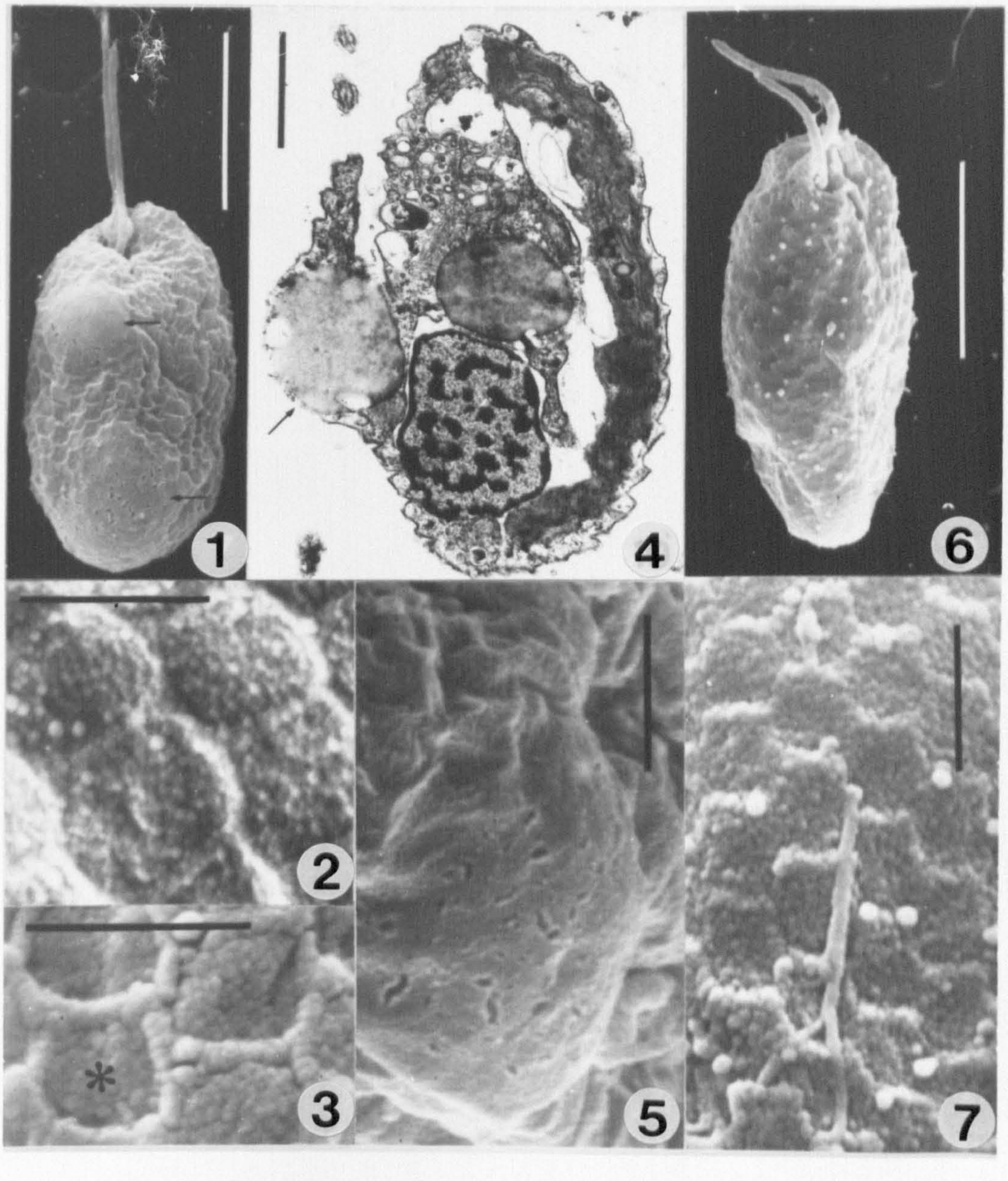

PLATE 8

PLATE 9

Rhinomonas reticulata et var., nucleomorph and periplast features, TEM. Glutaraldehyde/osmium fixation unless otherwise stated.

Fig. 1. Transverse section of Theta/C, showing the location of the nucleomorph (arrowhead) in relation to the pyrenoid (PY) and other cell organelles (S, starch cap around the pyrenoid; CHLP, chloroplast with several plastoglobuli (Pg); and N, nucleus). Scale bar = 1 µm. Fig. 2. Nucleomorph of Theta/C at higher magnification. The double membrane of the chloroplast envelope (arrowhead) and that surrounding the nucleomorph (arrow) are clearly visible. Scale bar = 0.5 µm. Figs 3–7. Periplast features; INT = cell interior, EXT = cell exterior, scale bars = 50 nm. Fig. 3. Theta/C. The internal periplast layer (arrows) is only discernible where the plasma membrane is swollen (arrowheads). Fig. 4. Rhodo, OTO. Note electron-dense internal periplast layer (arrows), and the moderately electron-dense gap separating it from the plasma membrane (arrowheads), which bears finely fibrillar material more than 100 nm long. Fig. 5. *Rhinomonas reticulata* var. *eleniana* 97825/C, OTO. The internal periplast layer (arrows) is roughly as thick as the plasma membrane (arrowheads), from which it is separated by a clear gap; a thin layer of granular material is present on the external face of the plasma membrane. Fig. 6. 3C. A distinct gap is visible between the thin internal periplast layer (arrows) and the plasma membrane (arrowheads), on which very little granular material is visible. Fig. 7. 995/2, OTO. The internal periplast layer (arrows) is moderately appressed to the plasma membrane (arrowheads), which bears a layer of granular material only a few nanometres thick.

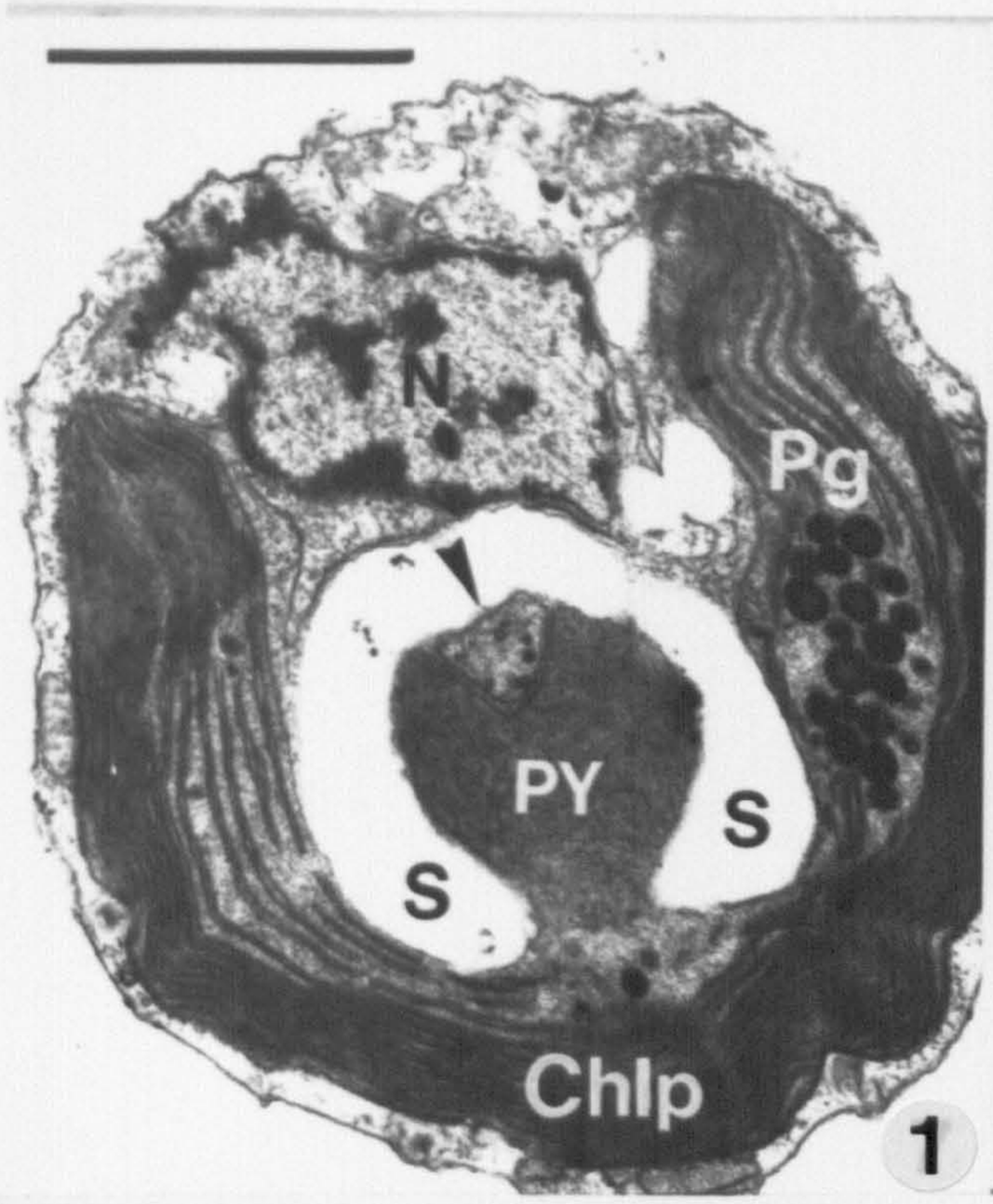

1

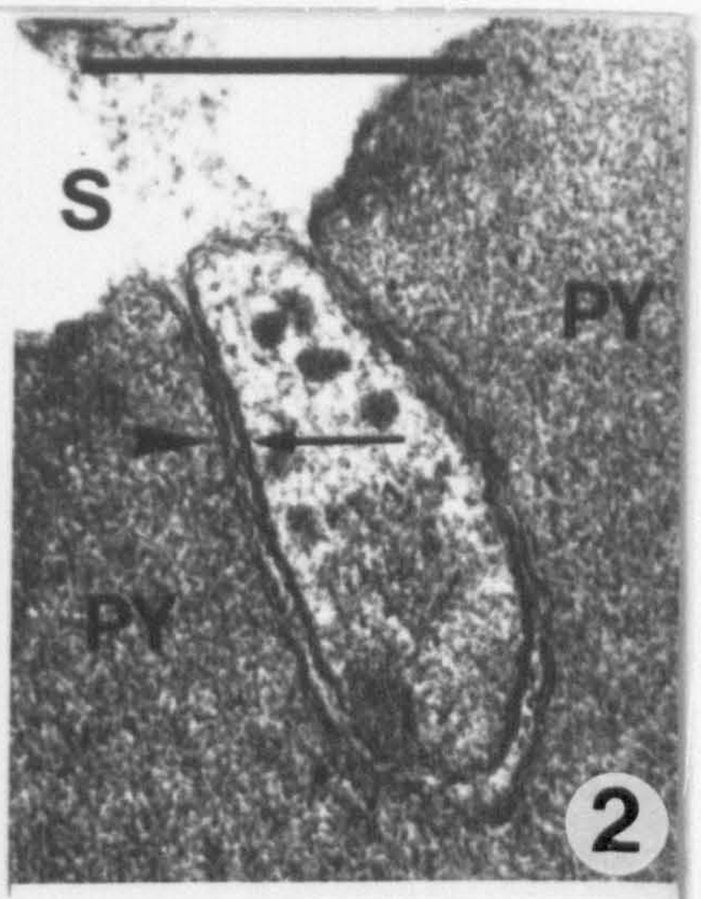

2

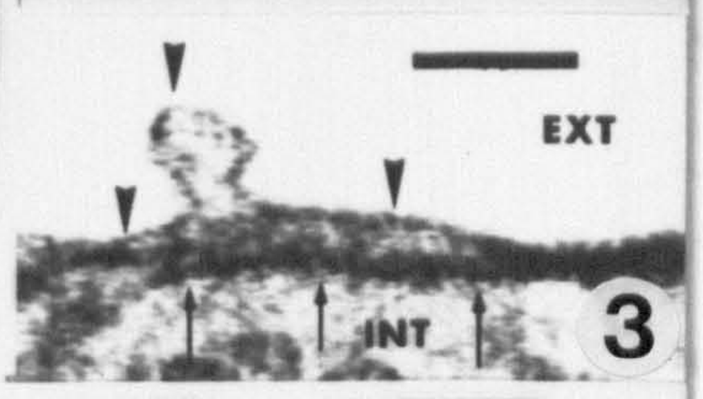

3

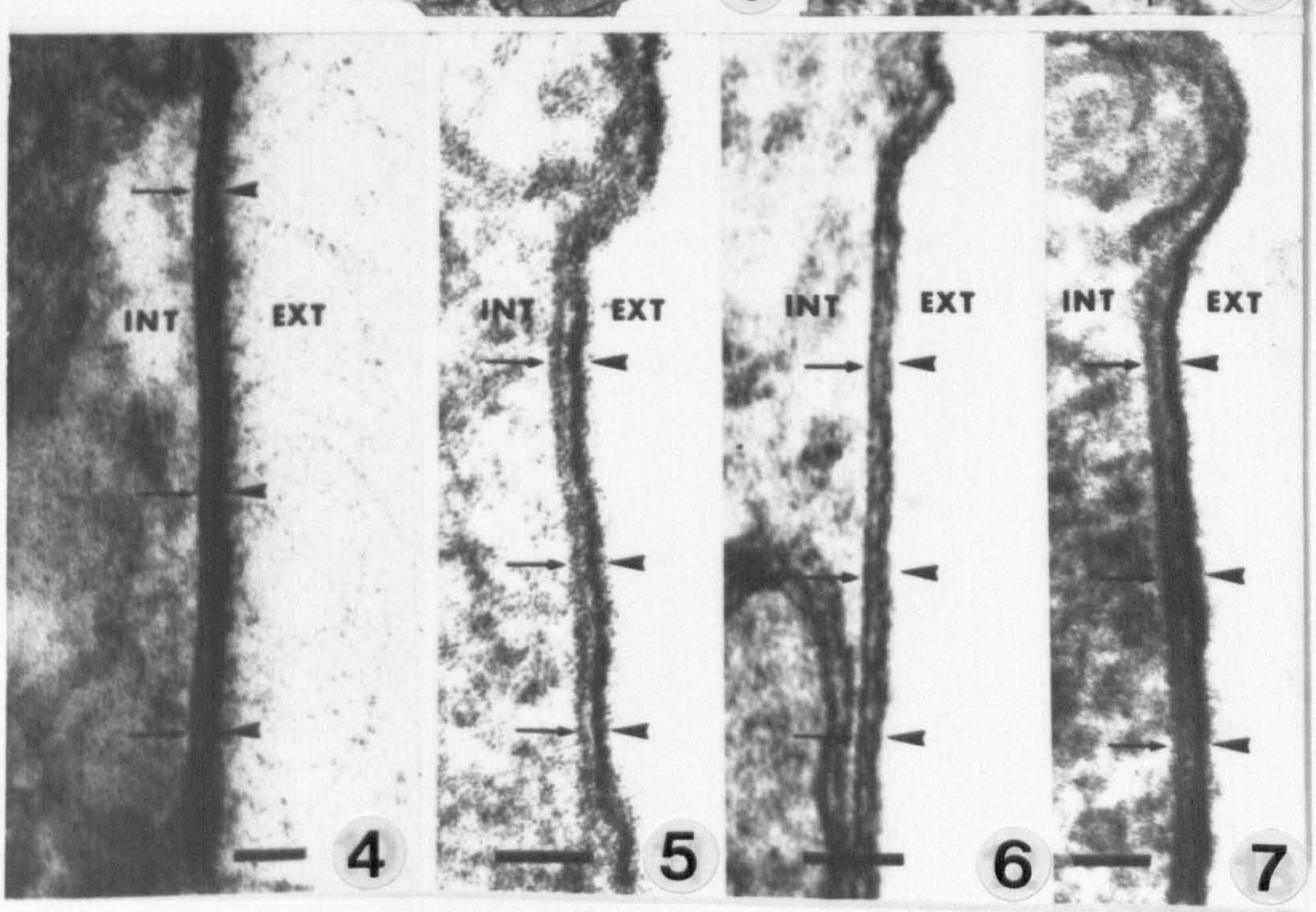

4 5 6 7

PLATE 9

PLATE 10

Bright-field light micrographs of *Rhinomonas reticulata* var. *reticulata* and a species of *Proteomonas*, which both fit into the diagnosis or later descriptions of *Rhodomonas baltica* Karsten (compare Plate 11)

Fig. 1. *R. reticulata* var. *reticulata* strain Theta/C, glutaraldehyde; pyrenoid (PY) and one flagellum (F) visible.
Fig. 2. A representative of *Proteomonas* (strain GN A from the author's collection), Lugol's; flagella (F), pyrenoid (PY), chloroplast (CHLP), and contractile vacuole (CV) clearly visible. Scale bars = 10 µm.

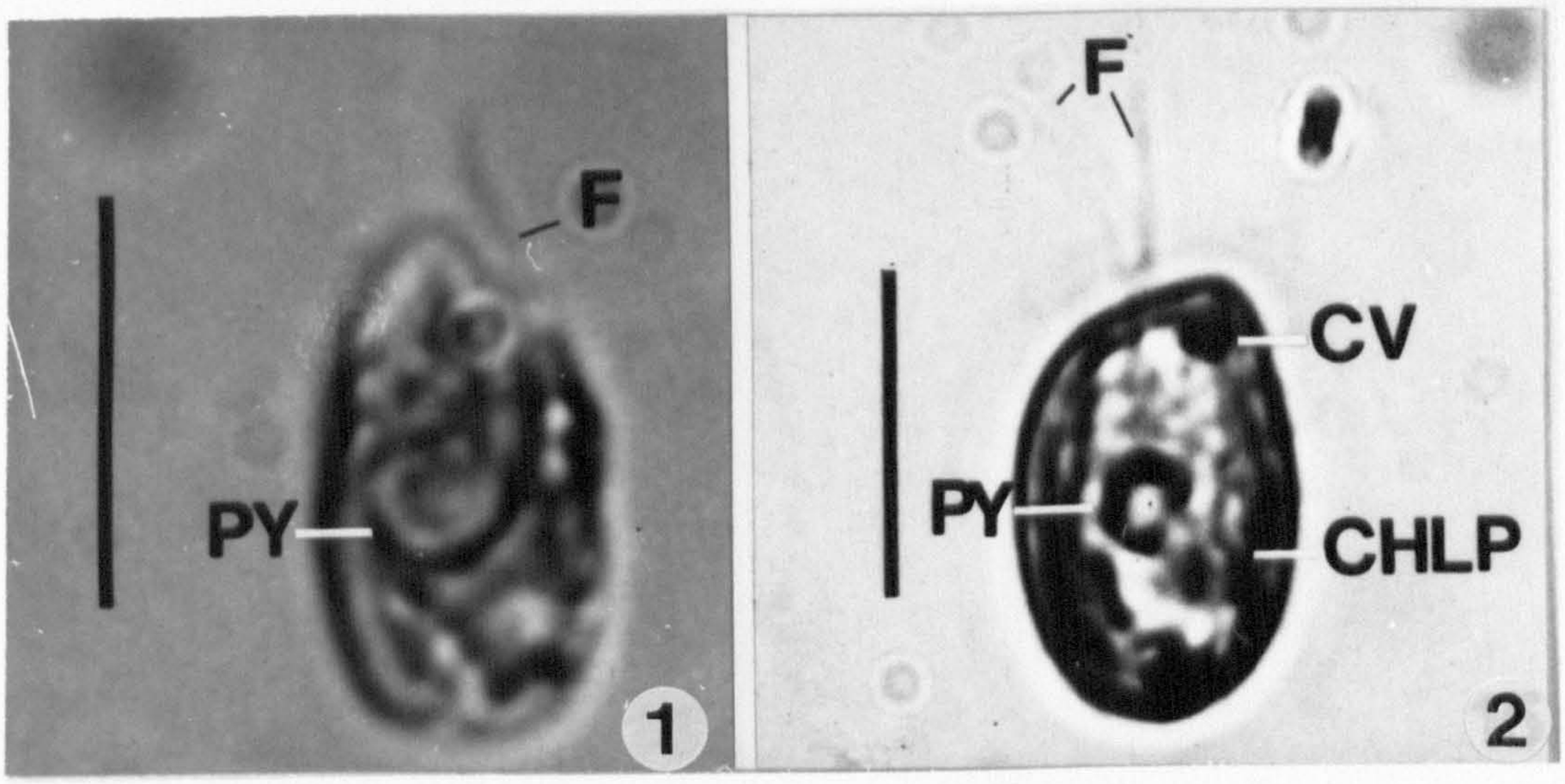

PLATE 10

PLATE 11

Schematic reproductions of illustrations of *Rhodomonas baltica* taken from the literature. All hatchings, shadings, and ejectosomes present in the original drawings have been omitted.

Fig. 1. From Karsten (1898), ≈ x1300. **Fig. 2.** From Zimmermann (1923), ≈ x1200. **Figs 3, 4.** From Kylin (1935), ≈ x2500. **Fig. 5.** From Zimmermann (1925), ≈ x2600.

1

2

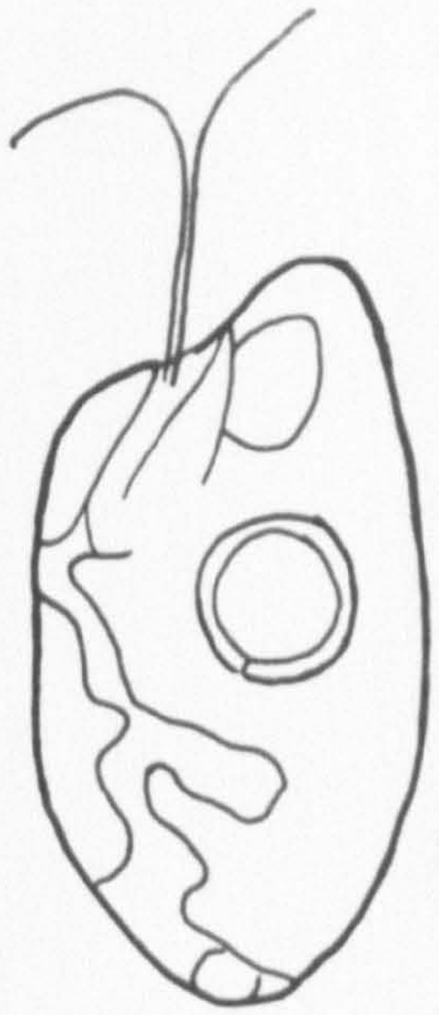

5

3

4

PLATE 11

PLATE 12

Schematic representations of the surface morphology of the periplast of *Rhinomonas reticulata* et var..

Fig. 1. Periplast with hexagonal periplast areas (PA), delineated by a hexagonal lattice (DL). Fig. 2. Periplast with roughly circular periplast areas (PA). White lines have been superimposed on the lattice delineating the PA's, to show that the overall hexagonal appearance is conserved in spite of the fact that the PA's are no longer hexagonal.

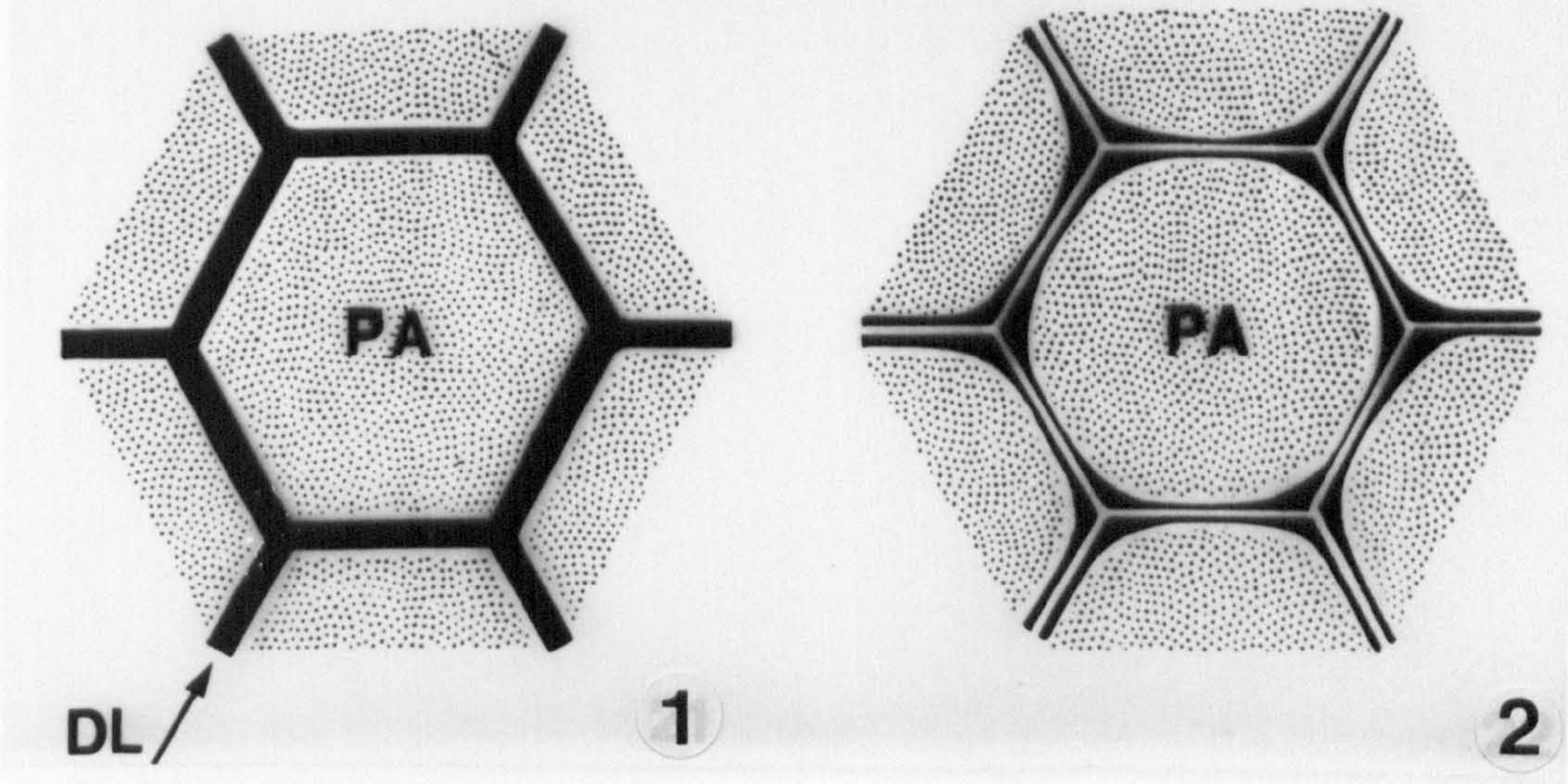

PLATE 12

PLATE 13

Proteomonas pseudobaltica comb. nov., strain CCAP 979/9, SEM (glutaraldehyde / osmium / critical point-drying unless otherwise stated), and LM (glutaraldehyde).

Fig. 1. Ventral view. **Fig. 2.** Ventro-lateral view. **Fig. 3.** Detail of the cell surface; the pores reflect the arrangement of the peripheral ejectosomes, whose discharge was caused by the use of glutaraldehyde as the sole fixative. **Fig. 4.** Lateral view; note the prominent central pyrenoid. Scale bars = 2.5 µm (Figs 1, 2), 1 µm (Fig. 3), or 10 µm (Fig. 4).

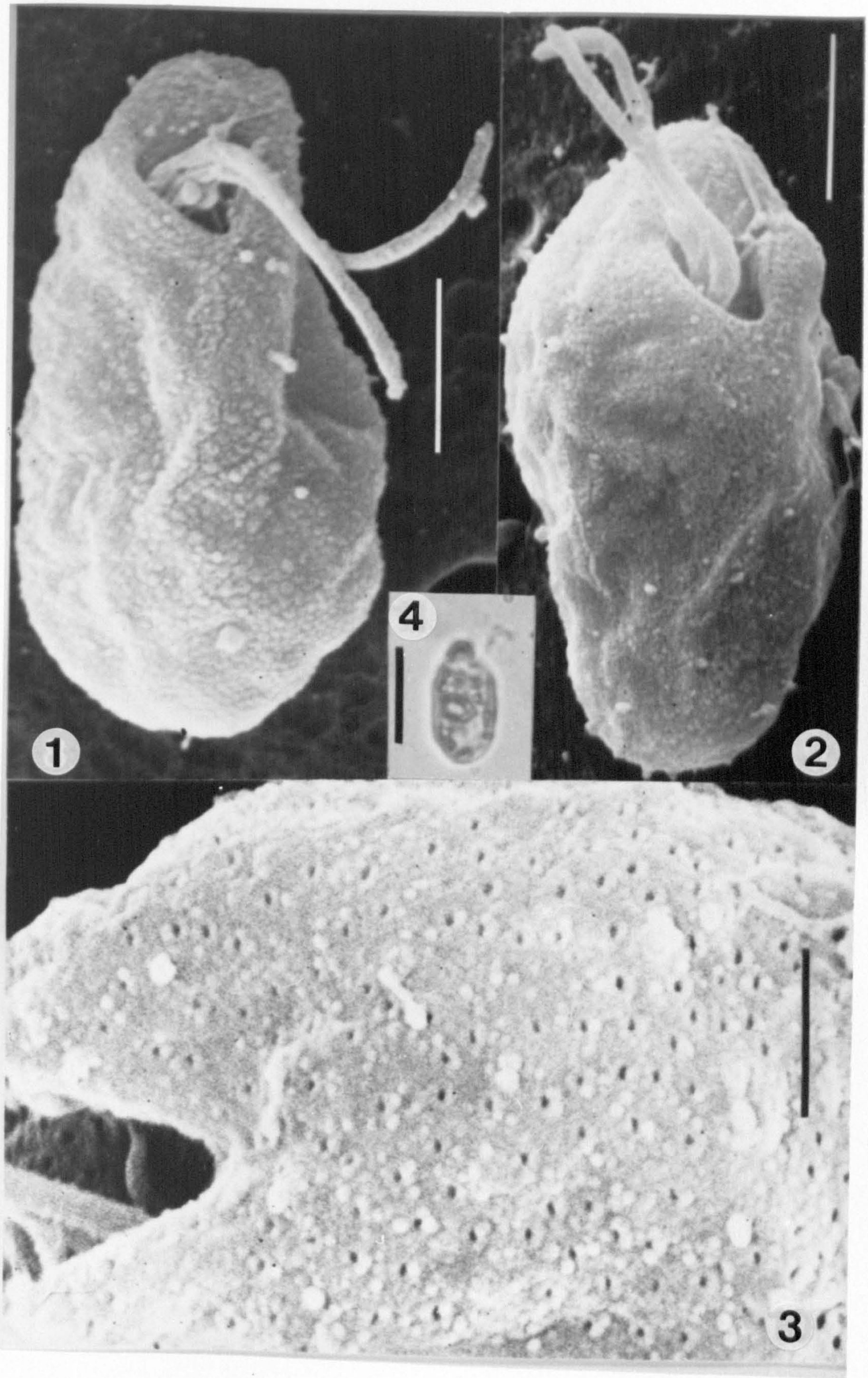

PLATE 11

PLATE 14

Proteomonas pseudobaltica comb. nov., strain GN A, SEM (glutaraldehyde /osmium /critical point-drying), and LM (Lugol's iodine).

Fig. 1. Dorso-lateral view. Fig. 2. Lateral view. Fig. 3. Ventro-lateral view. Fig. 4. Ventral view. Fig. 5. Lateral view; central pyrenoid and flagella clearly visible. Scale bars = 5 µm.

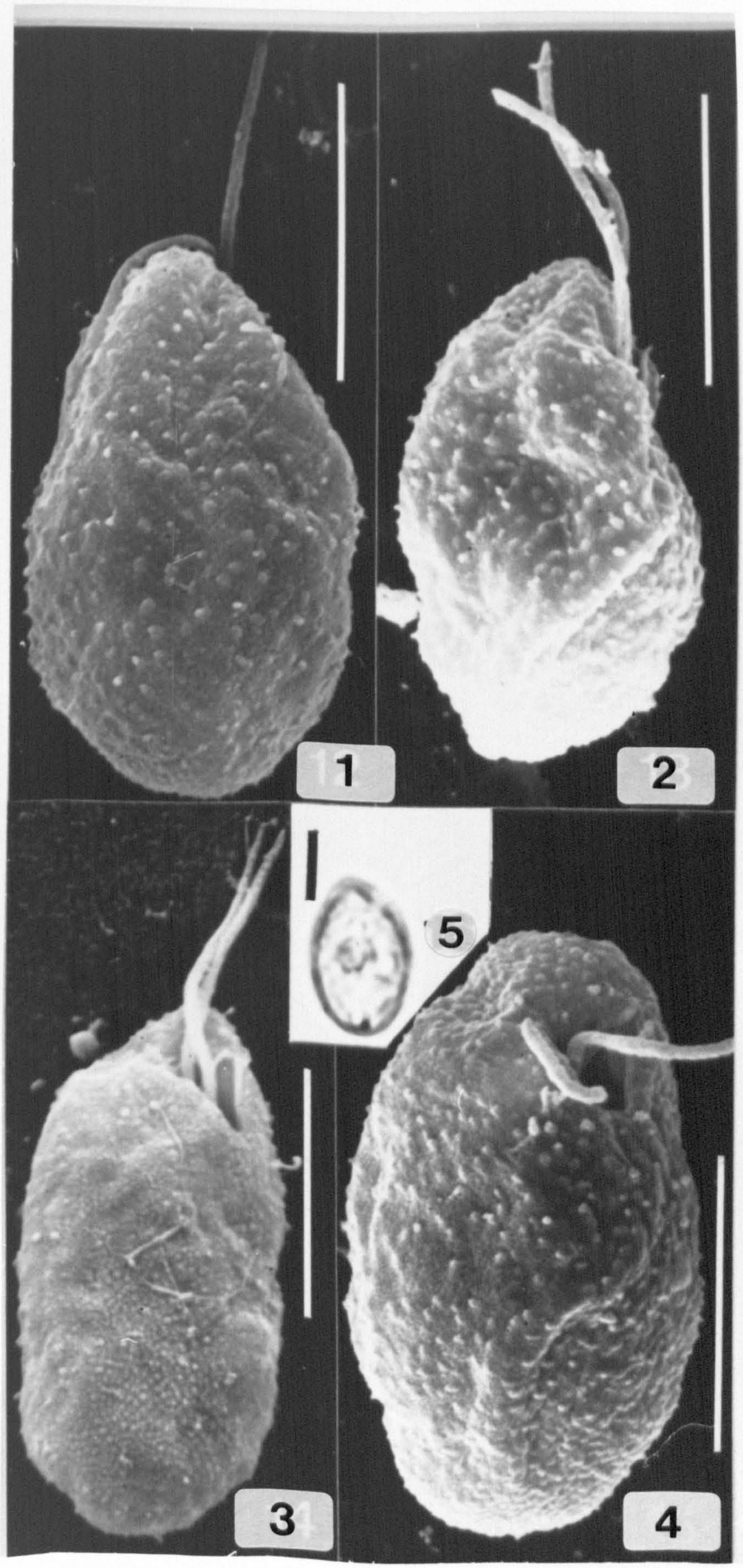

PLATE 14

PLATE 15

The freshwater *Cryptomonas marssonii* Skuja, strain SAG 26.80, SEM, (glutaraldehyde /osmium / critical point-drying), and LM (unbuffered glutaraldehyde)

Fig. 1. Lateral view. Fig. 2. Ventro-lateral view. The long furrow on the ventral cell face (arrows) is interpreted as a non-artefactual structure. Fig. 3. Cell with a narrow fold in the dorso-lateral region (arrows), probably caused by cell shrinkage. Fig. 4. Another cell with an artefactual fold, more pronounced than that in Fig. 19. Scale bars = 10 µm (Fig. 1) or 5 µm (Figs 2-4).

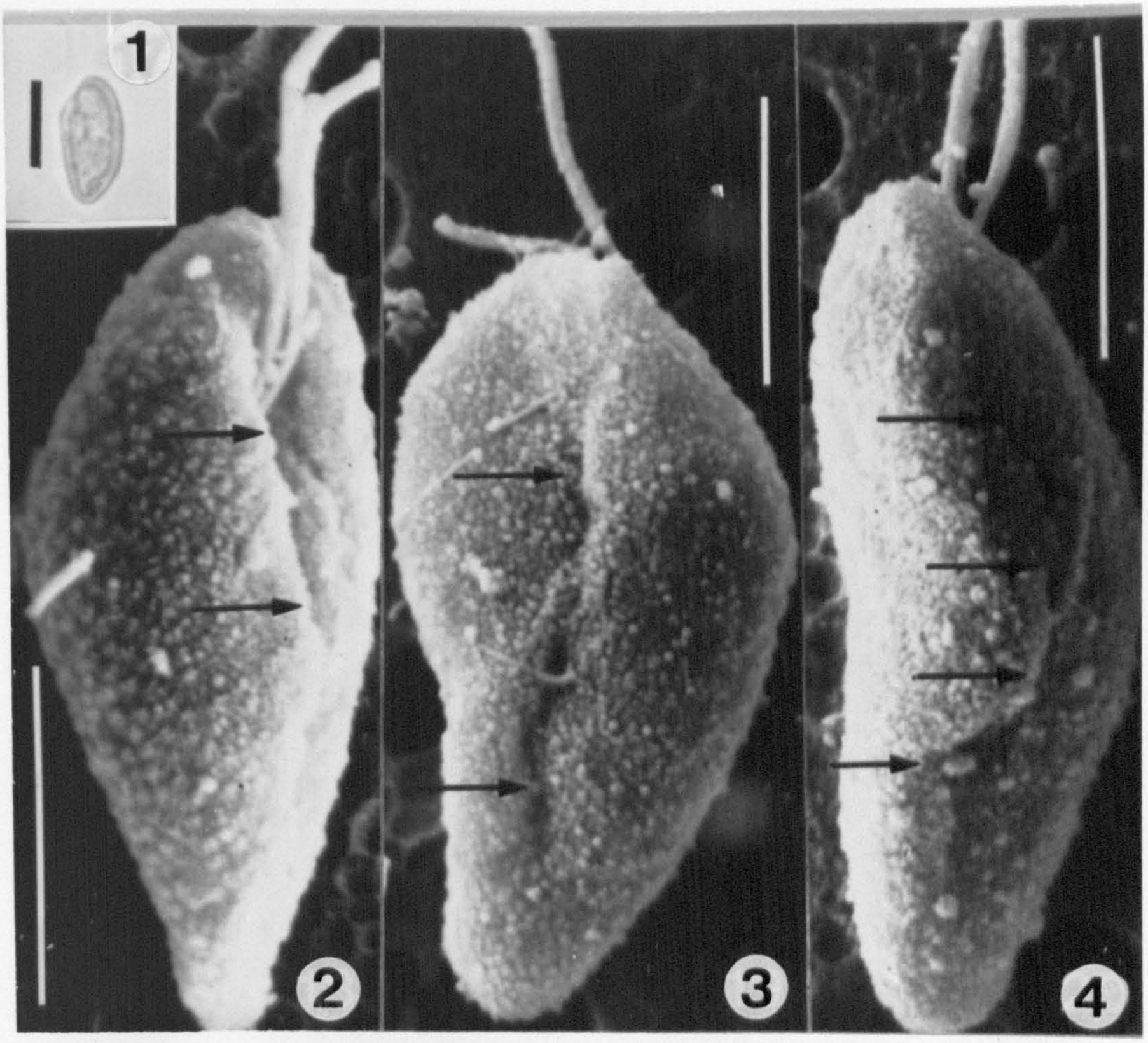

PLATE 15

PLATE 16

TEM views of *Proteomonas pseudobaltica* and *Cryptomonas marssonii*, glutaraldehyde /osmium.

Fig. 1. Longitudinal section of *Proteomonas pseudobaltica* strain CCAP 979/9, showing the vestibular opening (v), gullet (g), flagellar bases (fb), starch (s), nucleus (n), and two profiles of single chloroplast (chlp) with pyrenoid (py); scale bar = 2 µm. Fig. 2. Detail of the region of the cell surface between the arrows in Fig. 1. Note the single, sheet-like periplast layer (arrow) on the internal face of the plasma membrane (arrowhead); a discharged ejectosome vesicle (e) is also visible. Scale bar = 1 µm. Fig. 3. Detail of the cell surface of *Cryptomonas marssonii* SAG 26.80; a thin, sheet-like periplast layer (arrows) is present underneath the plasma membrane (arrowheads). Scale bar = 0.1 µm. Fig. 4. Longitudinal section of *Proteomonas pseudobaltica* strain GN A, showing the position of the single nucleomorph (nm) in relation to the chloroplast (chlp) and pyrenoid (py), the latter with a prominent starch cap (s); scale bar = 1 µm.

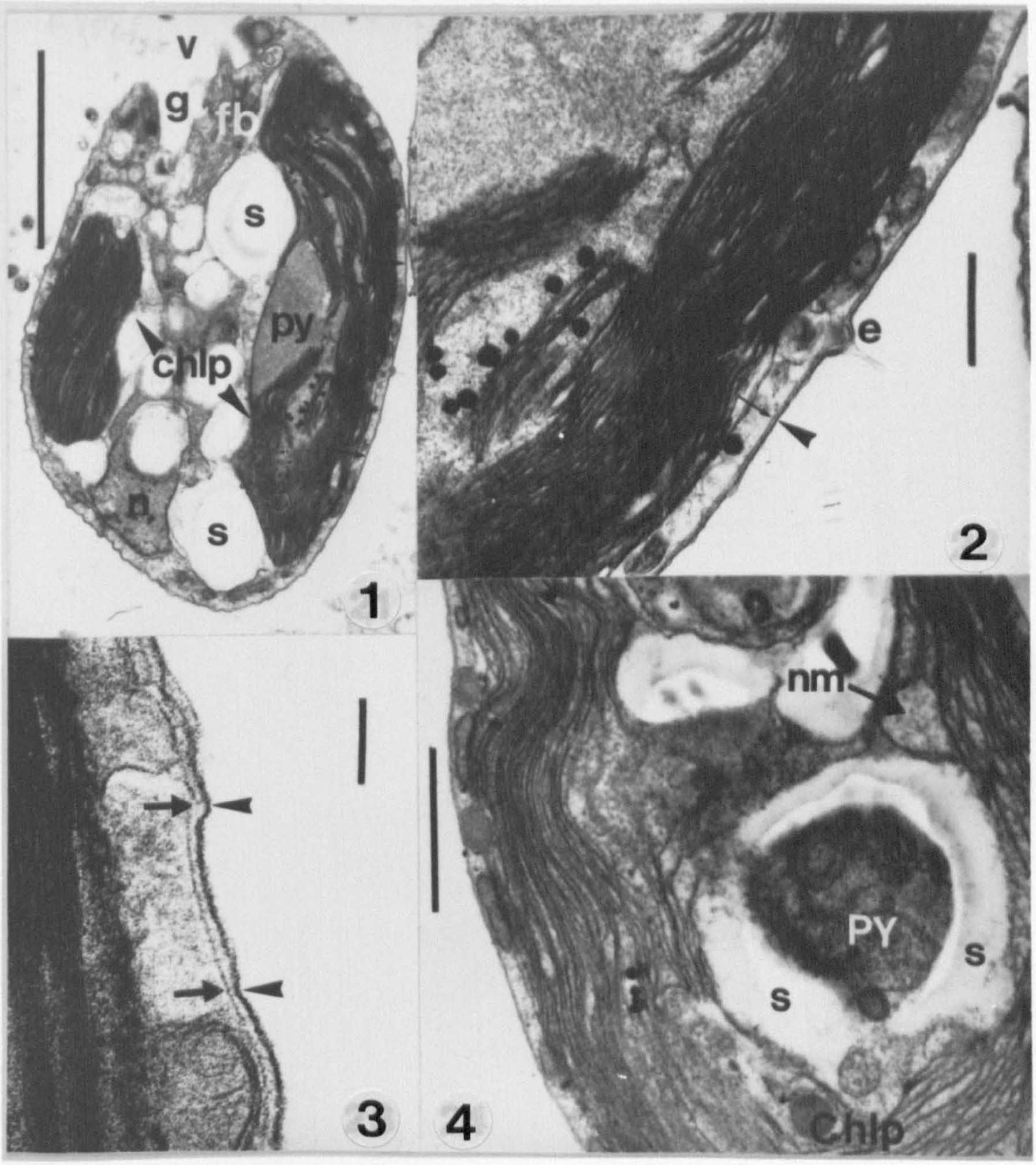

PLATE 16

PLATE 17

Proteomonas pseudobaltica var. *leonardiana* var. nov., SEM (glutaraldehyde / osmium /critical point-drying), and LM (Lugol's iodine).

Fig. 1 (holotype). Lateral view. Fig. 2. Ventral view. Fig. 3. Ventro-lateral view. Fig. 4. Dorsal view. Fig. 5. Lateral view; note prominent pyrenoid with starch cap. Scale bars = 10 µm.

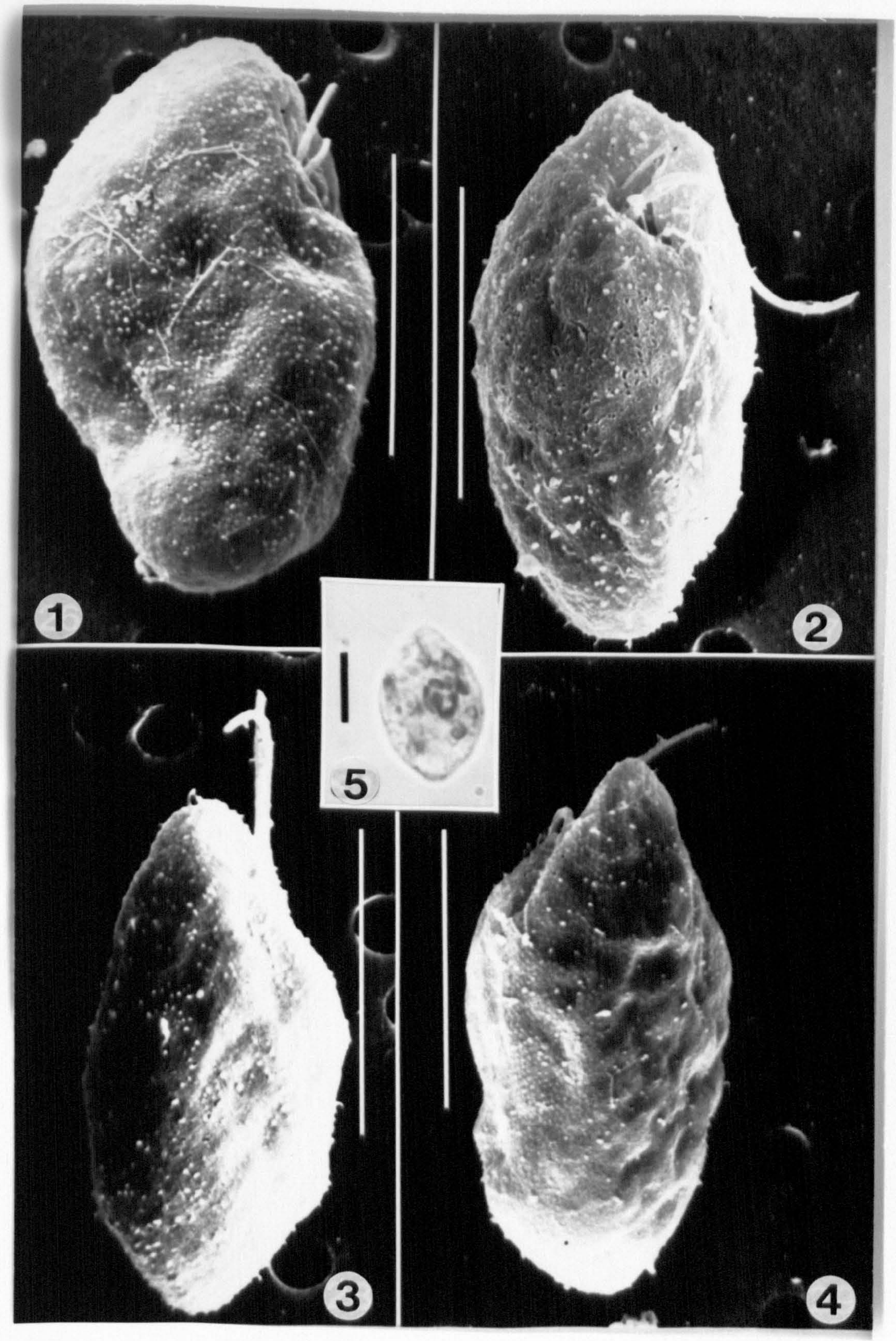

PLATE 17

PLATE 18

SEM views of *Rhinomonas reticulata* var. *elenlana*, strain IANL 97825/C, prepared according to different schedules.

Fig. 1. OGA fixation; signs of collapse at cell posterior, periplast indistinct, several flagellar hairs visible. Fig. 2. OGA fixation; severe signs of cell collapse at cell posterior and sides. Fig. 3. O/s fixation; detail of periplast, showing hexagonal arrangement of ejectosome pores. Fig. 4. O/s fixation; flagellar tips, with well preserved hairs. Scale bars = 5 µm (Figs 1, 2), 0.5 µm (Fig. 3), or 1 µm (Fig. 4).

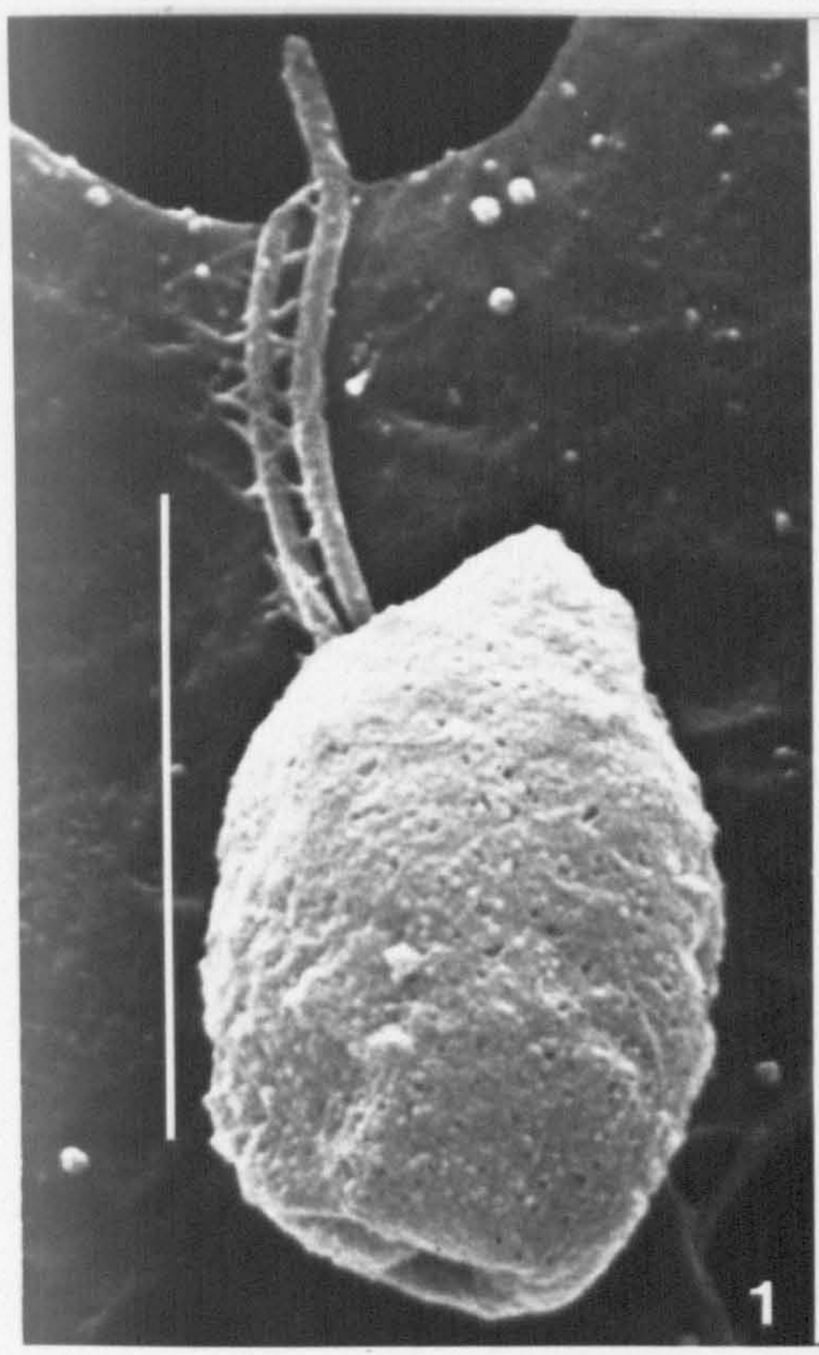

1

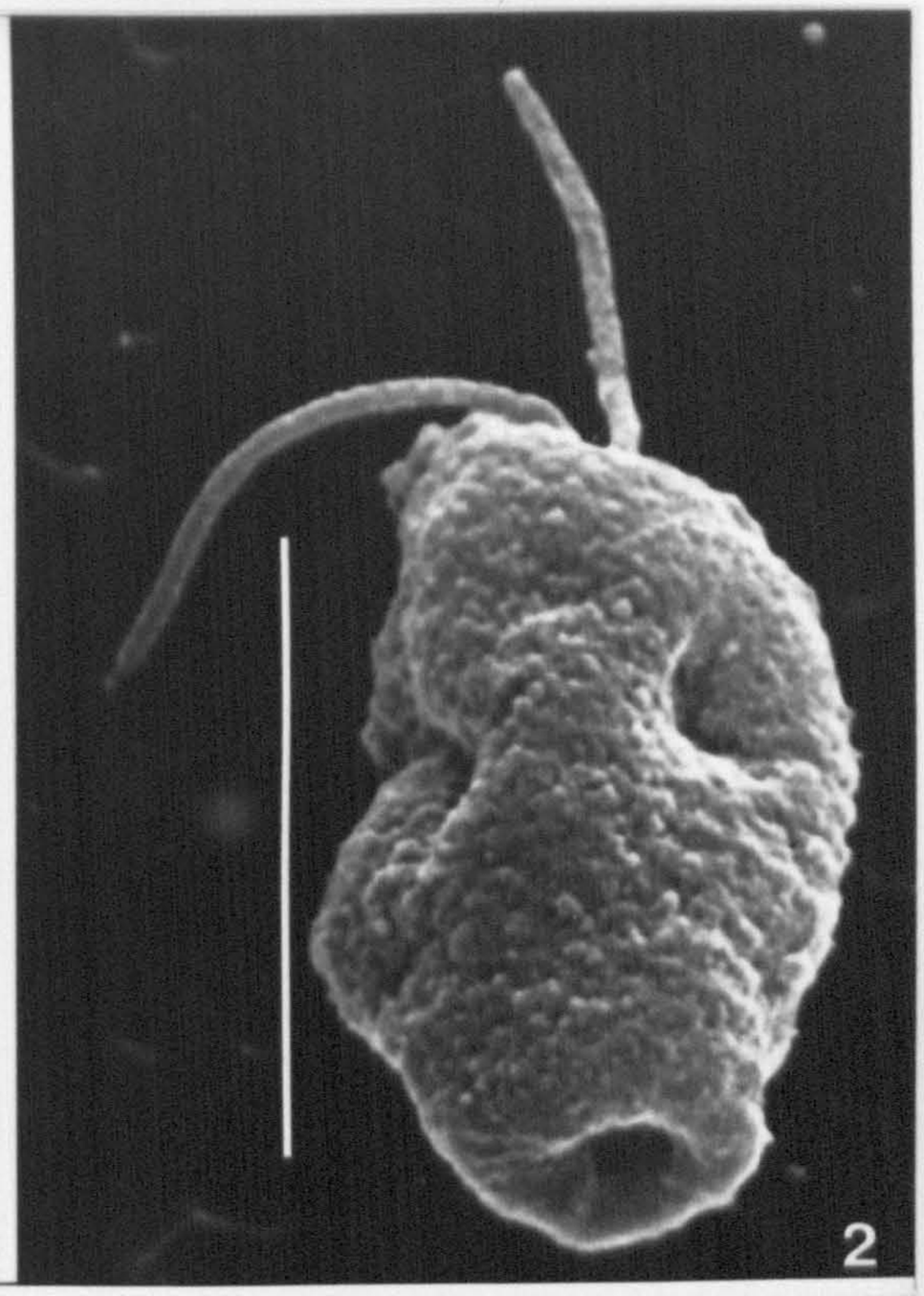

2

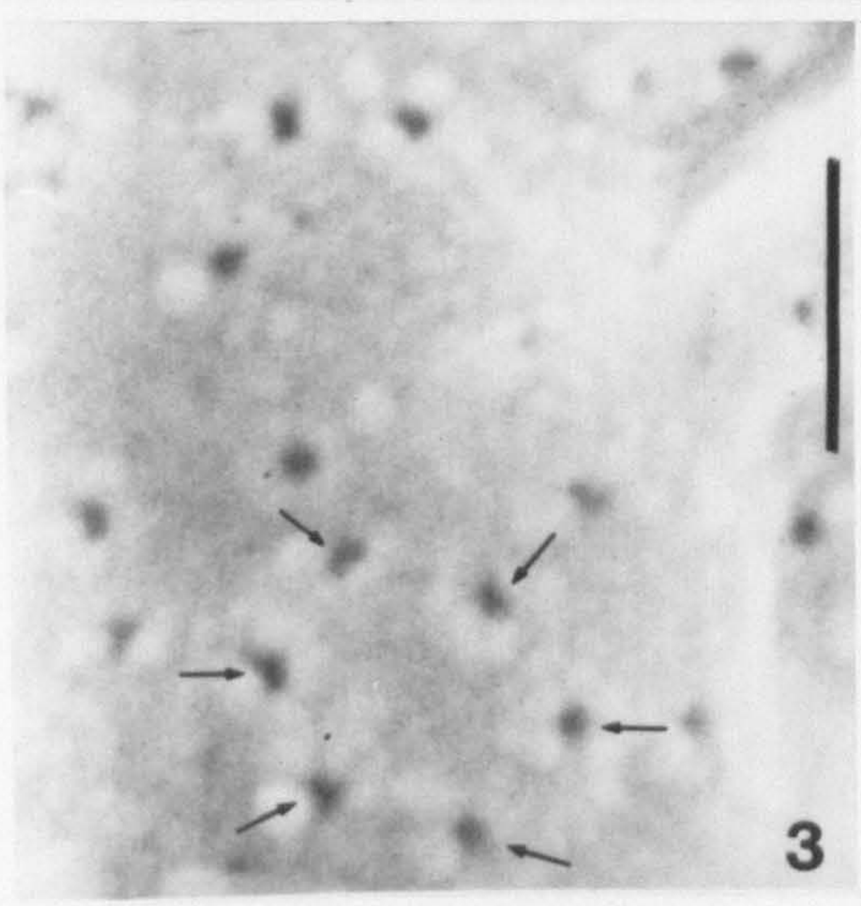

3

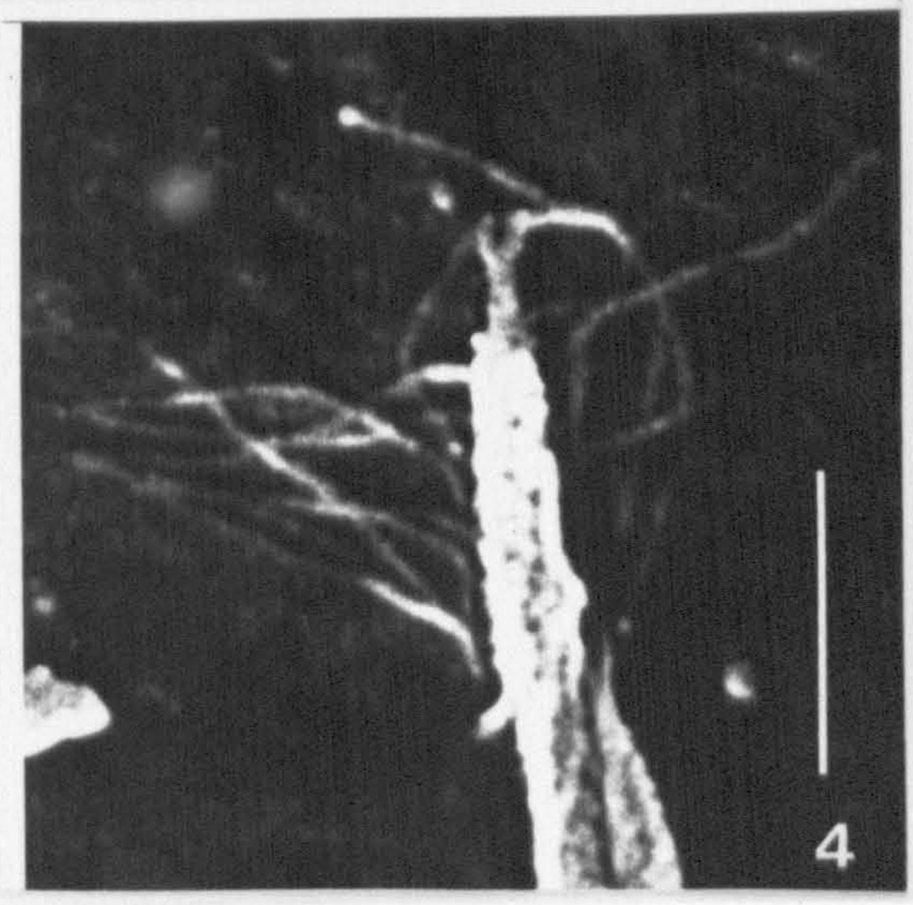

4

PLATE 14

PLATE 19

SEM views of *Rhinomonas reticulata* var. *elenlana*, strain IANL 97825/C, prepared according to the GA schedule.

Fig. 1. Cell with severely collapsed periplast. Fig. 2. Cell with several ejectosome pores; hexagonal periplast areas are faintly visible. Fig. 3. Cell with collapsed, rugulose periplast, and an everted internal organelle, probably the contractile vacuole (arrow). Fig. 4. Cell with numerous ejectosome pores, arranged according to an hexagonal pattern. Fig. 5. Cell with severe signs of collapse and shrinkage in the ventral region, simulating a 'furrow'. Scale bars = 5 µm (Figs 1-3), or 2 µm (Figs 4, 5).

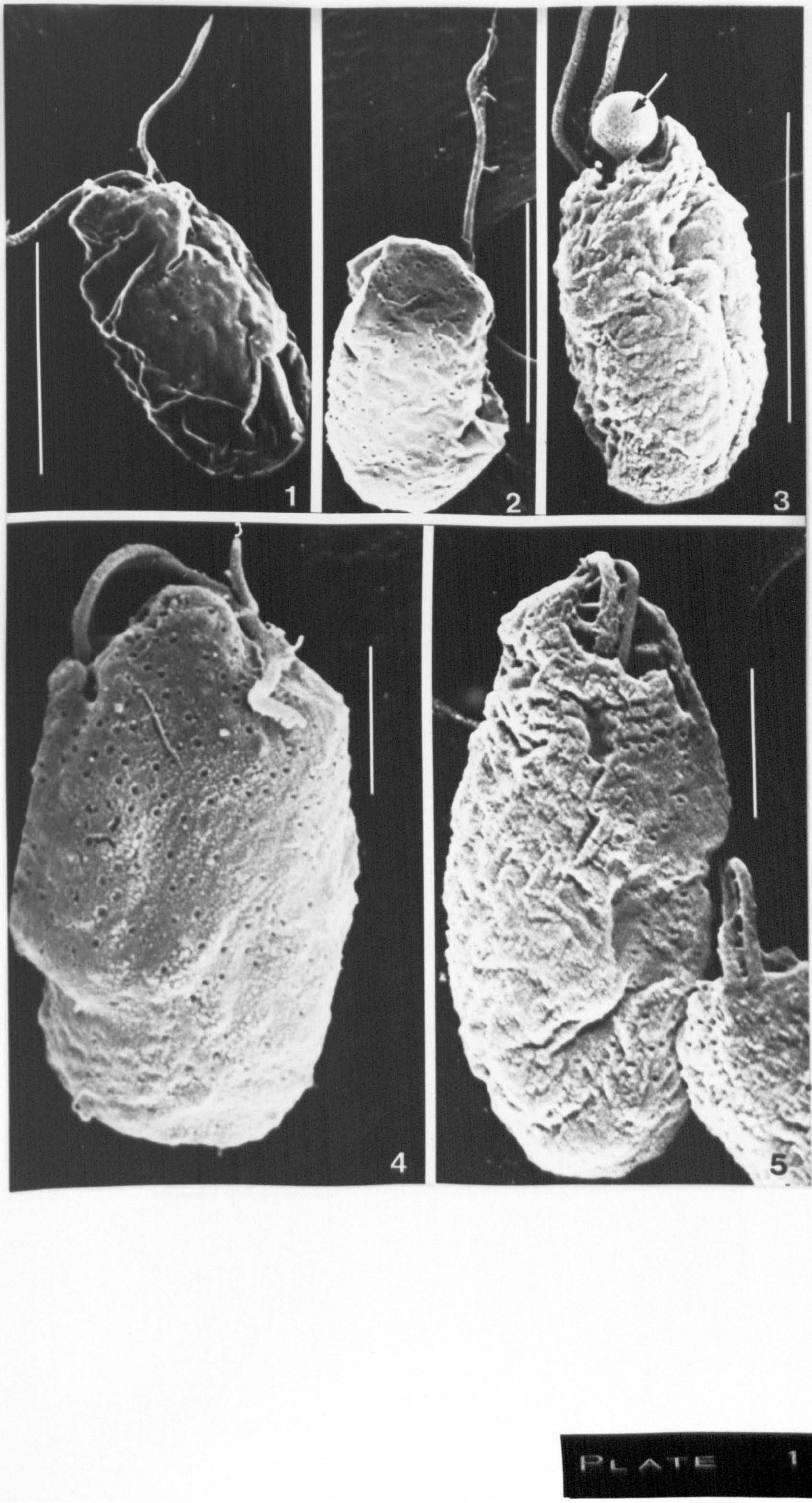

PLATE 19

PLATE 20

Cryptomonas acuta, SEM, Lugol /osmium / critical point-drying.

Fig. 1. Dorsal view; note length of flagella (F), and acute posterior. Fig. 2. Lateral view; furrow just visible (arrowhead). Fig. 3. Ventro-lateral view; wide furrow clearly visible (arrowhead). Fig. 4. Cell with regular, oblique spiral rows of pores, reflecting the arrangement of the underlying (discharged) peripheral ejectosomes. Scale bars = 10 µm (Fig. 1) or 5 µm (Figs 2-4).

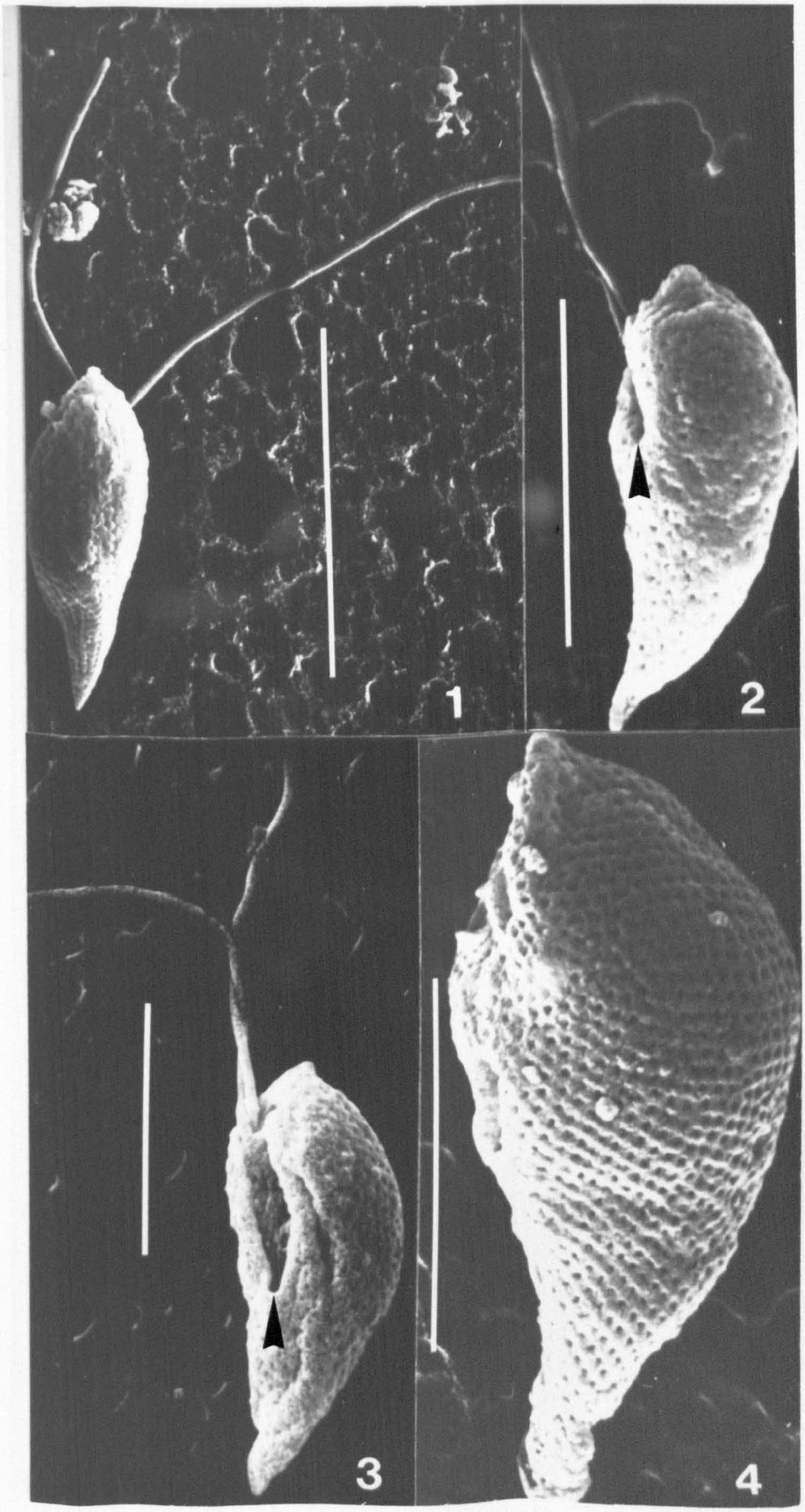

PLATE 20

PLATE 21

Plagioselmis sp., SEM, Lugol / osmium / critical point-drying.

Fig. 1. Dorsal view. Fig. 2. Dorso-lateral view. Fig. 3. Detail of the posterior 'tail'; note the absence of the hexagonal periplast pattern found on the rest of the cell surface. Scale bars = 5 µm (Figs 1, 2) or 1 µm (Fig. 3).

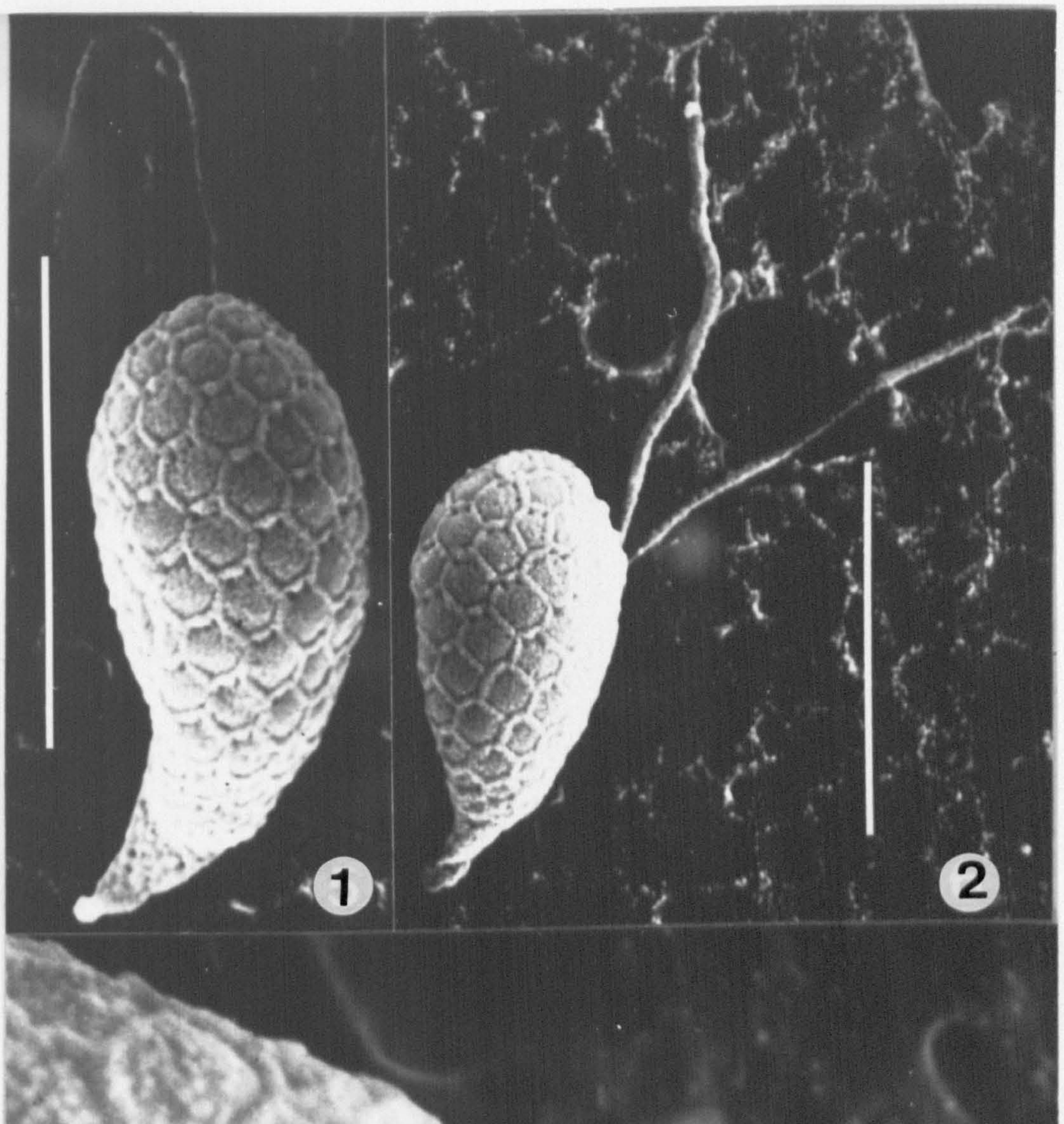

PLATE 21

PLATE 22

Strain CCAP 979/18, SEM, glutaradehyde / osmium / critical point-drying

Fig. 1. Dorso-lateral view. Fig. 2. Dorsal view. Fig. 3. Lateral view. The appearance of the periplast is that of a *Proteomonas*; however, TEM sections suggest that the nucleomorph may be housed within the pyrenoid, as in *Rhinomonas* and *Pyrenomonas*. Scale bars = 5 µm.

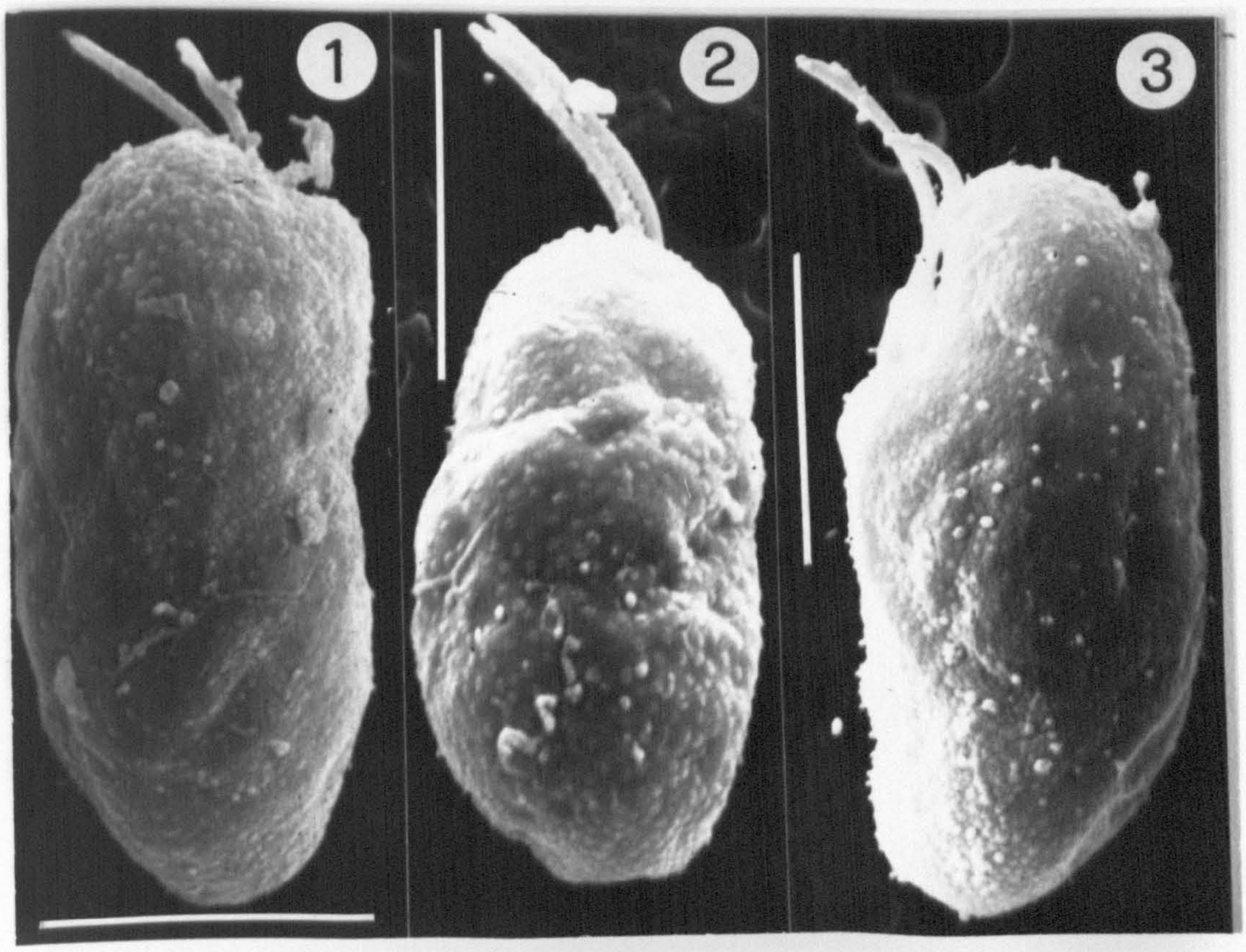

PLATE 22

PLATE 23

The freshwater '*Rhodomonas lacustris*' strain DK N750301, SEM, glutaraldehyde / osmium / critical point-drying.

Fig. 1. Ventral view. Fig. 2. Dorso-lateral view. Note the prominent posterior 'tail'. Scale bars = 5 µm.

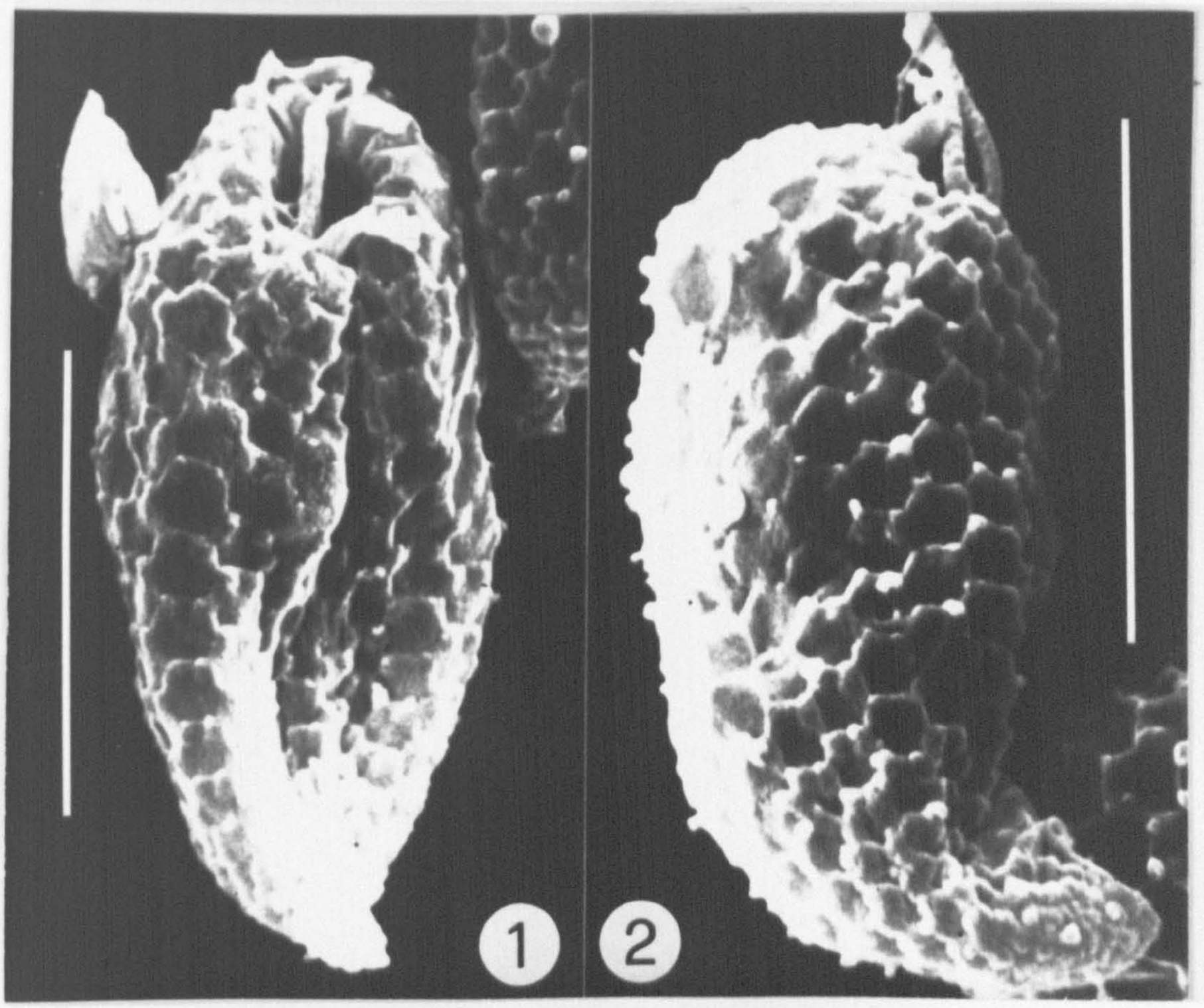

PLATE

PLATE 24

Pyrenomonas salina var. *curvata* var. nov., SEM, glutaraldehyde /osmium / critical point-drying, and phase-contrast LM, glutaraldehyde in seawater.

Fig. 1. Ventral view. Fig. 2 (holotype). Lateral view. Fig. 3. Dorsal view; note elongated, more or less rectangular periplast areas. Fig. 4. Dorso-lateral view. Fig. 5. Ventro-lateral view; the narrow fold (arrows) is probably an artefact caused by cell shrinkage. Scale bars = 5 µm.

1
2
6
3
4
5

PLATE 25

Rhinomonas reticulata var. *reticulata* , strain IANL M, SEM glutaraldehyde / osmium / critical point-drying.

Fig. 1. Dorso-lateral view. Fig. 2. Lateral view. Fig. 3. Ventral view. Fig. 4. Periplast at higher magnification. Scale bars = 5 µm (Figs 1-3), or 1 µm (Fig. 4).

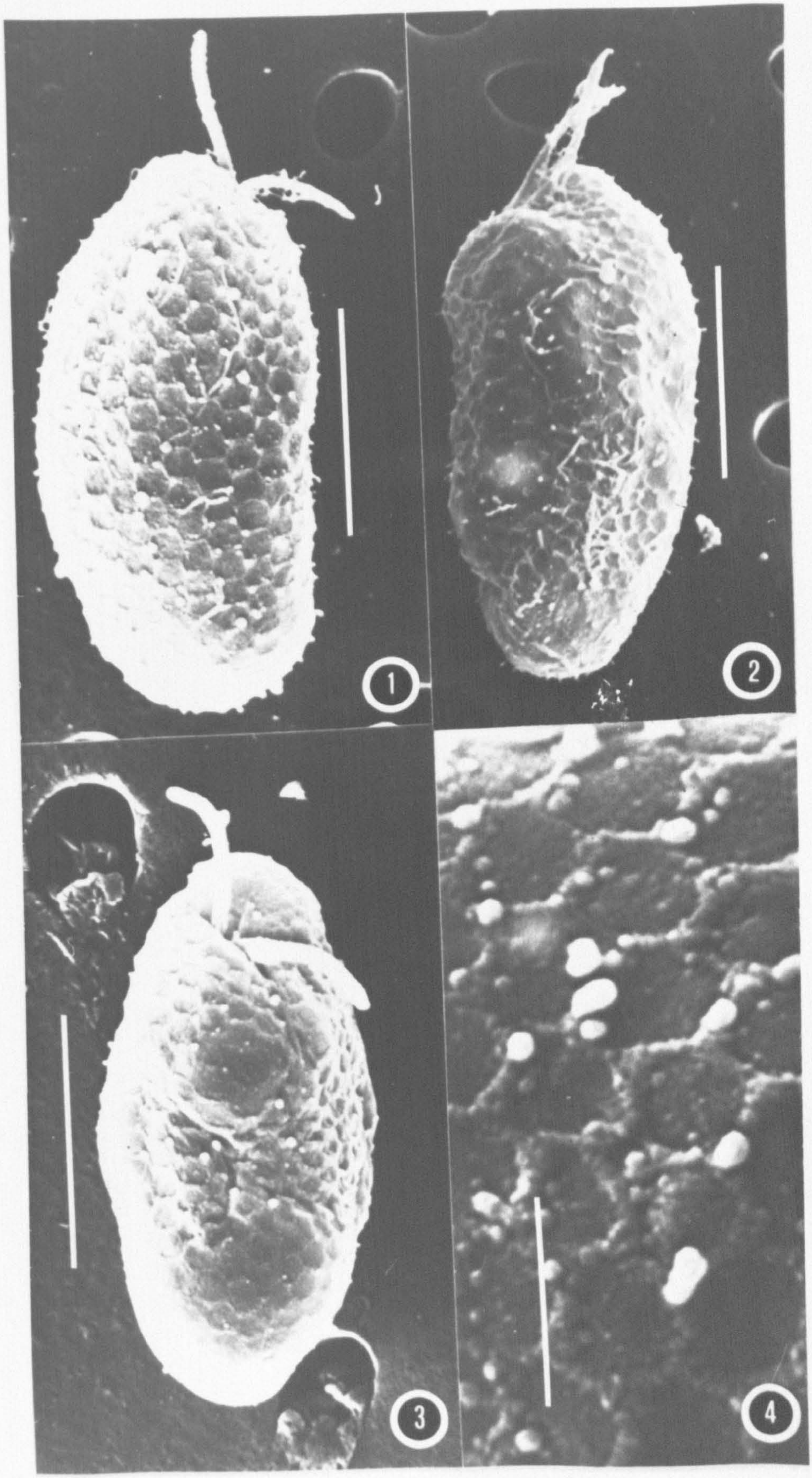

PLATE 25

PLATE 26

Pyrenomonas sp. strain PLY 175, SEM, glutaraldehyde / osmium / critical point-drying.

Fig. 1. Ventral view; note web of discharged ejectosomes covering the cell. Fig. 2. Periplast at higher magnification. Scale bars = 5 µm (Fig. 1), or 1 µm (Fig. 2).

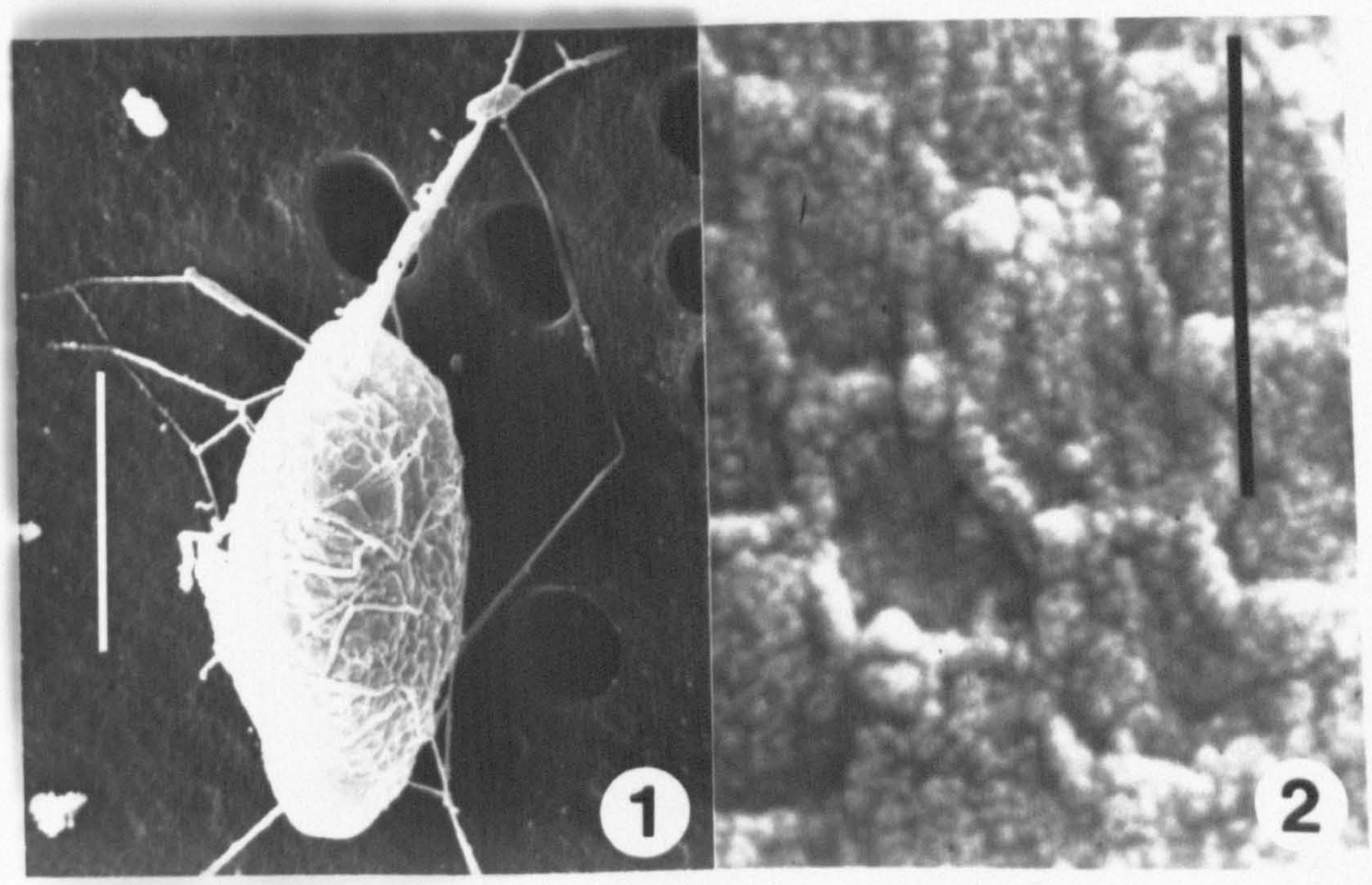

PLATE 24

PLATE 27

Rhinomonas reticulata var. *reticulata*, strain PLY 355, glutaraldehyde / osmium / critical point-drying.

Fig. 1. Ventral view; note short, notch-like 'furrow' (arrow), interpreted as an artefact arising from cell shrinkage, whose effects are also visible in other regions of the cell (arrowheads). Fig. 2. Ventro-lateral view; no obvious signs of cell shrinkage, notch-like 'furrow' absent. Fig. 3. Dorsal view. Fig. 4. Periplast at higher magnification; note partly discharged ejectosome vesicles (arrows). Scale bars = 5 µm (Figs 1-3), or 1 µm (Fig. 4).

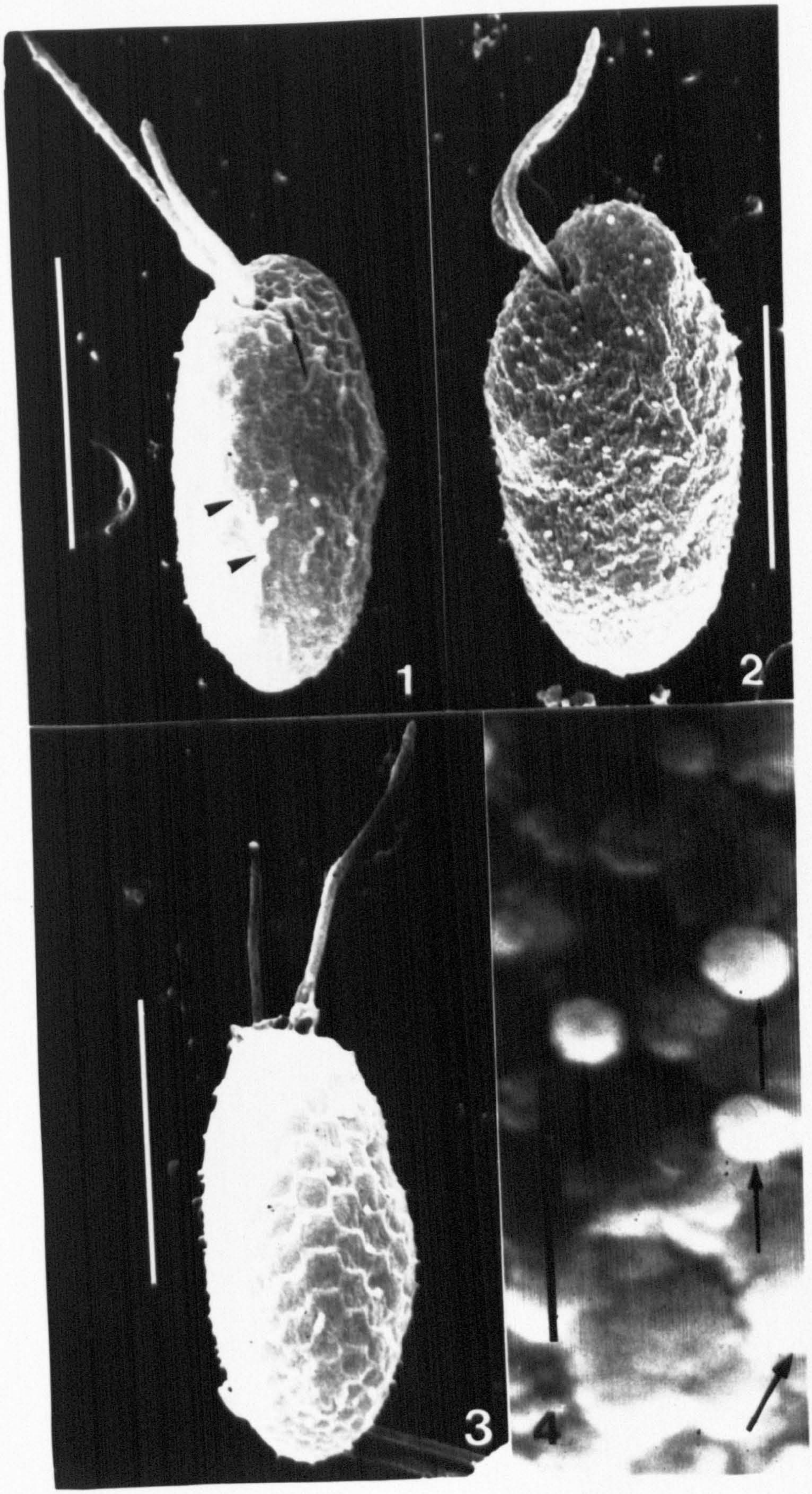

PLATE 27

PLATE 28

Rhinomonas reticulata var. *reticulata*, strain PLY 375, glutaraldehyde / osmium / critical point-drying.

Fig. 1. Lateral view. Fig. 2. Ventral view. Fig. 3. Dorsal view. Fig. 4. Detail of the periplast at higher magnification. Scale bars = 5 µm (Figs 1-3), or 1 µm (Fig. 4).

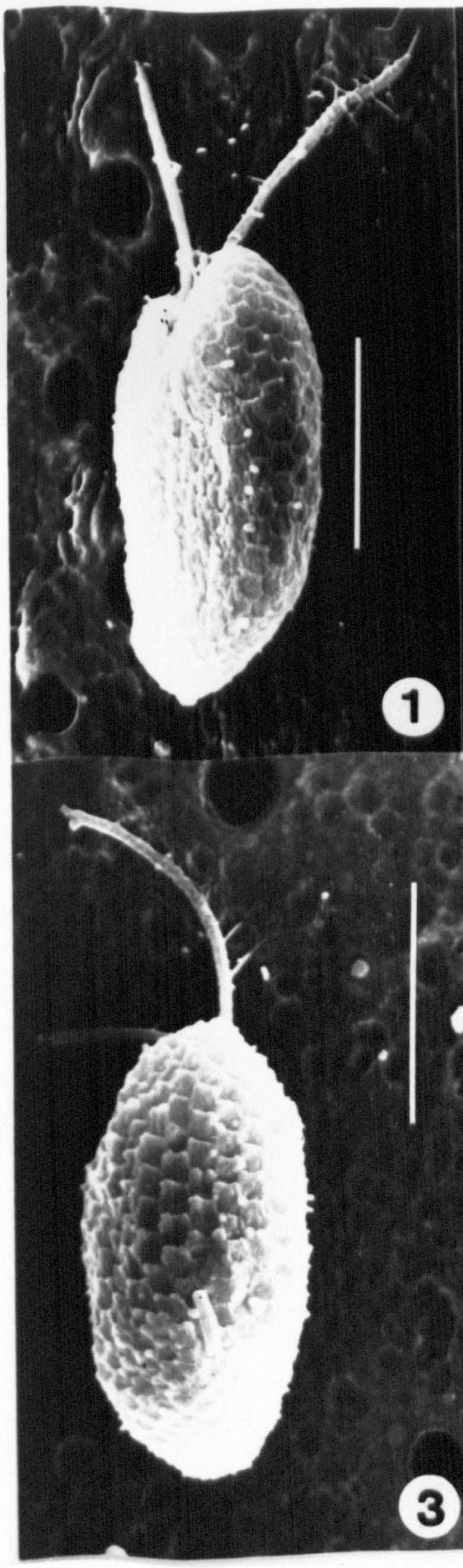
1

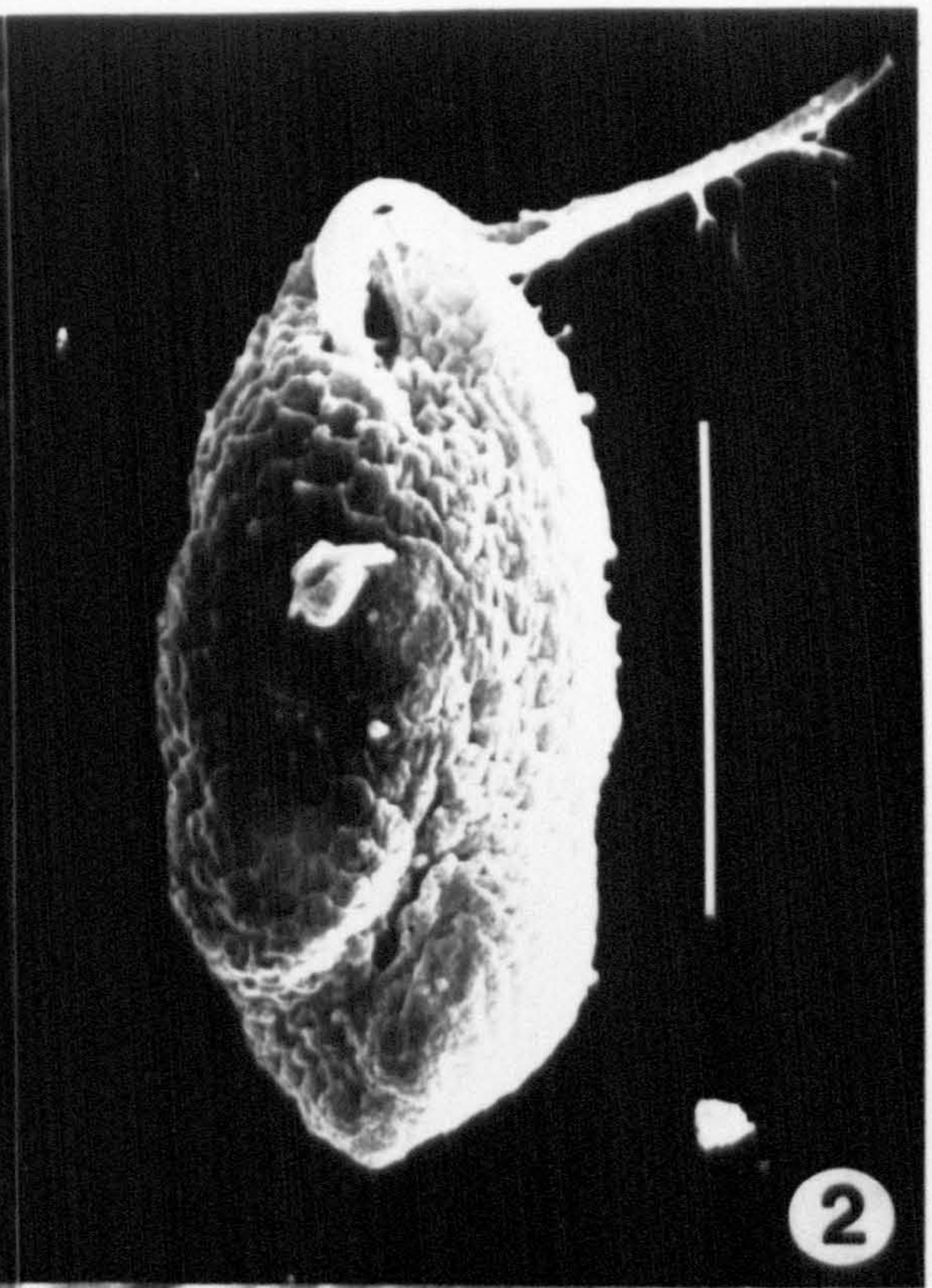
2

3

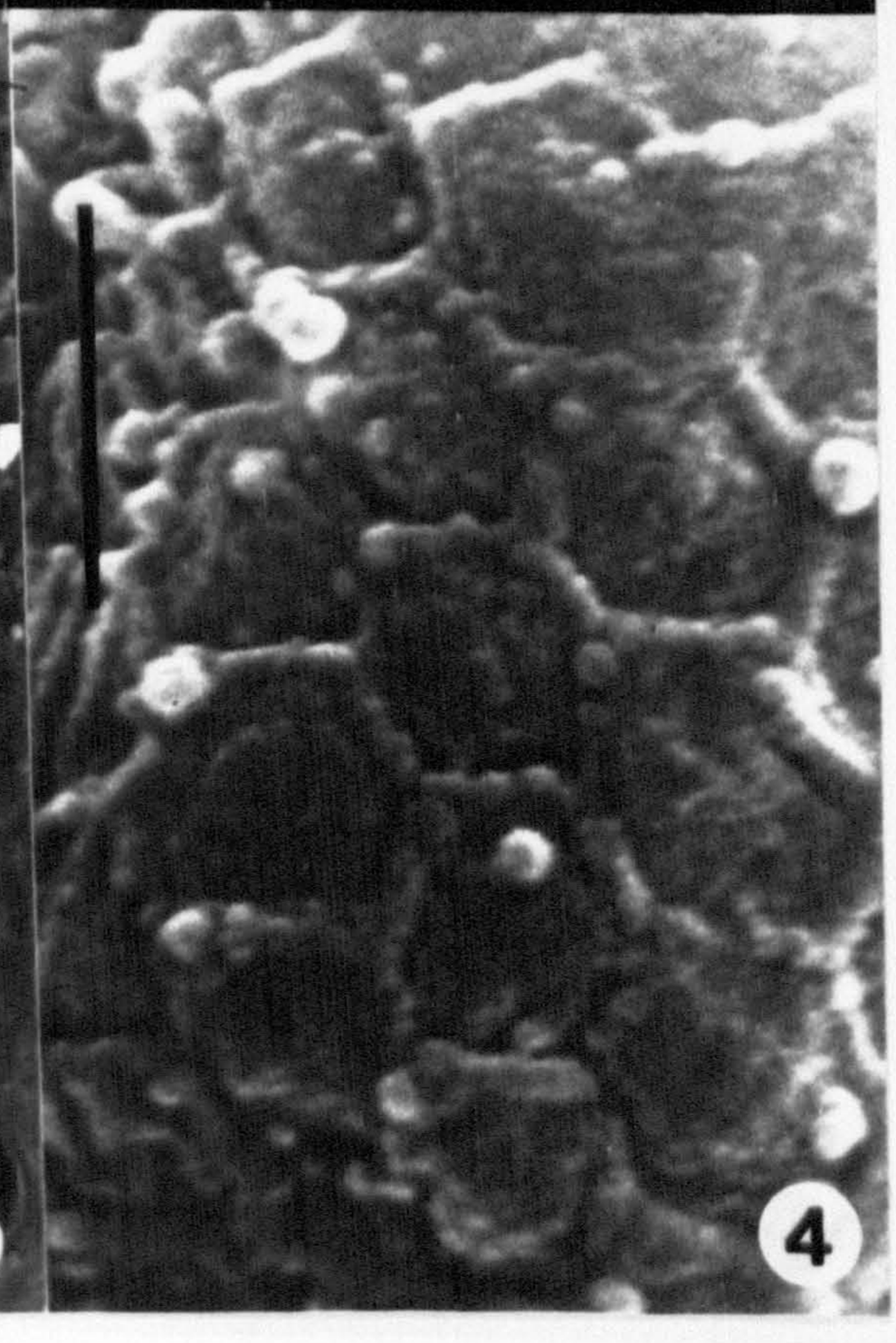
4

PLATE 28

PLATE 29

Rhinomonas reticulata var. *reticulata*, strains PLY 403 and 409, SEM, glutaraldehyde / osmium / critical point-drying.

Figs 1–4. Strain PLY 409; dorsal (Figs 1, 3) and ventro-lateral views (Fig. 2). Note artifactual S-shaped, furrow-like fold in Fig. 2 (arrowheads), associated with shrinkage in the median region of the cell (arrows); Fig. 3 shows an artifactual fold in the dorsal face. Fig. 4 shows the periplast at higher magnification. Figs 5–6. Strain PLY 403; dorso-lateral view (Fig. 5), and periplast at higher magnification (Fig. 6). Scale bars = 1 µm (Figs 1–3, 5), or 1 µm (Figs 4, 6).

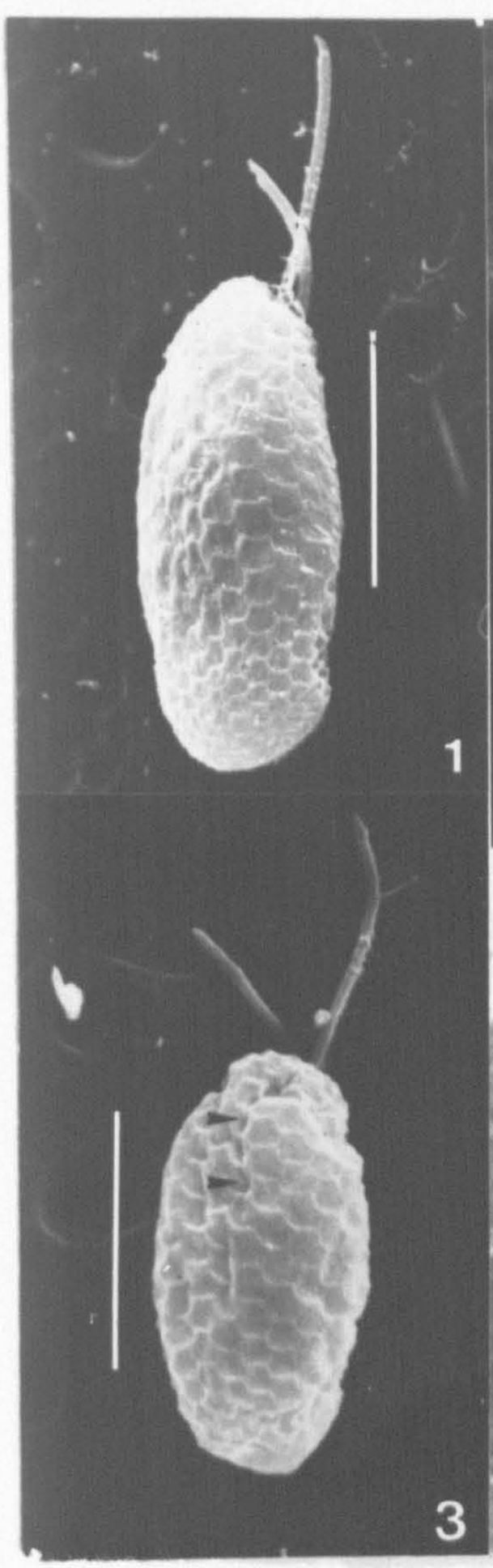

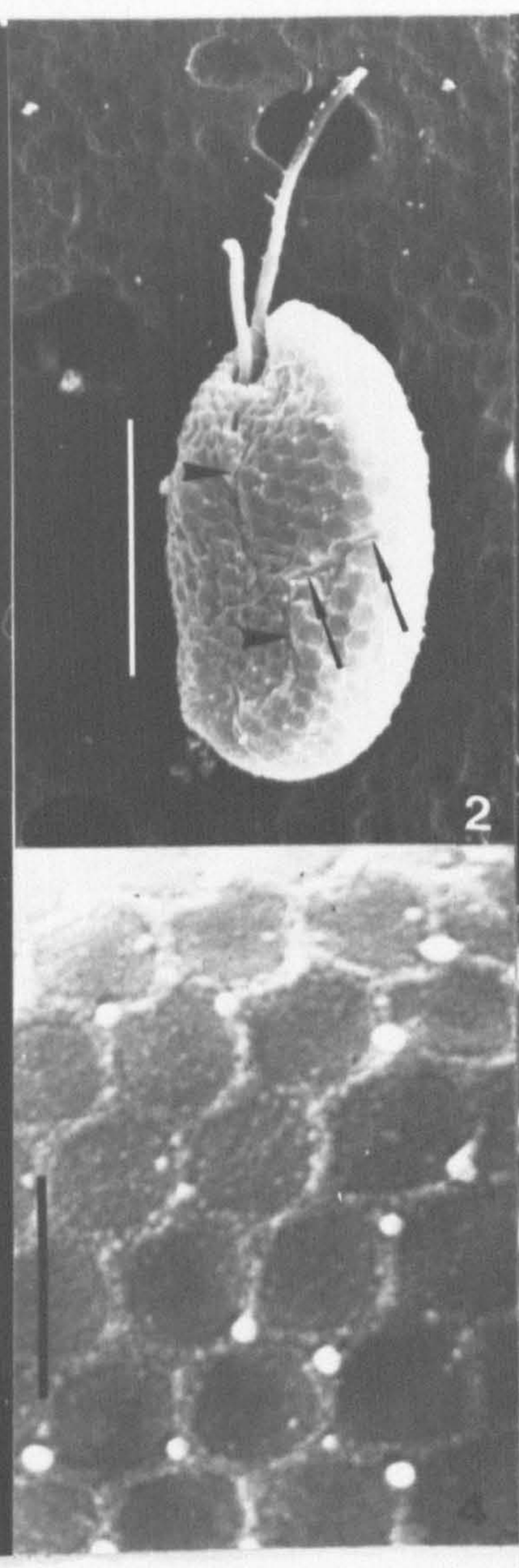

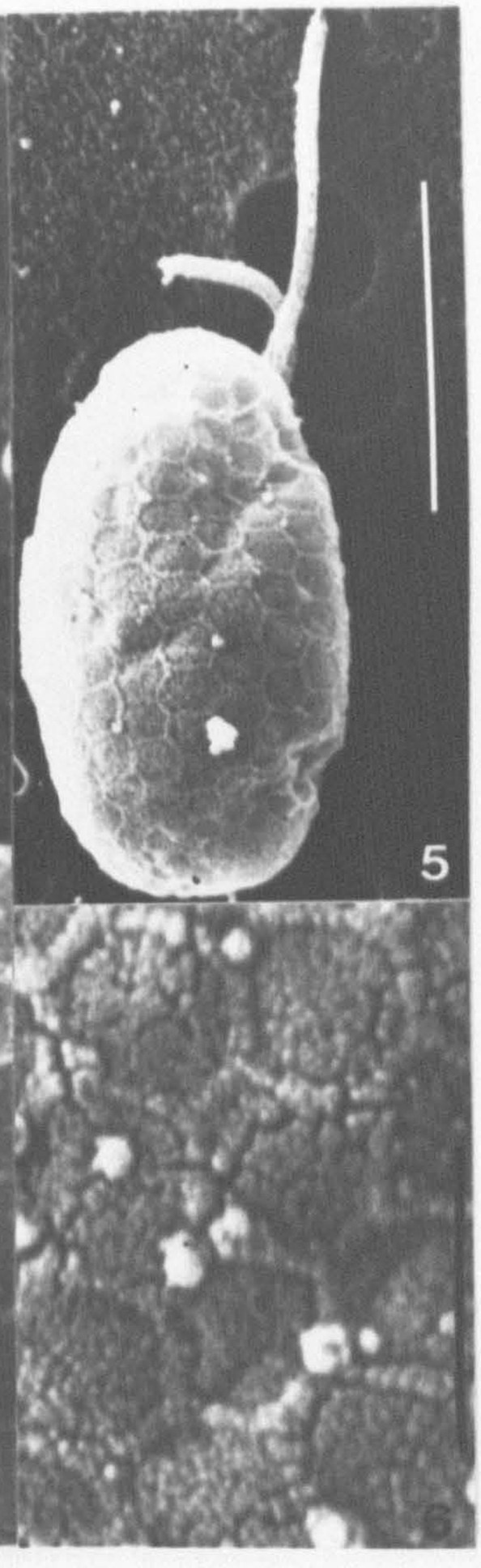

PLATE 29

PLATE 30

Strain UTEX LB 2422, SEM, glutaraldehyde / osmium / critical point-drying.

Fig. 1. Ventral view. Fig. 2. Dorsal view. Scale bars = 5 μm.

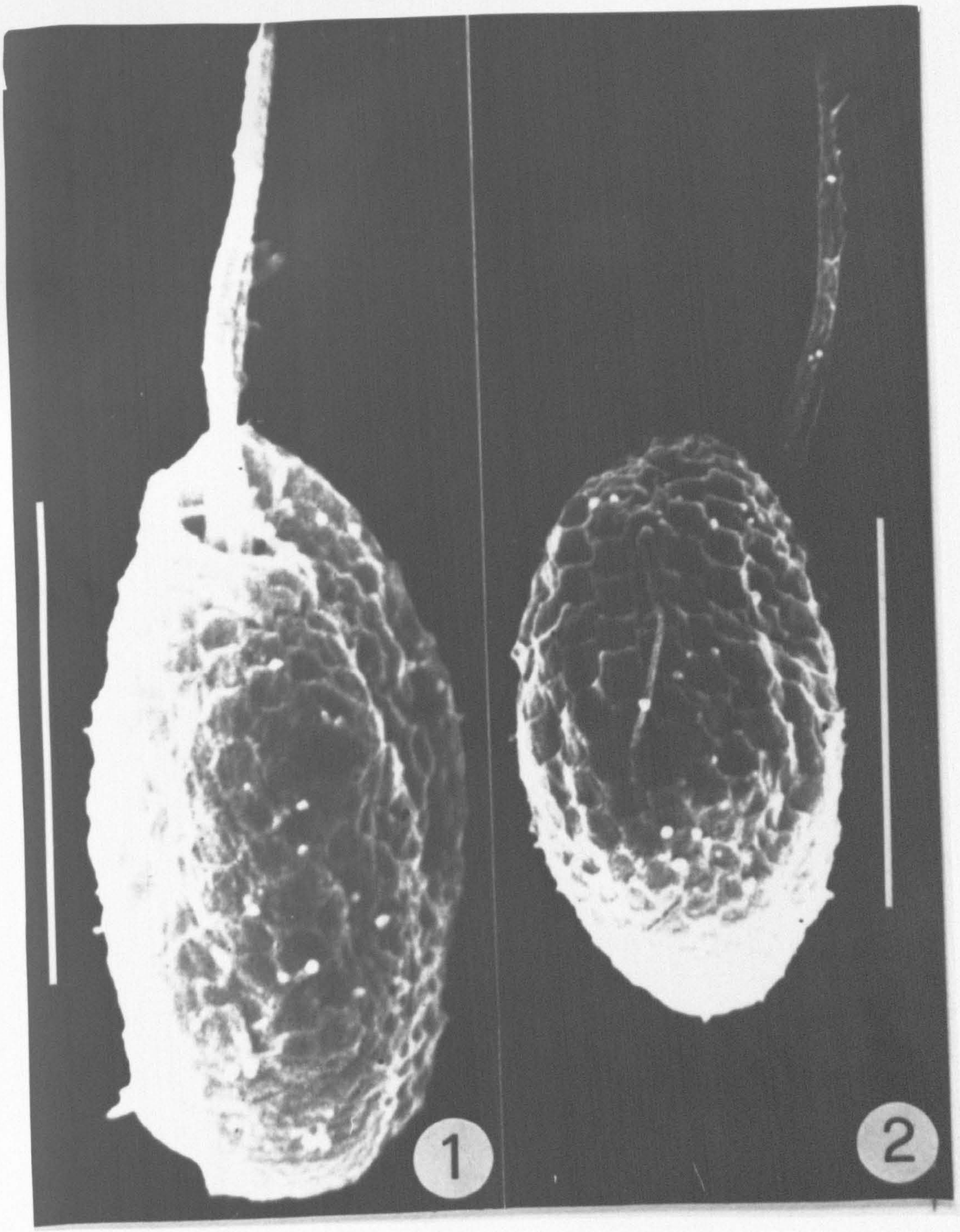

PLATE 30

PLATE 31 A

Some furrow-like artifacts, SEM, glutaraldehyde / osmium / critical point-drying.

Fig. 1. *Rhinomonas reticulata* var. *reticulata* strain PLY 403. The notch on the ventral margin of the vestibular opening (arrowhead) is probably a consequence of cell shrinkage. The effects of the latter are also visible in other cell regions, in the form of narrow folds (arrows); compare Fig. 2 , which shows another cell from the same SEM stub, having a vestibular opening without a notch, and lacking any sign of cell shrinkage. Fig. 3. The freshwater *Chroomonas* sp., strain SAG 980.1. Note the large, furrow-like fold, whose artefactual nature is demonstrated by the fact that its internal surface is lined with periplast areas. Scale bars = 5 µm.

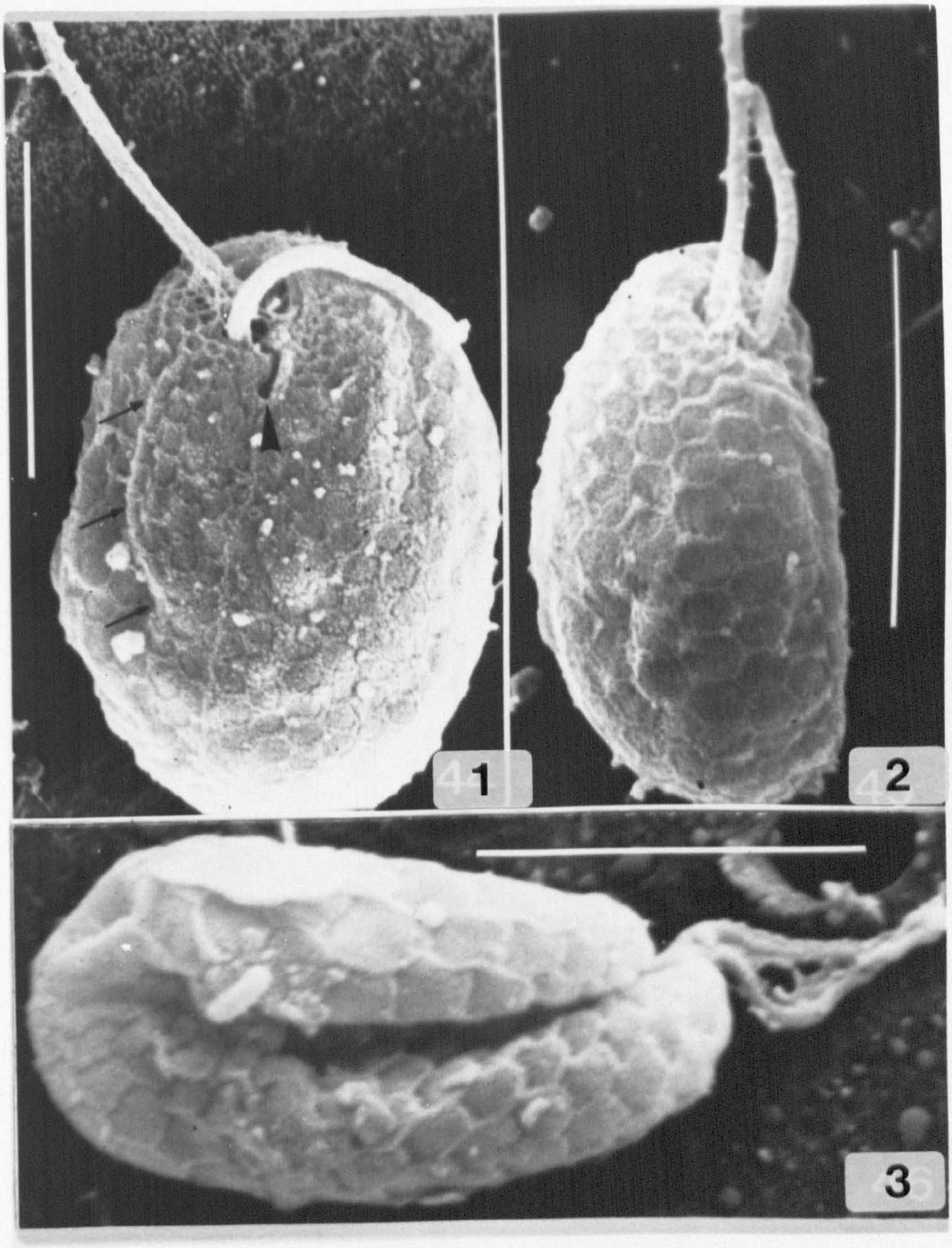

PLATE 31

PLATE 31 B

Visible absorption spectra of crude phycoerythrin (PE) extracts

Fig. 1. Type I PE of *Proteomonas pseudobaltica* CCAP 979/9. Fig. 2. Type III PE of *Cryptomonas marssonii* SAG 26.80. Fig. 3. Type I PE of *'Cryptomonas'* sp. CCAP 979/18. Fig. 4. Type I PE of *Proteomonas pseudobaltica* GN A. Fig. 5. Type I PE of *Rhinomonas reticulata* var. *reticulata* IANL Rhodo.

X-axis = wavelength (nm), Y-axis = absorbance (relative). Absorption peaks are indicated in bold type on the curves.

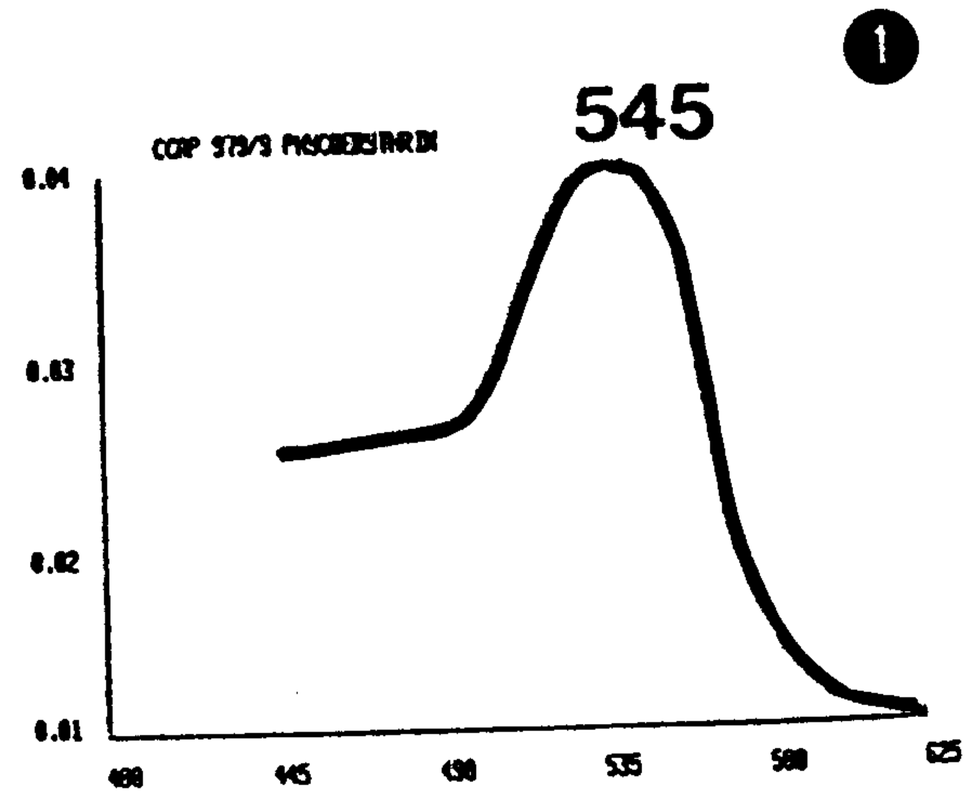
1
545
0.04
0.03
0.02
0.01
400
445
490
535
580
625

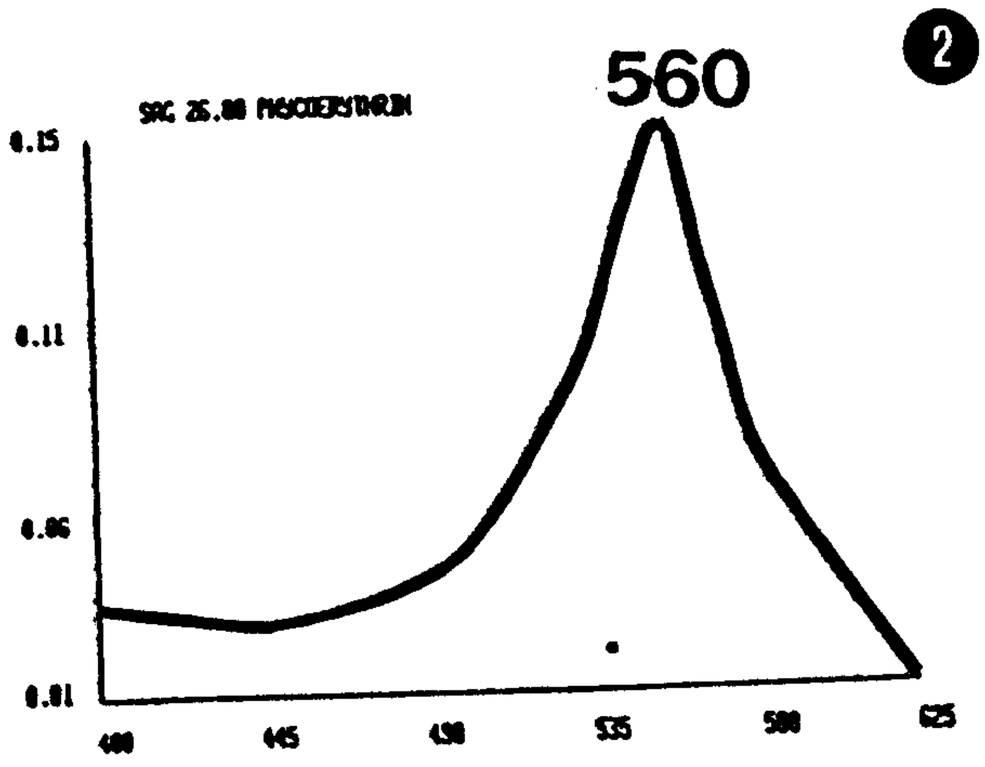
2
560
0.15
0.11
0.06
0.01
400
445
490
535
580
625

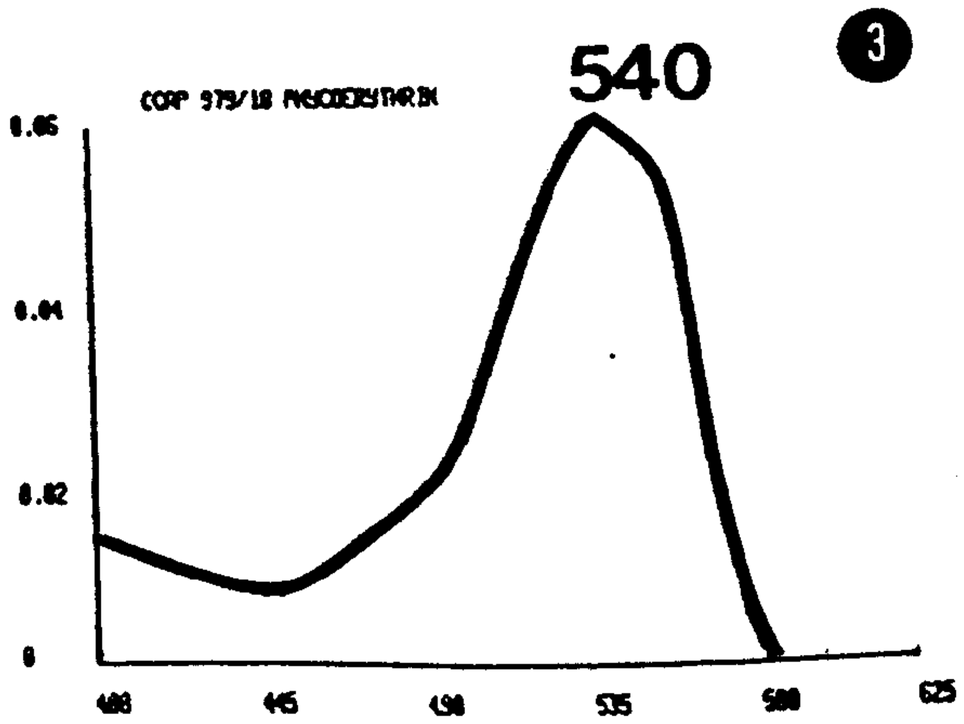
3
540
0.06
0.04
0.02
0
400
445
490
535
580
625

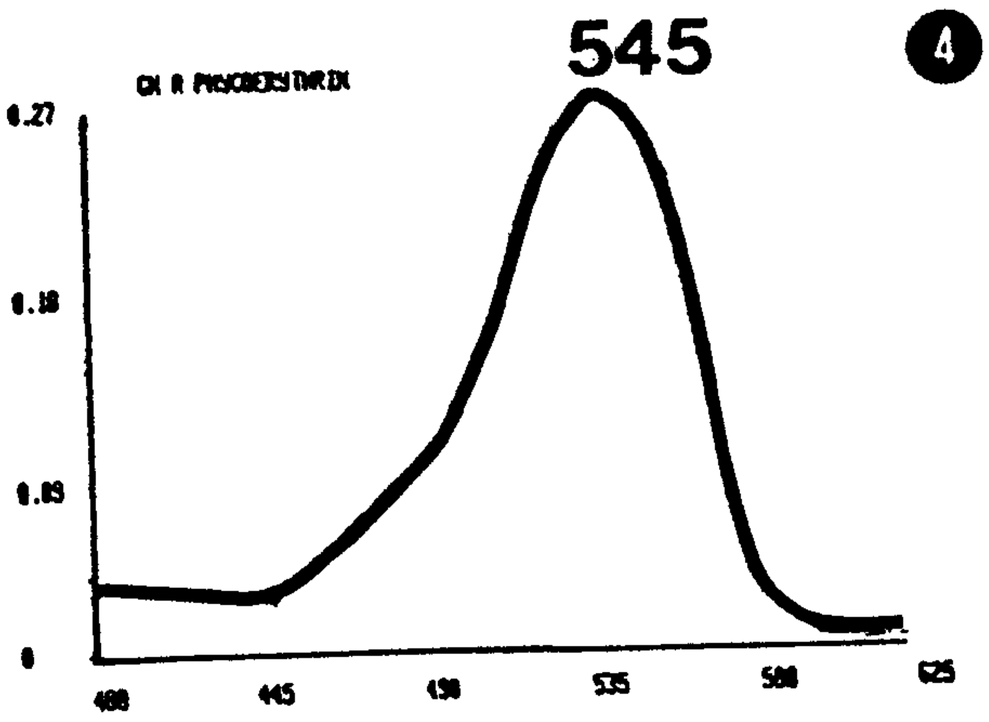
4
545
0.27
0.18
0.09
0
400
445
490
535
580
625

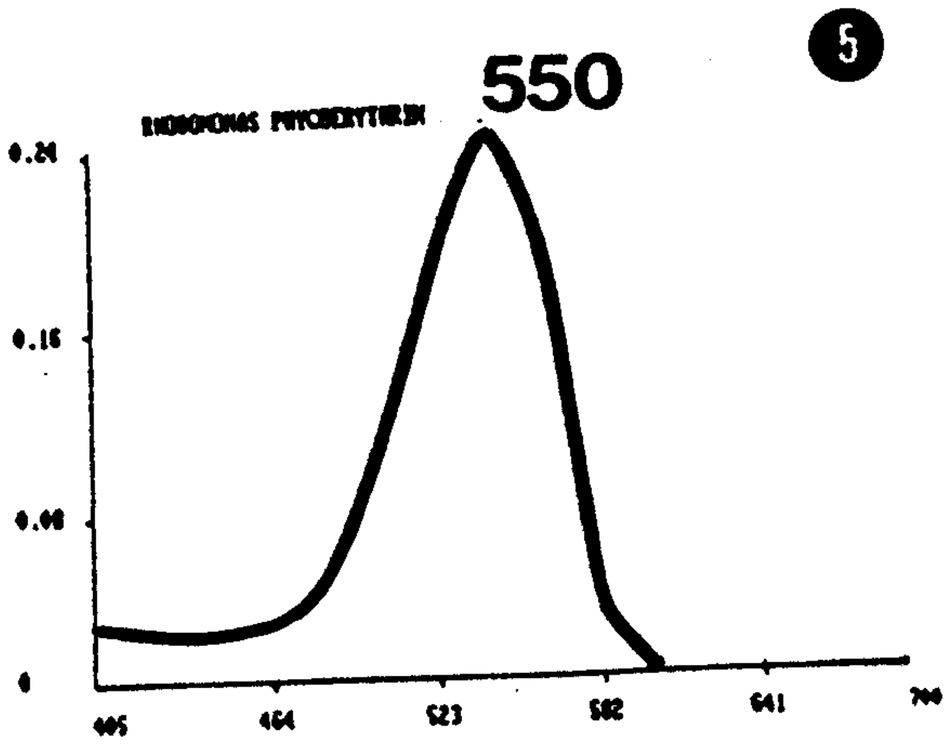
5
550
0.24
0.16
0.08
0
405
464
523
582
641
700

PLATE 31 B

PLATE 32

Chroomonas collegionis CCAP 978/11, LM

Fig. 1. A large colony of palmelloid cells; unfixed. Scale bar = 0.1 mm. Fig. 2. Detail of a smaller colony at higher magnification; unfixed. Scale bar = 20 µm.

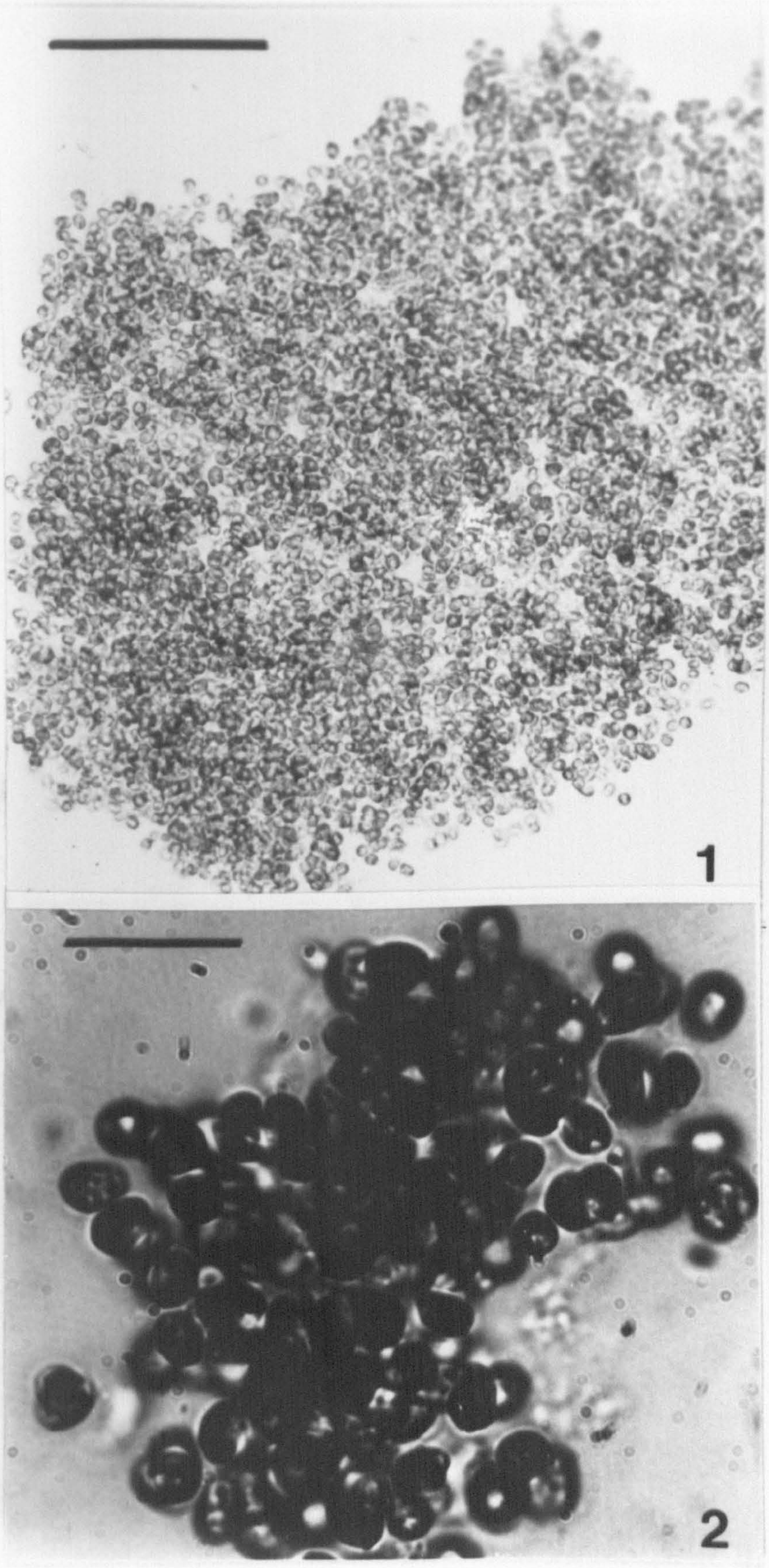

1

2

PLATE 32

PLATE 33

Chroomonas placoidea CCAP 978/8, bright-field (BF) and polarized (POL) light microscopy

Fig. 1. Palmelloid cell, showing two dense bodies (arrows) towards the periphery; unfixed, BF. Fig. 2. The same cell, POL; the dense bodies are highly refringent. Fig. 3. Motile cell seen from posterior, POL. Note refringent bodies (arrows). Scale bars = 5 µm.

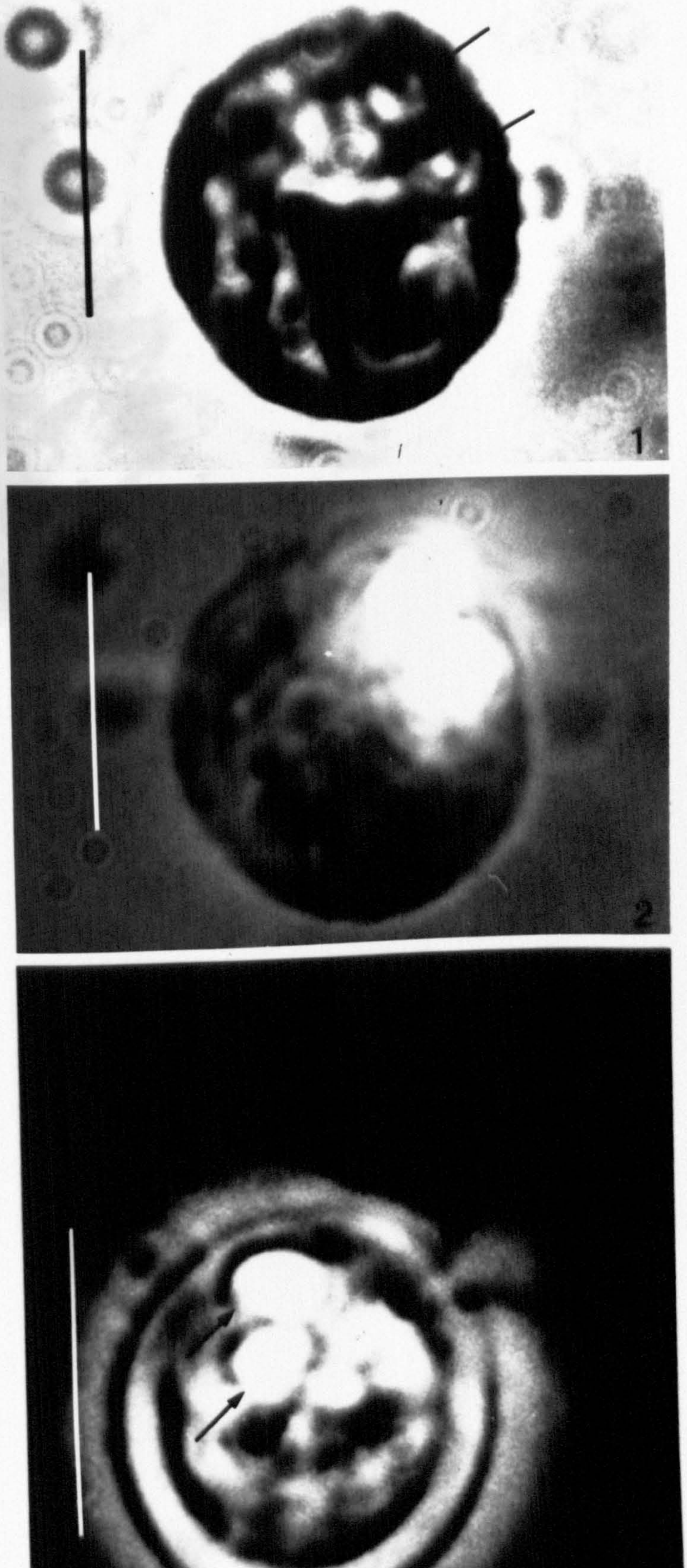

PLATE 33

PLATE 33

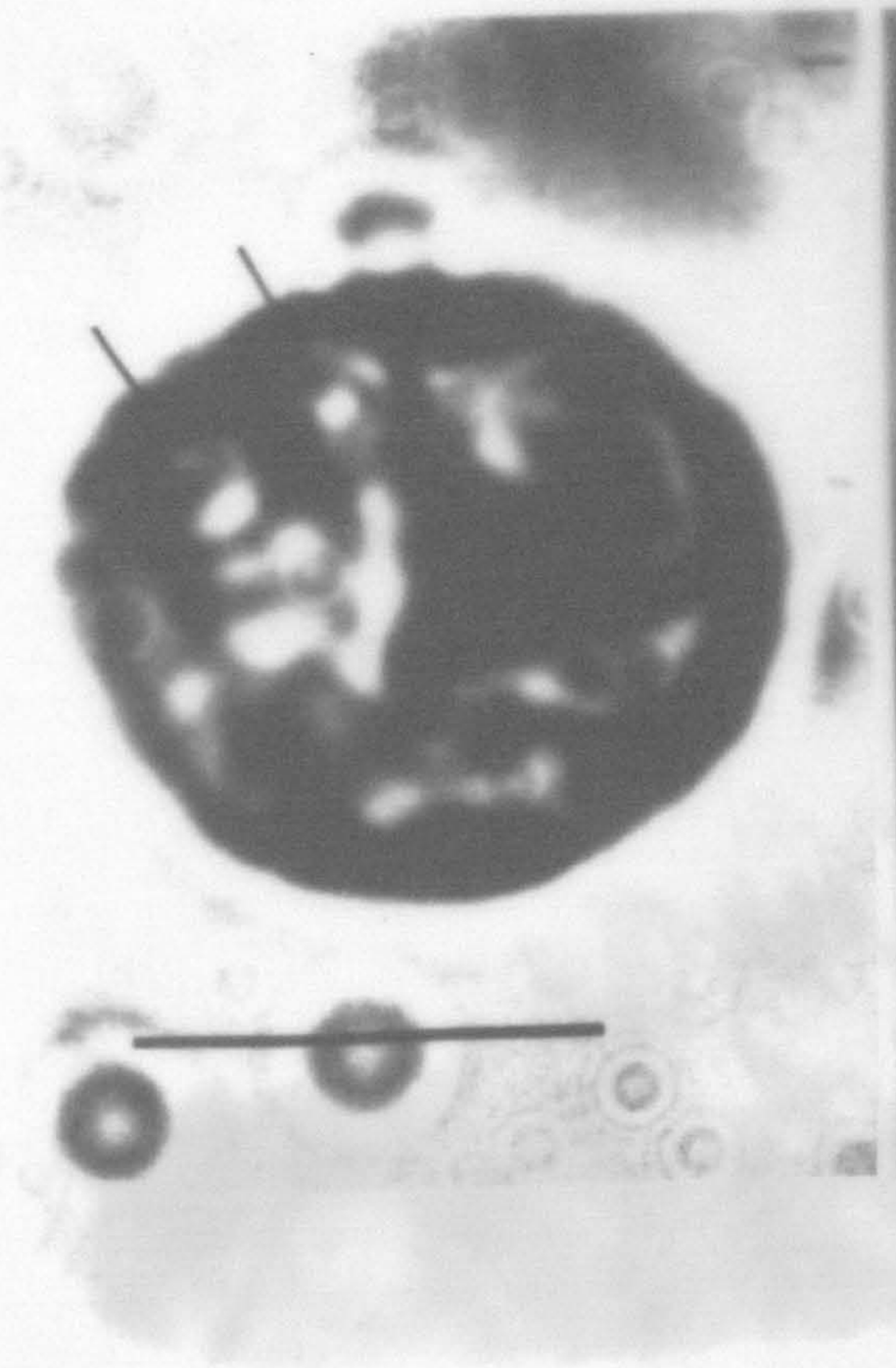

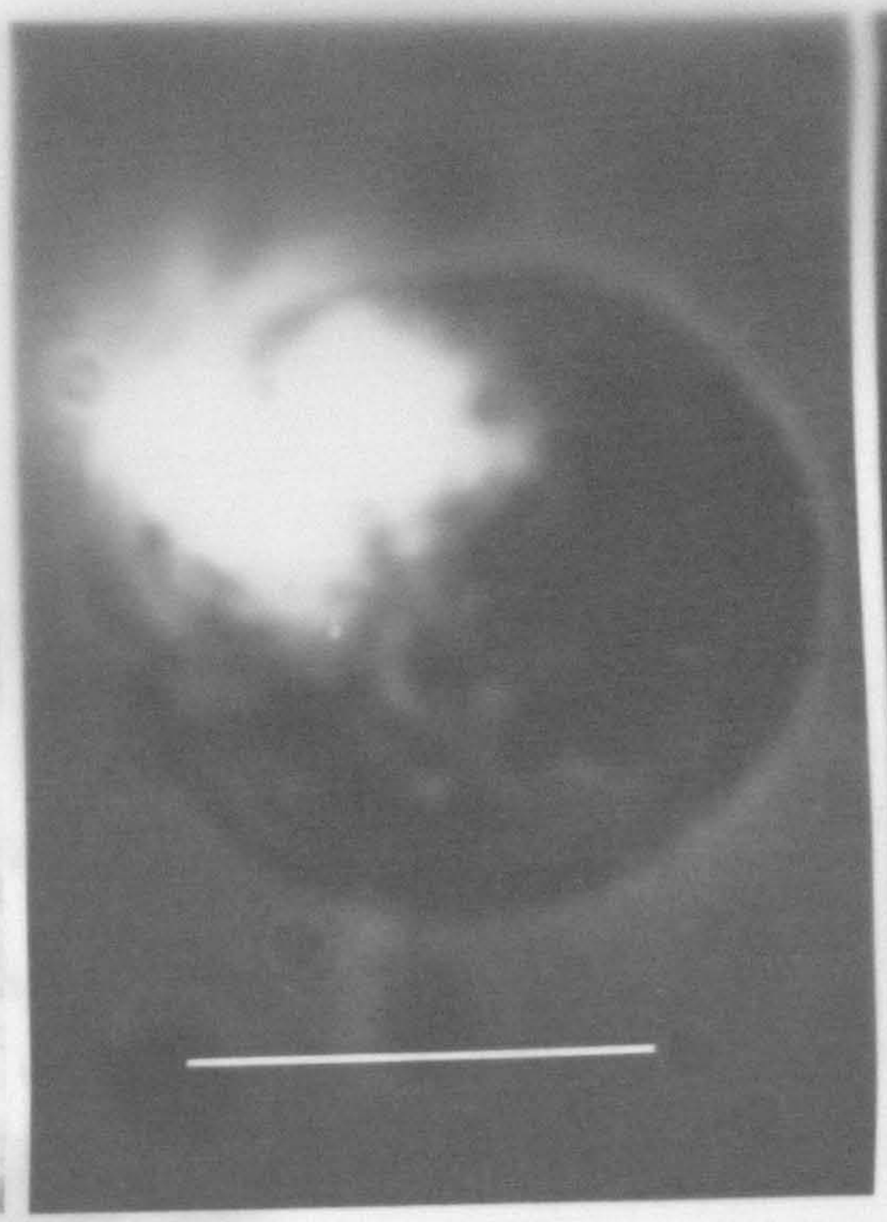

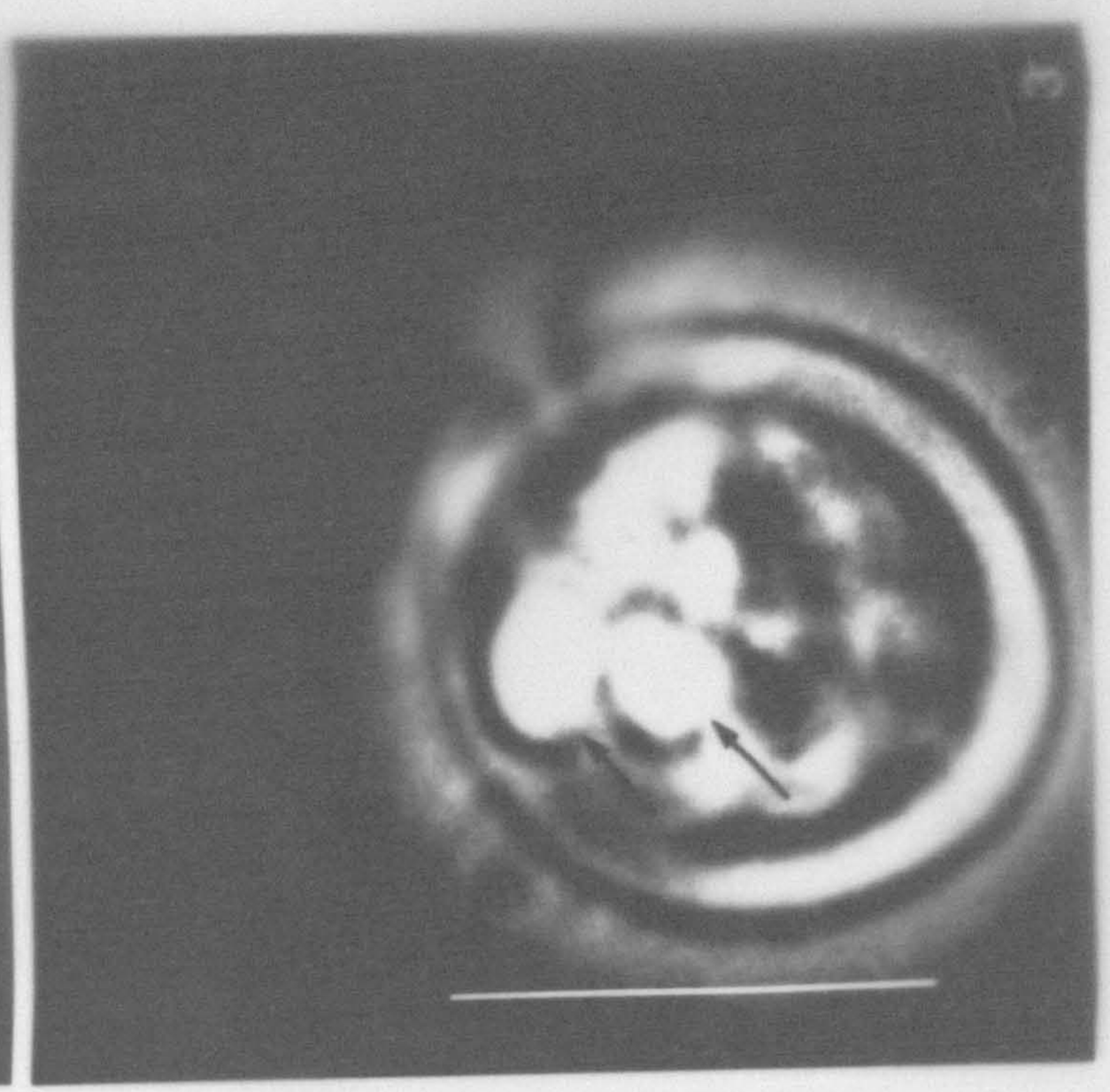

PLATE 34

Chroomonas placoidea CCAP 978/8, motile cells, SEM, glutaraldehyde / osmium / critical point-drying

Fig. 1. Cell seen from posterior. Scale bar = 5 µm. Fig. 2. Detail of the periplast at higher magnification. Scale bar = 1 µm.

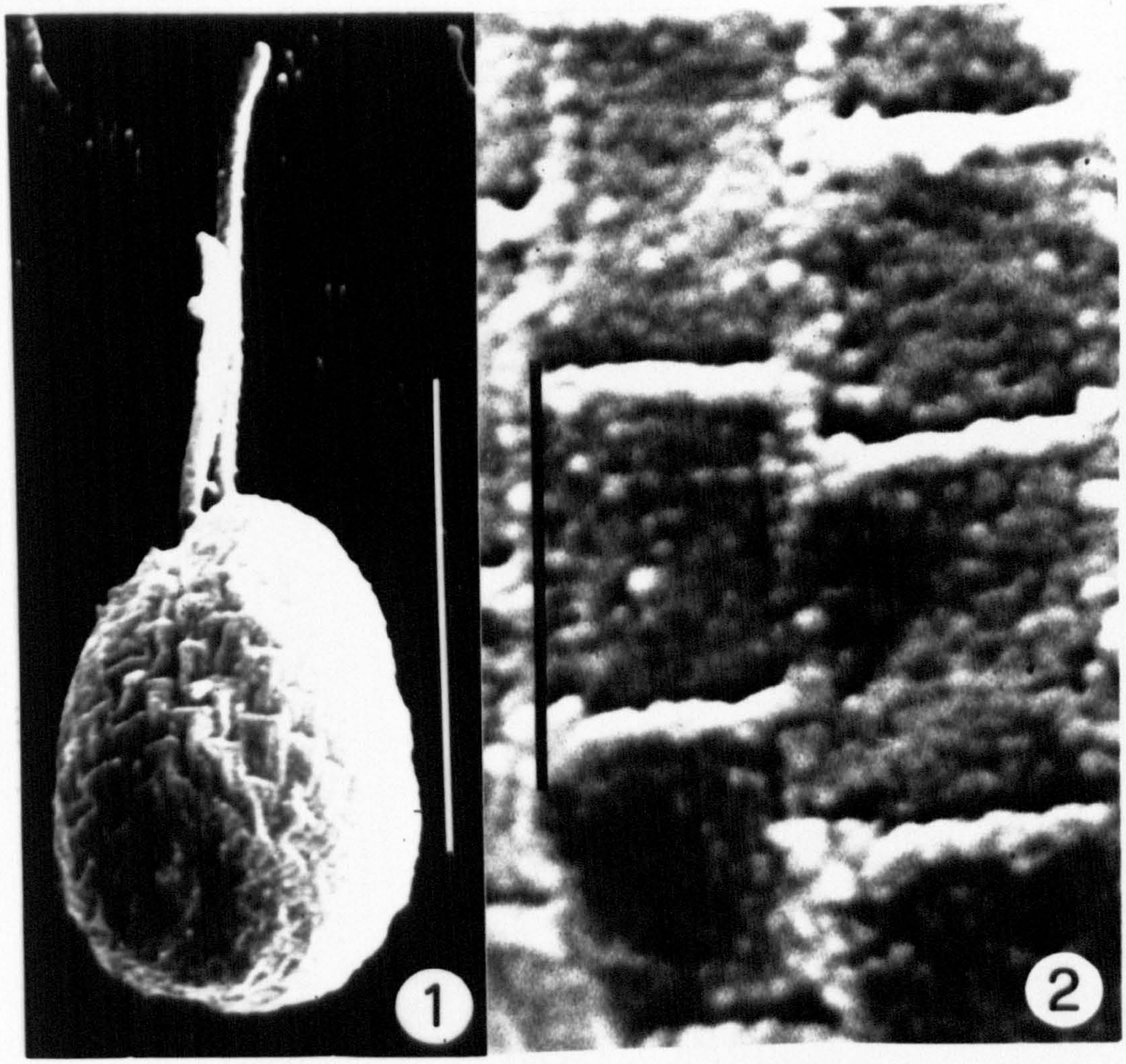

PLATE 34

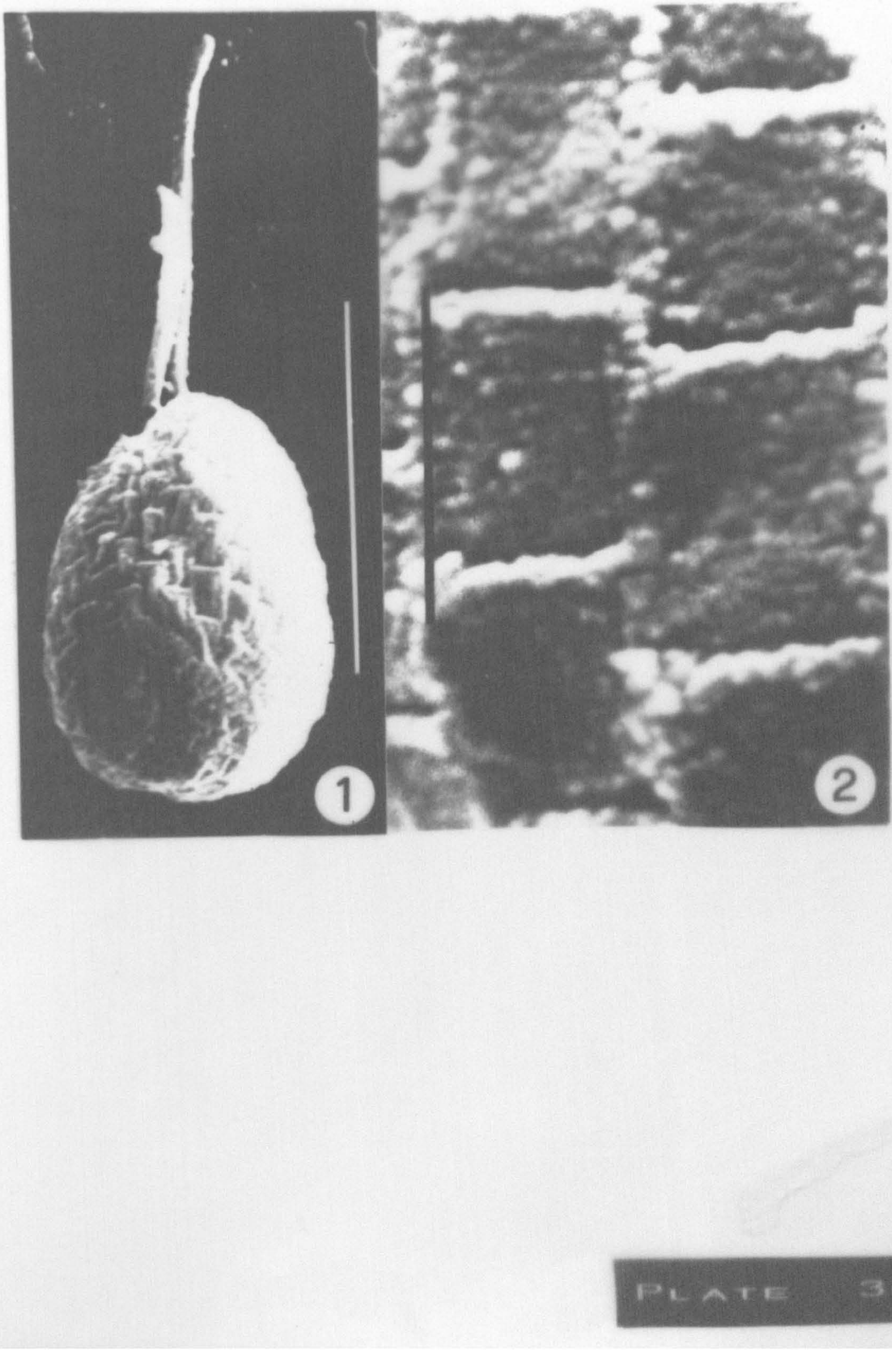

PLATE 34

PLATE 35

Chroomonas collegionis CCAP 978/11, SEM, glutaraldehyde / osmium / critical point-drying unless otherwise stated

Fig. 1. Motile cell, glutaraldehyde / critical point-drying. Scale bar = 2 µm. Fig. 2. At higher magnification, detail of the periplast of the cell in Fig. 1. Scale bar = 0.5 µm. Fig. 3. Motile cell. Scale bar = 2 µm. Fig. 4. Paired palmelloid cells, covered with mucilage. Scale bar = 5 µm.

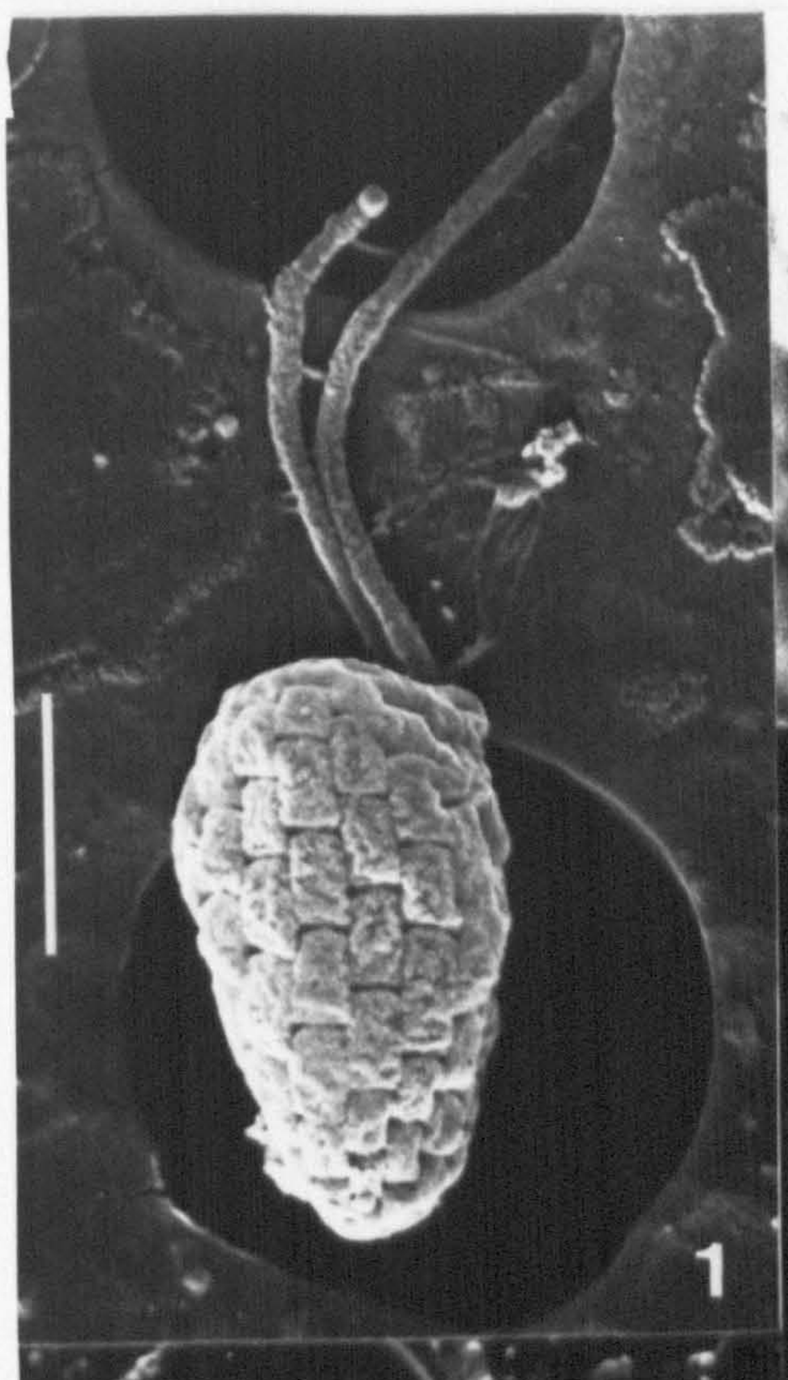

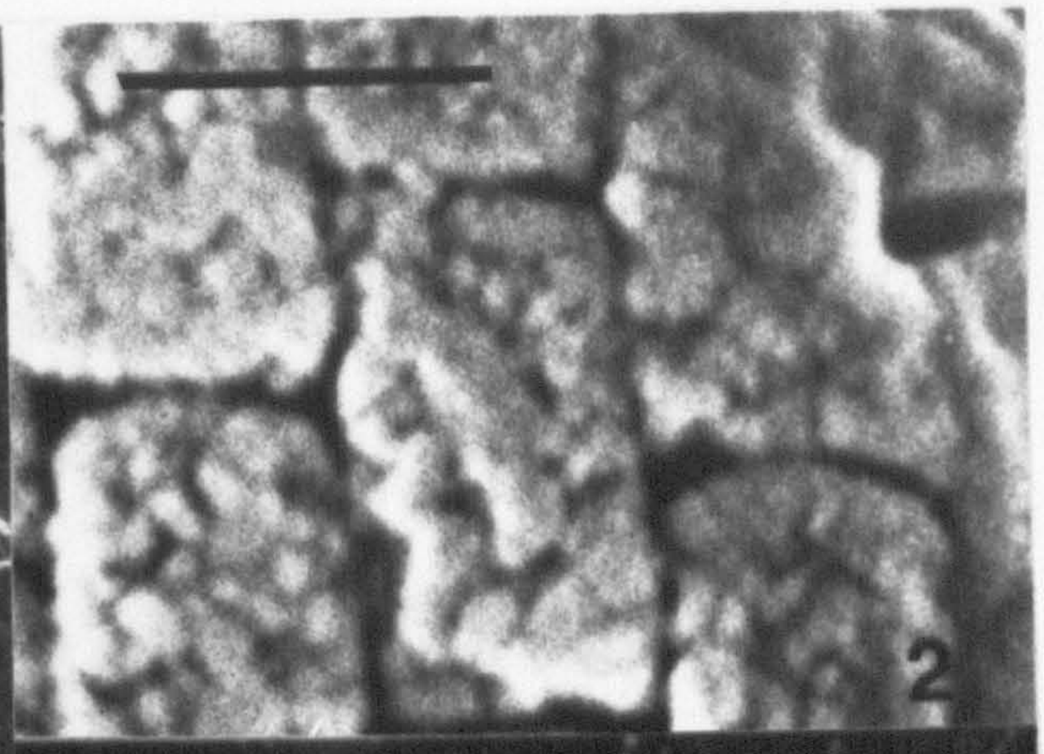

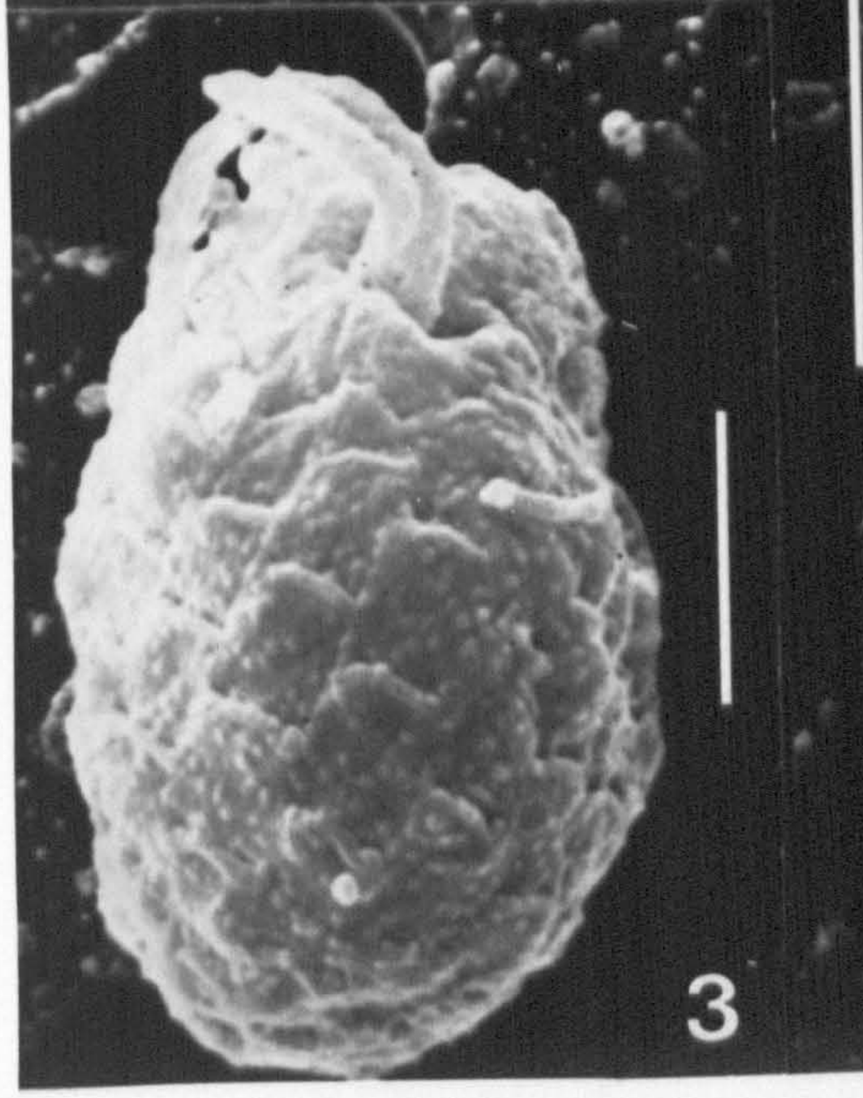

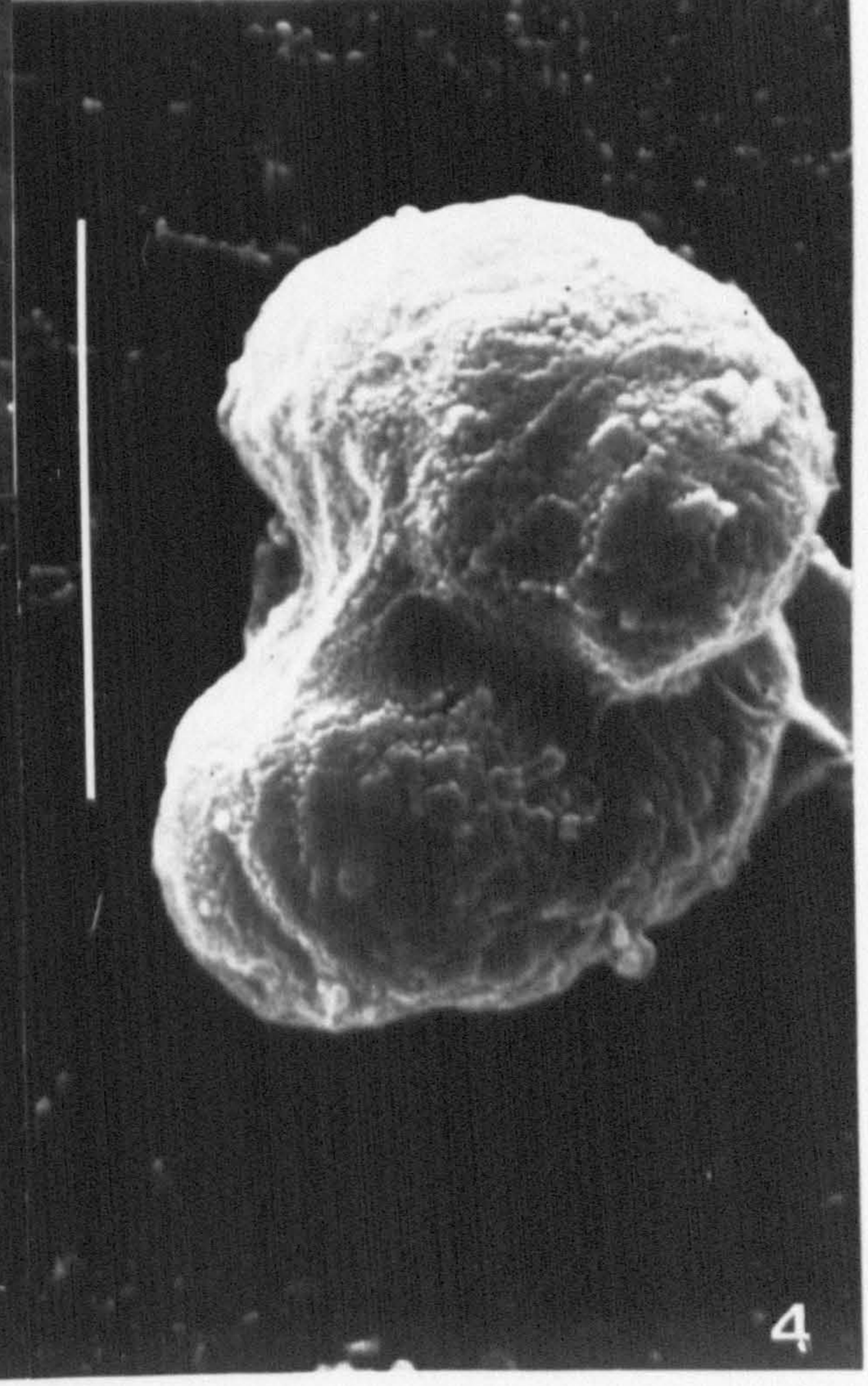

PLATE 35

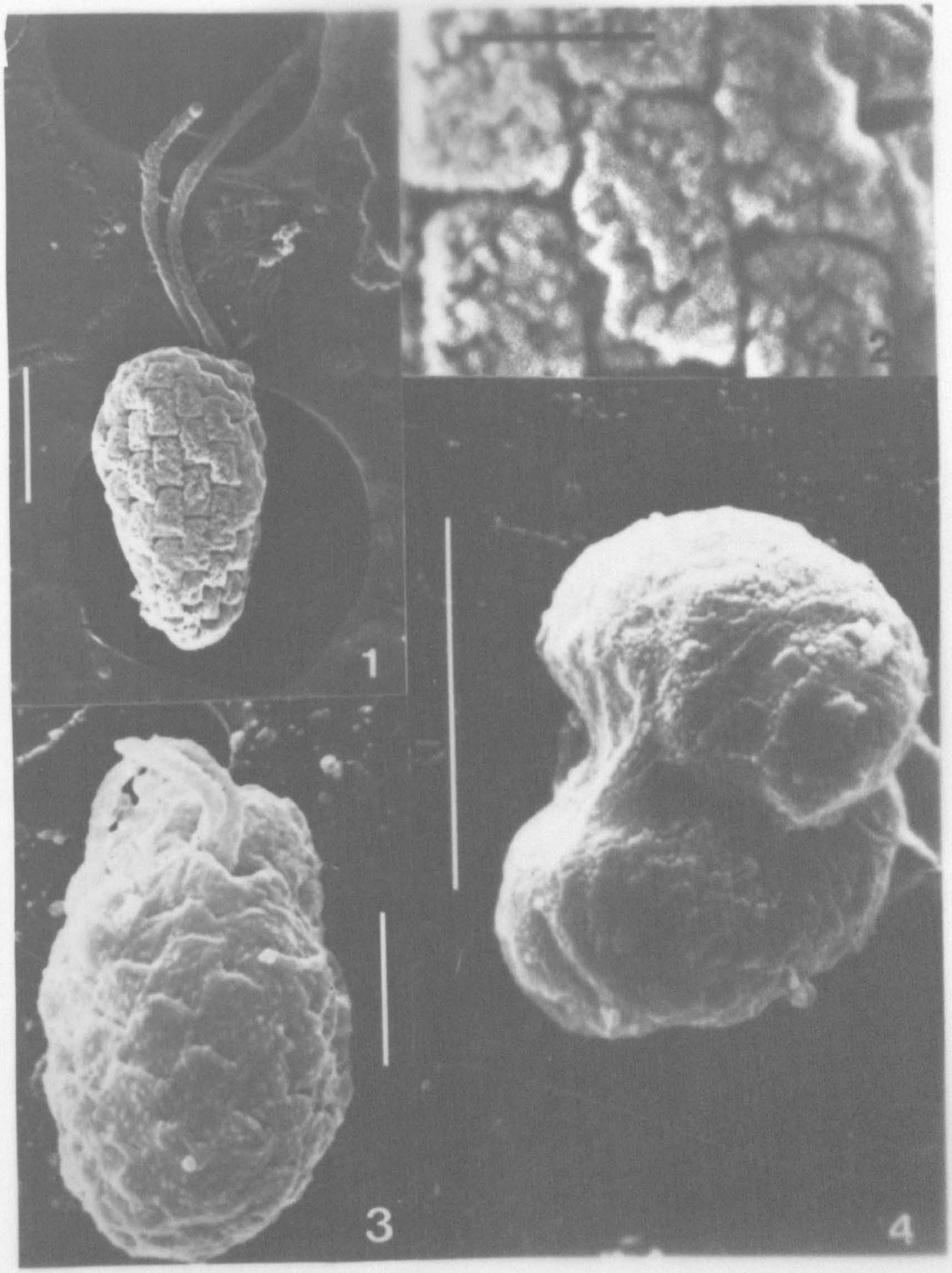
1
2
3
4

PLATE 36

Chroomonas sp. SAG 980.1, SEM, glutaraldehyde / osmium / critical point-drying

Fig. 1. Lateral view. Fig. 2. Ventro-lateral view. Fig. 3. Detail of the periplast at higher magnification. Scale bars = 5 µm (Figs 1, 2) or 1 µm (Fig. 3).

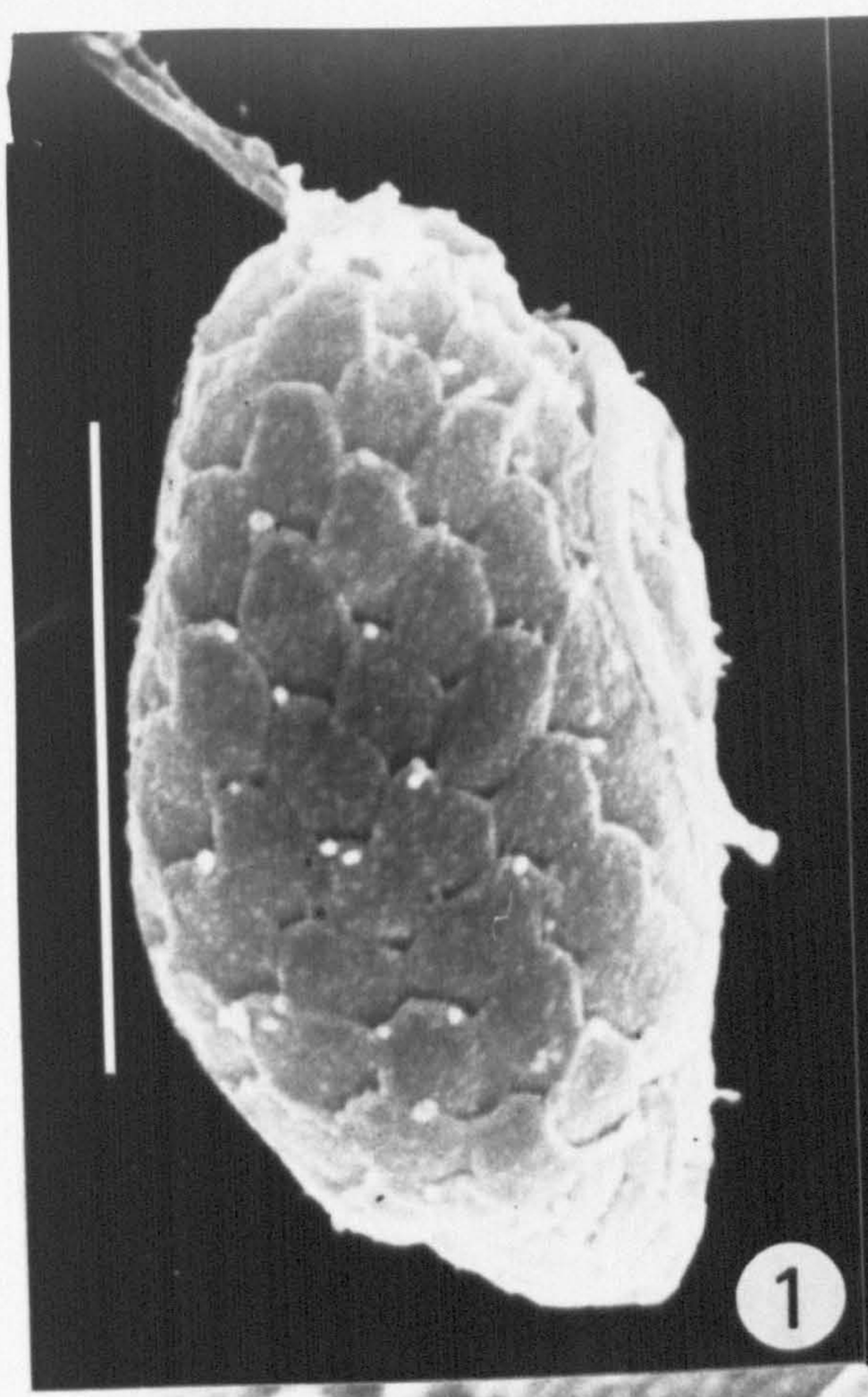

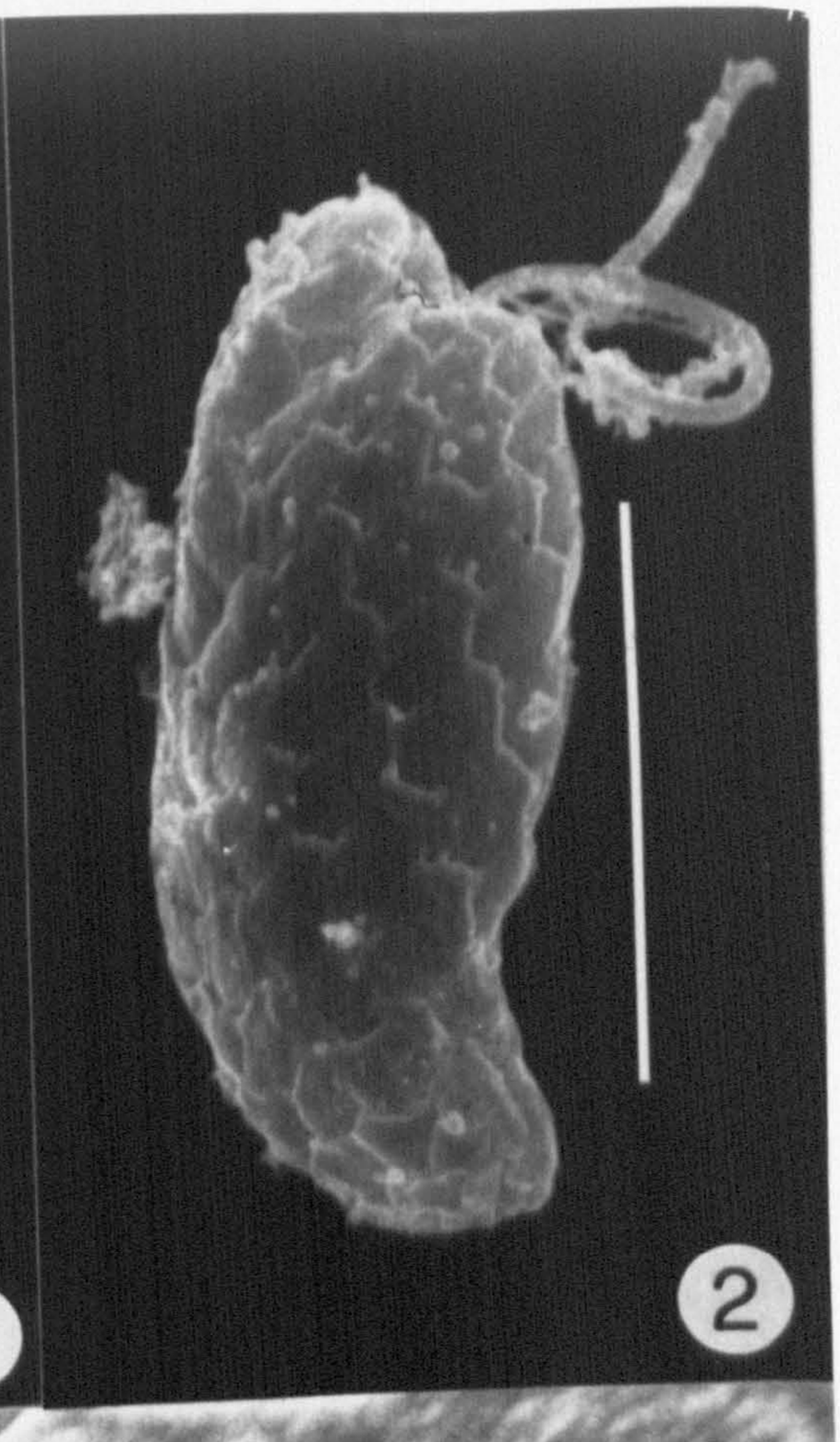

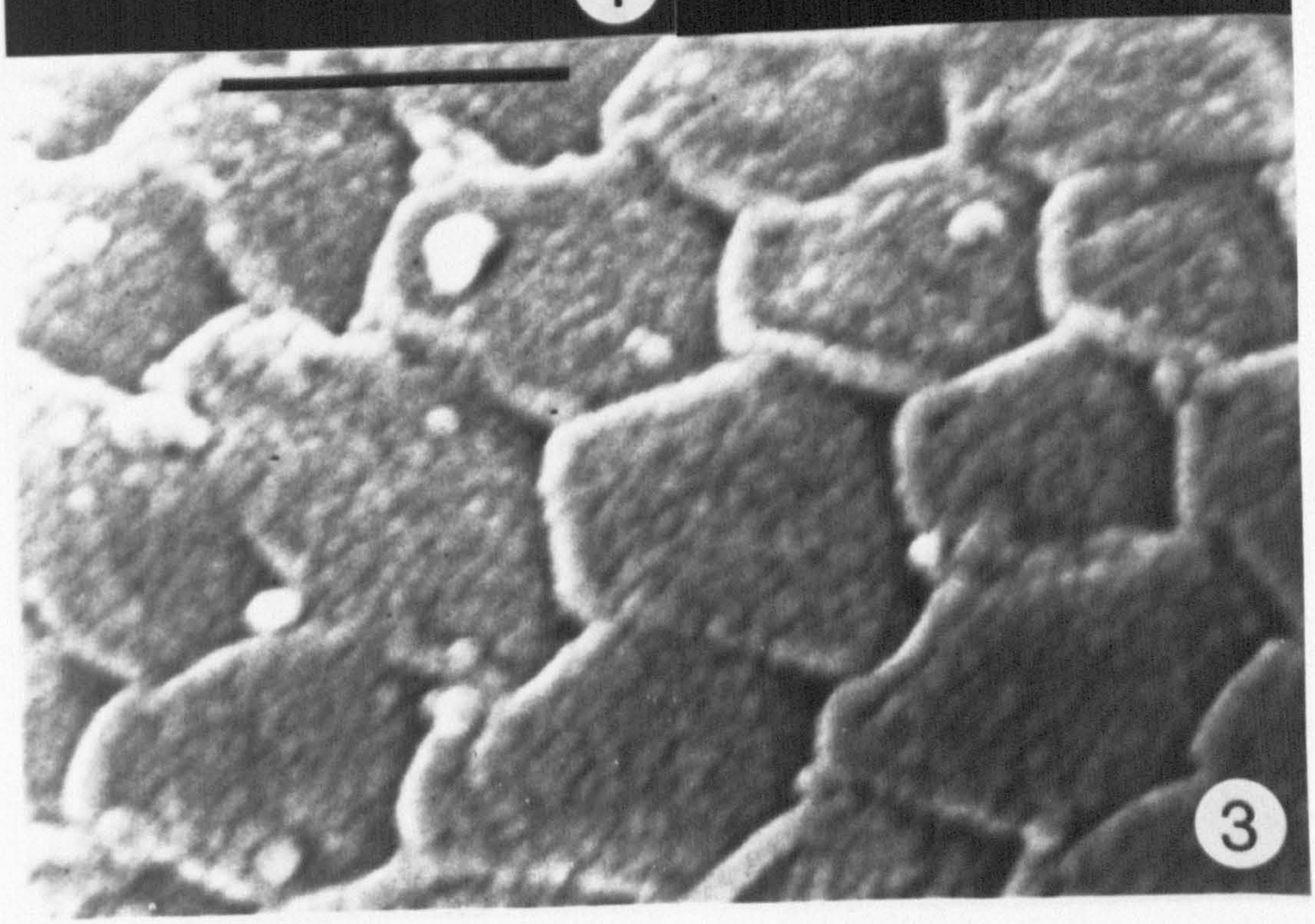

PLATE 36

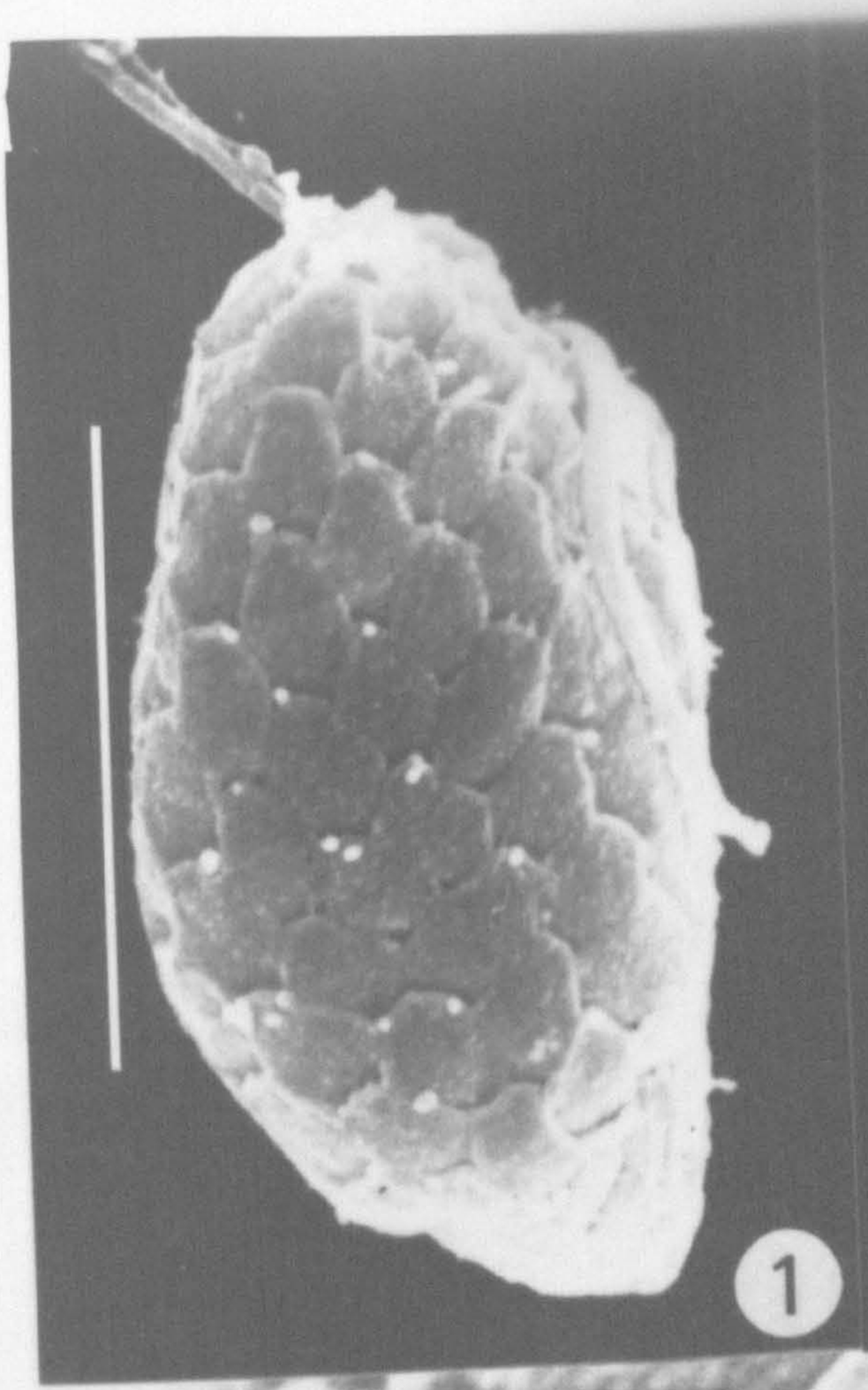

1

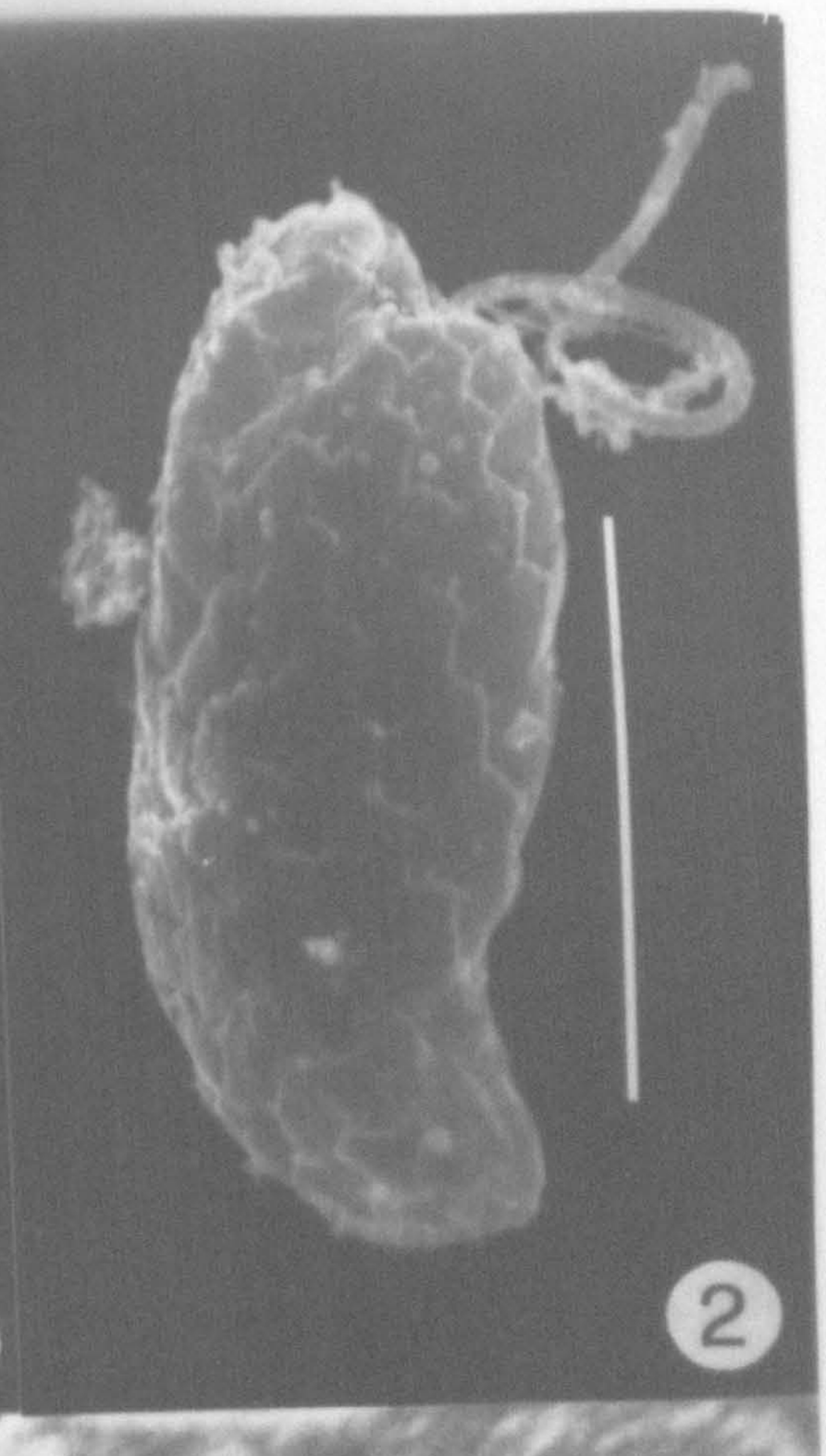

2

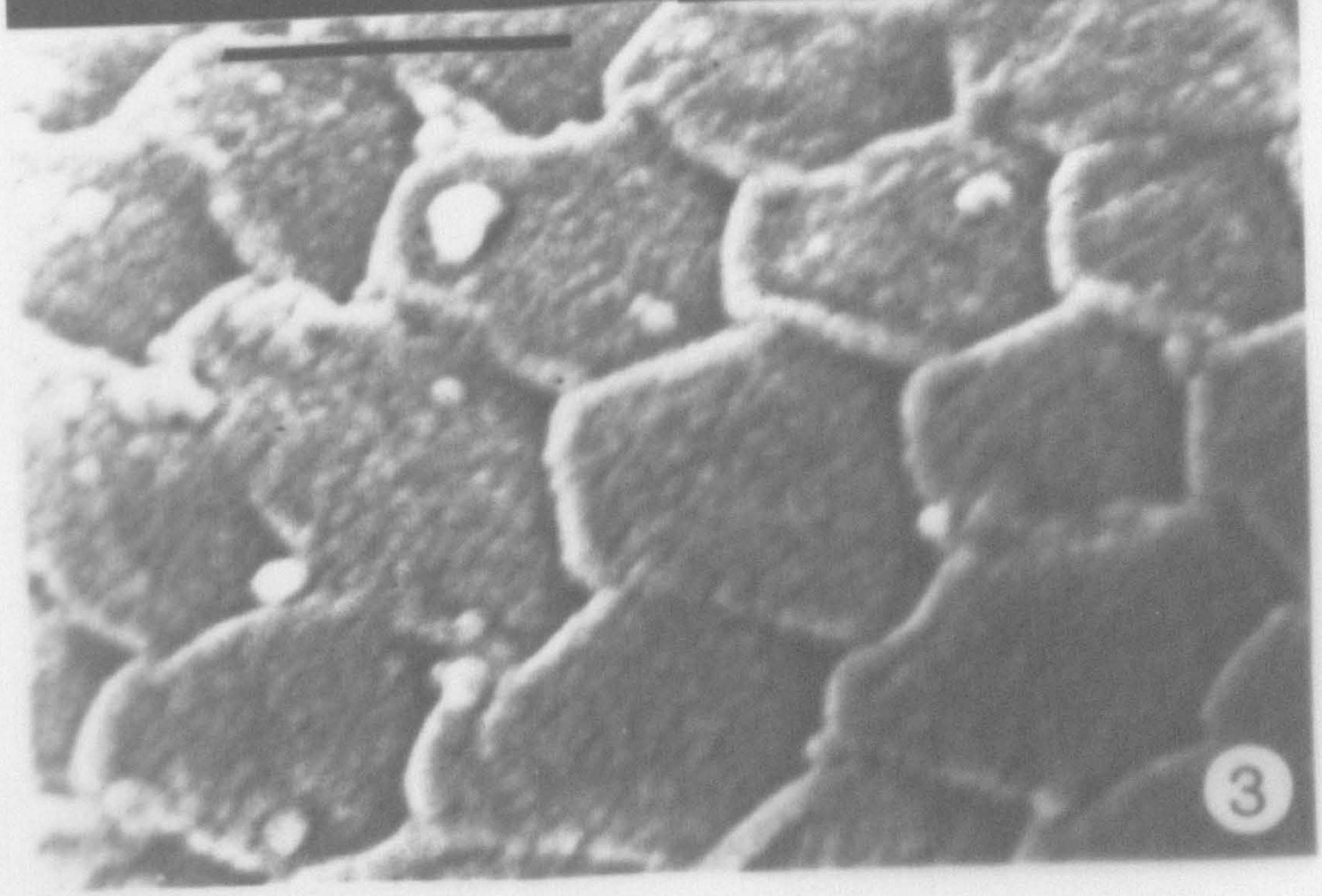

3

PLATE 37

Chroomonas collegionis CCAP 978/11, TEM, glutaraldehyde / osmium: details of the vestibular complex

Fig. 1. Transverse section showing the contractile vacuole (CV), close to the vertical gullet through which the flagella emerge. There is one row of ejectosomes, perpendicular to the gullet. Note the single, large Golgi body (GB). Fig. 2. A section similar to that in Fig. 1, but showing a ligule (L) in the gullet, and a narrow ejectosome channel (EC). Fig. 3. Longitudinal section, showing the wide external opening of the ejectosome channel (arrow). Scale bars = 5 µm.

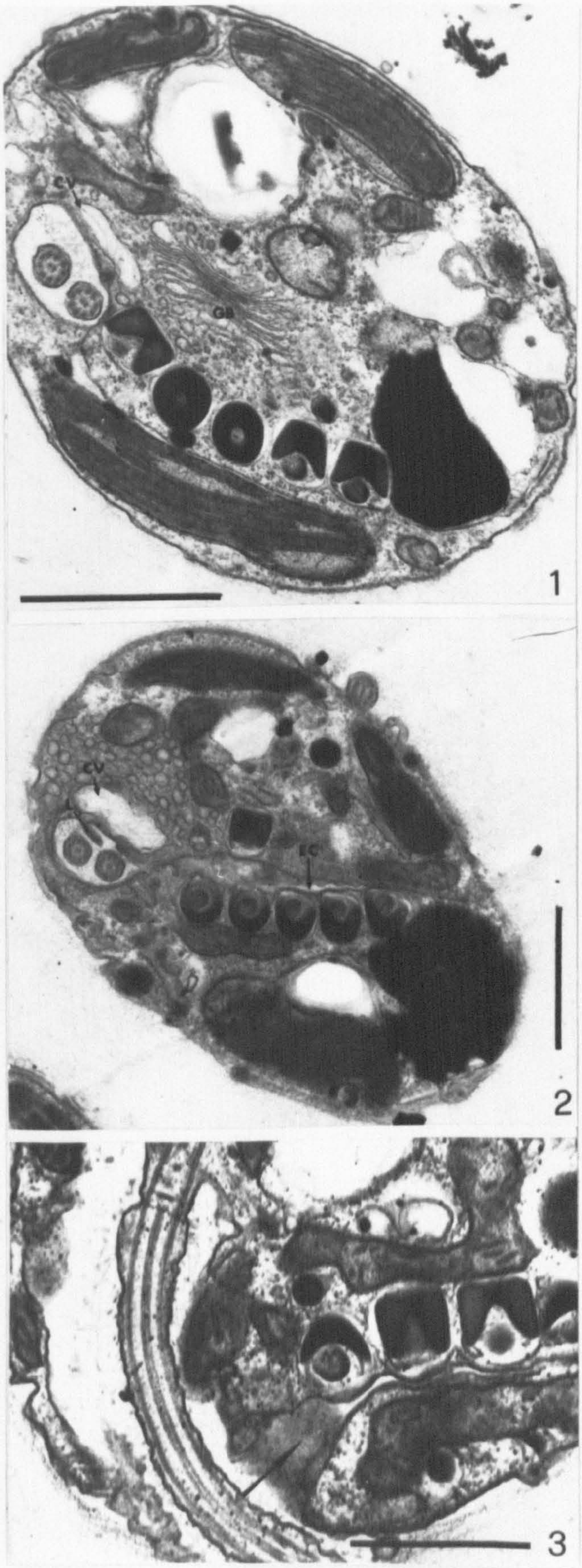

PLATE 37

PLATE 37

PLATE 38

Chroomonas collegionis CCAP 978/11, TEM, glutaraldehyde / osmium: single palmelloid cells in oblique sections

Fig. 1. In this cell, which seems to lack peripheral ejectosomes, there are two thin, elongated structures on the external face of the periplast, deeply embedded in the mucilage layer (M). Note the large, central nucleomorph (NM). Fig. 2. Cell with several small osmiophilic bodies (OB). Note eyespot (ES) surrounded by starch granules (S), and nucleus (N). Fig. 3. This cell shows the flagella (arrowheads) embedded in the mucilage layer (M). Note central nucleomorph (NM) and eyespot (ES). Fig. 4. Cell with several peripheral ejectosomes (arrowheads), and thin, elongated structures (arrows) embedded in the mucilage layer (M). Scale bars = 1 µm.

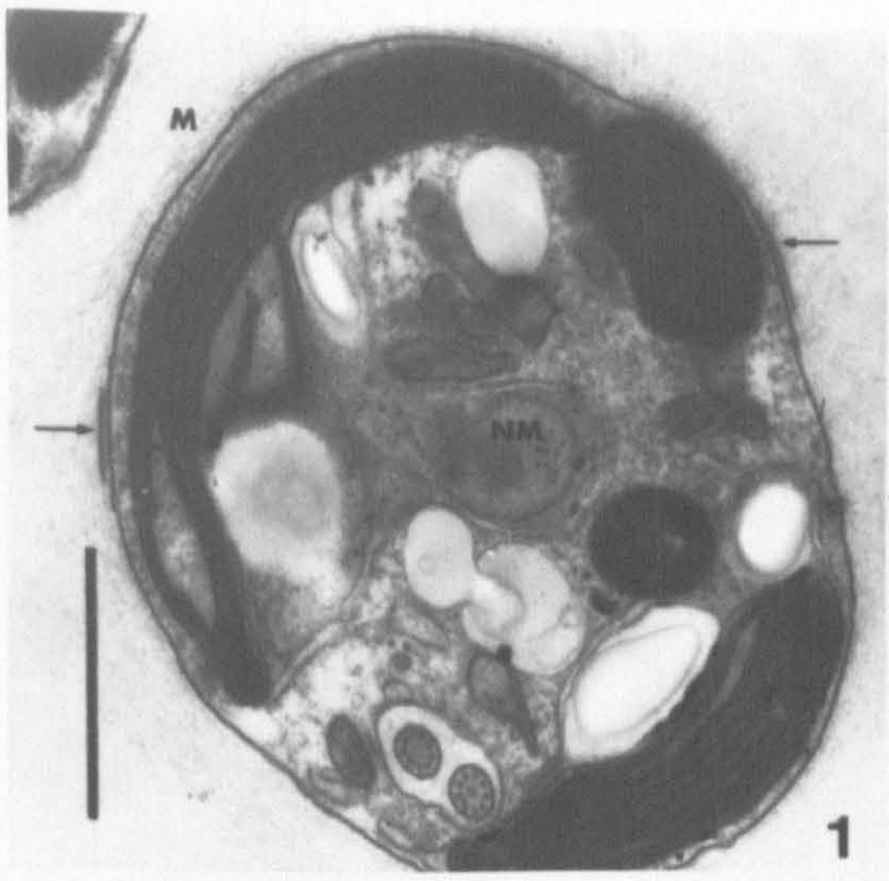

1

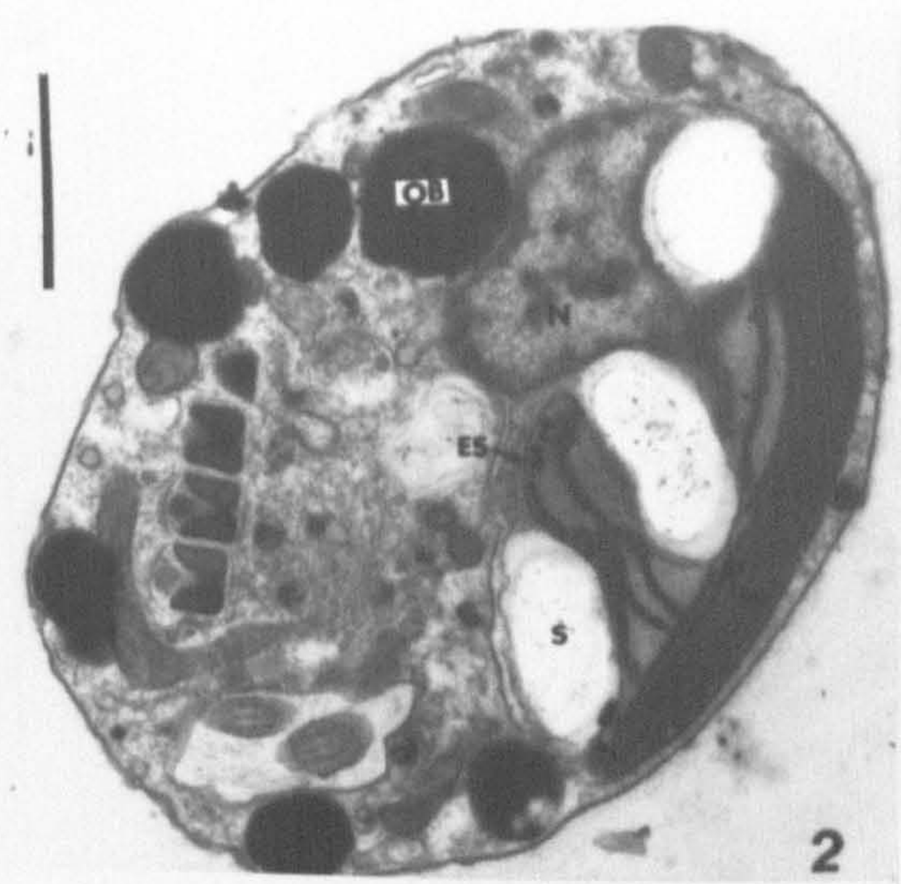

2

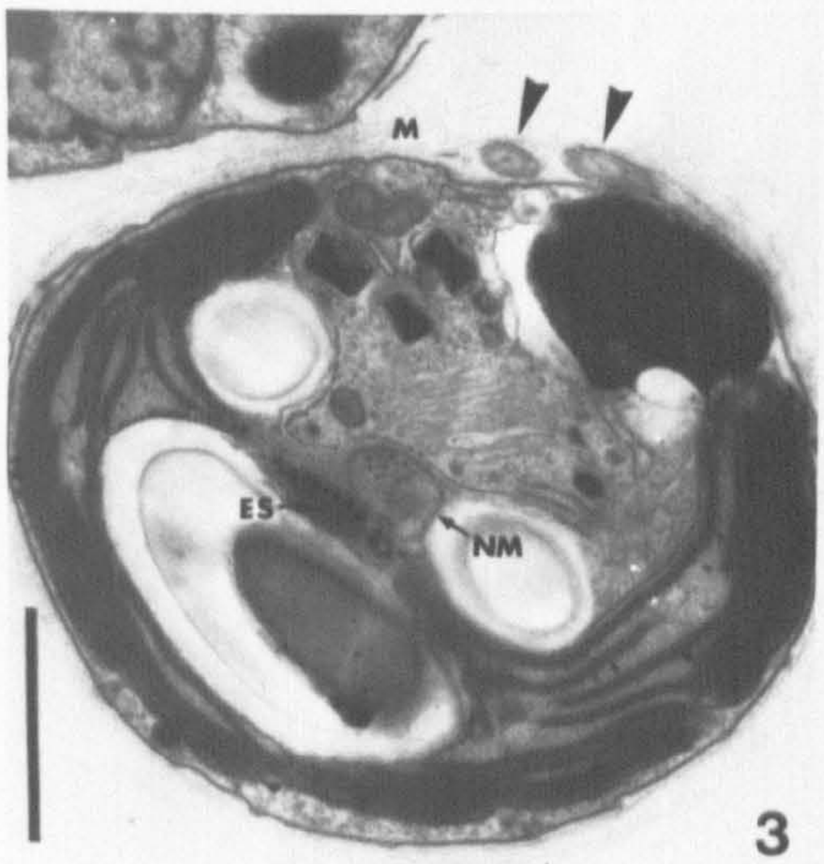

3

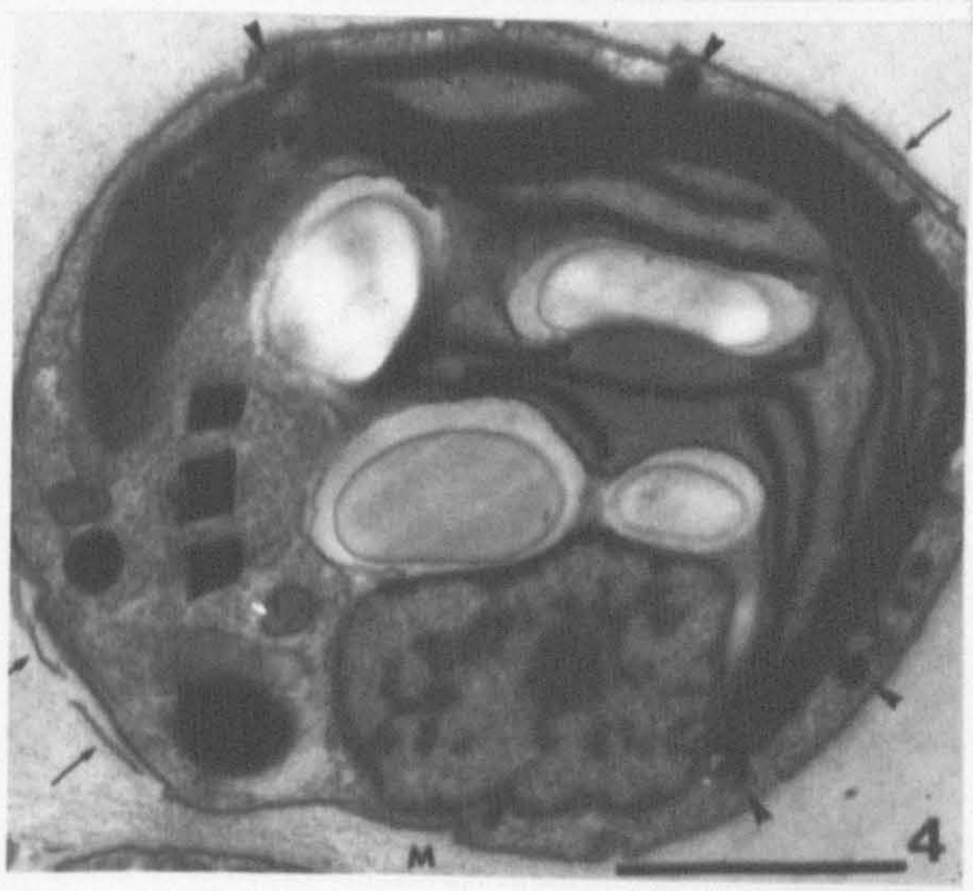

4

PLATE 38

PLATE 39

Chroomonas collegionis CCAP 978/11, TEM, osmium - thiocarbohydrazide - osmium: paired palmelloid cells

Fig. 1. General view of a palmelloid pair; note the flagella (arrowhead) embedded in the external mucilage layer (arrows). Scale bar = 2 µm. Fig. 2. Detail of the mucilage layer at the region of contact between cells; note dense (A_L) and loose (B_L) fibrillar layers. Scale bar = 0.5 µm. Fig. 3. Detail of the surface of one cell; note the periplast, whose discrete areas are marked by regularly spaced ridges (arrowheads), and the mucilage, with its dense (A_L) and loose (B_L) fibrillar layers. Scale bar = 200 nm. Fig. 4. In this cell the external (EPC) and internal (IPC) periplast components are apparently not subdivided in discrete periplast areas; note the tripartite plasma membrane (PM), sandwiched between the EPC and IPC, and the mucilage with its dense (A_L) and loose (B_L) fibrillar layers. Scale bar = 200 nm.

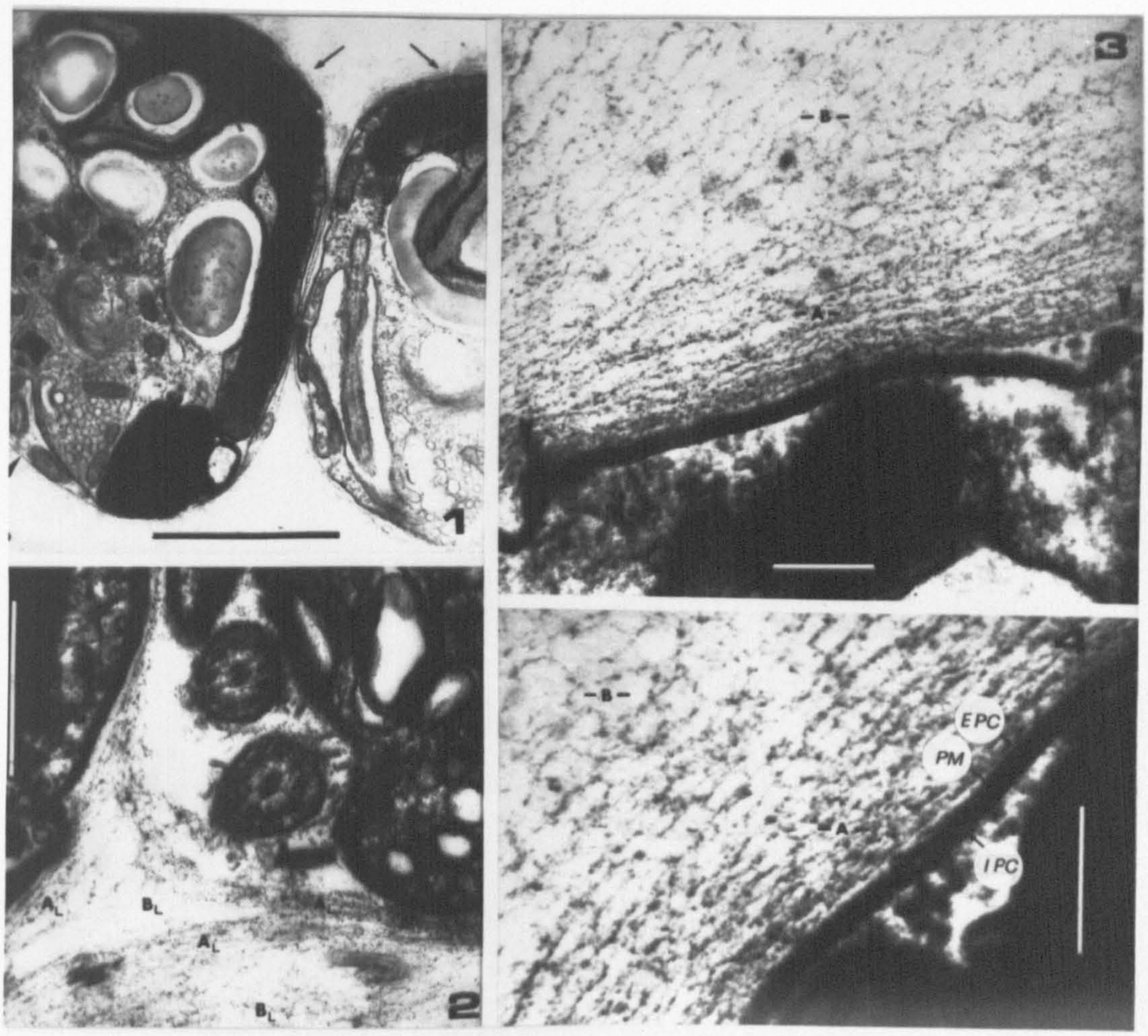

PLATE 39

PLATE 40

Chroomonas collegionis CCAP 978/11, TEM, osmium - thiocarbohydazide - osmium: influence of the development time of the photographic prints on the appearance of the mucilage layer

Each photograph corresponds to a doubling of the exposure time of the previous one. In Fig. 1 the mucilage layer is barely perceptible, although the internal cell components appear slightly overstained; note profiles of flagella (arrowheads), and the periplast, showing little evidence of being subdivided into discrete periplast areas. In Fig. 2 the mucilage is more distinct (arrows). In Fig. 3 the mucilage is clearly visible, and in Fig. 4 the dense (A_L) and loose (B_L) fibrillar layers are apparent; the internal cell components, however, are extremely overstained. Scale bars = 1 µm.

PLATE 10

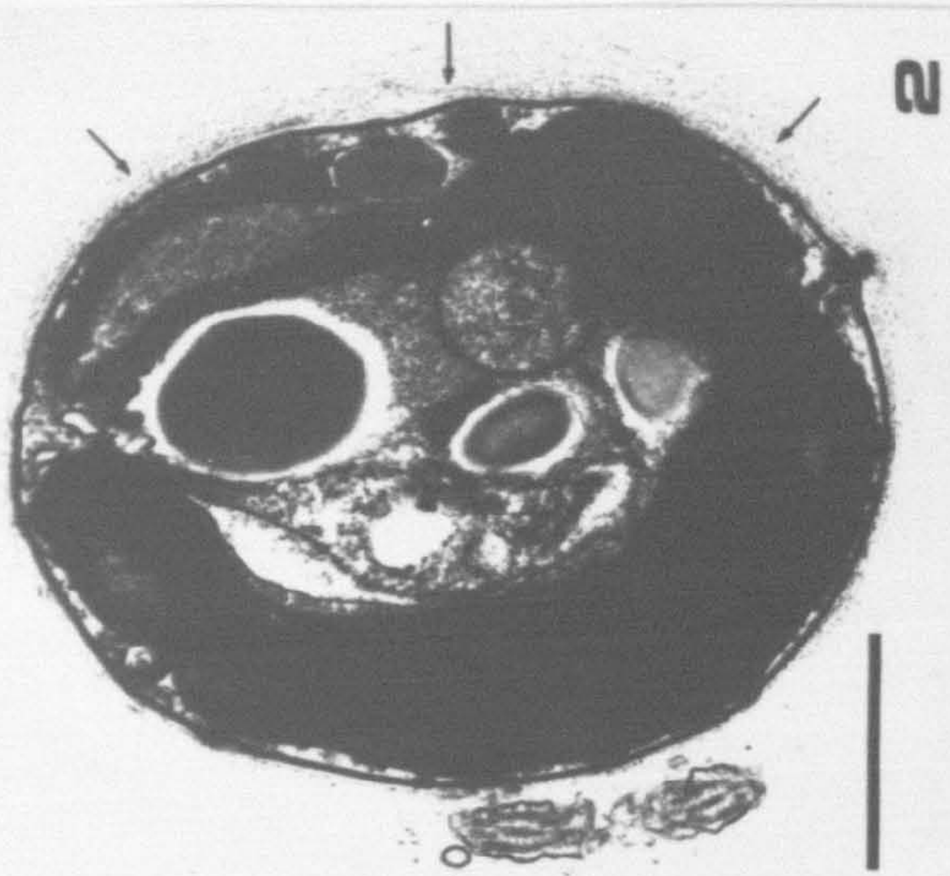

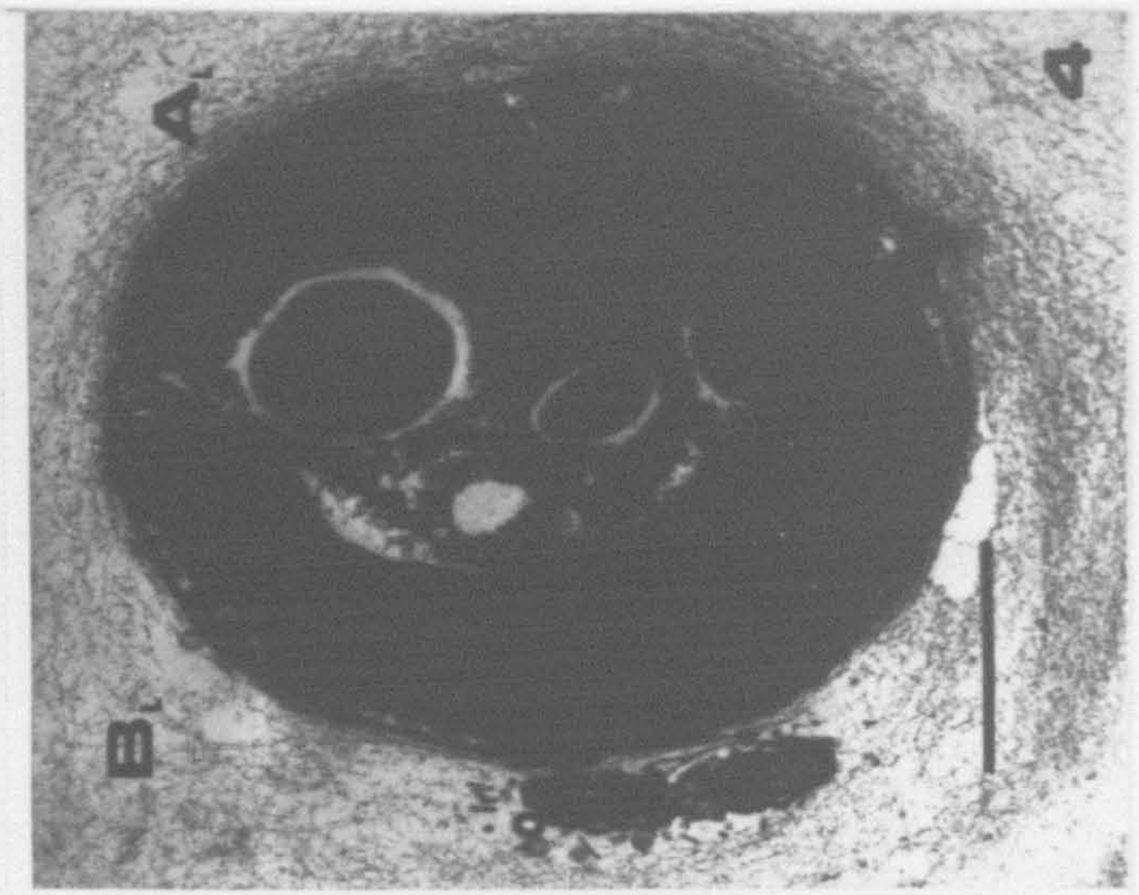

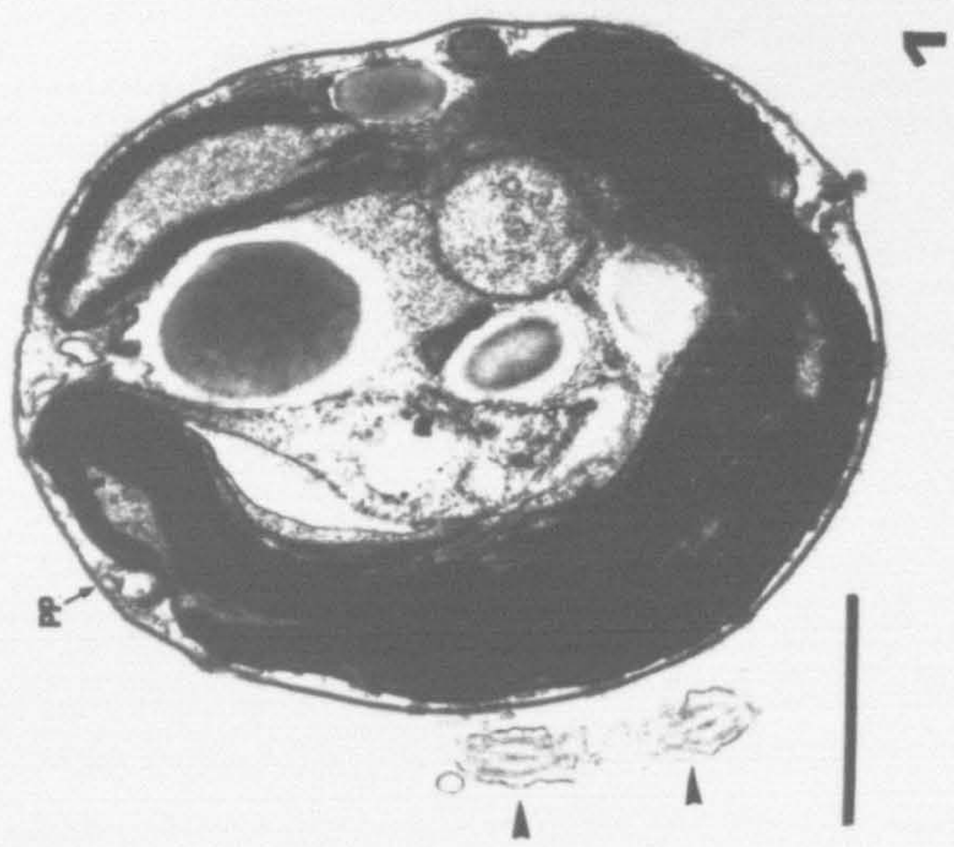

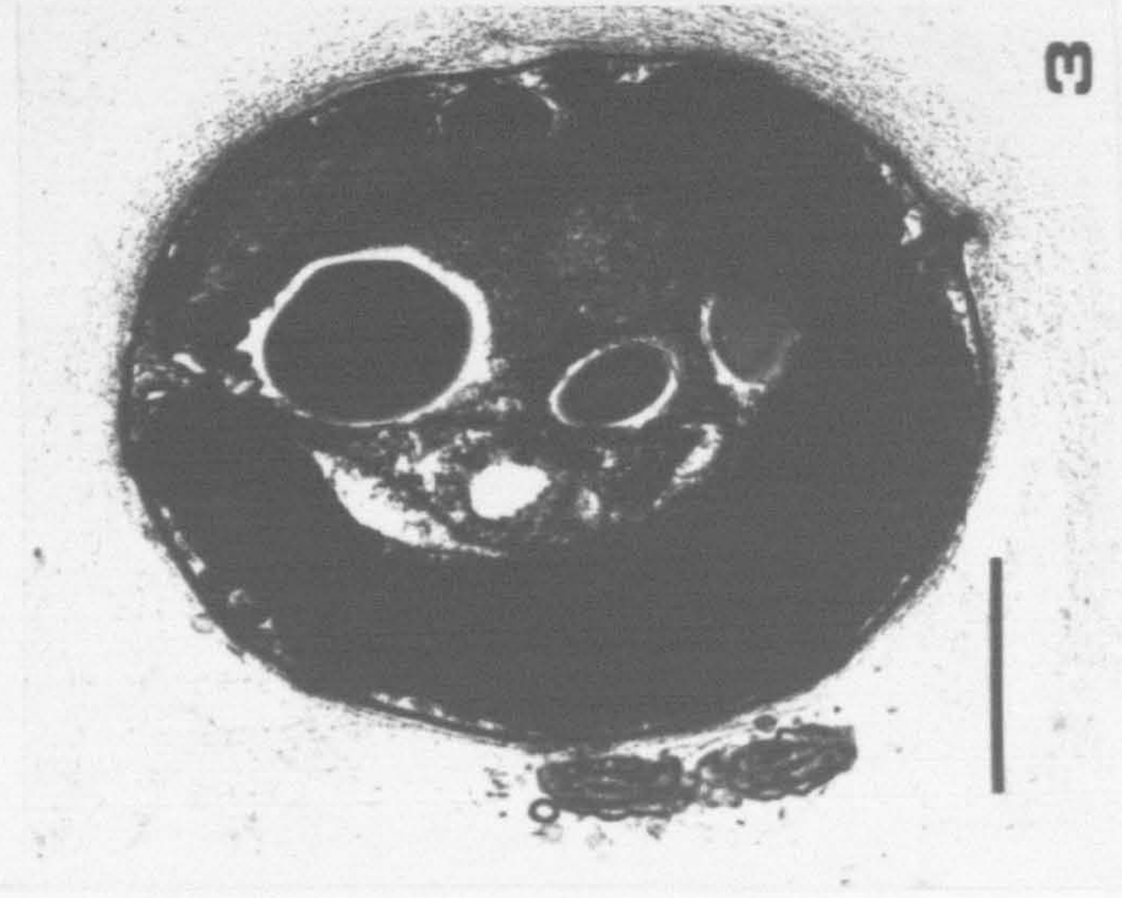

PLATE 41

Chroomonas collegionis CCAP 978/11, TEM, various fixation schedules: palmelloid cells

Fig. 1. Oblique section showing flagella (arrowhead) embedded in the mucilage layer (arrow); note the ligule (L) in the dorsal region of the gullet, anterior to the contractile vacuole. Osmium - thiocarbohydrazide - osmium (OTO). Fig. 2. Transverse section towards the mid-posterior region of the cell, showing the single H-shaped chloroplast with pyrenoidal bridge (PY); note the nucleomorph (NM) and nucleus (N) with nucleolus (NU). Glutaraldehyde - osmium (GAO). Fig. 3. Oblique section; note large mitochondrial profile (MT), nucleomorph (NM), and two Golgi bodies (arrowheads). GAO. Fig. 4. Section similar to that in Fig. 2, but showing the ligule (L) in the gullet. OTO. Scale bars = 1 μm.

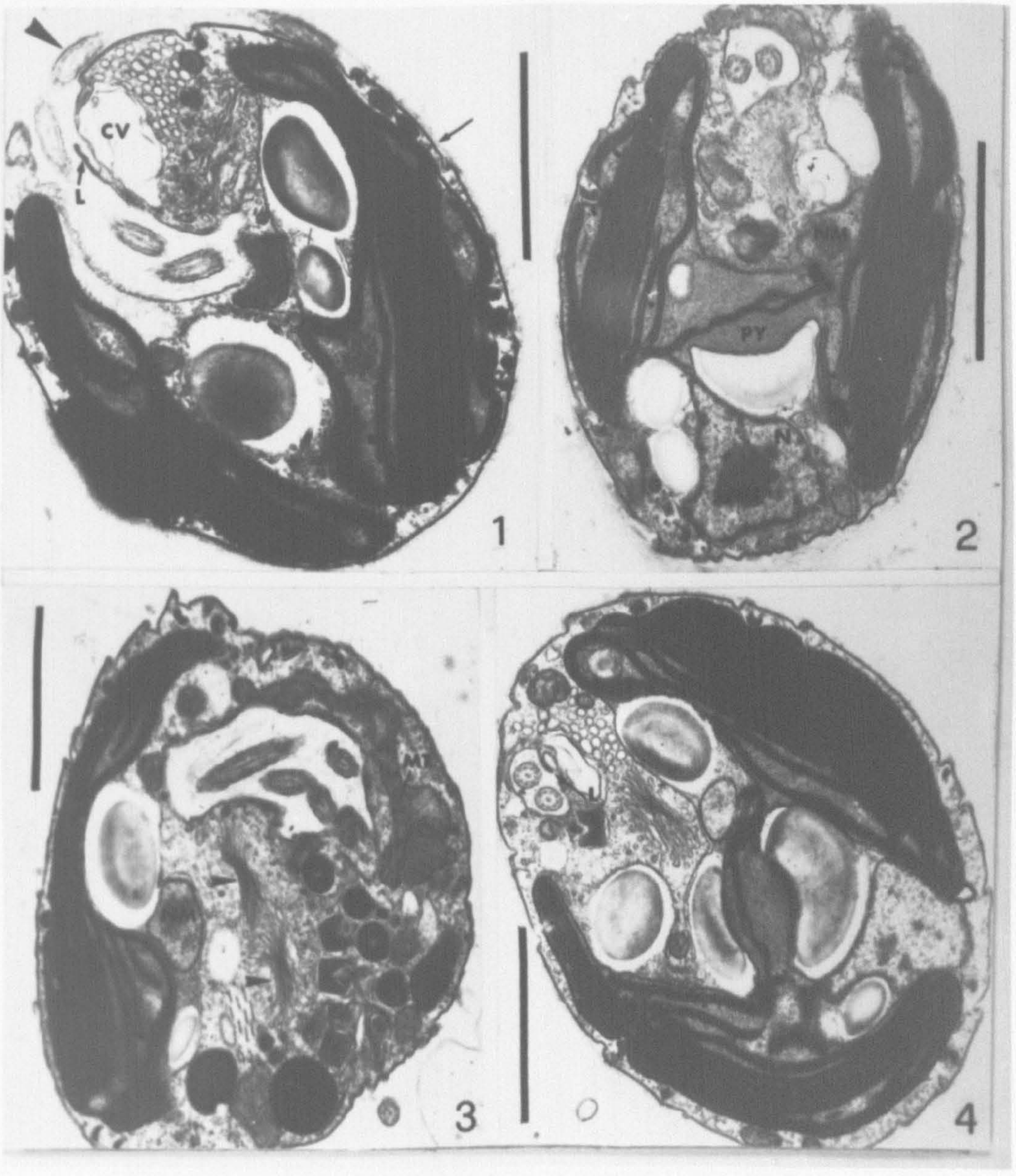

PLATE 41

PLATE 42

Chroomonas collegionis CCAP 978/11, TEM, glutaraldehyde - osmium: various appearances of the thylakoids

Fig. 1. Composite micrograph of palmelloid cell showing a regular arrangement of paired thylakoids. CE = double membrane of chloroplast envelope, CER = double membrane of chloroplast endoplasmic reticulum, E = peripheral ejectosome, PP = periplast, M = external mucilage layer. Scale bar = 250 nm. Fig. 2. Palmelloid cell with pairs of thylakoids, usually spaced, but showing stack-like regions here and there (asterisks). Scale bar = 300 nm. Fig. 3. Palmelloid cell with stacked thylakoids. Scale bar = 250 nm.

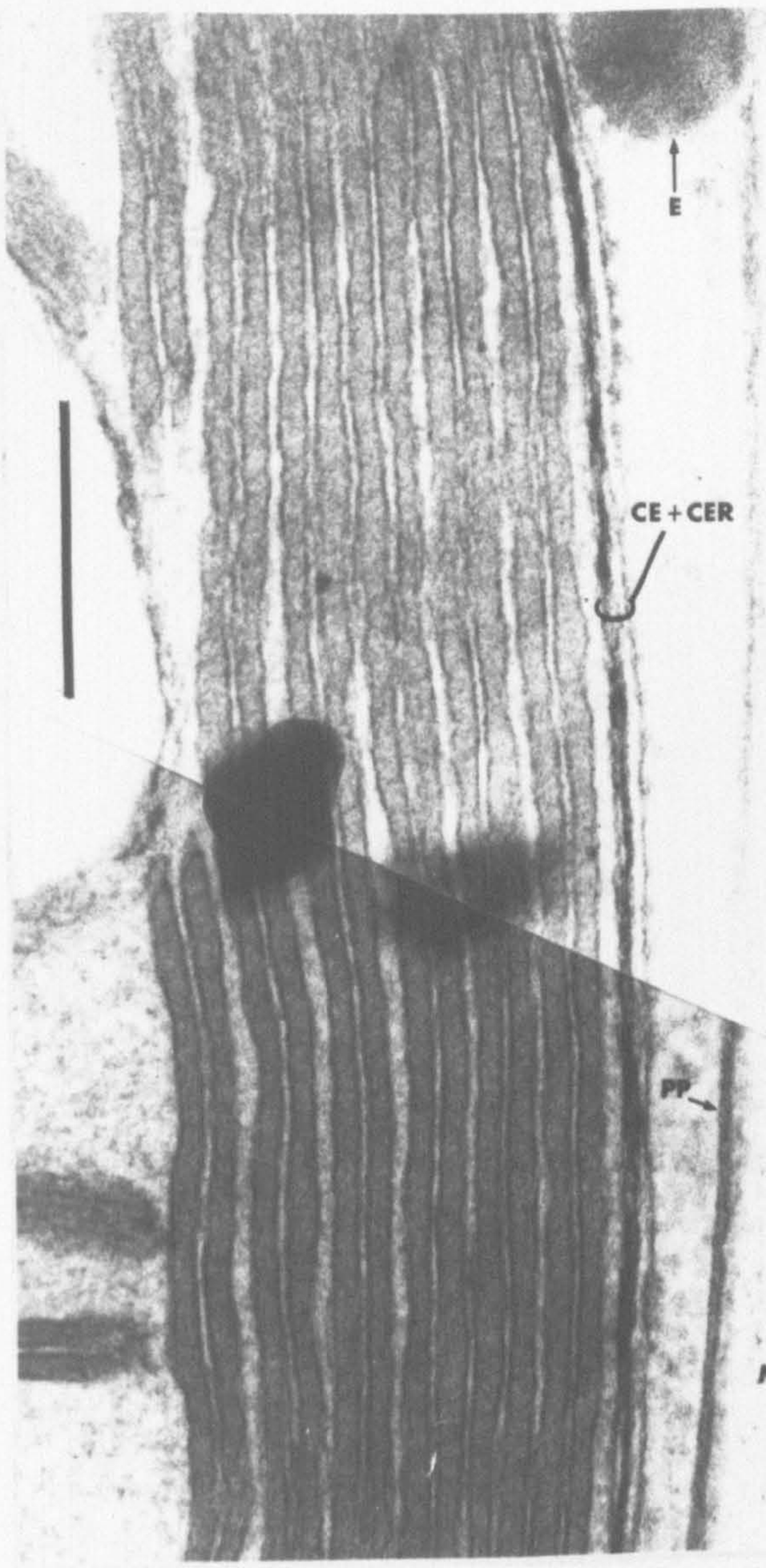

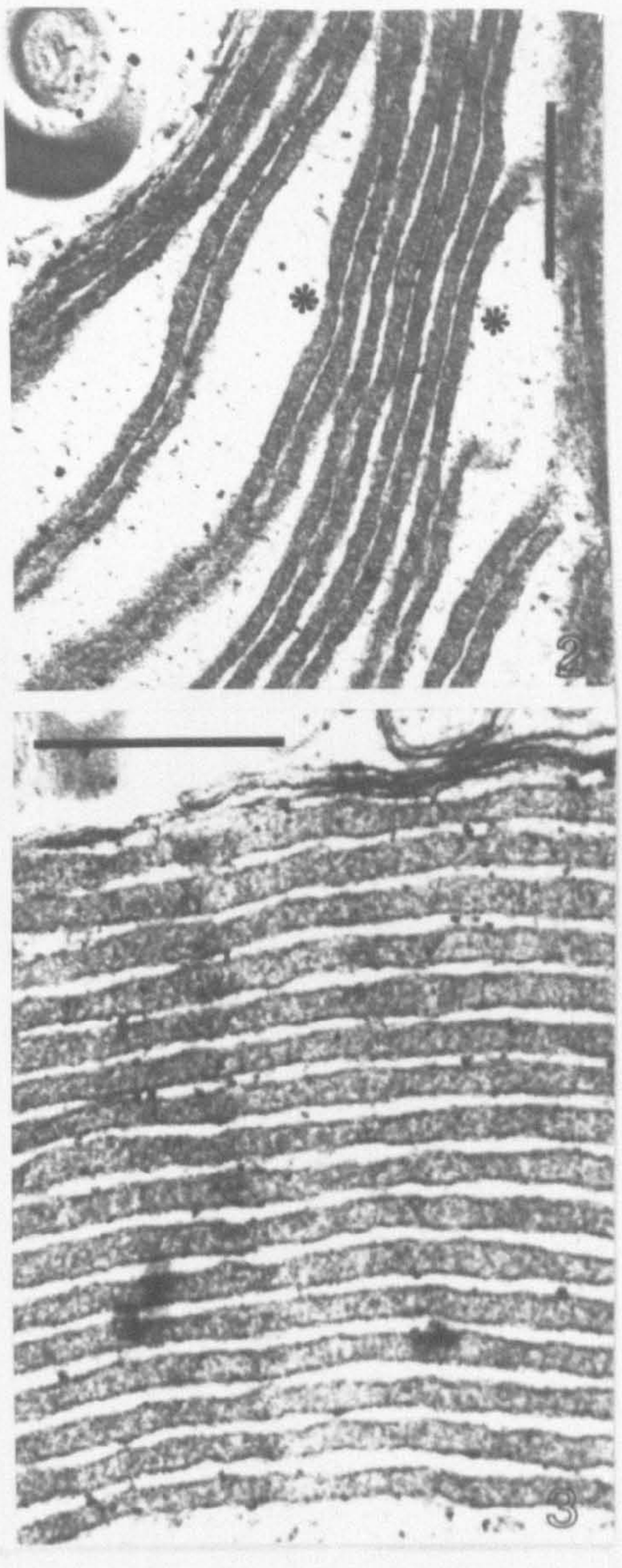

PLATE 42

PLATE 43

Chroomonas collegionis CCAP 978/11, TEM, glutaraldehyde / osmium: two consecutive oblique sections of a single palmelloid cell

The boxed regions in Figs 1 and 3 are shown at higher magnification in Figs 2 and 4. Note the eyespot (ES), and the transverse and longitudinal microtubular profiles (arrows) between it and the flagellar base (FB). In Fig. 2 there is also a vesicle with hair-like contents (arrowhead). Scale bars = 2 µm (Figs 1, 3) or 0.5 µm (Figs 2, 4).

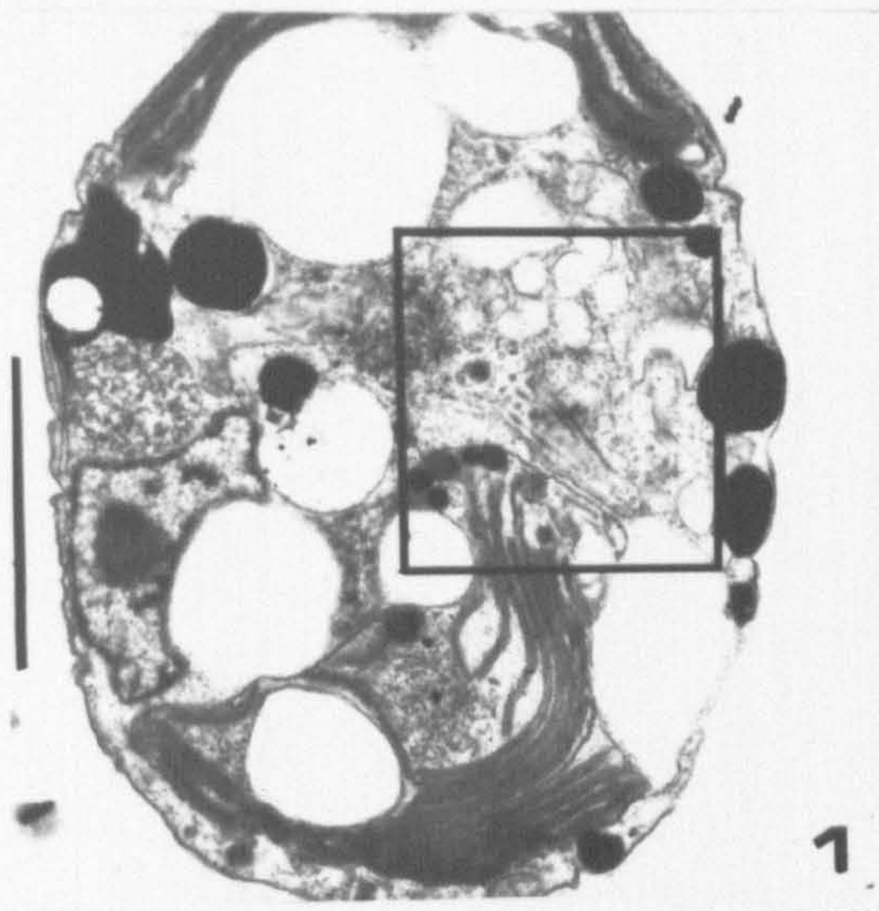

1

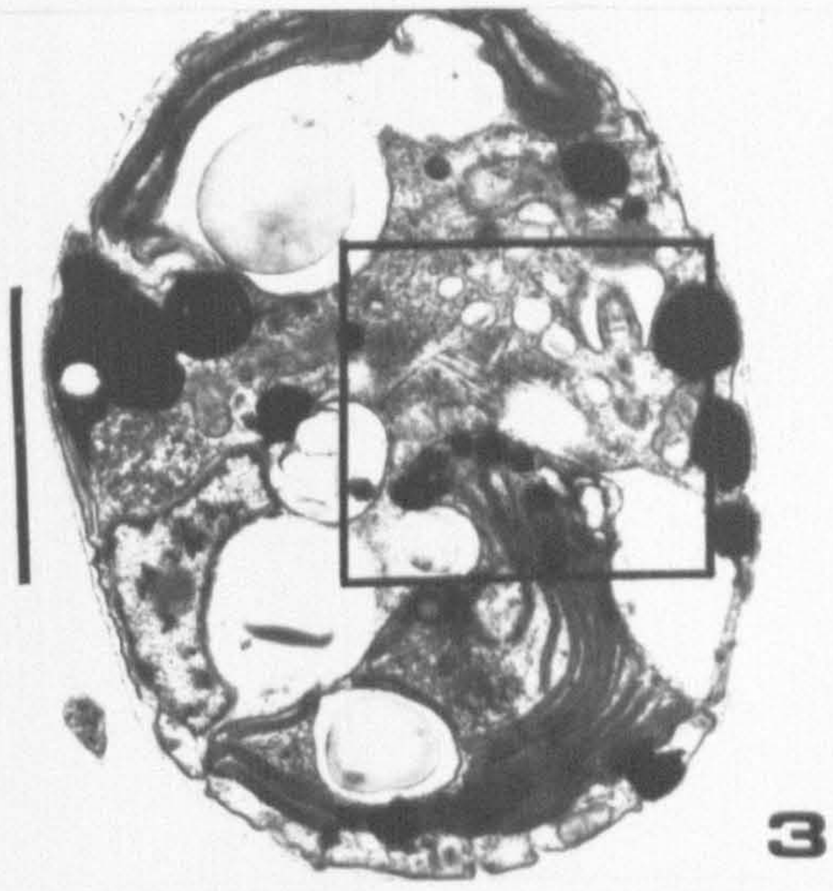

3

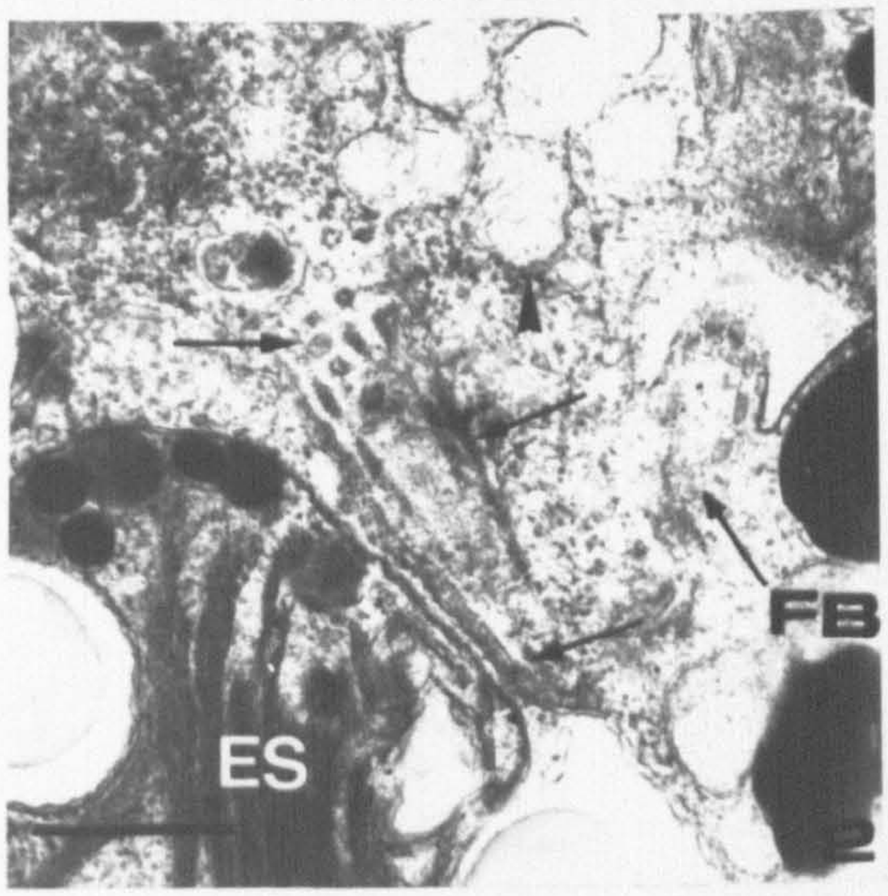

2

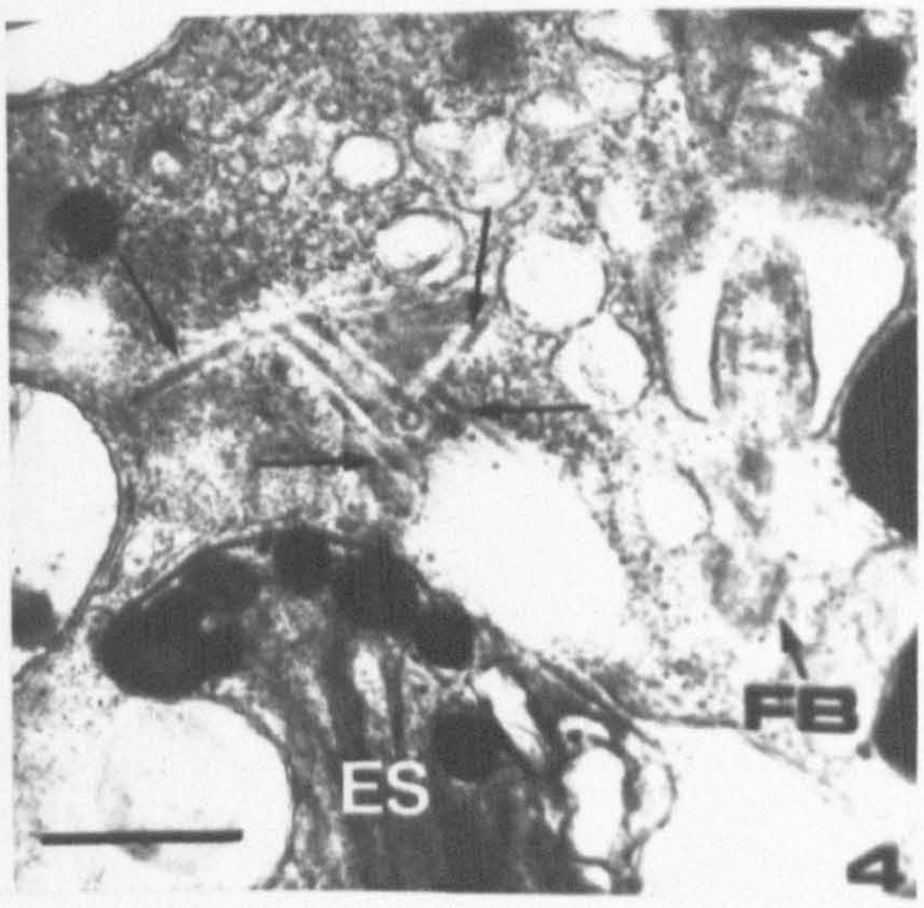

4

PLATE 43

PLATE 44

Chroomonas collegionis CCAP 978/11, TEM, glutaraldehyde / osmium unless otherwise stated: various views of the nucleomorph

In all Figs, G = dense globules, FGB = fibrillo-granular body; the arrowheads point towards the chloroplast.

In each Fig., note the different orientation of G and FGB relative to the chloroplast. Fig. 2 is an OTO-fixed specimen. Scale bars = 0.5 µm.

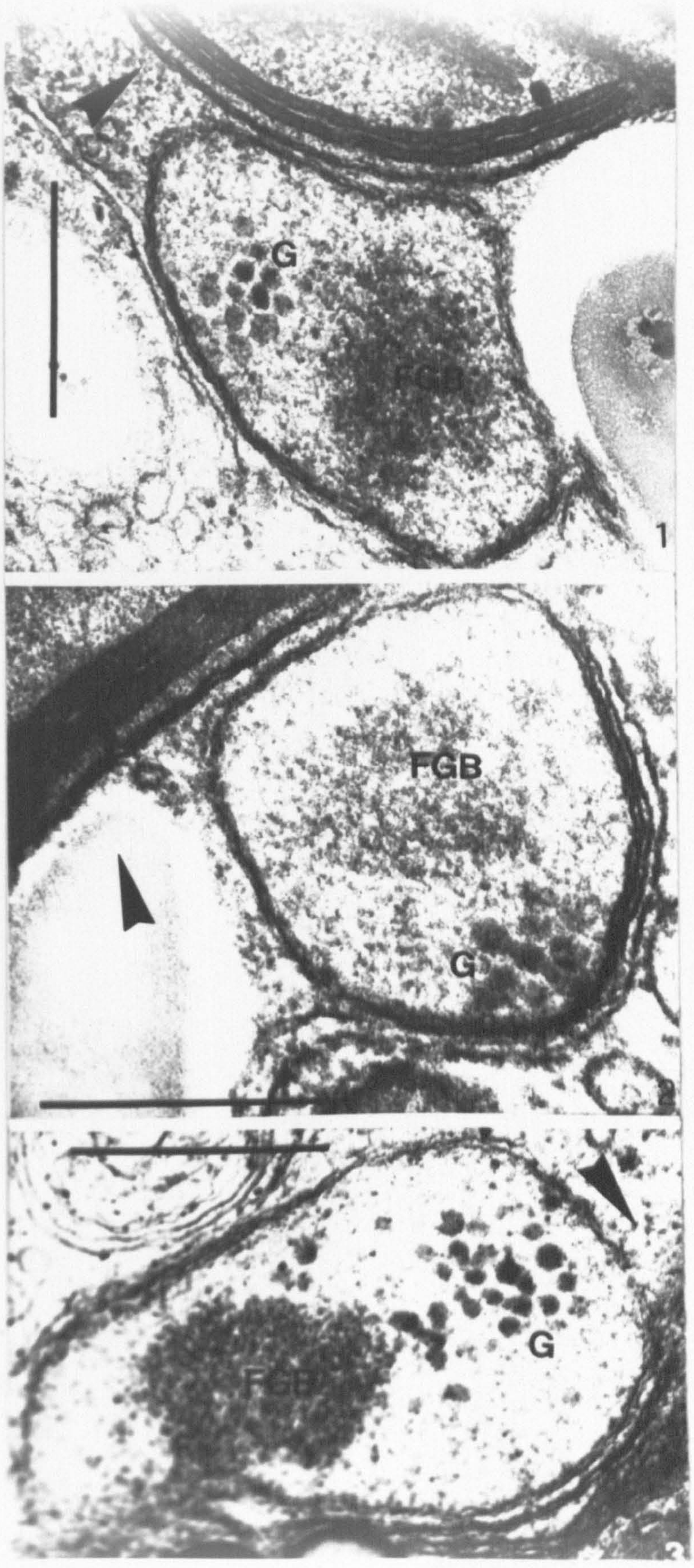

PLATE 44

PLATE 45

Chroomonas collegionis CCAP 978/11, TEM, glutaraldehyde / osmium: miscellanous inclusions

Fig. 1. A group of virus-like particles, contained in a membrane-bound vesicle. Scale bar = 100 nm. Fig. 2. A dense body within the chloroplast, surrounded by two thylakoids forming a closed loop. Scale bar = 250 nm.

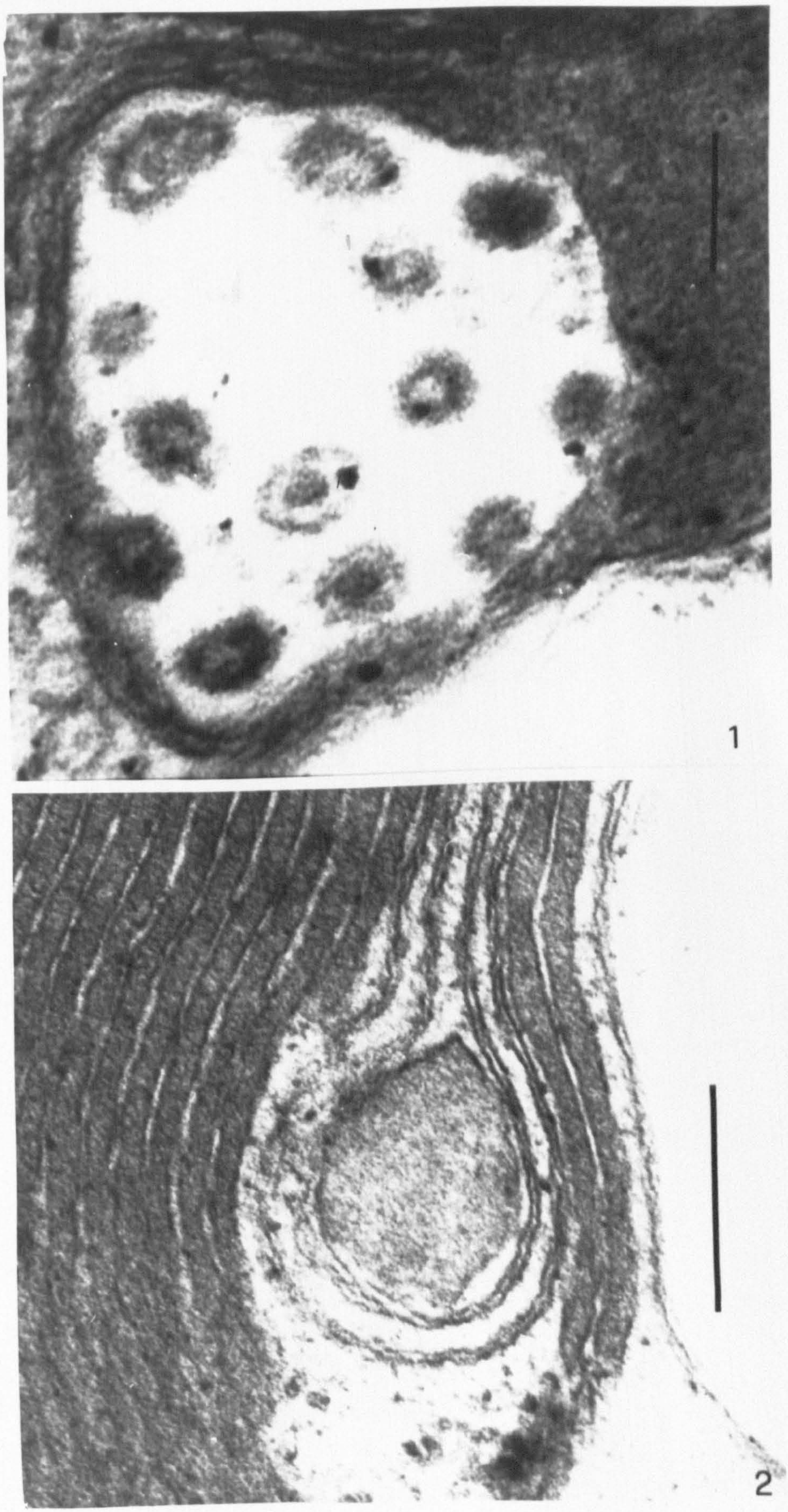

1

2

PLATE 45

PLATE 46

Further TEM views of the periplast of *Rhinomonas reticulata*, strain Theta/C

Fig. 1 shows an empty ejectosome vesicle fused with the plasma membrane. Figs 2 & 3 show the typical serrated appearance of the periplast. Scale bars = 0.2 µm.

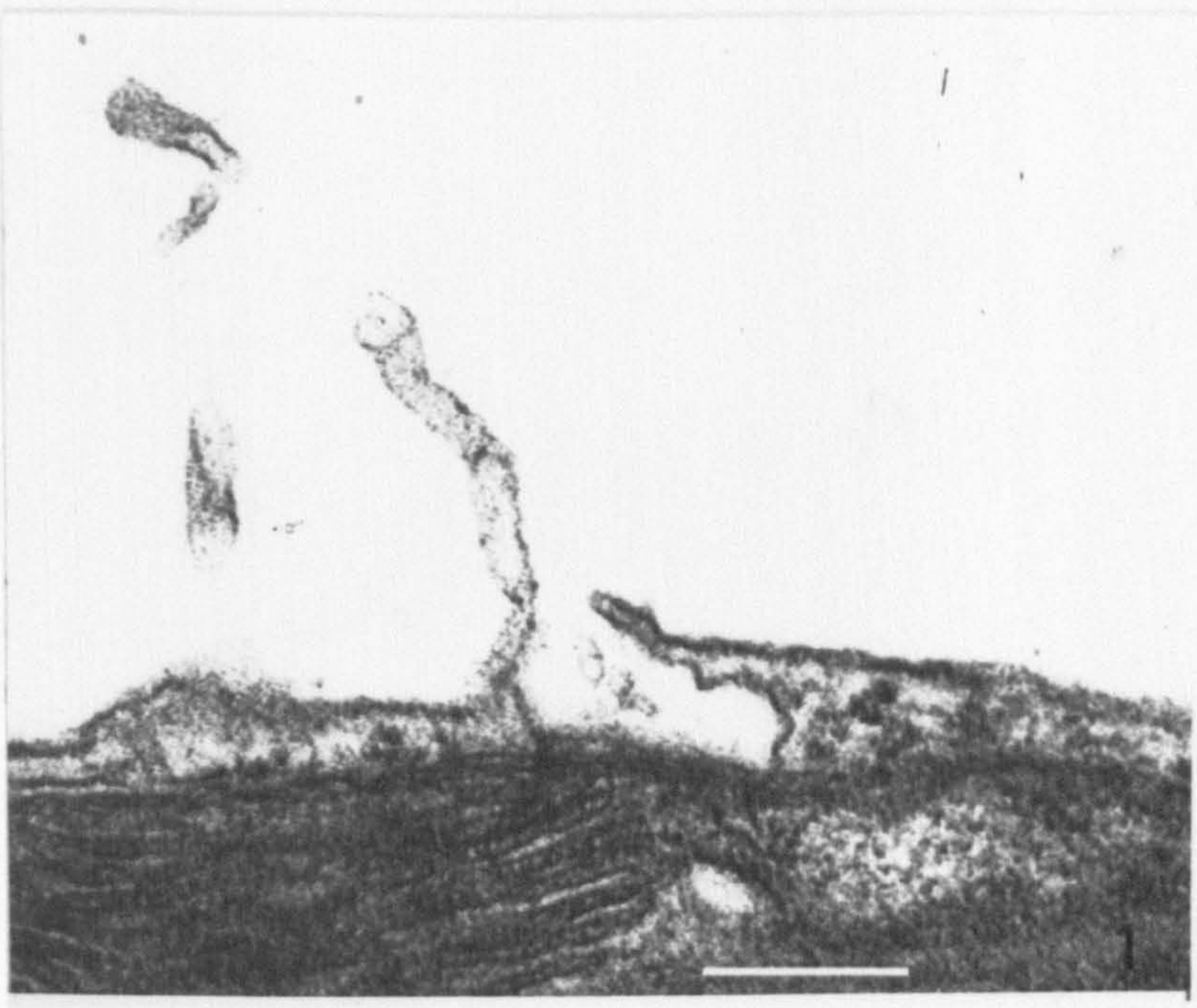

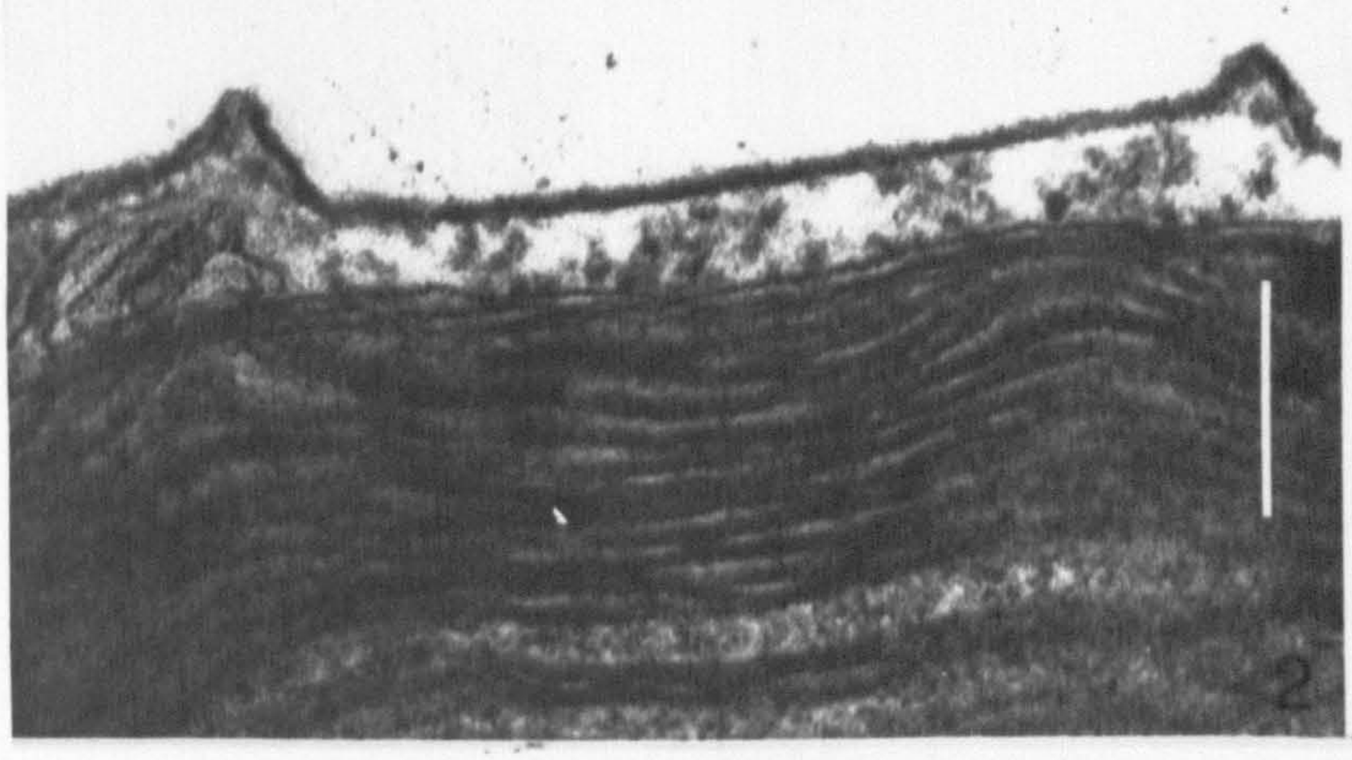

PLATE 46

PLATE 47

A comparison of the Golgi bodies in palmelloid cells of *Chroomonas collegionis* CCAP 978/11, and motile cells of *Rhinomonas reticulata*, strain CCAP 995/2. TEM, glutaraldehyde / osmium unless otherwise stated

Fig. 1. *C. collegionis*; three stacks of cisternae (dictyosomes) are present in this palmelloid cell (arrowheads). Each dictyosome is composed of few cisternae, moderately appressed in the median region, and distinctly swollen at the periphery.
Figs 2, 3. Two sections of different motile cells of *R. reticulata*, OTO fixation. Only one dictyosome is present. It is made up of numerous cisternae, considerably appressed in the median region, and only slightly swollen at the periphery.
Scale bars = 0.5 µm (Fig. 1) or 0.25 µm (Figs 2, 3).

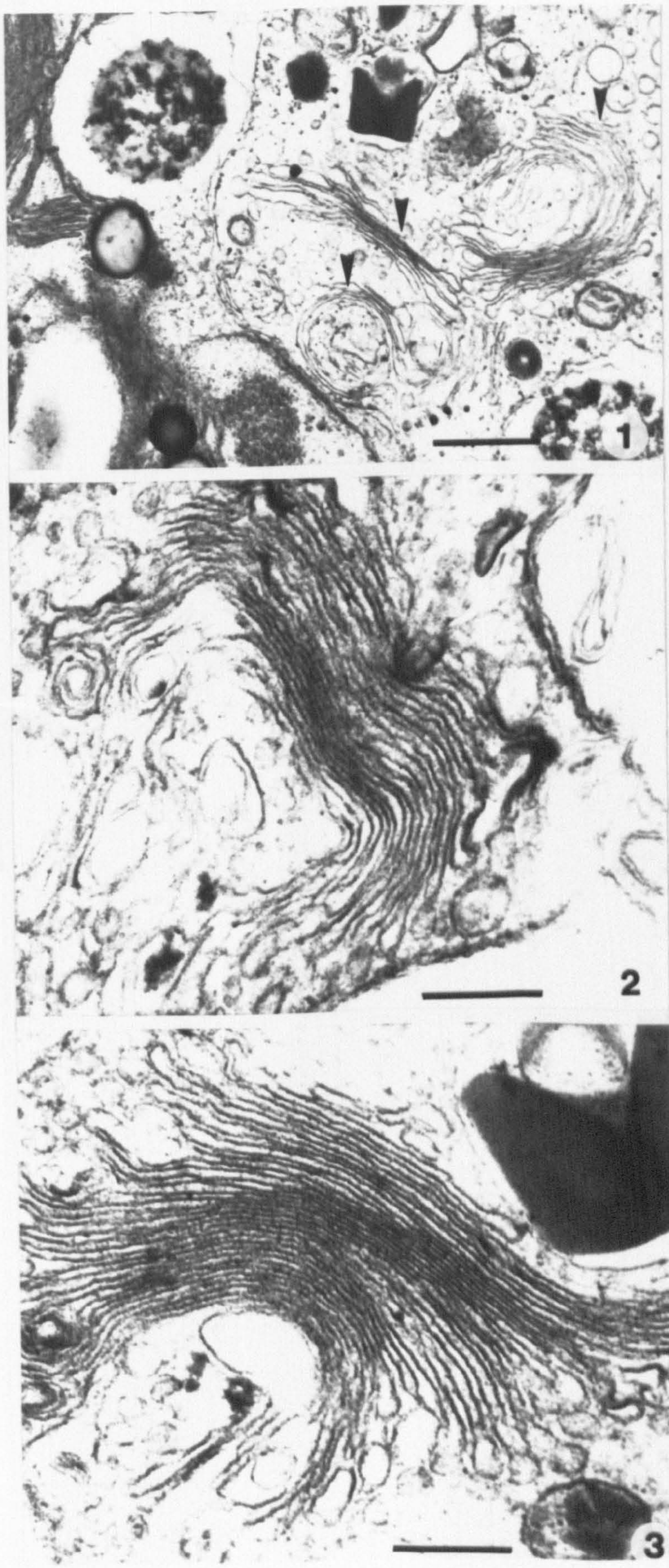

PLATE 47

PLATE 48

Flagellar features in *Chroomonas collegionis* and *Rhinomonas reticulata*, TEM, glutaraldehyde / osmium unless otherwise stated

Figs 1-3. *C. collegionis* (OTO fixation in Figs 1 & 2). Fig. 1 is a section of a flagellum inside the gullet, showing the usual 9 + 2 arrangement of microtubules in the axoneme; numerous tubular mastigonemes are also visible. Fig. 2 is a section in the transition region between the 9 + 2 axoneme and the 9 + 0 flagellar base (Fig. 3). Fig. 4. Longitudinal section of the flagellum of *R. reticulata*; the basal region is distinctly swollen. Scale bars = 0.2 µm (Figs 1, 3), 0.1 µm (Fig. 2), or 0.5 µm (Fig. 4).

PLATE 48

PLATE 49

Consecutive (non-serial) sections through the gullet of *Rhinomonas reticulata* strain CCMP 3C, TEM, glutaraldehyde / osmium

The sections show the typical 'platform' towards the basal region on the flagella, which carries a tuft of mastigonemes. Scale bars = 0.5 µm.

1

2

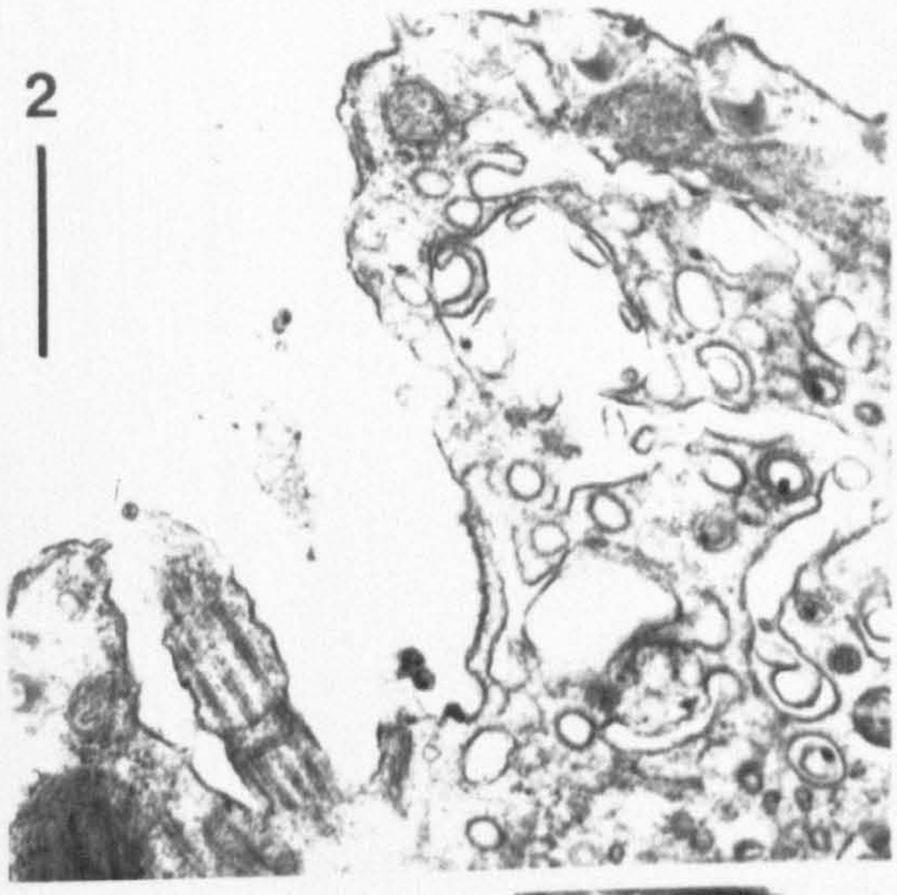

3

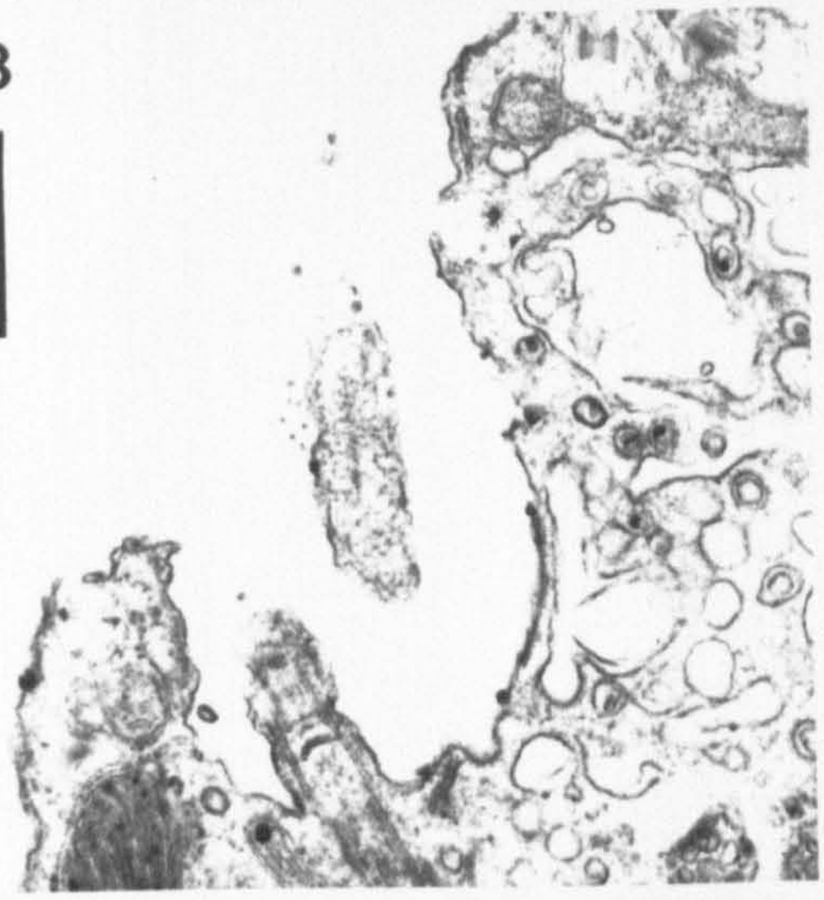

4

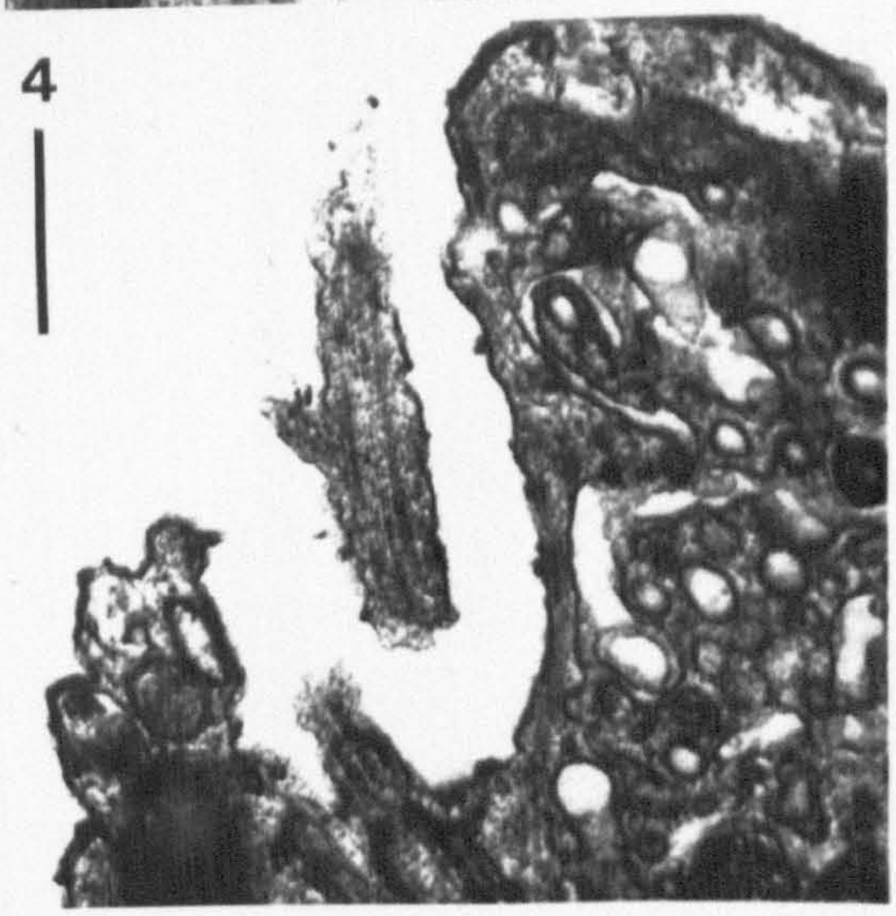

5

6

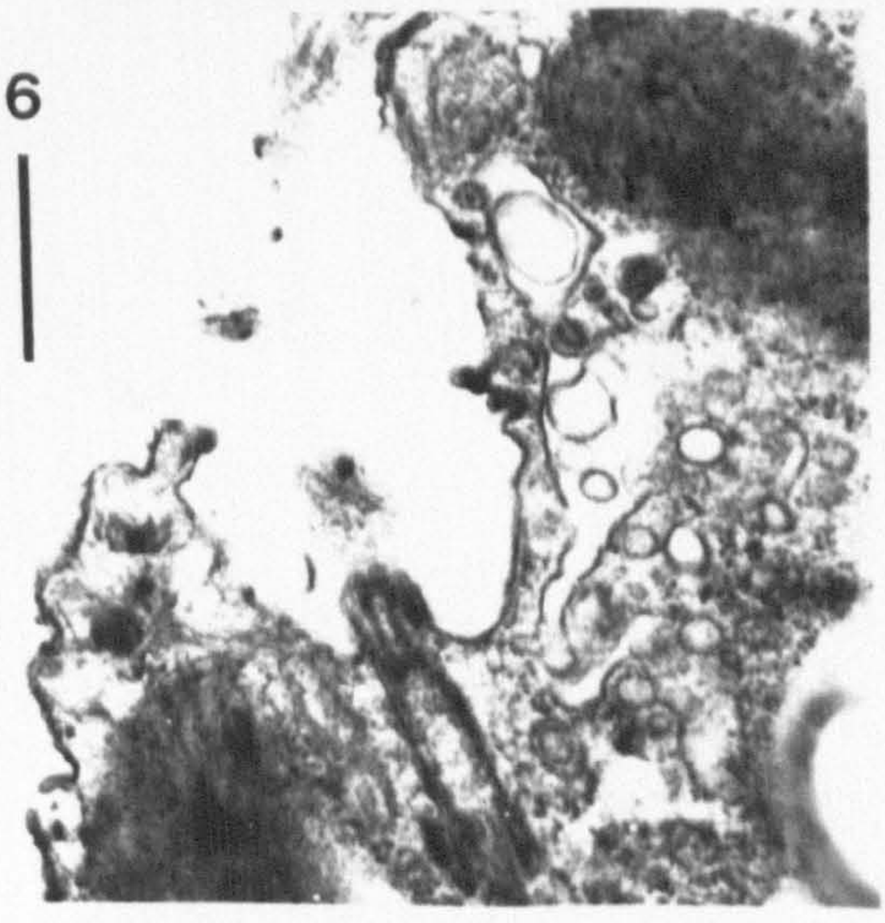

PLATE 49

PLATE 50

Ejectosome features, TEM, glutaraldehyde / osmium unless otherwise stated

Fig. 1. *Rhinomonas reticulata*, strain CCAP 995/2, OTO fixation. Note the difference in size between the gullet ejectosomes (arrowhead), and those present in the median region of the cell (arrow). The latter are probably newly formed peripheral ejectosomes, not yet transported to their final destination. Figs 2 - 4. *Chroomonas collegionis*: gullet ejectosomes. Note the typical subunits (Figs 2, 3), and the distinct lamellar appearance (Fig. 4). Scale bars = 1 µm (Fig. 1), or 0.25 µm (Figs 2 - 4).

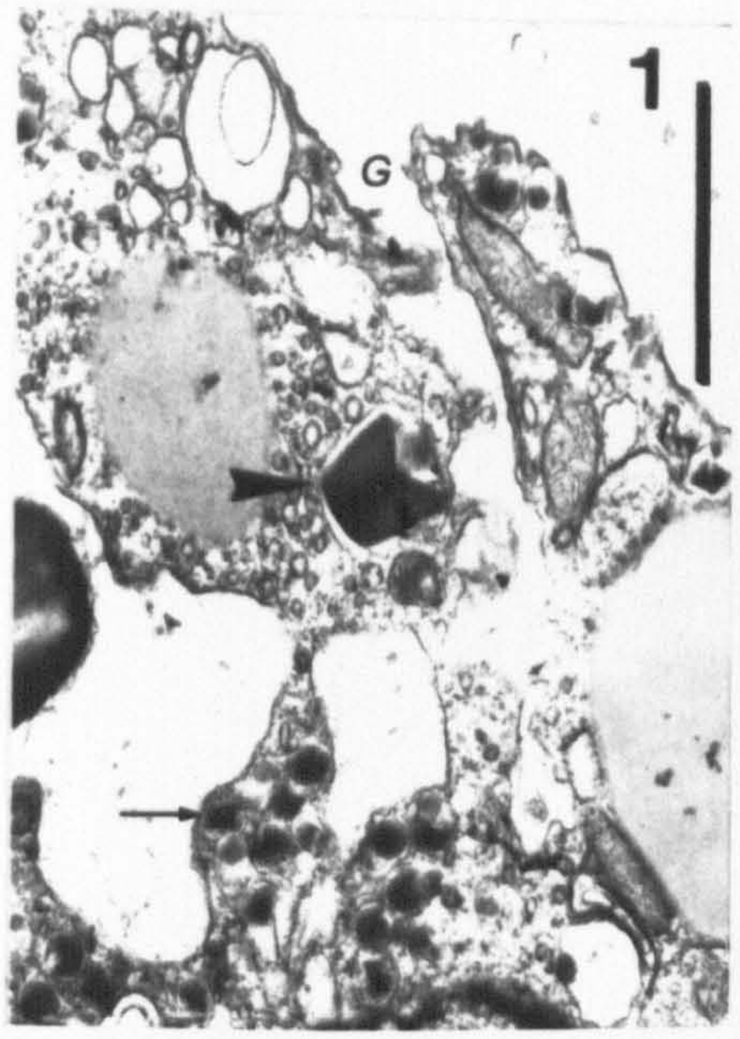

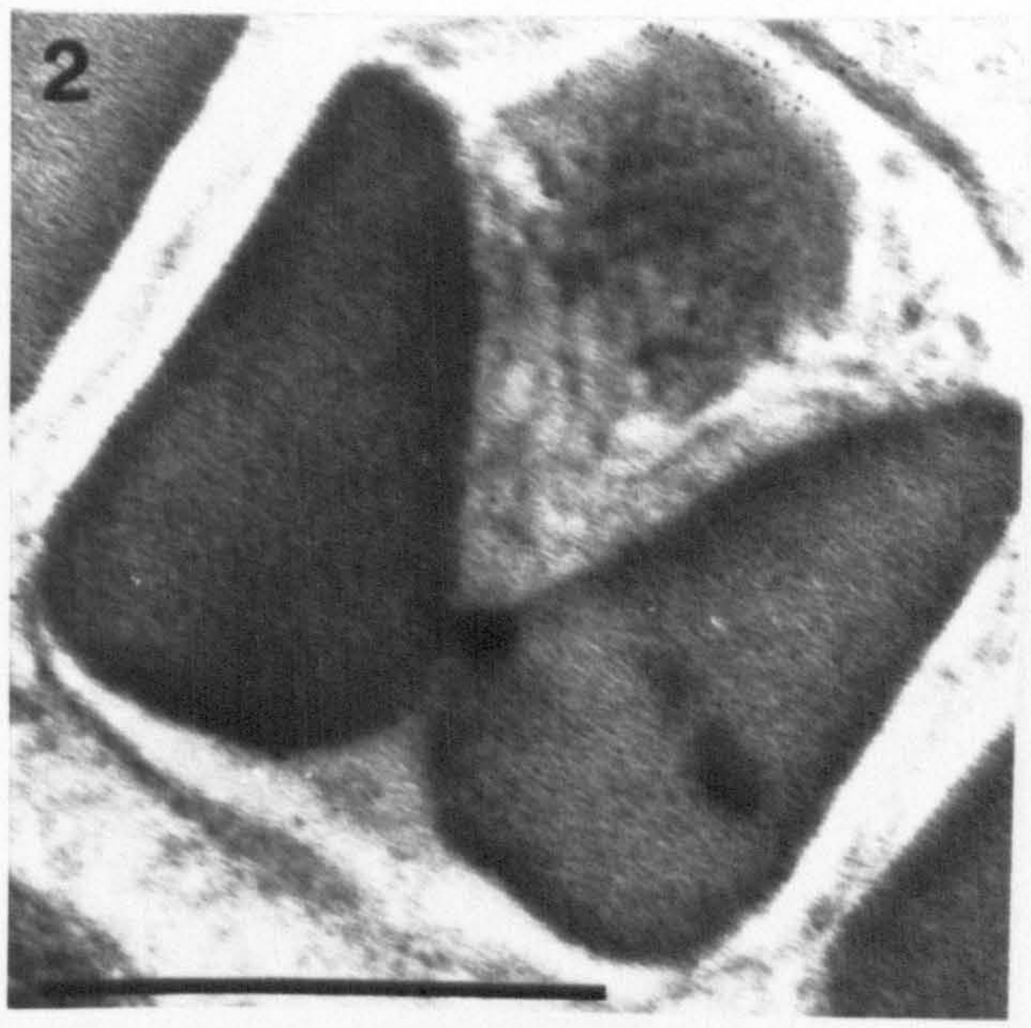

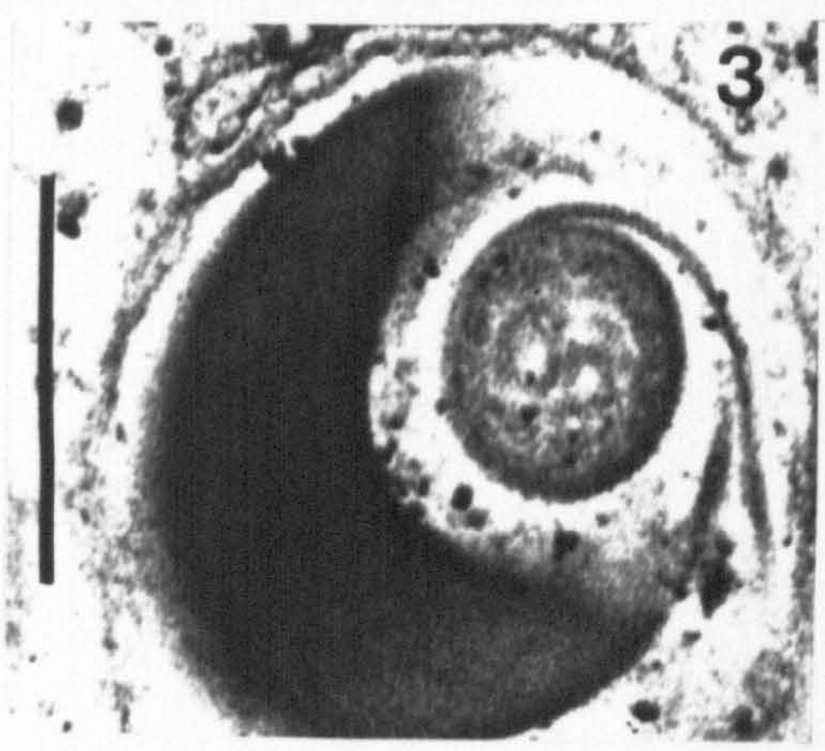

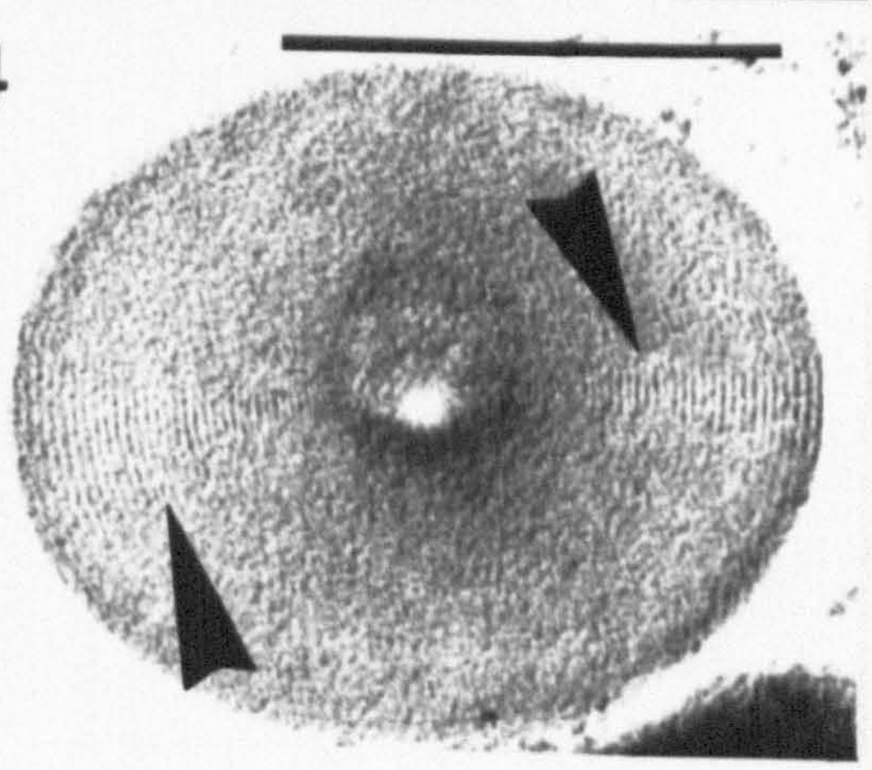

PLATE 50

PLATE 51

Mastogloia smithii, phase-contrast light microscopy

Fig. 1. External view of valve with circular central area. Fig. 2a. External view of broken valve with rectangular central area. Fig. 2b. Internal view of valve in Fig. 2a, showing the pseudoseptum (arrow). Fig. 3. Valvocopula in valve view, showing the partectal ring with a longitudinal element between its margins (small arrow), and the septum with its four protuberances (arrowheads) and U-shaped apices (large arrows). Fig. 4. Frustule in girdle view, showing the septa of the valvocopulae (arrowheads), and a pseudoseptum inside the valve apex (arrow). Fig. 5. Broken partectal ring in valvar view, showing the partectal ducts (arrows). Scale bars = 10 µm (Figs 1-4) or 5 µm (Fig. 5).

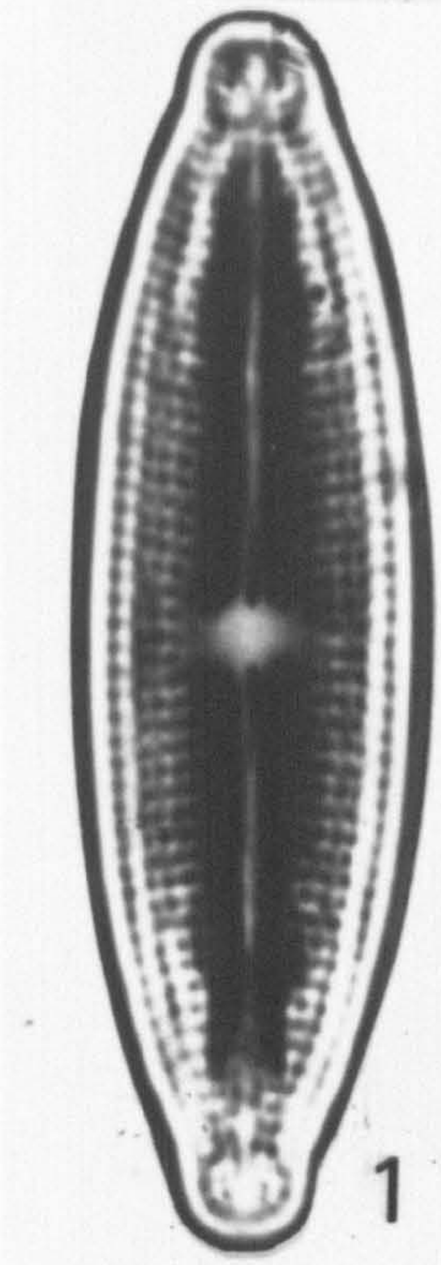

1

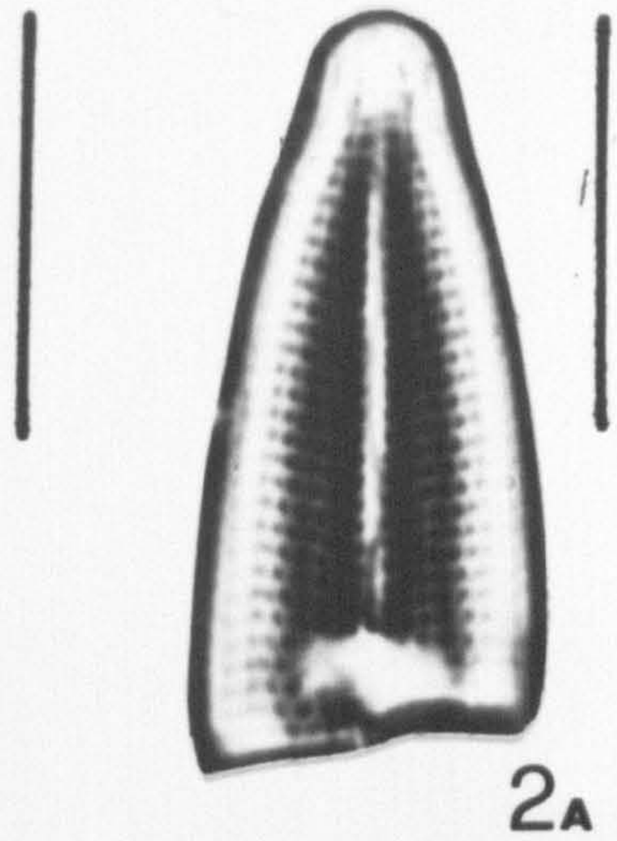

2A

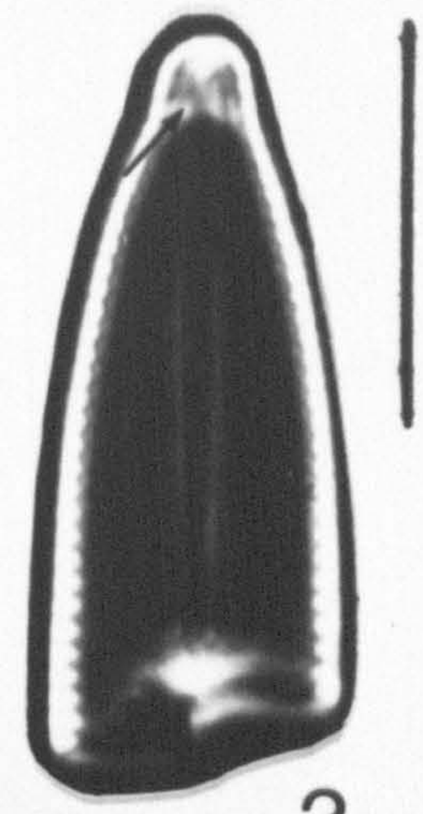

2B

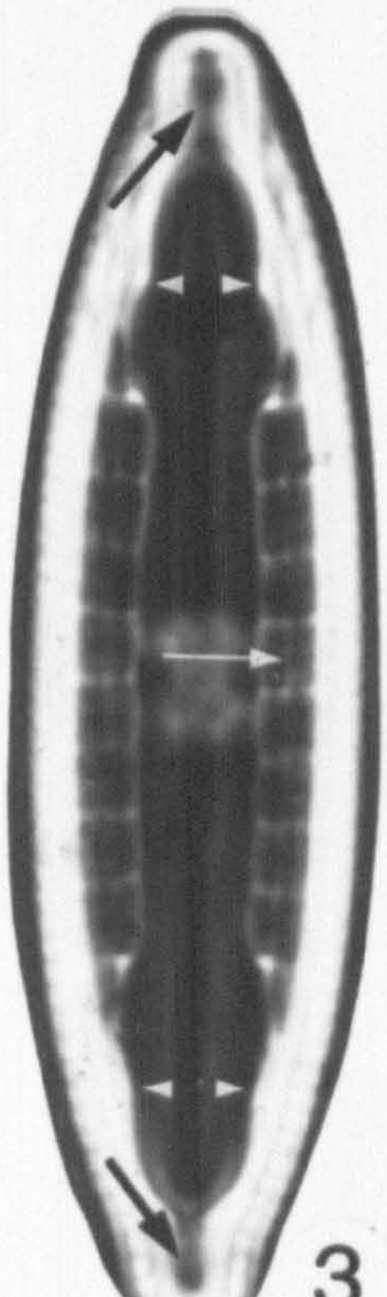

3

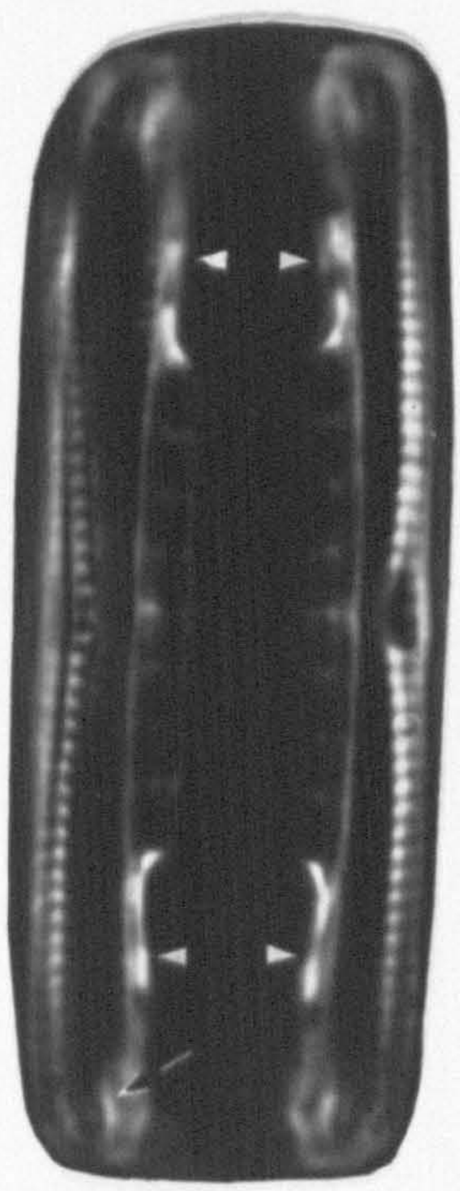

4

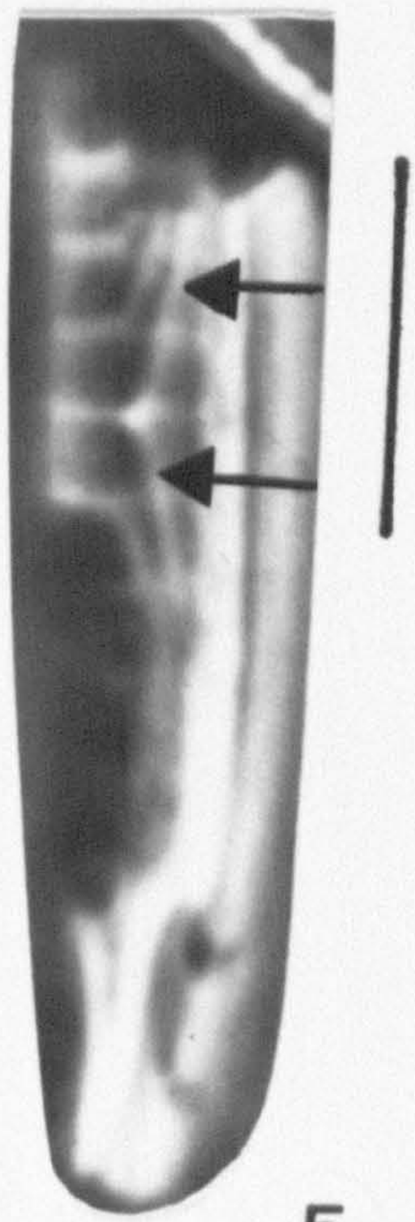

5

PLATE 51

PLATE 52

Mastogloia smithii, SEM: valve features

Fig. 1. External view of valve. Fig. 2. Broken frustule, with several slit-like areolae along the axial area (arrow). Fig. 3. Internal view of valve, showing a pseudoseptum at the valve apex (arrow). Fig. 4. Internal view of valve at higher magnification, showing depressions containing groups of four areolae, and thickened, transverse ribs (interstriae). Fig. 5. Broken valve, showing that each group of four small areolae on the internal face opens into a single pseudoloculus (arrowhead). Scale bars = 5 µm (Figs 1-3) or 1 µm (Figs 4, 5).

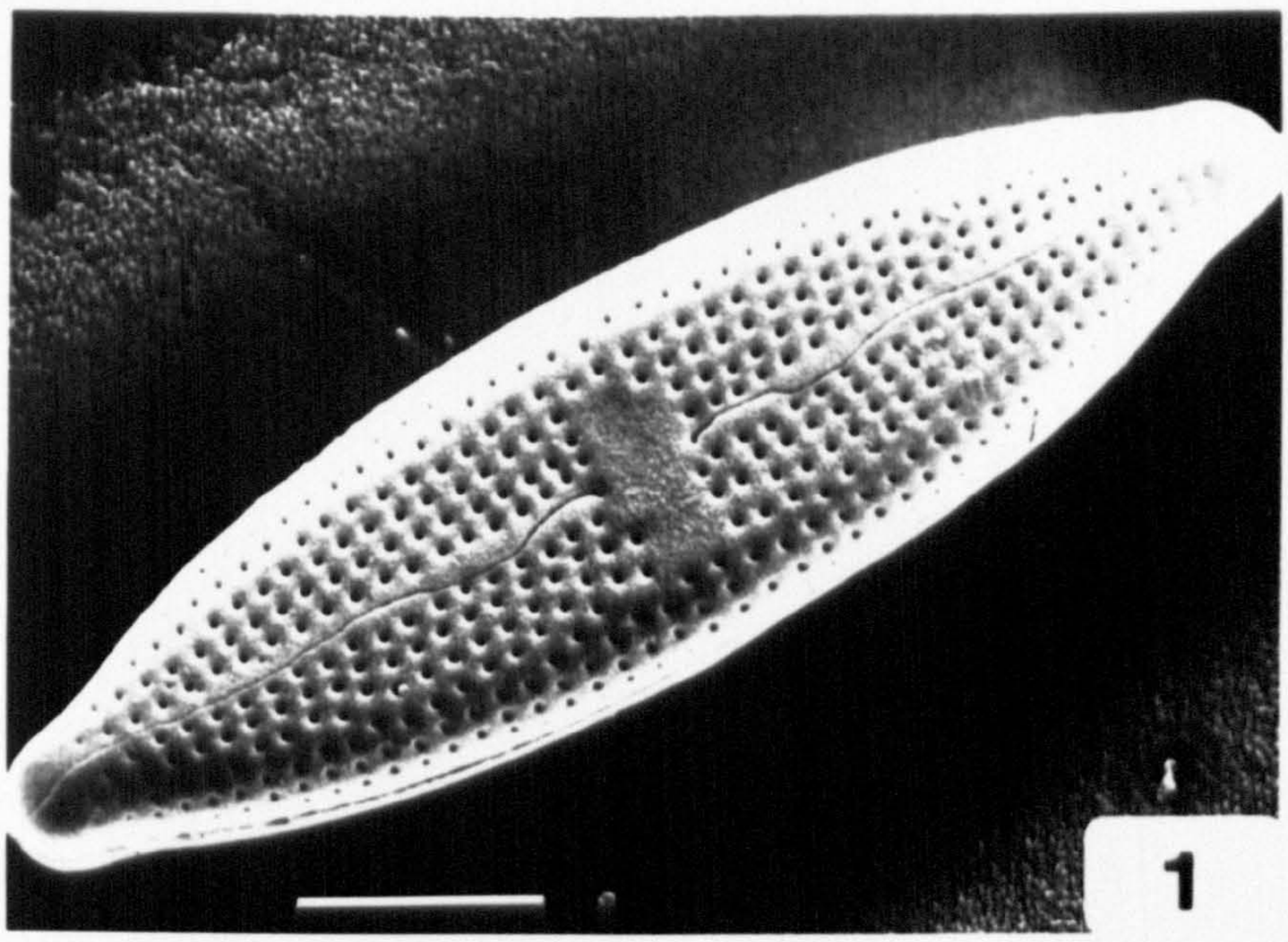

1

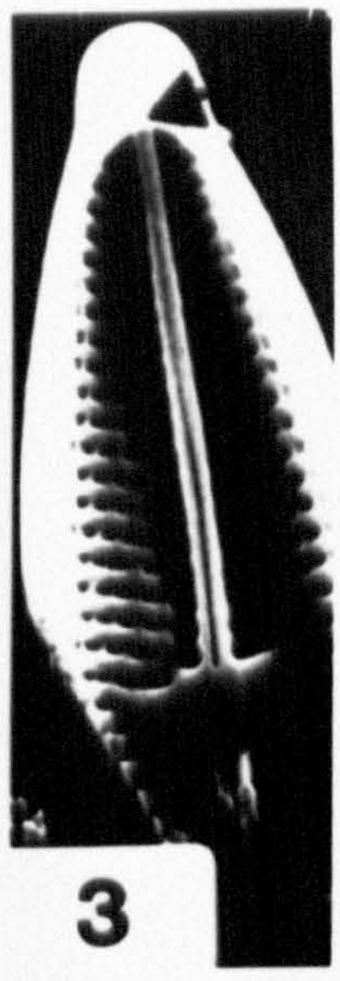

3

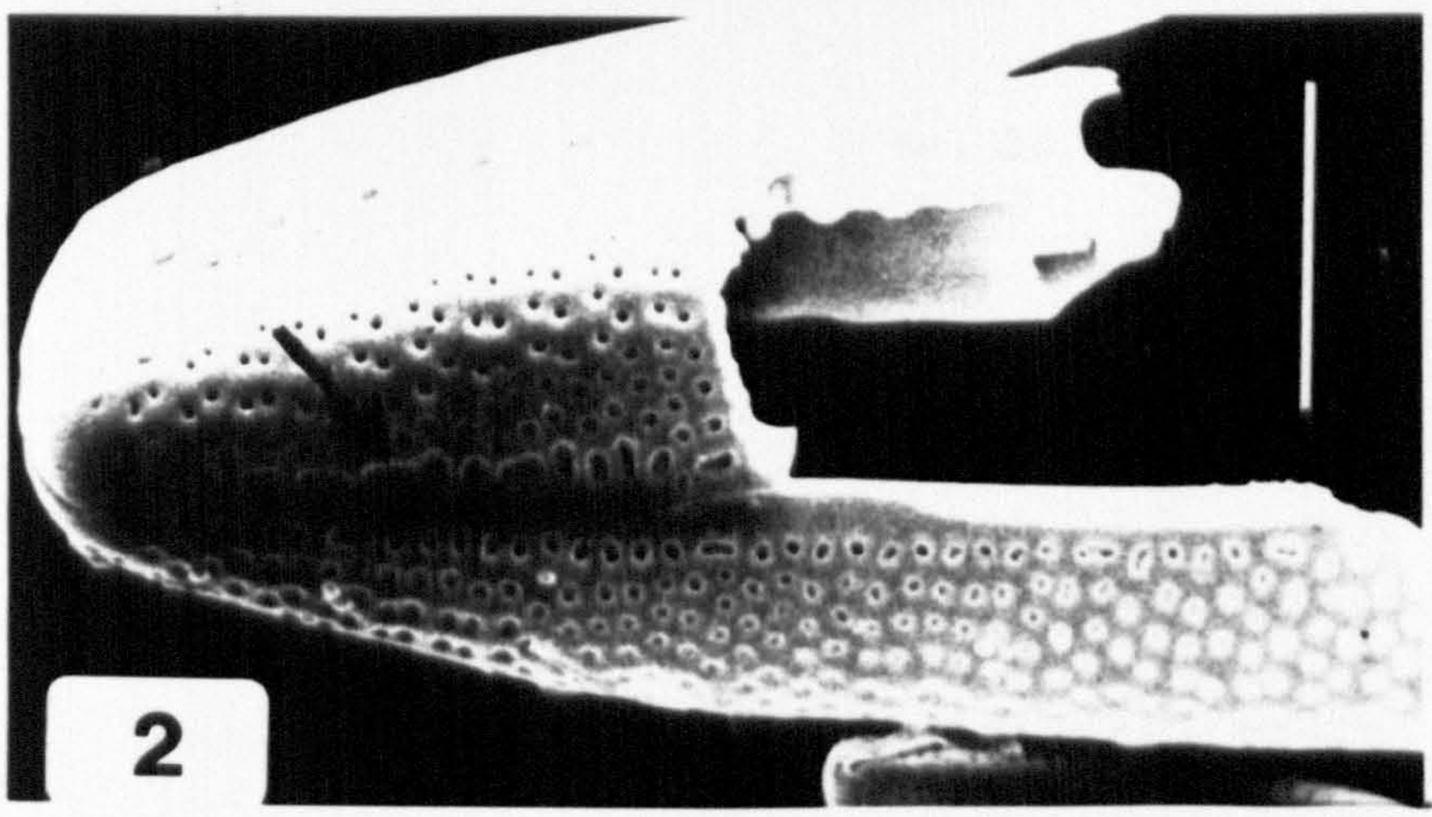

2

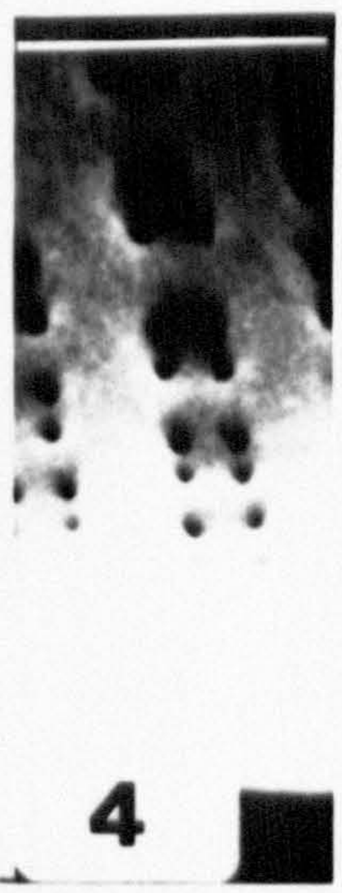

4

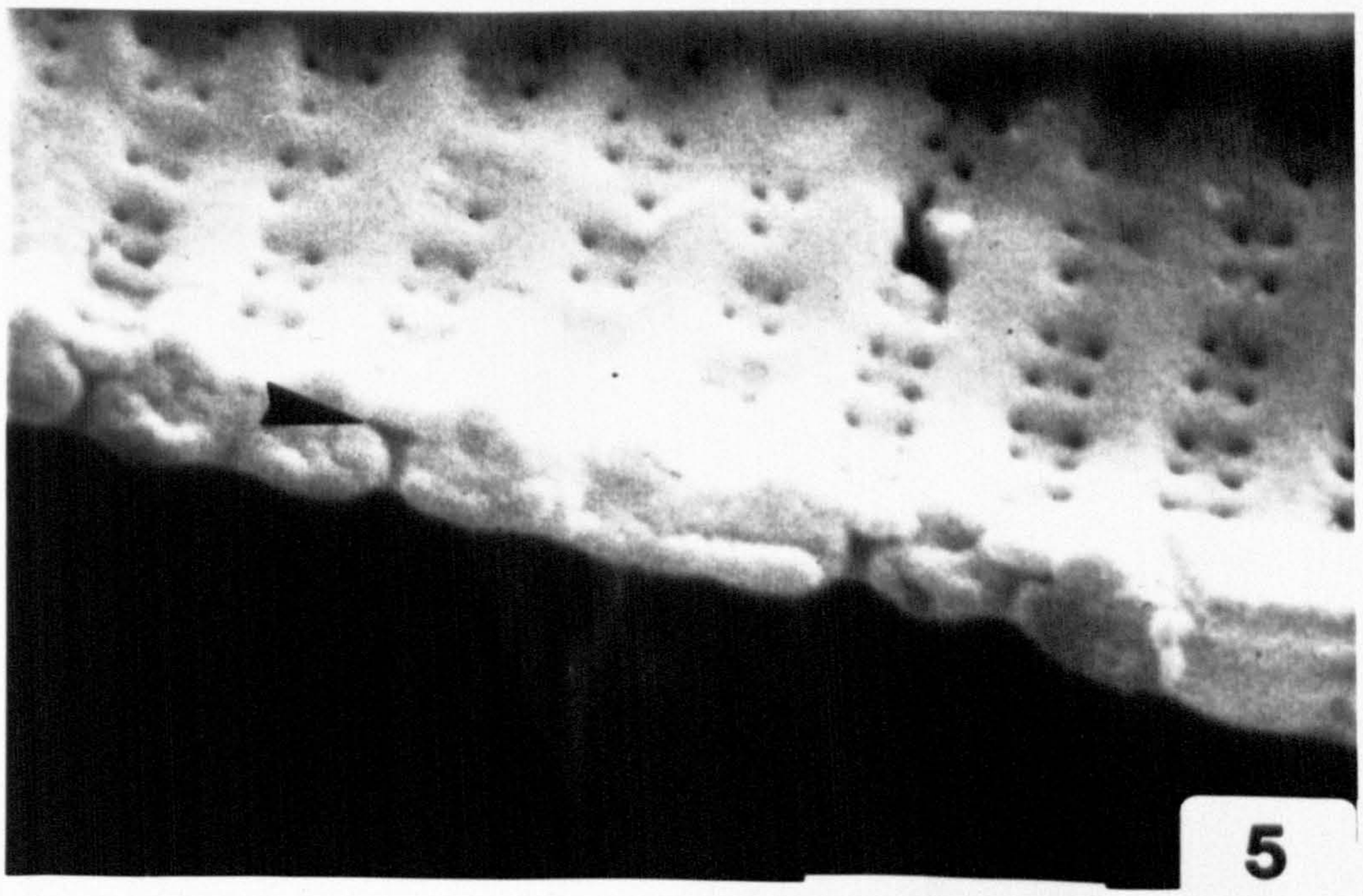

5

PLATE 52

PLATE 53

Mastogloia smithii, SEM: features of the valvocopula (mostly abvalvar views)

Fig. 1. Abvalvar view of a valvocopula attached to its parent valve; scale bar = 10 µm. Fig. 2. Abvalvar view of an apex of a valvocopula attached to its parent valve, showing the pseudopartecta (PP) terminating at one end with a pore-like cavity giving rise to a furrow (arrowhead), and forming a step at the other end (small arrow); note the U-shaped apex of the septum (large arrow); the abvalvar surface of the pseudoseptum of the parent valve is just visible through the slit of the U-figure; scale bar = 2 µm. Fig. 3. A fragment of a partectal ring, with a rupture in the wall (box); scale bar = 5 µm. Fig. 4. Detail of the rupture in Fig. 3, showing the external surface of the porous intrapartectal cylinder; scale bar = 0.5 µm.

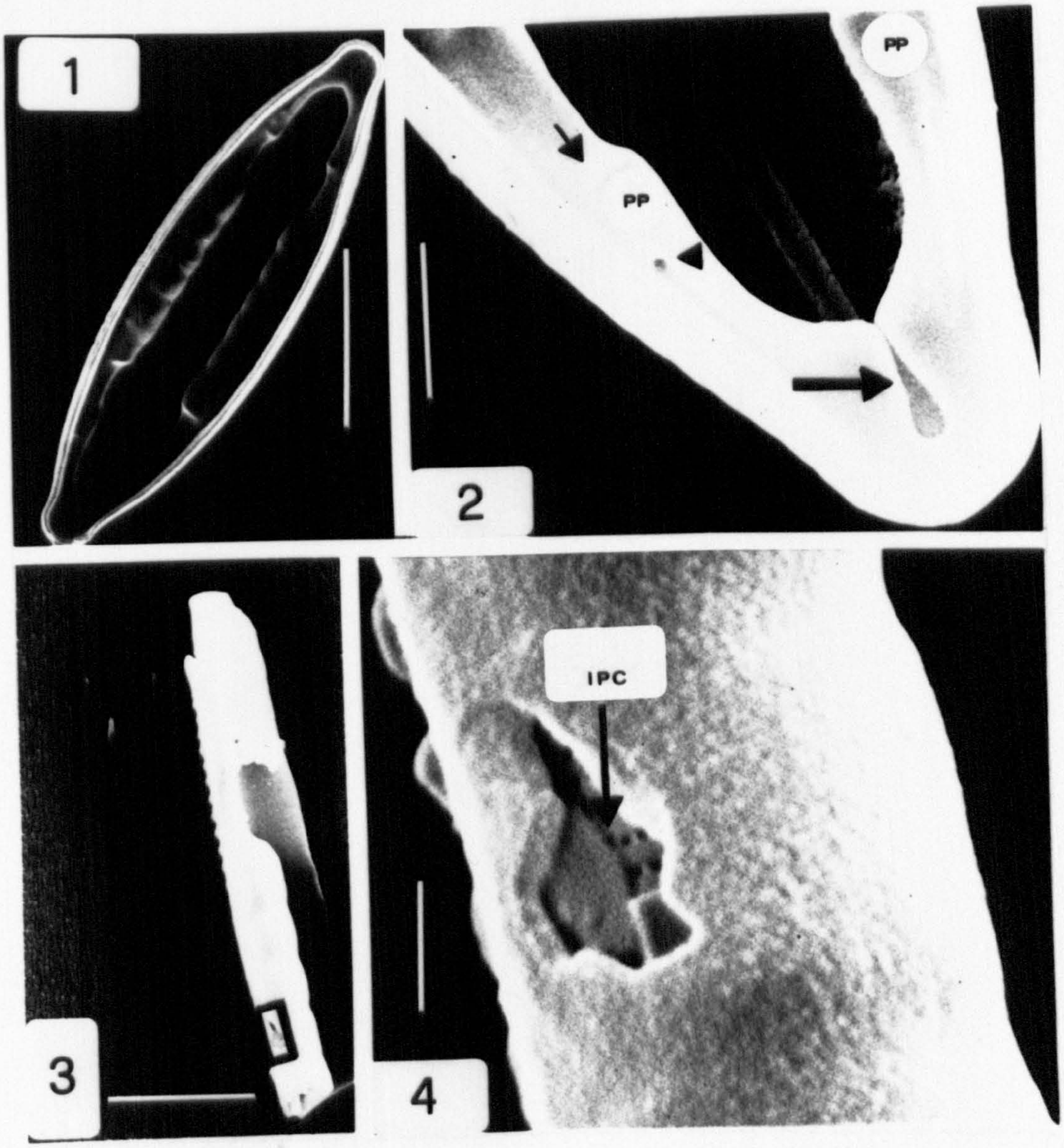

PLATE 53

PLATE 54

Mastogloia smithii, SEM: features of the valvocopula (ab- and advalvar views)

Fig. 1. Abvalvar view of a valvocopula, showing the pars exterior (C), septum (S), and partectal ring (PR); the intrapartectal cylinder is also visible (arrow). Scale bar = 5 µm. Fig. 2. Advalvar face of a valvocopula, showing the intrapartectal cylinder (arrowhead), wavy crest (large arrow), and two club-shaped structures at the apex of the septum (small arrows); scale bar = 5 µm. Fig. 3. Detail of the apex of the valvocopula in Fig. 2, showing the abutting club-shaped structures (arrowheads), and small pores on the external margin of the septum (arrows); scale bar = 1 µm.

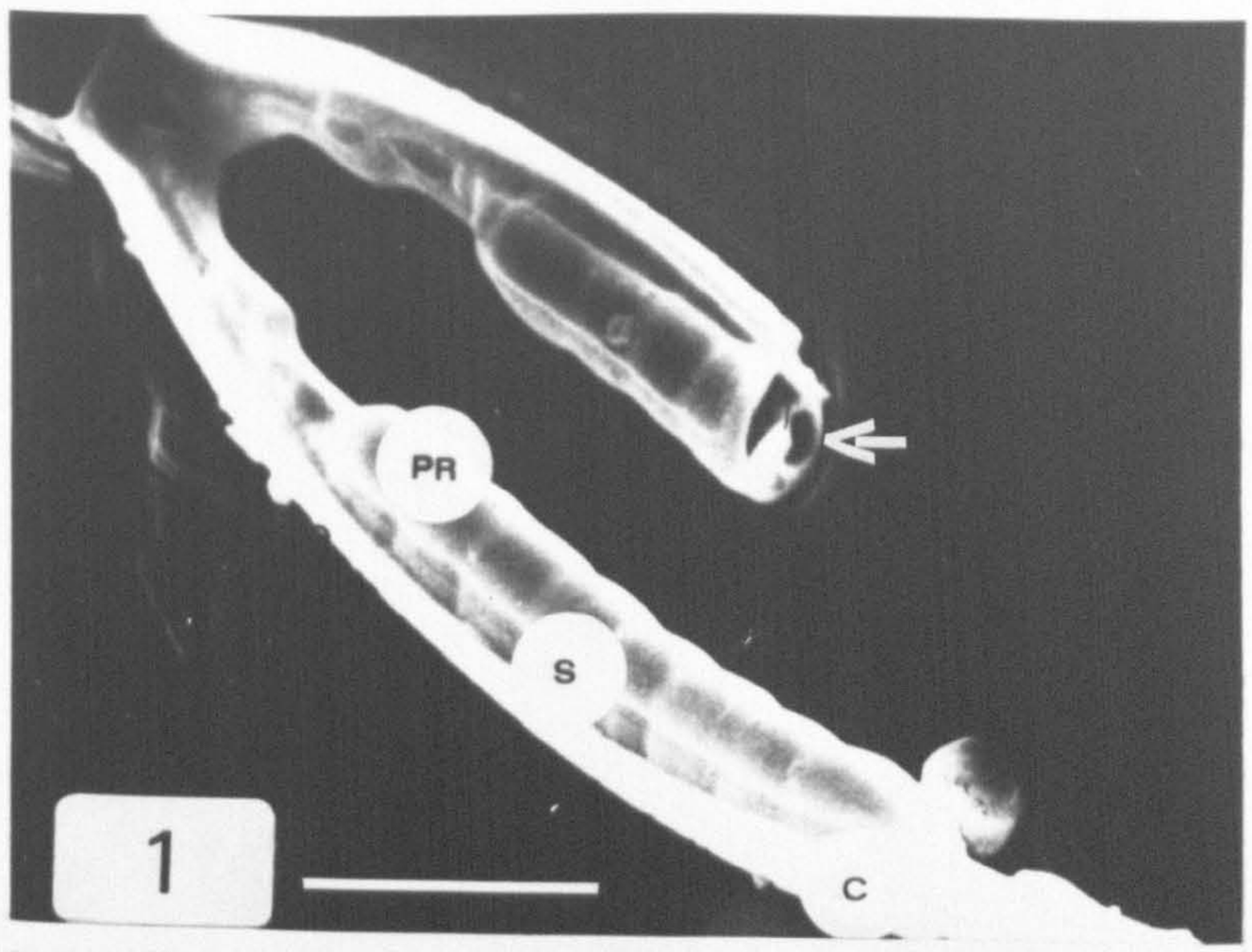

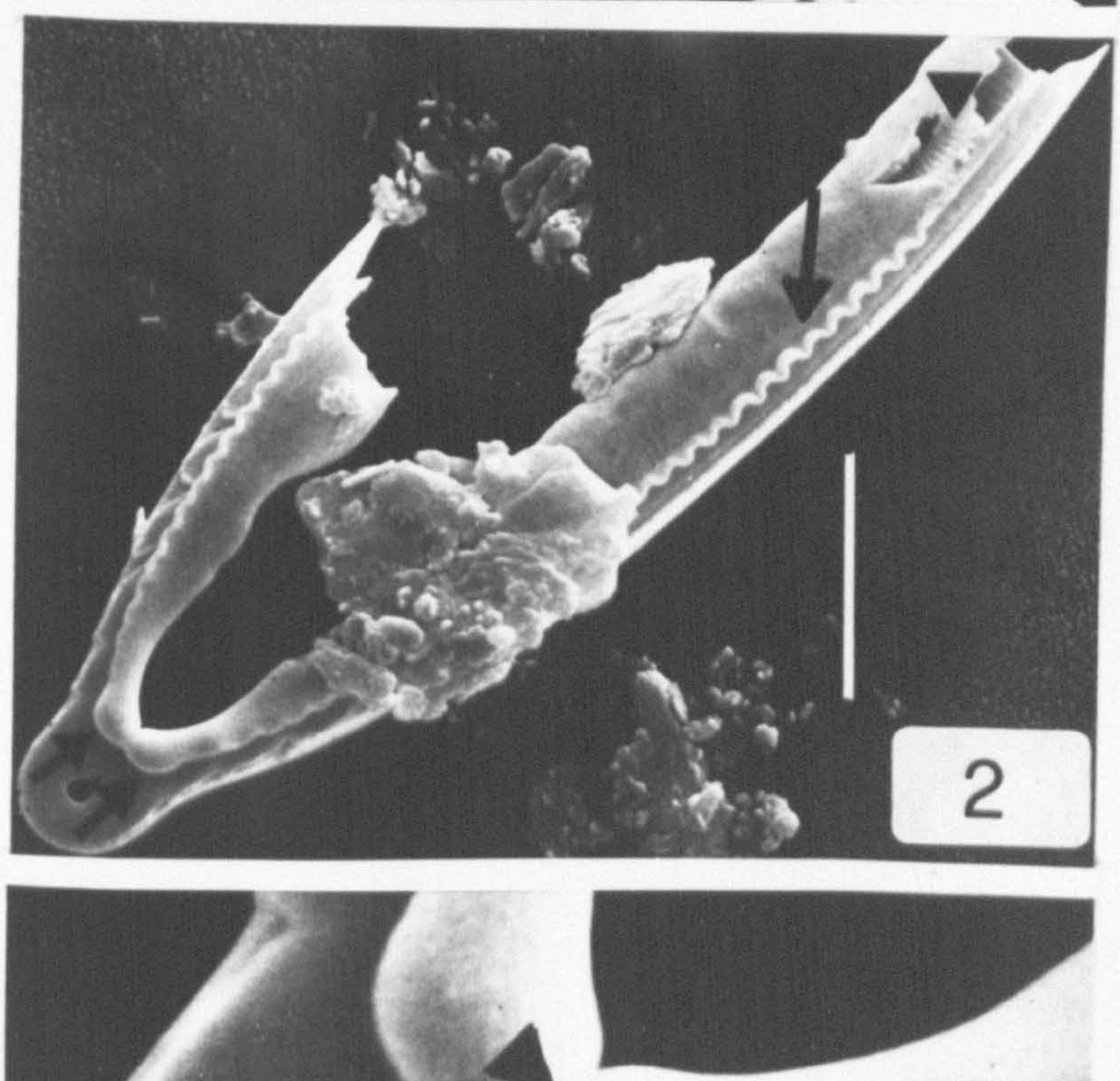

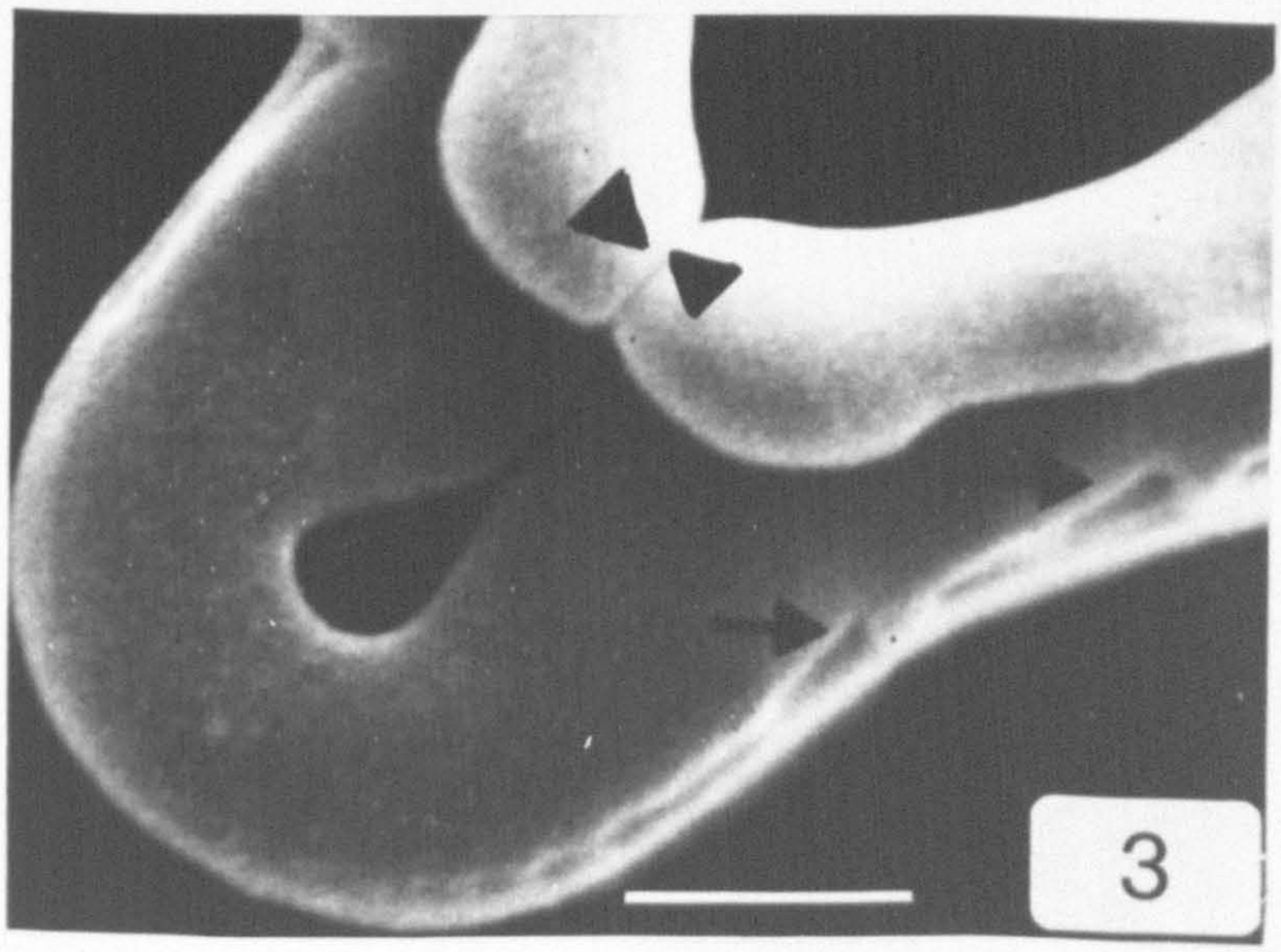

PLATE 54

PLATE 55

Mastogloia smithii, SEM: integration between the valve and the valvocopula

Fig. 1. Broken frustule, showing the wavy crest on the advalvar face of the valvocopula (arrowhead) and a club-shaped structure of the septum lying above the pseudoseptum of the valve (arrow); scale bar = 5 µm. Fig. 2. Detail of the advalvar surface of a partectal ring (PR), the undulating crest borne above the partecta (PU), septum (S), valve mantle (VM), and the pars exterior of the valvocopula (C); scale bar = 0.5 µm. Fig. 3. Higher magnification of the specimen shown in Pl. 52 Fig. 2; septum (S), partectal ring (PR), undulating crest (PU), planar pars exterior (C) with partectal pores, and valve mantle (VM) interacting with the undulating crest (large arrow); partectal ducts visible in the roof of the partectal ring and within the septum (arrowhead), intrapartectal cylinder visible inside the partectal ring (small arrow); scale bar = 2 µm. Fig. 4. Intact frustule, showing notches along the suture between the copula and valve mantle (arrowhead); scale bar = 10 µm. Fig. 5. Internal view of the copula; the club-shaped structures (white arrowhead) are produced by a 180-degree turn of the internal margin of the septum (black arrowhead), leaving a gap (a-b) of 0.5 um in the pervalvar direction; a pseudopartectum (PP) and a portion of the undulating crest (PU) are also visible. Scale bar = 2 µm. Fig. 6. Apex of a valvocopula, showing the partectal pores (arrowhead) in the pars exterior (C), which overlaps the mantle of the parent valve; a pseudopartectum (PP) is also visible. Scale bar = 2 µm.

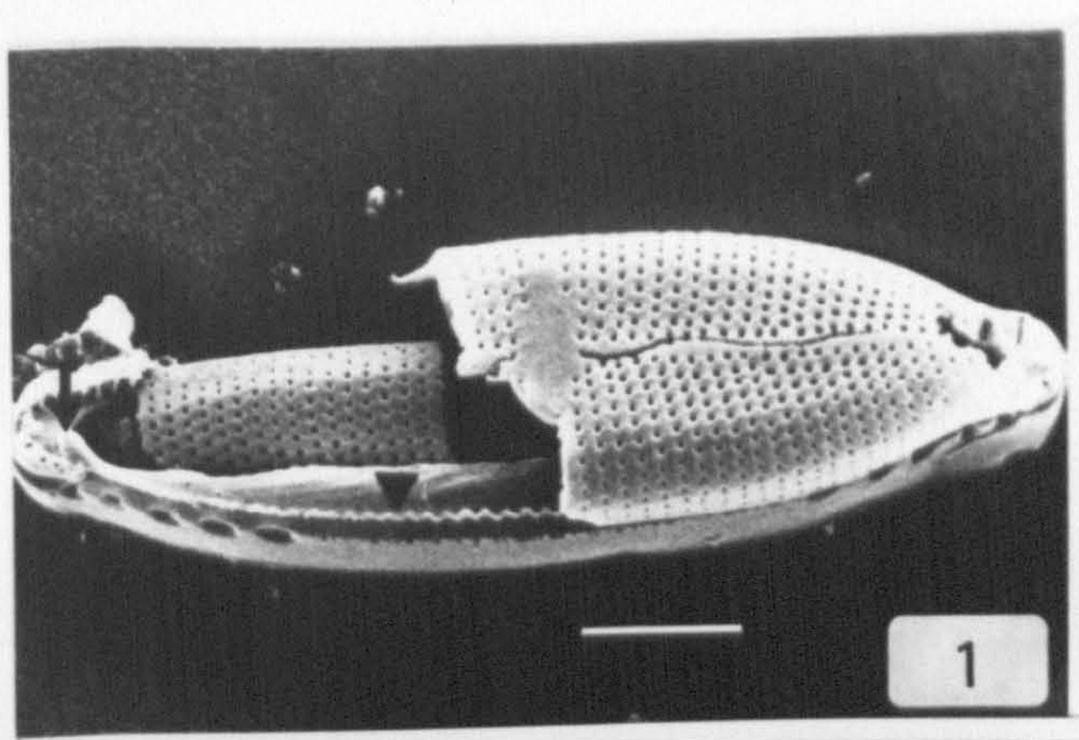

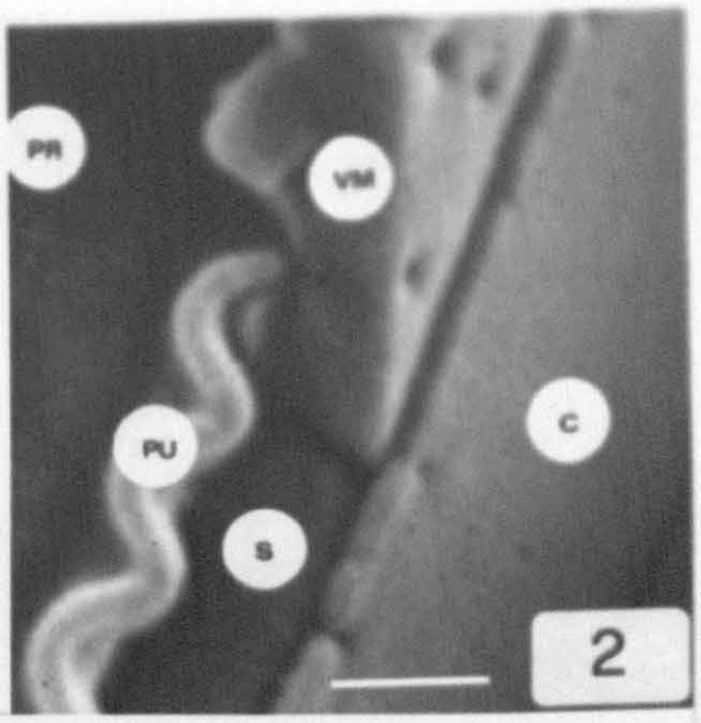

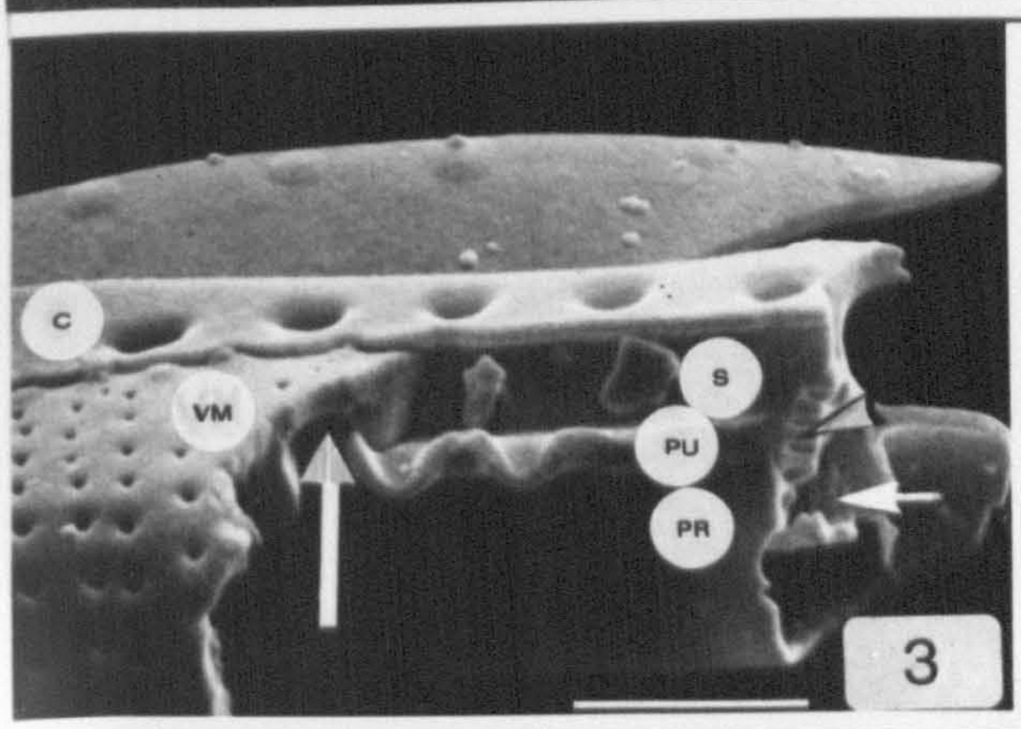

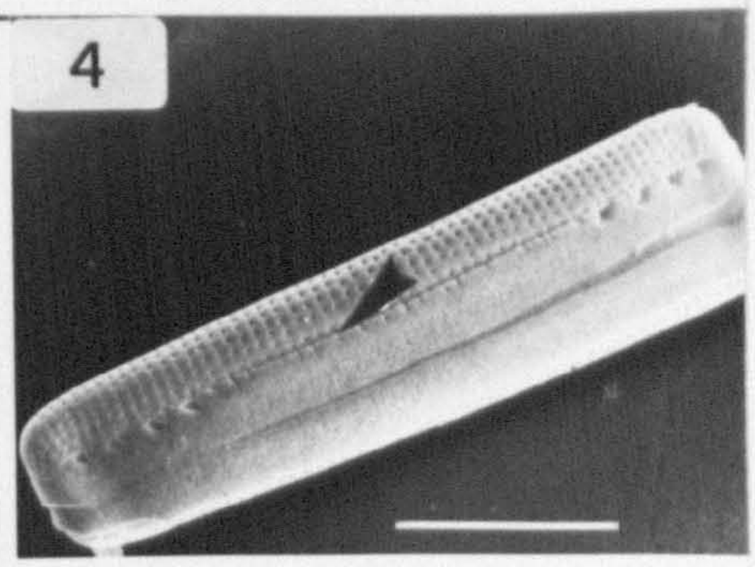

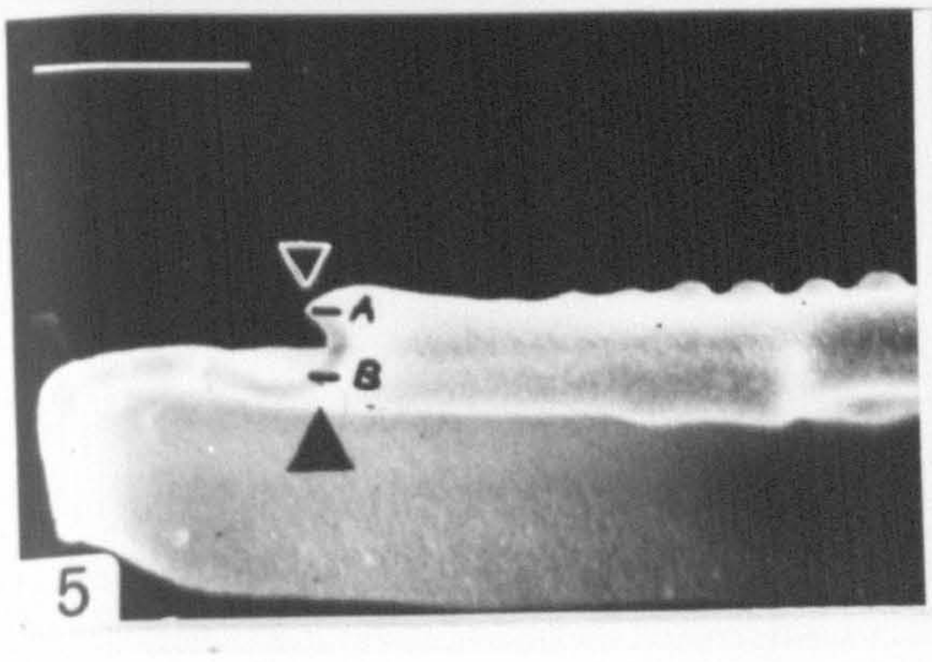

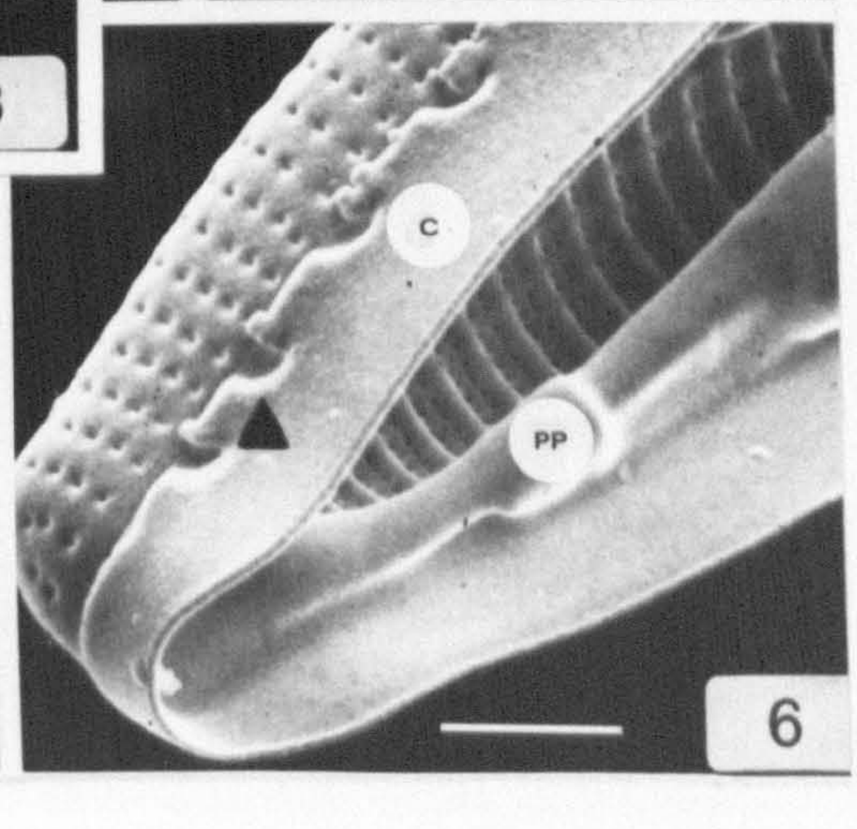

PLATE 55

PLATE 58

Mastogloia smithii: architectural features of the frustule

Figs 1, 2. Two whole frustules of different (pervalvar) width, SEM; V = valve, VC = valvocopula, and P = pleura, open at one pole (asterisk). The indices (E) and (H) refer to structural elements belonging to the epi- and hypotheca, respectively. Scale bars = 10 µm. Figs 3, 4. Reconstructions of the integration between the valve and the valvocopula; not to scale. Fig. 3. Valve face (VF), valve mantle (VM), pseudoseptum (PS), pars exterior of the valvocopula (C) with partectal pores (PPO), partectal ring (PR) with wavy crest (PU), and septum (S) with club-shaped structures (asterisks); the pseudoseptum (PS) fits within the gap present between the apex of the septum (S) and its club-shaped structures (asterisks), as indicated by the double arrow. Fig. 4. Diagrammatic representation of the interlock between an apex of the valve and the intercalary band, sectioned parallel to the transapical plane of the frustule; VF = valve face, VM = valve mantle, PS = pseudoseptum, asterisks = club-shaped structures of the septum (S), and C = pars exterior of the valvocopula.

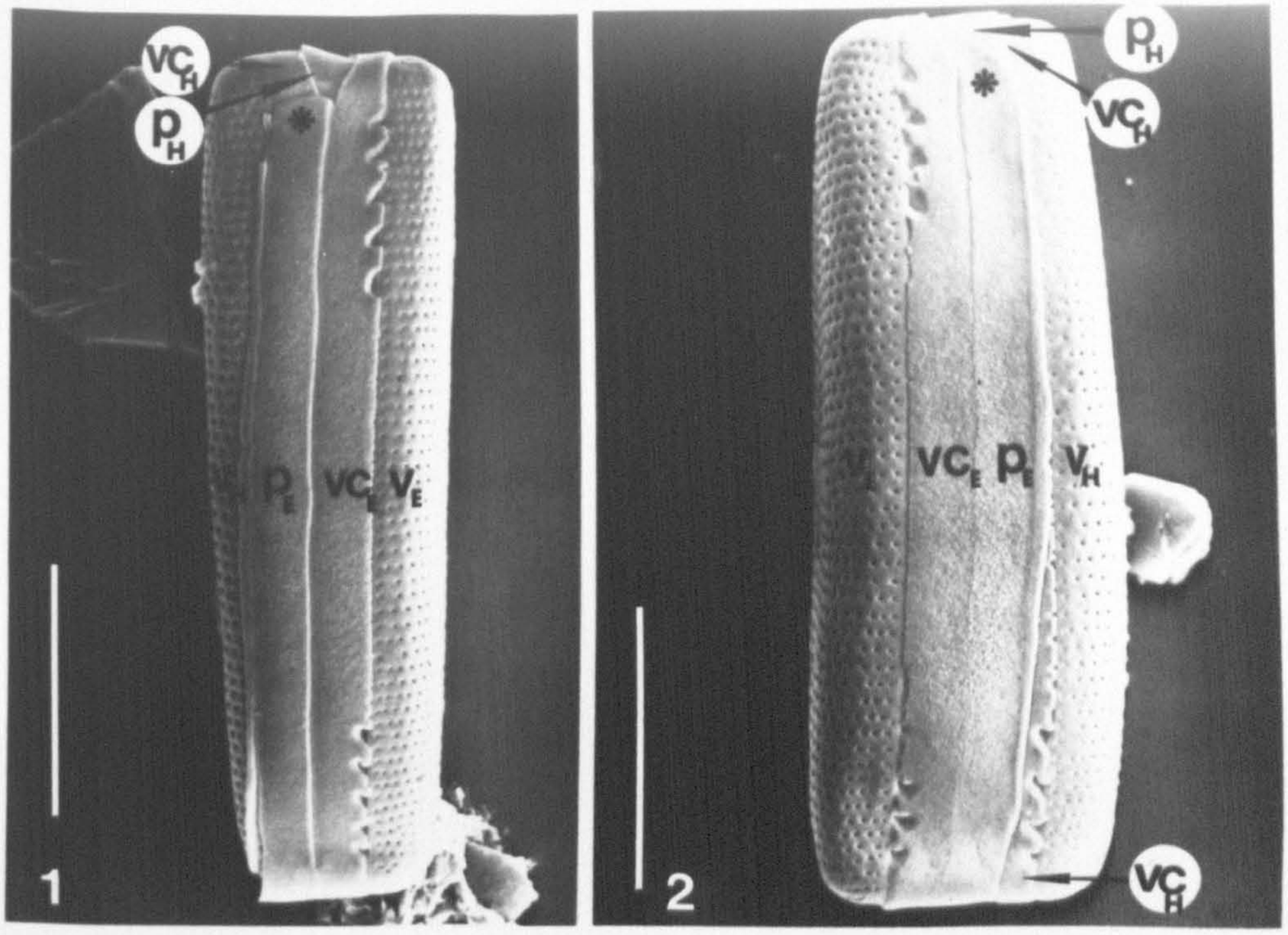

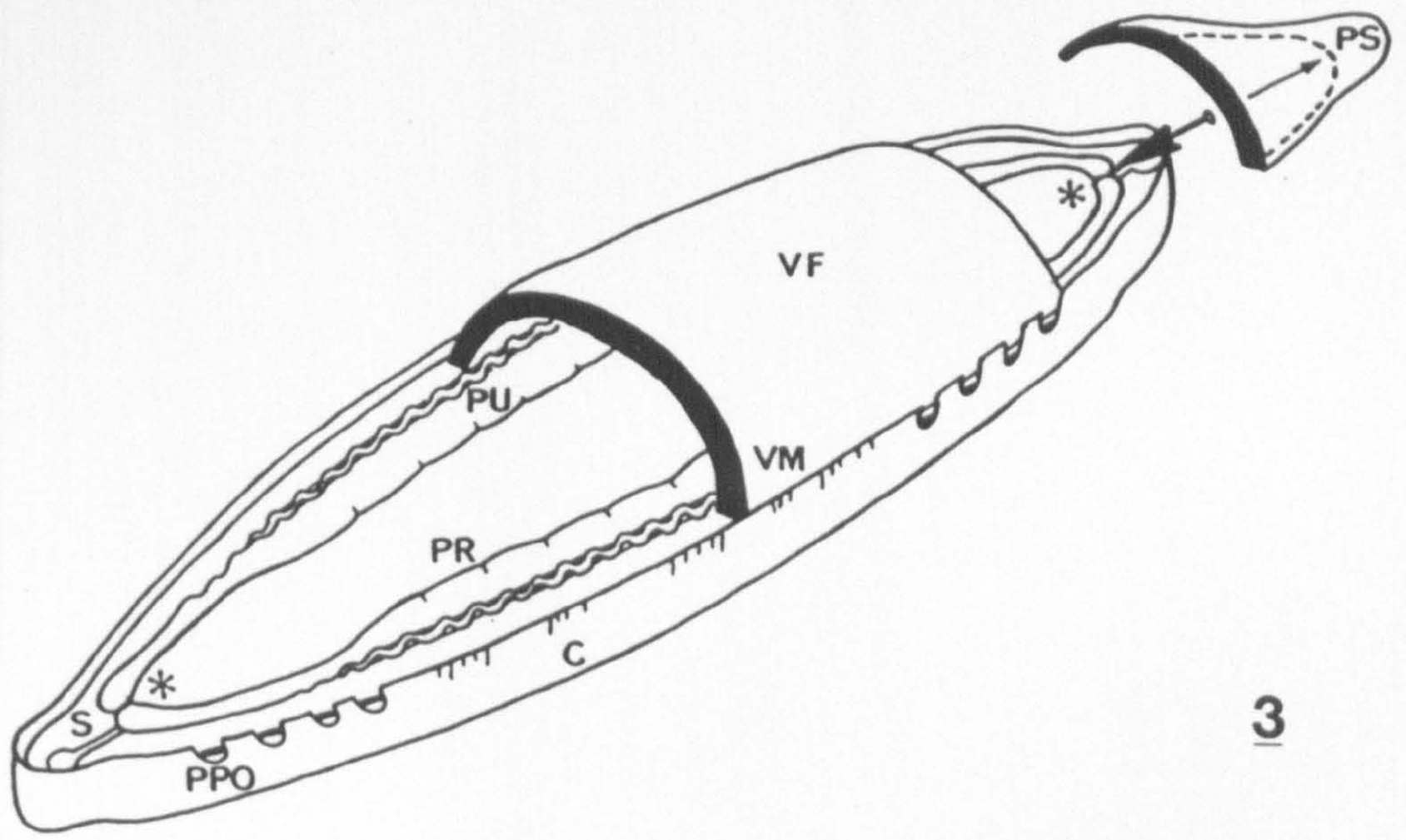

G. Novarino del.

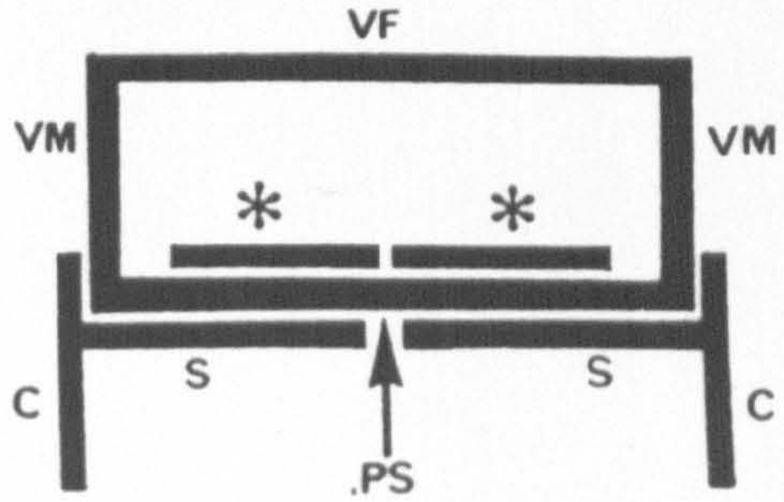

PLATE 56

PLATE 57

Cocconeis scutellum var. *stauroneiformis*, SEM

This is an internal view of the raphid valve. Along the margin, it bears the valvocopula of the araphid valve (AVVC), seen from its advalvar face. The *pars interior* of the AVVC is distinctly undulate, in relation with the fact that it interacts with the internal face of the mantle of the araphid valve (compare Pl. 58). Scale bar = 5 µm.

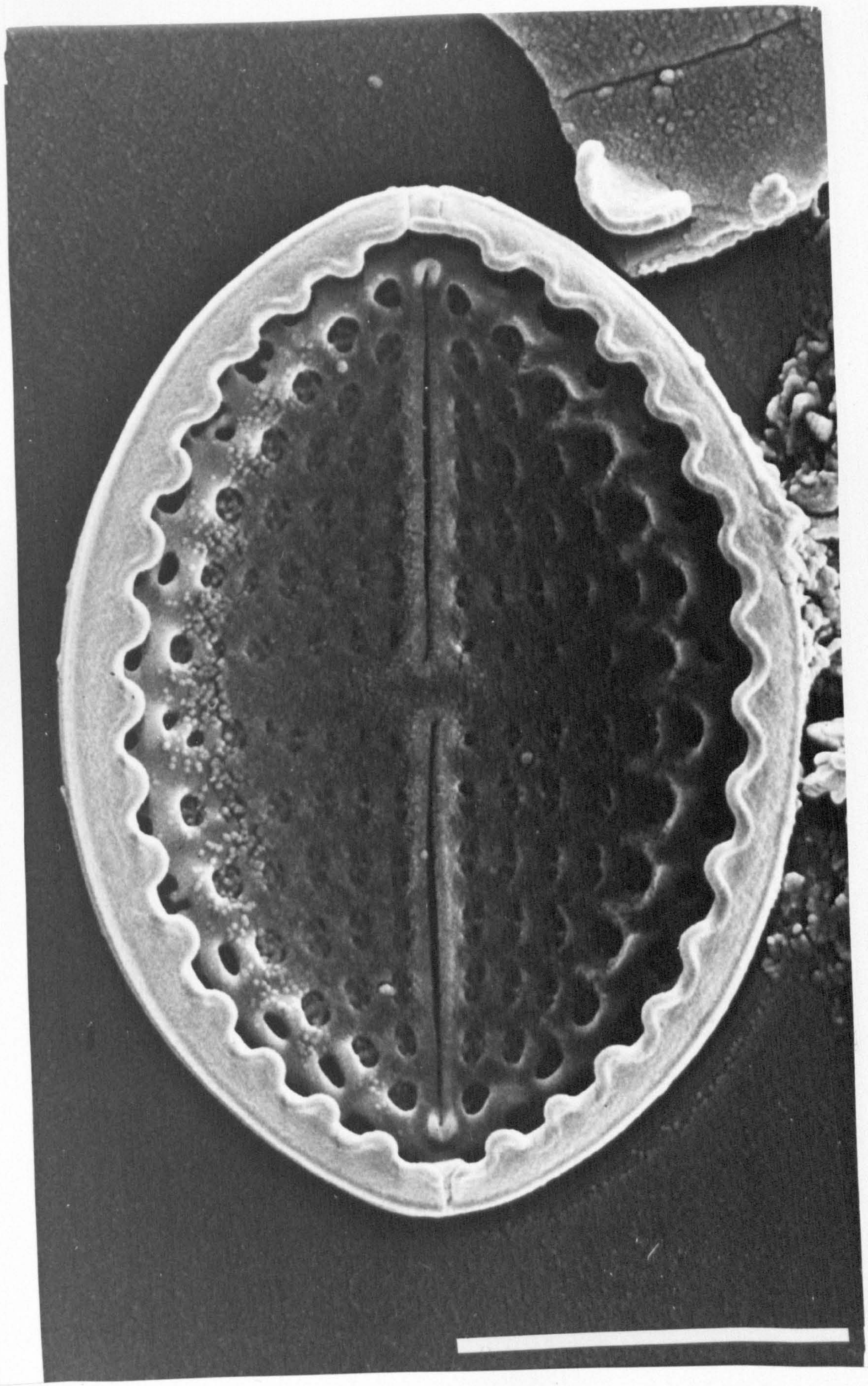

PLATE 57

PLATE 58

Cocconeis scutellum var. *stauroneiformis*, SEM

This is an external view of a broken araphid valve, with the undulate *pars interior* of the valvocopula just visible through the rupture. Scale bar = 5 µm.

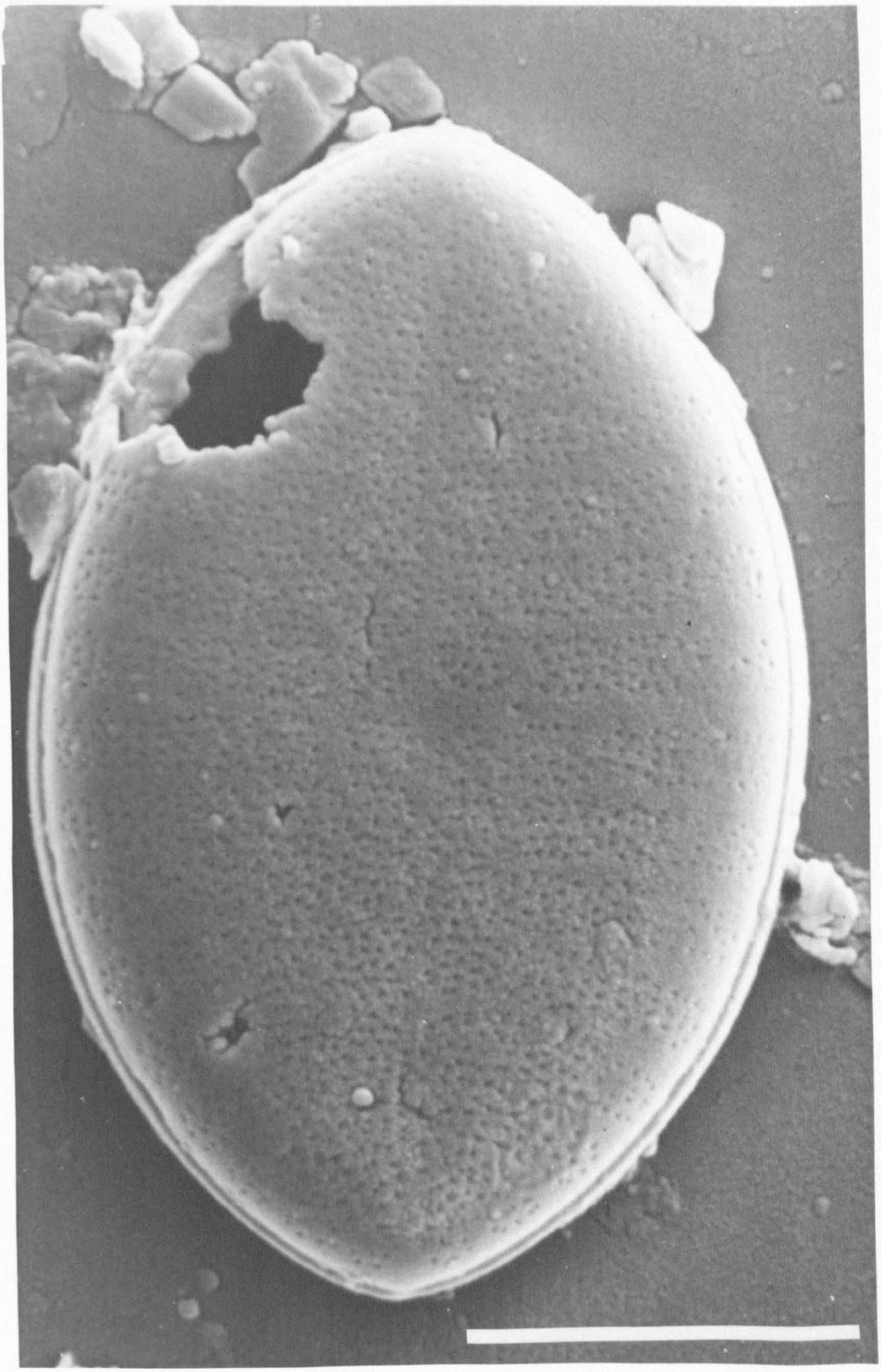

PLATE 58